
实验室学术委员会

顾问

苏纪兰 中国科学院院士，自然资源部第二海洋研究所研究员

主任

陈大可 中国科学院院士，自然资源部第二海洋研究所研究员

副主任

吴立新 中国科学院院士，中国海洋大学教授

张 经 中国科学院院士，华东师范大学教授

委员

秦大河 中国科学院院士，中国科学院寒区旱区环境与工程研究所研究员

王成善 中国科学院院士，中国地质大学（北京）教授

彭平安 中国科学院院士，中国科学院广州地球化学研究所研究员

周成虎 中国科学院院士，中国科学院地理科学与资源研究所研究员

陈发虎 中国科学院院士，中国科学院青藏高原研究所研究员

戴民汉 中国科学院院士，厦门大学教授

宗永强 香港大学教授

赵冲久 新疆维吾尔自治区人民政府副主席，原中华人民共和国交通运输部研究员

唐丹玲 中国科学院南海海洋研究所研究员

魏 皓 天津大学教授

杨守业 同济大学教授

王厚杰 中国海洋大学教授

丁平兴 华东师范大学教授

高 抒 华东师范大学教授

实验室行业技术委员会

主任

王光谦 中国科学院院士，青海大学校长

委员

张建云 中国工程院院士，南京水利科学研究院教授级高工

傅伯杰 中国科学院院士，中国科学院生态环境研究中心研究员

王 超 中国工程院院士，河海大学教授

胡春宏 中国工程院院士，中国水利水电科学研究院教授级高工

李家彪 中国工程院院士，自然资源部第二海洋研究所研究员

蒋兴伟 中国工程院院士，国家卫星海洋应用中心研究员

张洪涛 国务院参事，原国土资源部总工程师

仲志余 水利部长江水利委员会总工程师

李文学 水利部黄河水利委员会总工程师

石小强 中国长江三峡集团公司上海勘测设计研究院有限公司董事长

朱剑飞 交通部长江口航道管理局总工程师

崔丽娟 中国林业科学研究院湿地研究所研究员

汤臣栋 上海市绿化和市容管理局副局长

潘增弟 自然资源部东海局研究员

实验室领导

主任: 高 抒

副主任: 吴 辉 张卫国 江 红

目录 Contents

01

实验室简介
SKLEC Introduction

02

大事记
Headlines

05

科研课题与进展
Research Programs
& Highlights

114

交流与合作
Academic Communica-
tions & Cooperations

123

论文专著
List of Peer Reviewed
Publications

144

专利与软著
Patents & Software
Copyright

147

平台设施与野外观测
Facilities & Field
Observations

155

人才培养
Student Programs

161

研究队伍
Research Staff

实验室简介

SKLEC Introduction

河口海岸学国家重点实验室缘自1957年由教育部批复建立的华东师范大学河口研究室，依托华东师范大学，于1989年由原国家计委批准筹建，1995年12月通过国家验收并正式向国内外开放。

经过二十多年的建设，实验室已拥有一支结构合理、多学科交叉、专业互补、老中青结合的研究队伍；配备了先进的野外勘测及室内测试与分析仪器。实验室现有固定人员113人，其中研究人员103人（教授/研究员52人，副教授/副研究员26人，博士后25人；全部具有博士学位），技术人员7人，管理人员3人。秉承“开放、流动、联合、竞争”的运行机制，实验室瞄准国际学科前沿，围绕国家重大需求，在河口海岸学科前沿领域深入进行应用基础性研究，已成为代表我国河口海岸最高水平的科研基地与高层次人才培养基地。



大事记 Headlines

运行管理

Operations and Managements

2019年12月，河口海岸学国家重点实验室召开第六届学术委员会第四次会议，学术委员会顾问苏纪兰院士、学术委员会主任陈大可院士、副主任吴立新院士，学术委员会委员唐丹玲教授、王厚杰教授、杨守业教授、丁平兴教授、高抒教授；华东师范大学校长钱旭红院士、副校长孙真荣教授，校相关职能部门领导以及实验室全体成员出席会议。会议由陈大可院士主持。

1月12日，上海市海洋湖沼学会召开第九届会员大会，河口海岸学国家重点实验室李道季教授当选为学会新一届理事长。

10月28日，校党委第六轮第二巡察工作组入驻河口海岸科学研究院和河口海岸学国家重点实验室开展为期4周的巡察工作。实验室上下配合，确保巡查工作稳步推进。

研究生培养

Student Programs

4月至7月间，根据《华东师范大学博士研究生培养工作规定》（华师研[2019]347号）、《华东师范大学硕士研究生培养工作规定》（华师研[2019]348号）等文件的要求，在参考了国内外著名海洋科学有关院校培养方案后，经过研究生院培养方案交叉复议、各科学学位评定分委员会会议、培养方案修订工作小组会议等多次会议讨论，在原“海洋科学”研究生培养方案基础上，实验室/河口院对2020级起执行的新研究生培养方案进行了较大程度的修订。新的培养方案的变化主要体现在：在一级学科内优化了课程体系，新增发明专利、开发模块/方法、重量级期刊论文为科研成果可选条件，强化博士生的培养过程管理等方面。

6月22日，河口海岸科学研究院、河口海岸学国家重点实验室2020届毕业典礼暨学位授予仪式隆重举行。46名毕业生们依次接受了何青院长和高抒主任颁发的学位证书并拨穗，同时收获各位师长最诚挚的祝福。

7月14日，为了促进全国高校优秀大学生之间的学习和交流，激发大学生对河口海岸研究的兴趣，增进大学生对河口海岸事业的认识和了解，河口海岸学国家重点实验室“2020年优秀大学生夏令营”如期举行。此次夏令营首次尝试云端模式，通过实验室云参观、野外调查云直播等方式，吸引了来自全国40余所知名院校的138名优秀大学生前来参加。

学术交流

Academic Communications

6月1日，华东师范大学2020年度青年科学家（学者）在线国际论坛-海洋科学分论坛举行。来做国内外高校和研究机构的13名青年学者和与会专家相聚云端，进行了精彩的学术报告和科学探讨。

10月18-20日，2020河口三角洲动力与沉积地貌综合青年学者论坛举行。来自领域内的50余位专家学者和青年新星齐聚河口海岸学国家重点实验室，共同就当前研究领域内的前沿和热点问题进行讨论交流。

10月20-21日，中国科学院学部第106次科学与技术前沿论坛“中-欧海洋科学与技术进展”在上海举行。论坛由中国科学院地学部张经院士、欧洲科学院地学部Paul Tréguer院士和欧洲科学院地学部Louis Legendre院士共同召集。

11月9-13日，李道季教授出席联合国环境规划署海洋垃圾和微塑料不限成员名额特设专家组第4次会议并作重要发言。

国际合作

International Cooperation

1月，华东师大与海洋生物圈整合研究（Integrated Marine Biosphere Research, IMBeR）科学计划合作备忘录签约仪式暨战略合作伙伴研讨会在中山北路校区举行。双方约定自签约之日起，华东师大将承办IMBeR国际项目办公室（IMBeR IPO-China）。

1月，日本岛根大学河口研究中心主任Yoshiki Saito教授一行来访，与国重室签署了合作协议备忘录，双方就今后在项目申报、研究生培养等方面的合作进行了详谈。

5月，我室河口海岸水安全创新引智基地入选“111计划”2.0。河口海岸水安全创新引智基地于2008年立项，主要研究河口海岸的水资源和水安全问题。因执行情况良好，2012年获得滚动支持，2018年圆满完成“111计划”十年建设期。“111计划”2.0作为“111计划”的提升和延续，是教育部和科技部根据国家创新型发展战略需要来巩固和提升“111计划”在世界一流学科建设中的独特优势实施的专项计划。

11月，国家重点研发计划政府间国际科技创新合作重点专项“应对转型中的河口三角洲 (Coping with Deltas in Transition)”项目年度研讨会举行。该项目于2018年5月在华东师范大学正式启动，是由中国科技部 (MOST) 和荷兰皇家科学院 (KNAW) 联合发起的政府间科技合作项目，意在确立中国与荷兰长期的科学战略合作关系。

科研项目 Research projects

1月，李道季教授应澳门环保局邀请赴澳门签署合同，《澳门微塑料调查及应对策略研究》项目正式立项。10月，李道季教授团队赴澳门参加工作会议和采样工作。

10月，2019年度长江口共享航次积极应对疫情、顺利完成三个航段调查任务。

由我室何青教授主持申请的上海市科委社会发展领域重点项目“长江河口滩涂生态脆弱区监测与安全预警关键技术”获批立项，并在12月召开了项目启动会。

2020年度，实验室共获批国家自然科学基金项目18项，包括重点项目2项、长江联合基金2项、面上项目7项，青年项目7项。刘东艳教授主持的“我国陆架海硅藻稳态转换特征及环境驱动机制研究”项目和侯立军教授主持的“河口海岸湿地硝化微生物自养固碳机制研究”双双获得基金委重点项目资助。

人物 People

赵宁研究员入选国家级高层次青年人才支持计划。

唐剑武教授入选上海市高层次人才支持计划。

高灯州博士、苏磊博士、赵小双博士入选上海市“超级博士后”激励计划。

徐凡博士发表在GRL上的成果A universal form of power law relationships for river and stream channels被Editor选为亮点成果，并在AGU官方著名的EOS上加以重点宣传。

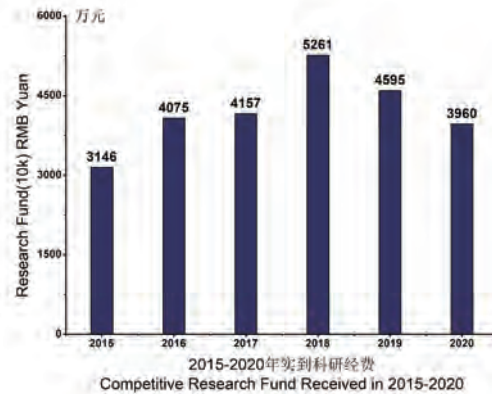
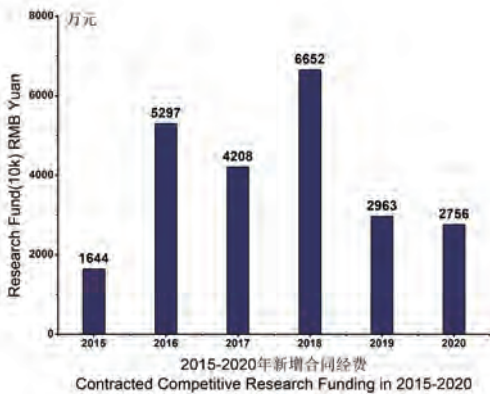
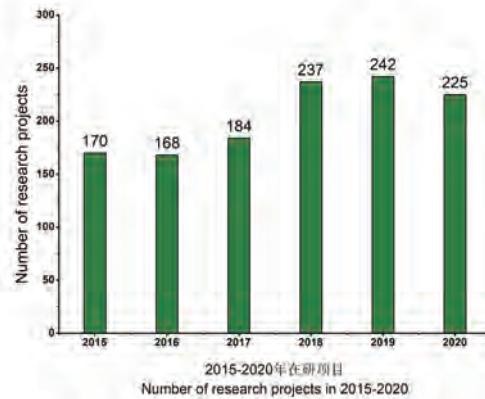
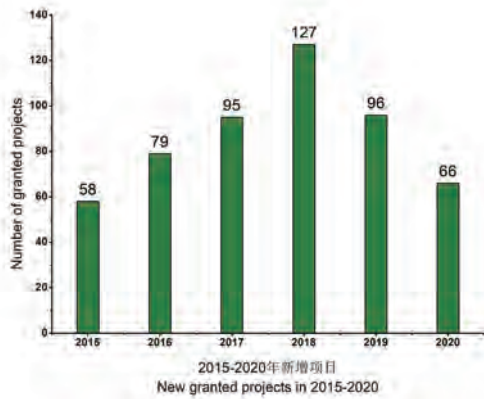
科研课题与进展

Research Programs and Highlights

科研课题

Research Programs

2020年度，实验室新增项目66项，新增合同经费2756.21万元。其中，新增国家、省部级项目24项，新增合同经费1696.08万元。2020年度，实验室合计承担课题220余项，实到经费3959.94万元，其中国家和省部级课题130余项，实到经费2986.60万余元。此外，实验室还获得科技部国家重点实验室专项经费510.38万元，其中205.68万元用于自主研究课题的部署，304.70万元用于实验室管理运行和开放课题。（数据统计截止2020年11月）



新增重大项目介绍

Brief Introduction of Selected New Projects

国家自然科学基金重点项目：河口海岸湿地硝化微生物自养固碳机制研究（42030411）（2021.01-2025.12）

项目拟以我国河口近岸作为典型研究区，综合利用地球化学、微生物分子生态学与生物化学等多学科研究方法与技术手段，系统研究河口近岸硝化微生物（AOB、AOA、NOB、Comammox）菌群动态（结构组成、多样性和丰度）的变化特征，阐明河口近岸硝化微生物驱动的化能自养固碳与氨氧化、亚硝氮氧化耦联计量关系，揭示河口近岸硝化微生物自养固碳的分子调控机理，定量分析河口近岸硝化微生物自养固碳的生态与环境效应，以期深化对河口近岸碳氮耦合循环机制的理论认识，并力争为河口近岸碳源汇功能评估、全球变化应对与可持续发展提供重要的科技支撑。

国家自然科学基金重点项目：我国陆架海硅藻稳态转换特征及环境驱动机制研究（42030402）（2021.01-2025.12）

全球变化背景下，海洋生态系统稳态转换特征与未来变化趋势是海洋科学的前沿热点。浮游植物贡献了全球约50%的初级生产力，硅藻是其中一个至关重要的类群。不同时空尺度的观测资料表明，硅藻在多个海区出现衰退信号，并引起浮游植物群落间的稳态转换，影响到海洋食物网、生物地球化学循环等多个关键过程，增加了有害藻华爆发规模与频率。因此，阐明硅藻衰退特征与环境驱动机制是十分重要的科学问题。本项目拟利用学科交叉优势，集成遥感、观测与古生态数据，结合模拟实验与统计模型，定量给出我国陆架海硅藻稳态转换的早期预警信号（临界慢化）、突变拐点及转换模态，构建关键种生态阈值，解析硅藻群落结构稳态转换特征与富营养化、暖化及自然气候变率三个关键过程的响应关系。研究对揭示我国陆架海浮游植物乃至生态系统的稳态转换特征具有重要参考价值，有助于理解生态系统结构与功能的稳定性以及未来生物生产力变化趋势。

上海市科学技术委员会社会发展领域重点项目：长江河口滩涂生态脆弱区监测与安全预警关键技术（20DZ1204700）（2020.09-2023.08）

滨海滩涂是全球陆海交界的生态脆弱区。长江河口滩涂是长江生态大保护的重要组成部分，但面临着流域减沙及滩涂萎缩、外来物种入侵及生境退化等严峻挑战，加强滩涂生态实时监测与安全预警，对长江大保护及长江经济带生态绿色发展等重大战略具有引领作用和标杆意义。本项目针对长江河口典型浅水滩涂生态脆弱区的滩涂、生态和环境等安全问题，以“滩涂生态系统-全程实时监测-综合阈值评估-安全预警管控”为主线，研发：
1. 基于ARGUS系统的滩涂植被和水文地貌综合监测技术；2. 外来物种入侵全过程防控监测技术；3. 空天地滩涂生态环境多元信息融合解译与定量反演技术。建立：1. 崇明东滩ARGUS生态动力地貌综合监测示范；2. 崇明东滩互花米草二次入侵监测和风险预警示范；3. 长江河口典型滩涂水沙动力实时监测示范。实现长江河口滩涂生态系统立体监测、安全评估和风险预警的全链条过程，为长江河口滩涂保护利用与管理决策提供科技支撑。

在研重要项目进展 Progress of Important Projects

国家重点研发计划项目：长三角典型河口湿地生态恢复与产业化技术（2017YFC0506000）（2017.07-2020.12）

本年度基于水沙-地貌-植被耦合的盐沼植被扩散机制机理研究进一步深化，发现本地种海三棱藨草的扩散不仅受上年种子库的影响，而且当年新产生的种子也有贡献，快速扩散时间集中在7-8月份高温期；在多项湿地修复技术支持下，本地种恢复面积达到1500亩以上，超过了项目考核指标要求的1200亩；修复区鸟类、底栖动物和鱼类种数和个体数量进一步提升；基于互花米草生物矿质液的新产品“肝知宝”固体颗粒投产；针对分散湿地秸秆研发的可移动式生物炭制取装备各模块进一步智能化；项目组与自然资源部东海局合作，撰写《外来物种互花米草蓝皮书》，并共同起草“十四五规划”项目建议材料；项目负责人和骨干作为技术支撑专家，起草了“上海市海岸带生态保护与修复重点工程项目规划”，被上海市采纳并上报自然资源部，本项目实施过程中获得的技术和理念将纳入未来上海市海岸带系列生态修复工程中。基于上述研究，产生了一批新的高水平研究论文、专利和研究报告。

国家重点研发计划“海洋生态环境保障”专项：海洋微塑料监测和生态环境效应评估技术研究（2016YFC1402200）（2016.09-2020.12）

2020年度，本项目在海洋塑料和微塑料污染监测分析技术、海洋塑料和微塑料分布、来源、运输和归趋以及生态环境效应评估技术研究等方面相继又取得了重要进展，产生了一系列创新性研究成果，进一步推动了海洋微塑料研究。本年度发表论文10篇，其中SCI论文9篇，SCI一区top研究论文8篇，申请专利3项；项目成员出席各类国内、国际会议15次，特邀报告9次。至2020年，本项目在海洋塑料和微塑料研究方面SCI研究成果名列全球第一，领跑世界。

本年度项目主要进展和成果总结如下：1. 完成了海洋塑料和微塑料监测指南，并通过联合国教科文组织政府间海洋学委员会西太平洋分委会（IOC-WESTPAC）专家评审，将向区域乃至全球推广；2. 根据先前研发的海洋微塑料大体原位采样技术方法，首次定量给出了海洋微塑料在西太平洋和东印度洋深海水层中的浓度分布，并提出了海洋微塑料在深海的可能运输模式，为亚太区域及全球海洋微塑料3D运输模型建立的数据采集奠定了前提技术条件；3. 构建了中国东海区域微塑料运输模型，发现漂浮、悬浮和沉降型微塑料的运输路径存在差异，受动力条件的影响运输路径存在季节变化特征，从微塑料河口排放—归宿来看，中国近海超过80%的微塑料滞留在中国近海海域，剩下的只有14%进入了太平洋，为我国在国际海洋微塑料污染治理中提供科学数据支持；5. 首次探明了我国东海近海海底塑料垃圾的分布热点及特征，为我国近海海底塑料垃圾污染治理提供了强有力的科学数据支撑；6. 首次报道了中国南海及印度洋大气中微塑料的污染特征，并进一步评估了全球塑料纤维向海洋的输送，为探明大气向海洋输送微塑料通量及全球运输模型的建立做出了开创性的贡献，并参与组织和促成GESAMP在全球范围开展海气塑料通量的研究；7. 通过进一步深入研究鱼类摄食微塑料的行为，从全新的角度阐明了鱼类摄食微塑料鱼类潜在的反应机制，为微塑料生态风险评估提供了新的途径。

与此同时，基于项目的研究成果，项目组专家还积极为国家提供应对政策建议和咨询，推动了我国在海洋塑料垃圾和微塑料污染管控方面相关政策和法规制定进程；项目研究成果也为我国应对海洋塑料垃圾和微塑料污染问题的行动、措施制定、国际政治与外交谈判提前奠定了科学研究基础，并提供了强有力的政策咨询和科技支

撑，项目成员在多个国际组织中任职，为我国掌握相关领域的国际话语权做出了重大贡献，极大地提高了中国在该议题的国际影响力。

国家自然科学基金重点项目：北部湾红树林潮滩响应陆海水沙变化的沉积动力过程 (41930537) (2020.01-2024.12)

红树林潮滩是全球极为重要的生态与环境资源。过去60年间，地球上约1/3的红树林因气候变化、海平面上升以及人类活动干扰等因素导致其出现永久性损失，全球红树林潮滩目前仍以每年0.2%的速率消失。占全国约1/3红树林的北部湾亦不例外，与建国前比较，红树林发生明显锐减且潮滩侵蚀后退。基于此，本项目瞄准国家《南红北柳》重大工程实际需求，以北部湾红树林潮滩沉积动力过程作为突破点，研究北部湾陆海边界条件变化和人类活动是如何改变红树林潮滩泥沙通量的存储与输运，以及如何影响潮滩沉积过程及地貌演变机制，最终揭示潮滩沉积与地貌跨尺度变化格局，提出高强度人类活动和海平面上升胁迫作用下的红树林潮滩变化趋势及侵蚀风险防范对策。目前为项目开展的第一年，已在海岸动力、悬沙及沉积、生物地貌等耦合方面取得初步成果，并在Marine Geology、Continental Shelf Research及海洋学报等国内外高档次期刊发表4篇。取得的主要进展包括：1. 定量识别不同动力分带区湍流动能、波浪和悬沙浓度的耦合关系，发现湍流动能是影响海滩水体悬沙浓度变化的最重要因素，其中仅占12.2%的湍流动能事件可产生42.9%的高浓度悬沙事件；2. 揭示了建国以来经历北部湾最大的台风威马逊对中强潮动力控制的北海海滩沉积物影响过程，研究发现沉积物粒度分布模式上由台风前以低潮带含量达39%的极细砂组分的显性特征，转变为台风后冲流带含量高达76%细砂组分的显性特征。其中波浪作用是破波带和低潮带内沉积物粒度分布模式发生转变的主要原因，潮位和海滩形态会影响冲流带内沙坝和沙槽表层的粒度分布；3. 揭示北部湾充填和溺谷型河口的红树林分布格局，研究发现充填型南流江河口和溺谷型大风江河口红树林自海向陆基本展现“红树林纯林(桐花树、秋茄、无瓣海桑种类混生)→红树植物与半红树植物(黄槿、苦朗等)混生→红树植物、半红树植物与非红树植物混生→红树植物镶嵌→稀疏红树林小苗”的分布模式格局，但大风江河口向陆界限主要以红树、红树幼苗及半红树混生为主。其中红树被浸淹时长是控制河口红树空间分布结构的主要因素。潮水上溯时长影响红树向陆生长的极限位置，宜林滩地是红树发育生长的必要条件。

国家自然科学基金山东省联合基金项目：黄河三角洲地貌演变的动力机制与环境效应 (U1706214) (2018.01-2021.12)

黄河三角洲曾是世界上淤进最快的大河三角洲。近年来，受流域气候变化和强烈的人工调控影响，入海水沙出现了新的情势，三角洲面临严峻的侵蚀危机。在入海水沙变异、河口流路变迁，以及海洋动力和人为干预作用下，黄河三角洲地貌演变出现了新的格局。围绕项目“河流入海水沙、海洋动力与三角洲地貌演变的耦合机制”和“陆海相互作用下三角洲演变的定量模拟技术”的两个关键科学技术问题，系统研究了黄河三角洲地貌演变动力机制及其环境效应。主要研究进展包括：量化了流域气候变化和人类活动对黄河三角洲地貌演变的影响，发现在人类活动维持高水平的情况下，气候变化的显著影响；从长时间尺度地貌演变的视角，探讨了转型中的黄河三角洲演变过程和机制，得到2000年是冲淤转型年，现行黄河口演变主要受调水调沙和口门出汉的控制；定量评估了调水调沙以来现行黄河口岸线动态，提出了维持冲淤平衡的水沙阈值；动态监测了人类活动和水动力作用下黄河三角洲北部潮滩动态，发现高滩围垦低滩侵蚀导致潮间带变窄；基于水沙耦合模型，计算了“尾闾河道-河口滨海区-外海”泥沙源汇通量，发现入海泥沙主要堆积在河口滨海区，其次输往莱州湾；进一步考虑极端事件的影响，定量模拟揭示了风暴对黄河三角洲近岸水沙动力和地貌演变的影响。

研究成果分别发表在Geomorphology、Catena、Journal of Hydrology、Marine Geology、Estuarine、

Coastal and Shelf Science、Continental Shelf Research、Environmental Monitoring and Assessment等国际著名刊物上。研究成果得到了山东省黄河三角洲可持续发展研究院管理中心的高度肯定，将对黄河三角洲生态保护和高质量发展规划提供重要的科学依据。

上海市科学技术委员会重点项目：长江河口河势稳定及控制关键技术研究与应用（18DZ1206400）（2018.11-2020.10）

由我室与中交上海航道勘察设计研究院有限公司、上海市水务(海洋)规划设计研究院、上海市水利工程设计研究院有限公司、长江勘测规划设计研究有限责任公司合作的项目，目标是服务长江口综合整治规划修编，为长江口保护和利用提供科技支撑。本年度主要进展如下：1) 系统总结了近百年长江口河势演变格局及其驱动机制，基于动力地貌模型对为未来减沙和海平面上升情景下的地貌变化进行了分析；2) 分析了长江口资源利用和保护的问题和需求，就未来河口河槽、沙洲、岸线、滩涂资源的保护和利用策略进行了研究，提出了长江口综合整治规划修编的建议方案。



部分新增项目

Selected New Projects

国家自然科学基金重点项目 NSFC Key Program	
北部湾红树林潮滩响应陆海水沙变化的沉积动力过程 (41930537) (2020.01-2024.12)	戴志军
国家自然科学基金面上项目 NSFC General Project	
全新世长江三角洲沉积中胶黄铁矿磁性诊断及其古环境意义 (41976158) (2020.01-2023.12)	张卫国
河口潮滩湿地氨氧化微生物驱动的氧化亚氮产生过程与调控机制 (41971125) (2020.01-2023.12)	董宏坡
基于溶解氧同位素来量化水柱和沉积物耗氧对低氧贡献的演替特征 (41976042) (2020.01-2023.12)	朱卓毅
鱼类对微塑料的摄食特性与机制 (41977344) (2020.01-2023.12)	施华宏
太湖南北两翼支流河谷全新世成陆过程及其对古文明发展的影响 (41971007) (2020.01-2023.12)	刘 演
北部湾典型砂质海岸海底地下水溶解有机碳结构组成及其入海通量研究 (41976041) (2020.01-2023.12)	张芬芬
海洋牧场生态环境对海底地下水输送营养盐通量的响应——以象山港为例 (41976040) (2020.01-2023.12)	杜金洲
国家自然科学基金青年科学基金项目 NSFC Young Scientist Fund	
基于长距离TLS强度数据的潮滩含水量反演研究 (41901399) (2020.01-2022.12)	谭 凯
潮汐影响下长江口盐沼水体溶解有机质的来源及降解转化机理 (41906145) (2020.01-2022.12)	曹 芳
长江口邻近海域浮游植物群落对黑潮次表层水入侵年际变异的响应特征 (41906121) (2020.01-2022.12)	周 鹏
省部级项目 Project Funded by Provincial and Ministerial Commission	
长江河口滩涂生态脆弱区监测与安全预警关键技术 (20DZ1204700) (2020.09-2023.08)	何 青
基于地球系统模式的北冰洋初级生产力演变研究 (20ZR1416300) (2020.07-2023.06)	冯志轩
渤海西北缘中全新世以来的沉积运输模式及其源汇效应 (20ZR1416800) (2020.07-2023.06)	刘世昊
海底地下水排放对盐沼湿地蓝碳生态系统的影响研究--以崇明东滩为例 (2020M671048) (2020.07-2023.06)	刘建安

上海市未来风暴潮的历史事件摄动法模拟研究 (20YF1411300)
(2020.07-2023.06) 张 凡

其他重要项目

Other Important Projects

澳门微塑料调查及应对策略研究 (2020.05-2021.11) 李道季

中挪国际合作项目: 海洋废塑料及微塑料管理能力建设项目 (2020.03-2023.06) 李道季

获批重要项目

Selected Approved Projects

我国陆架海硅藻稳态转换特征及环境驱动机制研究(国家自然科学基金重点项目)
(42030402) (2021.01-2025.12) 刘东艳

河口海岸湿地硝化微生物自养固碳机制研究(国家自然科学基金重点项目)
(42030411) (2021.01-2025.12) 侯立军

长江口埋藏盐沼土壤碳汇稳定性及其主控因子研究(国家自然科学基金面上项目)
(42077279) (2021.01-2024.12) 陈庆强

近海浮游植物分类的高光谱遥感探测机理与方法研究(国家自然科学基金面上项目)
(42076187) (2021.01-2024.12) 沈 芳

河口水环境中生物降解塑料的化学特征与生物效应研究(国家自然科学基金面上项目)
(42077371) (2021.01-2024.12) 陈启晴

杭州湾南翼全新世环境分异耦合过程与新石器人类响应与适应(国家自然科学基金面上项目)
(42071110) (2021.01-2024.12) 孙千里

风暴影响下潮滩沉积动力过程-底栖动物相互作用与反馈机制(国家自然科学基金面上项目)
(42076170) (2021.01-2024.12) 史本伟

长江口互花米草生态治理工程对底栖原生动动物群落的影响(国家自然科学基金面上项目)
(42076103) (2021.01-2024.12) 许 媛

长江河口新桥水道动力地貌变化及其对人类活动干扰的响应研究(国家自然科学基金面上项目)
(42076174) (2021.01-2024.12) 梅雪菲

河口潮滩底栖微型藻对反硝化型甲烷厌氧氧化的调控机制研究(国家自然科学基金青年项目)
(42001085) (2021.01-2023.12) 牛玉慧

潮滩盐沼植被对风暴过程的响应和生态护岸机制研究(国家自然科学基金青年项目)
(42006149) (2021.01-2023.12) 邢 飞

碎屑金红石U-Pb年龄和微量元素组成特征示踪长江与黄河物源研究初探(国家自然科学基金青年项目)
(42001001) (2021.01-2023.12) 尚 媛

南海碎碟壳体重金属元素记录的海洋环境特征和人类活动(国家自然科学基金青年项目)
(42006172) (2021.01-2023.12) 梅衍俊

未来多重复杂因素影响下的杭州湾风暴潮增水变化机理研究(国家自然科学基金青年项目)
(42006151) (2021.01-2023.12) 张 凡

海洋浮游桡足类摄食微塑料的行为模式及选择机制研究(国家自然科学基金青年项目)
(42006124) (2021.01-2023.12) 徐佳奕

潮沟分汊系统形态特征及动力机制研究(国家自然科学基金青年项目) (42006150)
(2021.01-2023.12) 徐 凡



科技部实验室专项基金 MOST Special Fund

2020年，科技部实验室专项共资助重点项目1项，人才队伍项目5项，技术队伍项目1项。

专项基金资助一览表

List of Recipients of Special Fund

项目名称 Project	负责人 Investigator
联合国教科文组织政府间海洋科学委员会海洋塑料和微塑料区域培训和研究中心建设项目	李道季
申请《采取应对崇明世界级生态岛建设潜在风险措施研究》项目前期调研	袁琳（茅志昌）
环境特征背景下海鲈鱼对微塑料的摄入量与赋存量解析	苏磊
我国典型陆海水域有机碱的地球化学特征及其对CO ₂ 体系的影响	宋淑贞
互花米草入侵对滨海湿地N ₂ O产生和消耗过程的影响	高灯州
Quantifying water quality change due to expansion of deltaic aquaculture ponds	Dhritiraj Sengupta
长江口水文监测浮标运行维护	胡进

科研进展 Research Progresses

2020年度，河口海岸学国家重点实验室在科技部、国家自然科学基金委员会和上海市科委等国家、省部级各类项目和国际合作项目及应用研究项目的支持下，在实验室的三大研究方向上围绕国家重大需求、聚焦前沿科学问题，持续地展开了科学研究。2020年实验室科研人员共发表各类论文255篇，其中SCI论文207篇，二区及以上论文134篇（top期刊论文102篇）。其中，以我室为第一单位或通讯单位发表的1区top期刊论文有30篇，发表刊物包括Nature Sustainability, Communications Biology, Geophysical Review Letters, Earth-Science Reviews, Water Research, Journal of Hazardous Materials, Journal of Geophysical Research-Oceans, Remote Sensing of Environment和Marine Geology等本领域权威刊物。其中，有两篇发表在GRL上的论文得到美国地球物理学会AGU会刊EOS的亮点推荐和重点评述（数据统计截止2020年11月）。

3.1 河口演变规律与河口沉积动力学

围绕变化条件下的河口三角洲系统演变规律和格局转变特征，以黄河口、长江口、杭州湾、珠江口、湄公河口、密西西比河口等典型案例，结合沉积地质分析、水沙现场原位观测、河床演变分析、遥感监测、数值模拟等多种研究手段，在河口潮汐动力、河道河相关系、河口三角洲泥沙源汇格局变化、极端事件影响等方面取得重要成果，包括：理论推导出河道河相关系的统一数学表达式，揭示了水流的紊动耗散是控制河势系统河相关系的根本原因及普适性规律，该成果得到美国地球物理学会AGU会刊EOS的亮点推荐和重点评述，仅有不到2%的AGU期刊论文可获此殊荣；揭示了潮波进入河口后的频散现象，阐述了以往忽略的低频信号对河口特高潮位的放大作用，拓展了关于河口空间范围的认识；揭示了河口三角洲系统对河流减沙的缓冲效应和适应性，体现在河口系统内的泥沙空间再分配过程和源汇格局转变，同时极端台风天气对河口侵蚀发生具有显著的补偿作用。这一成果大大深化和拓展了以往关于河口三角洲侵蚀风险的研究认识；综合历史沉积地貌分析和水动力模拟的多尺度研究方法，揭示了古河口海岸地貌演化与台风淹没事件之间的相互作用关系，为认识河口海湾演化及人类文明演替提供了有力支撑。

3.2 海岸动力地貌与动力沉积过程

实验室人员通过改进研究方法在不同时空尺度上进行海岸动力地貌与动力沉积过程的精细研究，取得如下主要成果：揭示沉积特征与风暴强度的对应关系，从陆架长时间序列中取得了地理地带性变化因素与西边界流强度关系的关键证据，获AGU会刊EOS的亮点推荐和重点评述。对中强潮型海滩湍流动能，波浪和悬沙浓度的权衡关系，以整体地识别湍流动能，波浪和悬沙浓度的耦合关系，并进一步评估了不同波浪带下湍流动能和波浪对悬沙浓度的相对重要性；对黄河近年来入海水沙量锐减背景下，研究人员用Telemac数值模型和Delft3D模型，模拟了入海水沙变化对河口滨海区沉积动力过程，探讨了潮汐变化、切变锋、泥沙输运和沉积过程的机理；发现大型底栖生物活动对沉积动力学关键参数的有显著影响，推动生物地貌学的研究进展；提出了一种用多探头集成的系统观测（IOA），解决了由于信号的衰减则引起含沙量反演的不确定性问题；发现风暴后及时实施小规模 and 短间隔的沉积物补给可以有效地补偿海滩上泥沙流失措施，这为海滩管理提供重要参考；通过对渤海中央泥质区的钻孔沉积物进行沉积特征分析，发现冬季北极涛动的调节作用，是通过与ENSO和黑潮的遥相关作用实现的，这为中国边缘海的泥质区古代环境变化研究提供了重要信息。

3.3 滨海湿地生态研究

在滨海湿地生态方面，实验室人员取得如下主要研究成果：滨海湿地是大气中CO₂的汇并具有缓解温室效

应的能力，但是土地利用变化削弱了CO₂吸收能力并显著增加了CH₄和N₂O排放，导致全球增温潜势增幅达65.4—2948.8%；揭示了潮汐动态淹水对湿地生态系统CO₂通量的影响机理，提出通过合理引种植物和调控水文条件等方法，快速提升滨海盐沼湿地“蓝碳”和改善水质缓解水华的能力，为盐沼湿地恢复工作提供了技术支撑；发现河口潮间带沉积物的碳氮基质可利用性、pH、盐度和硫化物等会影响潮间带沉积物硝化/反硝化过程以及N₂O排放量，解释了长江口潮间带沉积物N₂O产生机制与排放过程；预测在未来海平面上升情景下，水-盐胁迫会交互作用于滨海湿地的固碳能力和温室气体排放通量，从而削弱亚热带地区滨海湿地对大气中CO₂的吸收能力；研究发现红树林湿地土壤根周细菌的碳源利用率随着潮滩高程的升高而降低，土壤湿度和氧化还原电位共同影响了滨海湿地土壤细菌群落多样性、铁膜形成和重金属转运等功能，为红树林湿地生态修复提供了科学依据；探讨了互花米草二次入侵的多阶段生态过程，定量了湿地植物不同繁殖体对水动力干扰的生态阈值，并提出施用除草剂是相对环境友好的互花米草治理方式，为控制海岸带外来物种提供了新思路。

3.4 河口近海生物地球化学研究

河口近海生物地球化学方向取得如下主要研究成果：在人类活动和全球变化背景下，通过典型热带河口的马来西亚河流中硒、氨基酸以及碳氮同位素等参数，发现马来西亚泥炭河流向海洋输送的硒等生源要素通量远超过其它报道的小河流，陆地是溶解态有机硒的主要来源；且泥炭河流溶解有机质存在很强的细菌改造信号，组成也发生了改变；而印度的NAMADA河流的有机物的来源、保存和成岩作用受到该地区强烈的季节性变化的控制。在南海陆坡海区中尺度涡旋混合过程中，不同水层混合体系具有不同的微生物组成及其功能，同时通过双涡流将TOC穿过陆坡向南海海盆的水平输出量估计大于 22.1×10^9 gC，表明中尺度涡旋可显著促进南海的碳固存。利用同位素示踪Pu同位素作为示踪剂，首次评估了外海输入对近海重金属的贡献，并指出对Hg的贡献不可忽视。基于Rn同位素示踪地中海喀斯特区域通过海蚀洞等点源输入的地下淡水是地中海“新”营养盐的重要来源，其可能对寡营养盐结构的地中海生物地球化学循环产生重要影响。同时通过一系列工作，阐明了在我国重要水产品养殖基地桑沟湾，东海嵎泗列岛，广西红树林保护区珍珠湾地下河口碳及其营养盐循环模式以及与微生物之间的耦合关系，地下河口细菌在驱动营养盐和碳的源汇过程中起着十分重要的作用。

3.5 近海生态环境研究

近海生态环境方向取得的主要研究成果如下：揭示了我国近海有害藻华物种来源、分布、碳固定途径和营养盐利用机制，阐明了我国黄海浒苔爆发的内部生理学机制；对金潮藻的研究确定了黄海和东海的金潮物种为Sagarasum horneri，发现S. horneri在不同的生境中呈现不同的形态特征；分析了我国典型赤潮藻-中肋骨条藻和东海原甲藻体内磷库分布及其在不同磷环境下的对磷利用的变化情况，为藻华形成提供理论依据；揭示了海盆尺度强迫在MAB潜在叶绿素a变化中的重要作用；发现围填海和石油开采等人类活动影响我国近海水体、沉积环境和生物分布，相关结果为我国近海和河口环境管理提供了理论参考；利用脂肪酸和正构烷烃等参数结合ENSO、PDO等事件变化，反演近海上升流强度的年际变化；发现人类活动对潮间带沉积物中PAHs的分布和沉积具有关键和不同的影响，为潮间带沉积物污染提供了大陆尺度的证据。以上研究为深入了解我国沿海有害藻华的形成机制，提出有效的有害藻华监测和防控策略提供了有力的科学支撑，也为潮间带生态系统健康保护提供了科学依据。

3.6 海洋微塑料研究

海洋微塑料方面继续发挥国内和国际引领作用，取得如下主要成果：首次报道了中国南海及印度洋大气中微塑料的污染特征研究，揭示了微塑料可以通过大气远距离运输到一千多公里以外的地方；结合空气动力学模型，研究估计得出2018年全球产生了7.64-33.76 t的大气微塑料纤维；构建了中国东海区域微塑料输运模

型，发现中国近海超过80%的微塑料滞留在中国近海海域，剩下的只有14%进入了太平洋，为我国在国际海洋微塑料污染治理中提供科学数据支持；研究揭示了地球上最深的已知区域—挑战者深渊，及深海平原和位于太平洋海底海沟（4900 m至10890 m）的沉积物中的微塑料赋存特征，表明深渊海沟将是大量塑料及微塑料的重要的储存库及最终的汇；调查了中国东海海底塑料的区域分布，组成和数量，为我国近海海底塑料垃圾污染治理提供了强有力的科学数据支撑；研究探索使用一种大体积采样的新技术应用于西太平洋和印度洋水柱微塑料丰度调查，据此得出大洋水柱的丰度值至少低于传统小体积采样有1 - 2个数量级；综述了水柱中微塑料采样方法、分布和理化性质的最新进展，提出使用体积梯度试验和统一的60-100 μm 拖网孔径的建议；揭示了大型蚤、珍珠龙胆石斑鱼等生物对微塑料颗粒的摄食行为及急性生长发育毒性和亚致死的内分泌干扰效应。

河口演变规律与河口沉积动力学 Estuarine Evolution and Sedimentation Dynamics

A Universal Form of Power Law Relationships for River and Stream Channels

Xu, Fan; Coco, Giovanni; Zhou, Zeng; Townend, Ian; Guo, Leicheng; He, Qing. *Geophysical Research Letters*, 2020, 47(20): e2020GL090493.

The description of the geomorphic characteristics in power law forms has been the subject of research, over the past 70 years, and has become the cornerstone of regime theory. However, just why power functions should represent such geomorphic relationships remains poorly understood. Hence, differences in the values of the regime exponents observed for different river systems remain largely unexplained. To address this issue, we derived generic forms of the power law relationships without postulating any power functions of the discharge. The theoretical approach accurately captures the systematic variations of the regime exponents shown by a number of large data sets from previous research. We also explain how frictional resistance is responsible for the systematic variability of regime exponents. Overall, our study provides a robust mechanism to describe the variations of the exponents, along with a deductive explanation of the power laws at the core of fluvial hydraulic geometry.

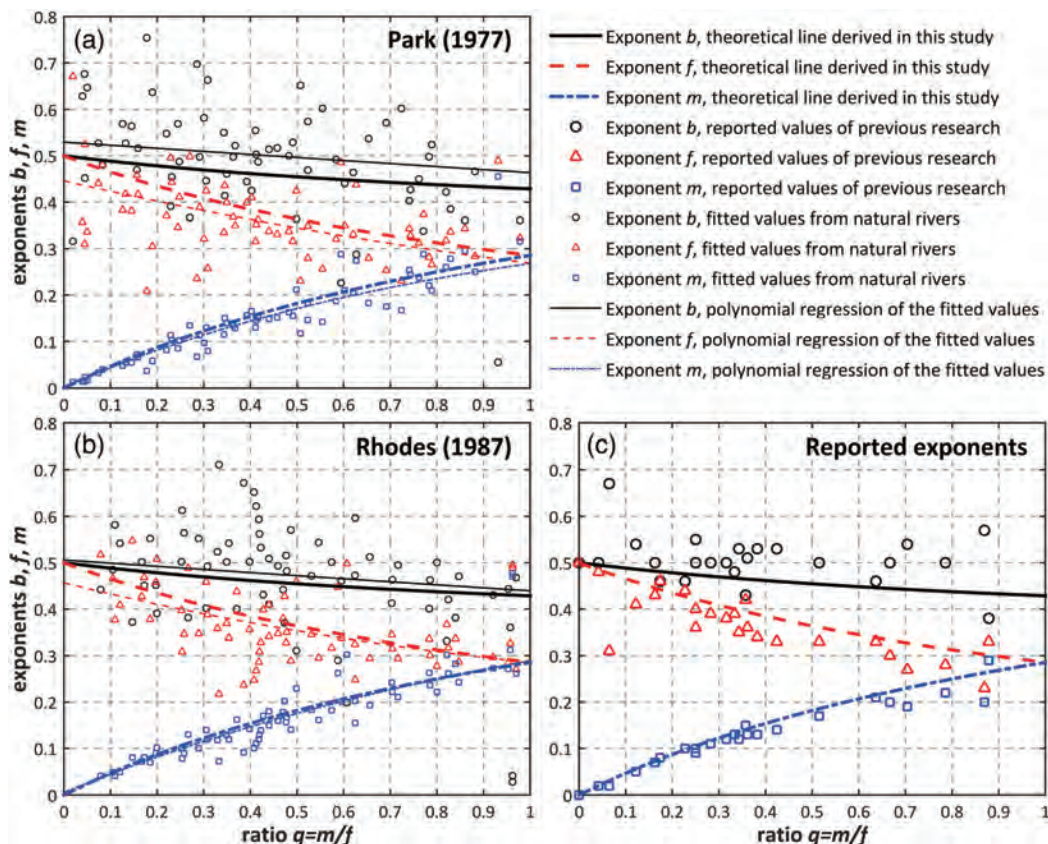


Figure 3. Variation of the exponents b , f , and m with q as derived in this study (thick lines), and fitted values collected from natural stream channels by Park (panel a) and Rhodes (panel b), and the values collated by previous researchers (panel c). The thin lines in panels a and b show the polynomial regressions of the fitted exponents (see Table 1 for the values). The values of R^2 of the regressions for b , f , and m are 19%, 47%, and 87% for Park (1977) and 17%, 55%, and 85% for Rhodes (1987), respectively. The relatively small values of R^2 for exponent b indicate that the slightly decreasing trend is a weak signal in the presence of a lot of noise. In contrast, the trends for the other two exponents are much larger relative to the noise and the regression coefficients reflect this.

河床演变学的核心科学问题之一是探究河道断面形态与水沙动力条件之间的内在联系，通常称之为河相关系。自50年代Leopold和Maddock的开创性工作起，河道的宽度、深度和流速基本都采用经验幂函数与流量关联： $B \propto Q^b$ 、 $H \propto Q^f$ 和 $U \propto Q^m$ 。其中B、H、U和Q分别为河道断面宽度、平均深度、平均流速和流量，b、f和m为幂指数。许多河流地貌学领域的研究人员致力于建立该幂函数关系的第一性原理，并尝试阐明b-f-m幂指数变化的物理机制，但至今尚未得到令人满意的结果。这一问题极大限制了河床演变学中对河相关系的普适性理解和相关模型预测能力。

针对这一难题，本研究首先收集了世界上约150条河流的数据拟合幂函数值以及50组不同学者提出的理论经验值。通过考察b-f-m幂指数随比值m/f的变化规律，发现了b-f-m拟合值的系统性变化规律。为了理解这一变化规律，本研究构建了动力学模型，数值模拟了河道横截面在不同演化阶段的几何形状和侵蚀潜势，并推导了平衡断面形态的理论解析形式。结果显示数值模型与理论推导之间完美吻合。研究首次揭示了河道断面平衡形态的解析表达，证明了幂函数形式河相关系的存在性，阐明了底摩阻对b-f-m幂指数变化的控制机制，对预测河道平衡形状提供了潜在可能。研究成果对基础科学和实际应用有系列贡献价值：包括流量监测、洪涝风险评估技术到对水生态系统的认识等。

研究成果在Geophysical Research Letters上发表，并被Editor推选为亮点成果，在AGU官方著名的EOS上加以重点宣传。

Morphodynamic couplings between the Biandan Shoal and Xinqiao Channel, Changjiang (Yangtze) Estuary

Lou, Yaying; Dai, Zhijun; He, Yuying; Mei, Xuefei; Wei, Wen. *Ocean and Coastal Management*, 2020, 183: 105036.

Channel-shoal systems (CSS) are some of the significant morphodynamic cells in estuaries, which provide immeasurable economic, ecological and environmental value. However, most CSS in mega-estuaries of the world are facing great challenges from serious risk of degradation due to intensive human activities and sea-level rise. Here, we focus on the tradeoff between the Biandan Shoal (BDS) and Xinqiao Channel (XQC), which is the largest CSS of the South Branch, Changjiang Estuary. The results show that the BDS area above the 5 m water depth had an observable increasing tendency with an interannual increasing rate of 1.43 km²/yr during 1996–2016. The corresponding XQC volume exhibited an obvious reduction trend with an annual decreasing rate of 3.79 X 10⁶ m³/yr. Meanwhile, the BDS presented lateral and downward extension with more than 4.7 km of downward movement, while the XQC indicated shrinking with the width of the upper reaches decreasing by nearly half since 1998. Furthermore, the morphodynamic evolution of the BDS-XQC system during 1998–2016 could be divided into four stages: pre-flood stage with the joint extension of the BDS and XQC (1996–1998); conversion stage due to impacts from the extreme flood (1998–2000); development stage with obvious deposition throughout the system (2000–2009); stabilization stage with deposition on the high flats but no lateral expansion of the BDS, and continuous shrinkage of the XQC (2009–2016). The dynamic balance of the BDS-XQC system was mainly determined by the tradeoffs between the BDS and XQC, even though the occasional extreme hydrological events disrupted the coupling of the BDS-XQC. Meanwhile, the local channel blocked by the construction of the Dongfengxisha Reservoir induced a decrease in water discharge into the XQC, which was responsible for the recent XQC recession. In light of the impact of future climate change and increasing human interference in the anthropogenic era, fragile CSS distributed in estuaries should be holistically considered with policies to support sustainable integrated coastal zone management.

滩槽系统是河口地区重要的地貌单元，具有极高的经济、生态和环境价值。然而，由于高强度人类活动和海平面上升影响，世界上大多数大型河口的滩槽系统正面临着严重的退化风险。本文重点研究了长江口南支最大的滩槽系统扁担沙和新桥水道之间的滩槽关系。结果表明，在1996 - 2016年间，5 m水深以上扁担沙面积明显增加趋势，年际增长率达 $1.43 \text{ km}^2/\text{yr}$ 。相应的新桥水道体积则呈现明显下降趋势，年际减少速率为 $3.79 \times 10^6 \text{ m}^3/\text{yr}$ 。同时，自1998年以来，扁担沙沙体呈横向向下游扩展趋势，其迁移距离超过4.7 km。而新桥水道却发生河道束窄现象，其水道上部河道宽度收缩了近一半。此外，1998年至2016年间，扁担沙和新桥水道这一滩槽系统形态动力学演化可分为四个阶段：大洪水前期扁担沙和新桥水道共同扩展阶段（1996 - 1998年）；受特大洪水影响的转换阶段（1998 - 2000年）；整个滩槽系统明显淤积的发展阶段（2000 - 2009年）；以及相对稳定阶段（2009 - 2016年），这一阶段扁担沙没有明显的横向扩展只存在高滩淤积状态，而新桥水道仍持续萎缩。尽管偶尔发生的极端水文事件破坏了扁担沙和新桥水道这一滩槽系统的耦合，但这一系统的动态平衡主要仍取决于扁担沙和新桥水道之间的相互影响。与此同时，由于东凤西沙水库的建设堵塞了当地河道，导致进入新桥水道的径流量减少，这是导致新桥水道近期衰退的原因。考虑到未来气候变化的影响以及日益增加的人为干扰，相关部门应着重关注这些广泛分布于河口区的脆弱的滩槽系统，通过工程措施因地制宜，进一步支持可持续的海岸带综合管理。

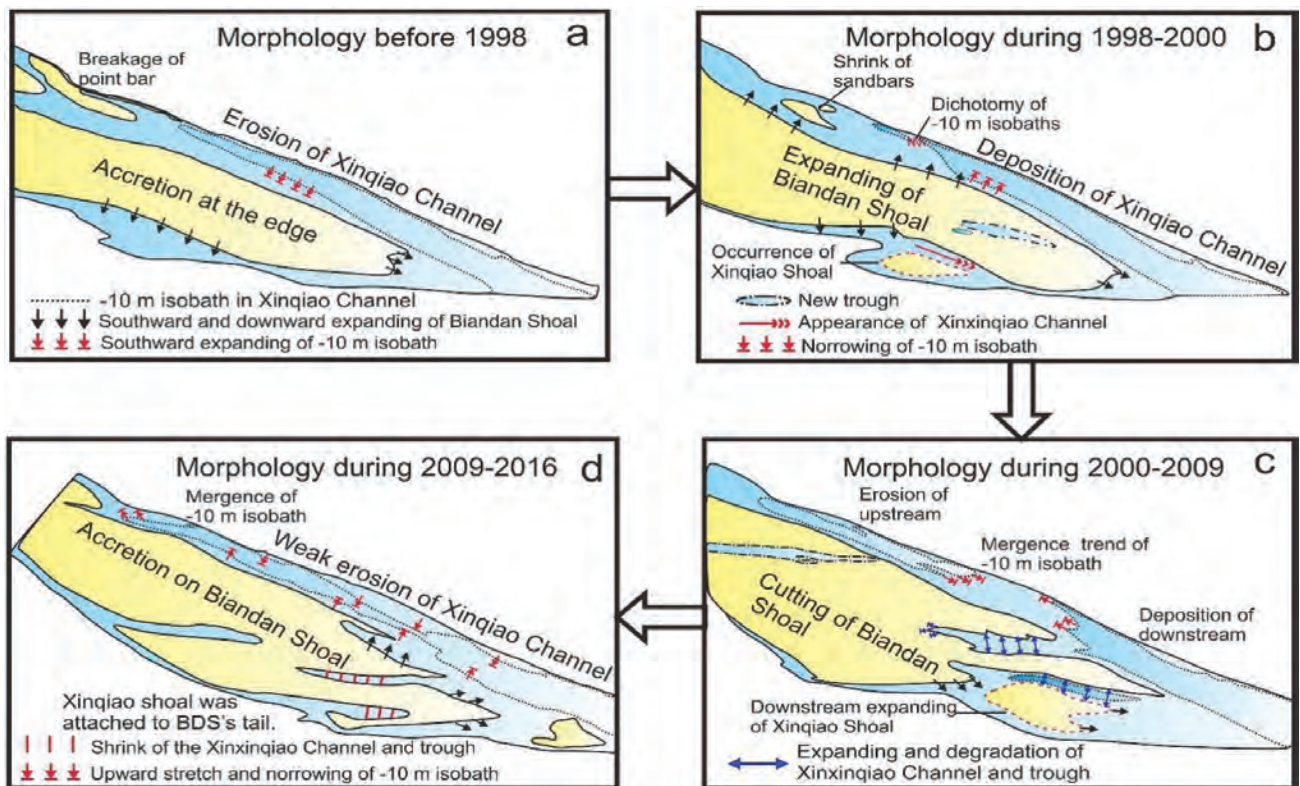


Fig. 15. Conceptual model depicting the morphodynamics of the BDS-XQC system between 1996 and 2016.

Spatial and seasonal variability in grain size, magnetic susceptibility, and organic elemental geochemistry of channel-bed sediments from the Mekong Delta, Vietnam: Implications for hydro-sedimentary dynamic processes

Jiang, Yamei; Saito, Yoshiki; Thi Kim Oanh Ta; Wang, Zhanghua; Gugliotta, Marcello; Van Lap Nguyen. *Marine Geology*, 2020, 420: 106089.

Understanding the relationship between depositional processes and their products in the fluvial–marine transition zone in tide-dominated depositional systems is fundamental to improving environmental and stratigraphic interpretations of long-term sedimentary records. The distributary channels of the Mekong Delta represent a typical example of a complex sedimentary environment characterized by strong fluvial and tidal interactions, and seasonal variability in hydro-sedimentary dynamic processes, particularly the migration of a salt wedge front linked to seasonal fluctuations in freshwater discharge. For this study, we analyzed grain size, magnetic susceptibility, and organic elemental geochemistry of channel-bed surficial sediments collected in 2015 from all distributary channels during the dry season and from the Mekong–Co Chien River during the flood season. This paper reports spatial and seasonal differences in the characteristics of channel-bed surficial sediments, which are closely linked to sediment sources and depositional processes during the dry and flood seasons.

Distributary channels are characterized by coarse-grained sediments in the upper reaches and fine-grained sediments in the lower reaches, in both dry and flood seasons, reflecting the difference between the upstream fluvial-dominated environment and the downstream tide-dominated environment. Flood season samples from the Co Chien River show higher magnetic mineral contents and a terrestrial source of organic carbon compared with dry season samples, indicating sourcing from the drainage basin and trapping of suspended materials in the distributary channel due to the barrier effect of the saltwater wedge at the river mouth. Compared with the flood season, during the dry season the mud content was lower in the downstream reach close to the river mouth and higher in the upstream reach of the Co Chien River, and the content of magnetic minerals was lower in both reaches, indicating dissolution of magnetic minerals during early diagenesis. Furthermore, the lower C/N ratios (< 10) and slightly enriched $\delta^{13}\text{C}$ values of the dry season samples from the Co Chien River imply an additional contribution of organic carbon from a marine source. These various features imply a landward import of mud into the Co Chien River induced by stronger salinity intrusion during the dry season. Along the downstream tract of the Bassac River, two mud-dominated reaches were identified during the dry season. The magnetic mineral contents, C/N ratios and $\delta^{13}\text{C}$ values indicate that the mud-dominated reach near the Bassac River mouth is also supplied from resuspended sediments by estuarine circulation and tidal pumping, whereas the mud in the reach that is transitional from fluvial to tide dominance has a riverine supply. The results suggest that the Mekong distributary channels are important sinks for suspended sediments during both the flood and dry seasons, controlled by a sediment trapping mechanism provided by either estuarine processes or the morphological configuration of the channels, both of which are controlled by fluvial–tidal dynamics. These depositional processes may be compensating for the incision of channels induced by sand mining in recent decades.

湄公河三角洲平原分流河道众多，前人的研究多集中在径流作用占优的下泄汉道（Bassac汉道）的沉积动力和地貌过程调查，较少关注潮汐作用占优的Mekong汉道下游各分汉。但是，随着入海水沙的减少和相对海平面上升，潮汐作用对三角洲平原分流河道的地貌演变作用可能加强。因此，本研究利用在Mekong汉道洪枯季和Bassac汉道枯季获得的表层沉积物，分析其粒度、磁化率和有机碳组成的时空变化，探讨潮汐在该三角洲平原汉道泥沙输运和沉积中的作用。研究结果显示，在空间上，径流优势的感潮河段表层沉积物普遍粗于潮汐优势的河口段；潮汐优势的河口段，洪季也有细颗粒泥沙在汉道内淤积并且有海洋藻类的贡献，反映盐水入侵的作用。枯季，潮汐优势的汉道，泥质沉积区向上游迁移，海洋来源泥沙、或者是经历早期成岩作用的泥沙贡

献增多，反映盐水入侵加剧。径流优势的Bassac河道在枯季也出现两个泥质沉积区，分别是盐水楔头部以及从近口段向河口段的过渡区，后一个泥质区的沉积机制推测和挖沙导致的河道地貌有关，但还需要更多现场调查。上述湄公河三角洲的研究结果说明，在人类活动和相对海平面上升的共同作用下，潮控河口的河道内淤积可能会增多。

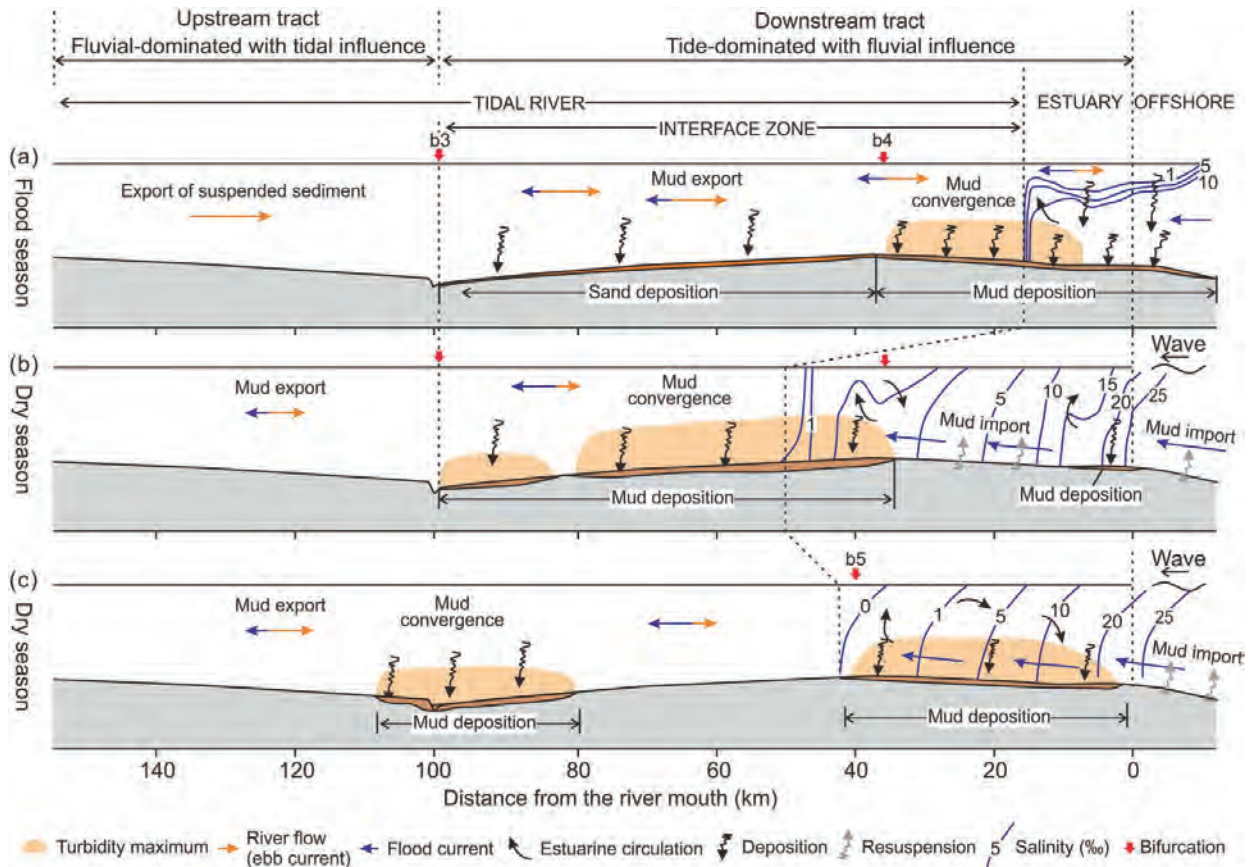


Fig. 9. Conceptual model of depositional processes in the Mekong–Co Chien–Cung Hau River during (a) the flood season and (b) the dry season and (c) in the Bassac–Dinh An River during the dry season. Mud convergence occurred in the interface zone between the tidal river and estuary and in the saltwater wedge as suggested by previous studies in the Mekong–Co Chien–Cung Hau River during both the flood (a) and dry (b) seasons (Wolanski et al., 1996; McLachlan et al., 2017). In contrast, two mud convergence zones occurred in the Bassac–Dinh An River during the dry season: one in the freshwater region and the other in the saltwater wedge (c).

Numerical simulation of mid-Holocene tidal regime and storm-tide inundation in the south Yangtze coastal plain, East China

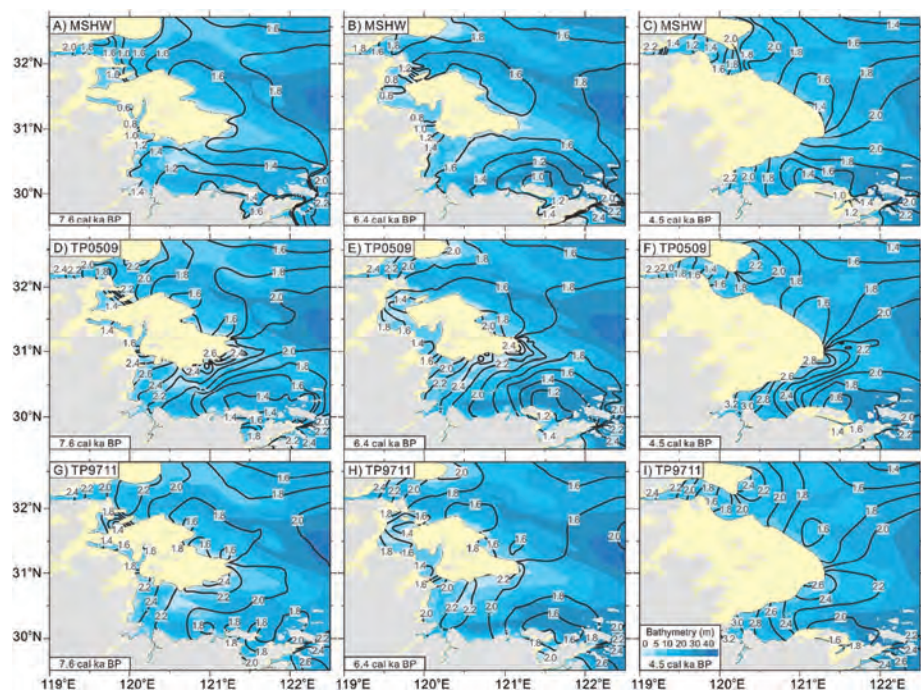
Wang, Shuo; Ge, Jianzhong; Kilbourne, K. Halimeda; Wang, Zhanghua. *Marine Geology*, 2020, 423: 106134.

Coastal flooding is reported as one of the major causes for the interruptions of Neolithic cultures inhabiting the south Yangtze coastal plain, China during the middle Holocene. The archaeologically sterile transgressive sedimentary layers could be the results of extreme events or relative sea-level rise induced by the enlargement of the local tidal range or global/regional sea-level rise. To clarify the mechanism of the transgressive deposits at typical Neolithic

sites and the termination of Neolithic Liangzhu Culture in the south Yangtze coastal plain, this study reconstructed the paleo-topography at 7.6, 6.4 and 4.5 cal ka BP on the basis of a database including 107 sediment cores and 644 radiocarbon ages and simulated the paleo-tidal regimes and the inundation areas induced by typhoon events under the paleo-topography and sea levels using a hydrodynamic model of high-resolution Changjiang Estuary Finite-Volume Community Ocean Model (CE-FVCOM). The simulation results of tidal regimes showed that the tidal amplitude increased from 1.6 m to 2.2 m in the head of Hangzhou Bay induced by the paleo-topographic change during the period 7.6–4.5 cal ka BP. By contrast, it reduced from 1.6 m to 1.0–1.2 m in the Ningbo Plain, southeast of the bay, which was unable to explain the long-lasting marine inundation there and supported our previous assumption of an event of abrupt sea-level rise at 4.5–4.4 cal ka BP. Simulation of the storm-induced inundation further suggested that coastal flooding mainly occurred along the coastline of the Taihu Plain under the combined effect of tidal amplification and typhoon events at 4.5 cal ka BP, while the inundation almost covered half of the Taihu Plain if all factors including tidal amplification, extreme event and the abrupt sea-level rise were considered. We therefore suggest that the obvious increase in flood risk under the backdrop of sea-level rise was a major cause for the abandonment of the Liangzhu Culture in the south Yangtze coastal plain at around 4.4 cal ka BP.

杭州湾沿海低地在新石器期间遭受多次海水入侵，甄别这些海侵事件的原因、即相对海平面上升、潮差放大还是极端风暴事件，对于重建海平面曲线和极端风暴事件时间序列都很重要。本研究利用大量的钻孔数据库，重建长江口-杭州湾7.6, 6.4和4.5 ka古地形，并利用CE-FVCOM对该区上述三个时间节点的天文潮进行数值模拟，揭示平均大潮高潮位随古地形的变化，同时选择了过去数十年气象记录中的两个极端风暴事件，进行上述三个时间节点的风暴潮增水和淹没模拟。模拟结果显示，随着古太湖湾的充填，杭州湾喇叭形的几何形状基本形成，湾内潮差因此增多，湾顶的平均大潮高潮位增加尤其明显。但在古宁波湾内，随着充填作用的发生，潮差随时间而减小，因此无法用来解释该区域良渚文化结束后长达近千年的海水入侵事件。风暴潮情景模拟进一步显示，只有类似9711的超强台风才能淹没鱼山遗址。另外，如果在良渚文化末期叠加海平面上升情景，则太湖平原和宁波平原在极端风暴发生时淹没范围显著增加，海侵大范围发生。

Fig. 6. Spatial distributions of MSHW at 7.6 (A), 6.4 (B), and 4.5 cal ka BP (C), peak water elevations at 7.6 (D), 6.4 (E), and 4.5 cal ka BP (F) in the scenario TC0509 and peak water elevations at 7.6 (G), 6.4 (H), and 4.5 cal ka BP (I) in the scenario TC9711. Numbers in A–C denote the highest tide levels in the one-month tide simulation, representing the mean spring high water (MSHW). Numbers in D–I denote the highest water levels in the storm-tide simulation under two typhoon scenarios.



Analysis of the Use of Geomorphic Elements Mapping to Characterize Subaqueous Bedforms Using Multibeam Bathymetric Data in River System

Yan, Ge; Cheng, Heqin; Teng, LiZhi; Xu, Wei; Jiang, Yuehua; Yang, Guoqiang; Zhou, Quanping. *Applied Sciences*, 2020, 10: 7692.

Riverbed micro-topographical features, such as crest and trough, flat bed, and scour pit, indicate the evolution of fluvial geomorphology, and have an influence on the stability of underwater structures and overall scour pits. Previous studies on bedform feature extraction have focused mainly on the rhythmic bed surface morphology and have extracted crest and trough, while flat bed and scour pit have been ignored. In this study, to extend the feature description of riverbeds, geomorphic elements mapping was used by employing three geomorphic element classification methods: Wood's criteria, a self-organization map (SOM) technique, and geomorphons. The results showed that geomorphic element mapping can be controlled by adjusting the slope tolerance and curvature tolerance of Wood's criteria, using the map unit number and combination of the SOM technique and the flatness of geomorphons. Relatively flat bed can be presented using "plane", "flat planar", and "flat" elements, while scour pit can be presented using a "pit" element. A comparison of the difference between parameter settings for landforms and bedforms showed that SOM using 8 or 10 map units is applicable for land and underwater surface and is thus preferentially recommended for use. Furthermore, the use of geomorphons is recommended as the optimal method for characterizing bedform features because it provides a simple element map in the absence of area loss.

河床微地貌特征，如顶槽、平床、冲坑等，反映了河流地貌的演变，对水下构筑物和整体冲刷坑的稳定性有影响。以往对河床形态特征提取的研究主要集中在有韵律的床面形态上，提取了河床的波峰和波谷，而忽略了平床和冲刷坑。在这项研究中，为了扩展河床的特征描述，采用了三种地貌要素分类方法：Wood准则、自组织地图（SOM）技术和地貌。结果表明，通过调整Wood准则中的坡度公差和曲率公差，利用SOM技术和地貌平坦度相结合，可以控制地貌要素的制图。相对平坦的河床可以用“平面”、“平面”和“平面”单元表示，而冲刷坑可以用“坑”单元表示。比较地形和河床形态参数设置的差异，发现使用8或10个地图单元的SOM适用于陆地和水下表面，因此优先推荐使用。此外，地貌被推荐为描述河床特征的最佳方法，因为它在没有面积损失的情况下提供了一个简单的元素图

Sedimentary zonation shift of tidal flats in a meso-tidal estuary

Wei, Wen; Dai, Zhijun; Pang, Wenhong; Wang, Jie; Gao, Shu. *Sedimentary Geology*, 2020, 407: 105749.

Understanding the spatial-temporal pattern of sedimentary dynamics on tidal flats is important for examining their ecological function and evolutionary trend. In this study, the dynamic state of sediments across an open-coast tidal flat of the meso-tidal Changjiang Estuary, China, on a monthly scale from December 2014 to June 2016 was examined, based on a high-spatial-resolution sedimentological-topographic survey and a collection of related meteorological-hydrological data. The results revealed a continuously distinct zonation of sediments, which transformed seaward from sand-dominance to silt dominance over a short distance. A zoning, to divide the tidal flat into a sand zone, a mixture zone and a silt zone, was delimited based on the cluster analysis of grain size frequency distributions. The zonation was highly dynamic, with the mixture zone migrating upward during summer and experiencing an uplift of 1 m in its lower boundary over the time period examined. Within each zone, the medium size and sorting coefficient of sediments tended to be smaller in winter than those in summer. Alterations of the mean tidal level likely controlled the zonation shift and sediment variations. A higher mean tidal level indicated a landward shift of the location exhibiting shear stress maxima and the mixture zone had to migrate upward to maintain an appropriate stress for the

development of mixed sediments. The impacts of waves were masked under normal conditions, but during storms strong waves dominated an embedded down-ward displacement of the mixture zone. Characteristics of sediments covering a large region of the tidal flat changed along with zonation shifts, resulting from altered proportions among sandy, mixed and silty sediments. The study highlights that sedimentary zonation shift, under the impacts of seasonal variations in tidal level, can be a major manifestation of tidal flat sedimentary dynamics.

弄清潮滩沉积物的时空变化对于诊断潮滩生态服务功能、预测潮滩发展演化趋势均具有重要的指示意义。本研究以2014.12-2016.6高密度沉积物现场调研、高精度潮滩地形监测与配套

气象水文资料为基础，对中等潮差、开敞环境的长江口南汇南滩沉积物空间分布模式及其月际动态进行系统解析。结果表明，所研究潮滩在横向上始终呈现泾渭分明的空间分异特征，沉积物自陆向海依次为砂质、砂-粉砂混合质和粉砂质。随后，我们对沉积物粒径频率数据进行聚类分析，精准划定了三种类型沉积物聚集区（砂区、混合区和粉砂区）的分带边界。最终发现，潮滩的沉积分带高度动荡，在夏季倾向于向高滩爬升；各分带内，沉积物在夏季粒径更细、分选更差。引入风、浪、流的沉积动力学分析指示，这些变化主要受控于河口平均潮位的升降。这是因为，较高的平均潮位预示着滩面切应力峰值位置的向岸和向高迁移，混合带为维持适宜发育砂-粉砂混合质沉积物的切应力区间必须向上爬升。在这一过程中，大片沉积物均经历分带归属及相应的砂、粉砂组分配比调整，最终体现出中值粒径和分选系数的变化。这一研究强调，季节性潮位升降诱发的潮滩沉积分带移动，可以是潮滩沉积物时空动态的主要表现形式。

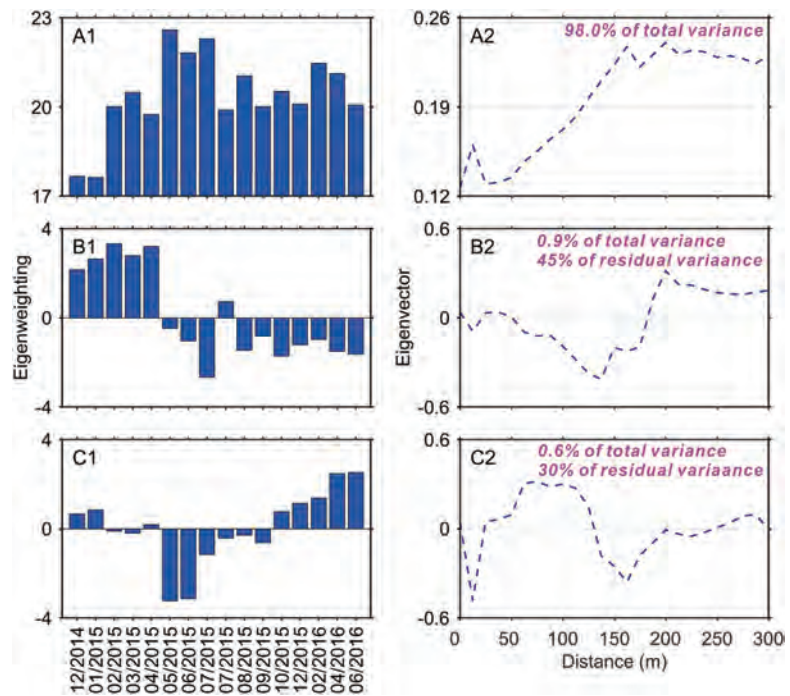


Fig. 6. EOF analysis on D50 of the cross-shore sediments between 2014 and 2016: (A1-2) the first eigenweighting and eigenvector; and (B1-2) and (C1-2) the second and third eigenmodes.

Tropical cyclones significantly alleviate mega-deltaic erosion induced by high riverine flow

Wang, Jie; Dai, Zhijun; Mei, Xuefei; Fagherazzi, Sergio. *Geophysical Research Letters*, 2020, 47(19): e2020GL089065.

The drastic decline in sediment discharge experienced by large rivers in recent years might trigger erosion thus increasing the vulnerability of their extensive deltas. However, scarce information is available on the erosion patterns in mega-deltas and associated physical drivers. Here a series of bathymetries in the South Passage, Changjiang Delta, were analyzed to identify morphodynamic variations during high riverine flow and tropical cyclones (TCs). Results indicate that high river flow during flood season triggers large-scale net erosion along the inner estuary, generating elongated erosion-deposition patches. Erosion magnitude gradually weakens moving seaward with few localized bottom variations in the offshore area. TCs transport sediment landward and are accompanied by an overall weak erosion, with a less organized spatial pattern of erosion-deposition. TCs can therefore significantly alleviate erosion, reducing the

sediment loss induced by riverine flows by over 50%. These results highlight the role of TCs on the sediment dynamics of mega-deltas.

近年来全球大河入海泥沙通量的急剧降低引起冲积地貌的侵蚀，从而增加三角洲的脆弱性。然而当前对于理解巨型三角洲的侵蚀模式及其驱动机制较为缺乏。本研究通过量化长江三角洲南槽地形的时空变化特征，来揭示长江洪季高径流和台风对其动力地貌过程和泥沙输运格局的差异影响。发现长江高径流造成南槽拦门沙口内泥沙大规模净侵蚀，诱发形成细长型带状地貌变化斑块，同时侵蚀量级向海逐渐转弱。而台风过程能够将海源沉积物的向陆输量增强，使得洪季南槽净侵蚀量降低，对应侵蚀-淤积的地貌斑块呈分散且无序状。结合历史时期长江三角洲地貌发育趋势及对台风的响应规律，研究甄别出台风可显著缓解洪季高径流引致三角洲侵蚀的地貌效应，对比发现其携带淤积的泥沙量可达洪水净侵蚀量的50%以上。面对极端水文事件增加和海平面上升等多重压力，凸显台风对巨型三角洲动力沉积和泥沙平衡关键作用的系统研究应当加深，特别是陆源供给泥沙锐减的三角洲生态地貌系统。

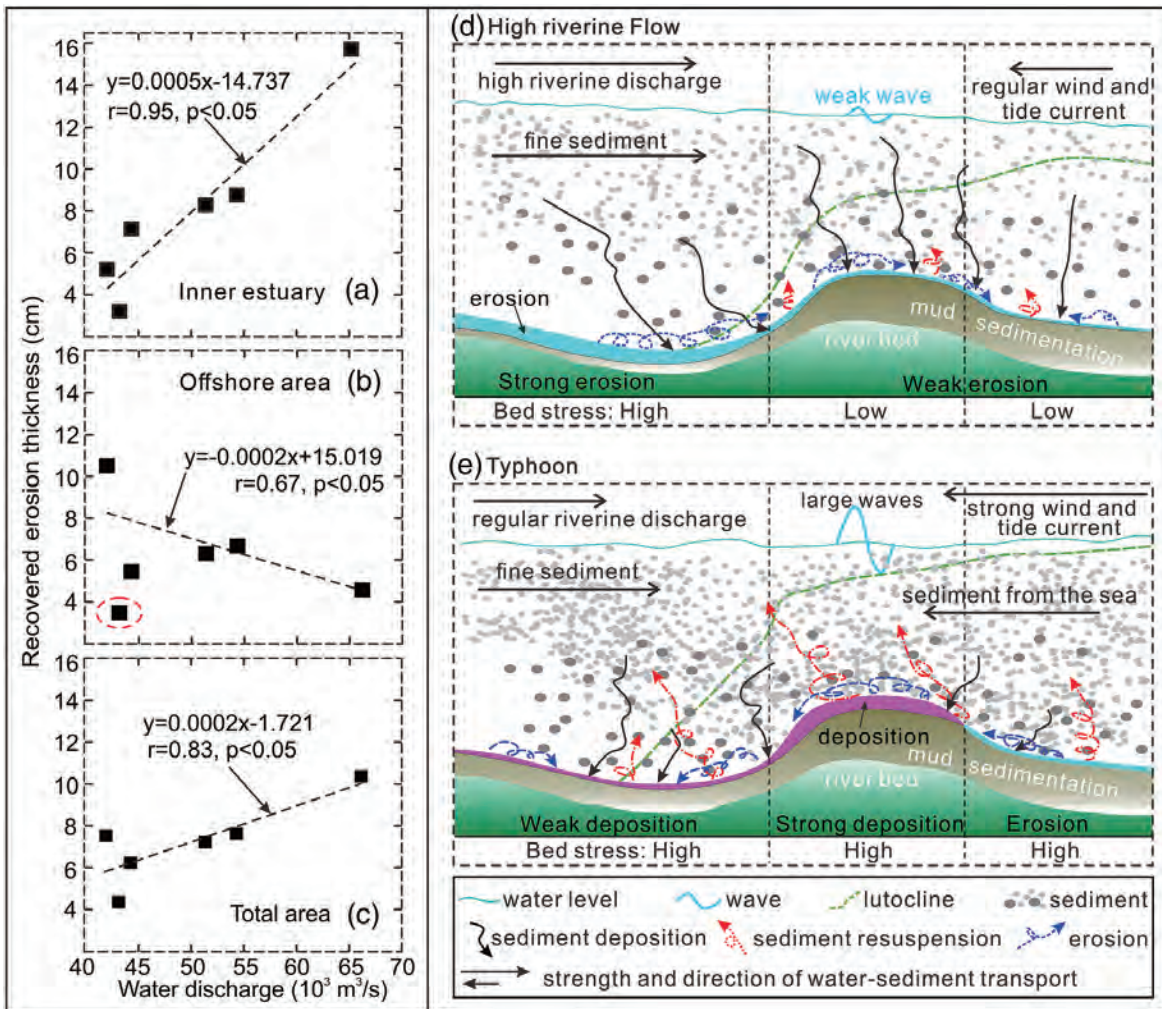


Figure 4. Relationship between annual recovered erosion thickness and average value of the top 30 river water discharges in each year: (a) inner estuary, (b) offshore area (value in red ellipse was excluded), and (c) entire SP. Conceptual model showing the hydrodynamics, sediment dynamics, and bathymetric changes in the inner estuary and offshore area induced by (d) high riverine flow and (e) typhoon.

The multi-decadal morphodynamic changes of the mouth bar in a mixed fluvial-tidal estuarine channel

Zhou, Xiaoyan; Dai, Zhijun; Mei, Xuefei. *Marine Geology*, 2020, 429: 106311.

Inner-channel mouth bars (IMB) are common and vital geomorphological structures in estuaries that can efficiently promote the progradation of a fluvial delta. However, these significant structures face serious interferences by natural and human forces. This study mainly focuses on IMB deposited in the mixed fluvial-tidal dominated South Passage (SP) of the Changjiang Estuary between 1959 and 2018 to reveal how multidecadal morphodynamic variability in a mouth bar responds to natural forcing and human interferences. The results show that the volume of the IMB in the SP increased from $1128 \times 10^6 \text{ m}^3$ in 1959 to $1636 \times 10^6 \text{ m}^3$ in 1989 and then decreased to $462 \times 10^6 \text{ m}^3$ in 2018. Meanwhile, the evolution of the IMB could be divided into five stages, the growing phase (1959 to 1979), which showed a 'V' shape, the partial adjustment phase (1999–2003), which showed a 'crest-dent' shape, the stable phase, which showed a flat shape (2004–2010), the partial adjustment phase (2011–2017), when Jiangyanan Shola inserted into the SP, and finally evolved into a flat shape in 2018. Fluvial water discharge and suspended sediment discharge (SSD) did not control the variation in the mouth bar. ENSO events were normally responsible for not only the periodic variations in the landward slope and the water depth of the crest of the IMB but also occasional extreme changes in the IMB. Moreover, local sandbar insertion, sediment from the seaside induced by strong tidal power and intensified engineering projects resulted in the continual shrinkage of the mouth bar by depositing more sediment at the mouth bar. Our work implies that understanding and governing this IMB will bring additional economic benefits to this fast-developing society, but the protection of this delicate estuarine geomorphology system should still receive great attention.

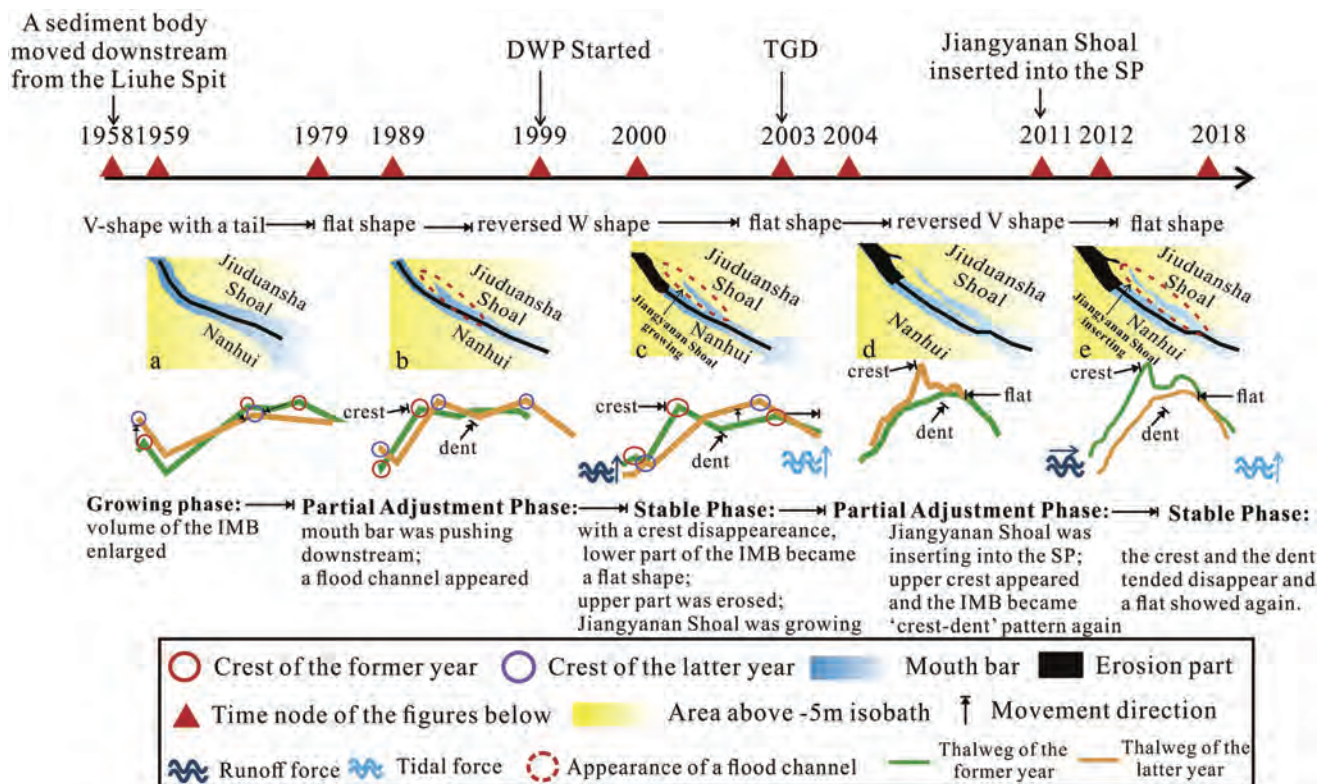


Fig. 13. Conceptual model of evolution of the IMB, when inner mouth bar was at the period of (a) 1959–1979: growing phase; (b) Partial adjustment phase: 1989–1999; (c) Stable phase: 2000–2003; (d) Partial adjustment phase: 2004–2011 and (e) stable phase: 2012–2018.

槽内拦门沙是河口地区常见且至关重要的地貌结构，它可以有效地促进河流三角洲的淤积。然而，这一关键的地貌结构单元现在却面临这来自自然与人类作用的双重胁迫。本研究主要聚焦于槽内拦门沙在1959-2018年间在潮控与河控混合型河口——长江口南槽沉积过程，揭示拦门沙多年尺度地貌变化对于自然与人类干预活动的响应过程。结果表明南槽拦门沙的体积自1959-1989年间，由 $1128 \times 10^6 \text{m}^3$ 增加至 $1636 \times 10^6 \text{m}^3$ ，至2018年，下降至 $462 \times 10^6 \text{m}^3$ 。同时，拦门沙整体的演化过程可分为五个阶段，分别是成长期（1959-1979年），表现出V型；局部调整期（1999-2003年），表现为“尖端-凹陷”型；稳定期，表现出平台型（2004-2010年）；当江亚南沙进入到南槽区域时，表现为局部调整期（2011-2017年间）、并且在2018年最终演化为平台型的稳定期。径流量与悬沙通量并未控制拦门沙的演化。ENSO事件通常影响拦门沙陆测角度与滩顶水深的周期性变化，并造成拦门沙形态的某些突变。更进一步的是，局部沙坝的侵入，逐渐增强的潮流动力所导致海侧方向增多的沉积物运输以及密集的河口局部工程，最终导致河口拦门沙的挤压。我们的研究结果表明在这个飞速发展的社会，了解并且治理槽内拦门沙将会带来额外的经济价值，但是如何保护这一脆弱的地貌结构单元同时需要获得更多的关注。

Effects of river discharge and tidal meandering on morphological changes

Wang, Xianye; Sun, Jianwei; Zhao, Zhonghao. *Estuarine, Coastal and Shelf Science*, 2020, 234: 106635.

A tidal creek represents a typical morphologic unit in an intertidal flat. The development and migration of a tidal creek can affect the mass transport, ecological environment, and geomorphologic evolution of the flat. By using field observations, this study links hydrodynamics, sediment transport processes with short-term changes in topography at a typical tidal creek system located at the Chongming Island of the Yangtze River estuary. Hydrodynamic and sediment transport associated with varying tidal cycles across both wet (flood) and dry seasons were measured through the field campaign. The wet and dry seasons represent higher and lower discharges of Yangtze River, respectively. The results indicated that most of the suspended sediment becomes entrained at the beginning of a flood tide. At a fixed point, 7.2 times of suspended sediments, which were entrained out of the creek in wet season, began to be transported along the creek compared to dry season. In the dry season, high flow velocity and shear stress conditions occurred in the tidal creek because the water level was below the top of the flat. In summary, the tidal creeks were found to serve as effective conduits for the transportation of sediments in the wet season, and the secondary flow enhanced the development of tidal meandering. Seasonal variations in creek morphological changes were also continuously monitored over two years at intervals of two months. The change of creek morphology varied from the high level to low level, and tidal meandering was strongly associated with flood and ebb tides.

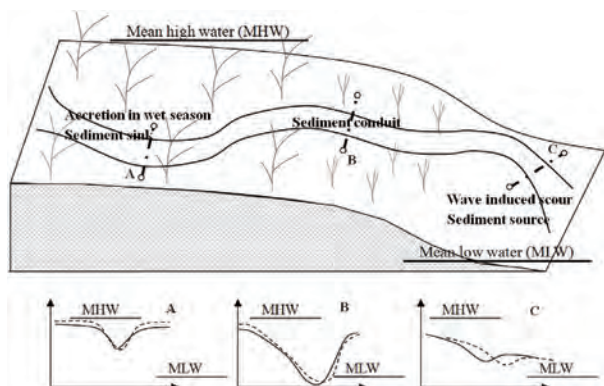


Fig. 1. The patterns of different sections of the tidal creek.



Fig. 11. The flow and sediment movement couple with the tidal meandering.

潮间带潮沟是典型的潮间带地貌单元。潮沟的发育和迁移会影响潮滩的物质运输、生态环境和地貌演化。本研究以长江口崇明岛典型潮沟系统为研究对象，通过野外观测，将水动力、泥沙输移过程与地形短期变化联系起来。通过野外实地观测，测量了在洪季和枯季不同潮周期下的水动力和泥沙输运。结果表明，大部分悬移质泥沙在涨潮初期被挟带。与枯季相比，在某一固定点，洪季从潮沟中向海运输的悬浮泥沙是枯季的7.2倍。枯季，由于大部分时期水位低于潮滩表面，潮沟出现了高流速和高剪切力条件，但是悬沙浓度反而偏低。综上所述，潮沟是雨季泥沙输移的有效通道，局部的潮沟弯曲形成的二次流促进了潮沟曲流的发展。两年监测期内，每隔两个月对潮滩的地貌季节变化进行了连续监测，地貌形态由高潮滩到低潮滩变化的演变机制不尽相同，潮沟的蜿蜒发育与涨潮、落潮密切相关。

Strong inland propagation of low-frequency long waves in river estuaries

Guo, Leicheng; Zhu, Chunyan; Wu, Xuefeng; Wan, Yuanyang; David, A. Jay; Ian, Townend; Wang, Zheng Bing; He, Qing. *Geophysical Research Letters*, 2020, 47: e2020GL089112.

Tidal waves traveling into estuaries are modified by channel geometry and river flow. The damping effect of river flow on incident astronomical tides is well documented, whereas its impact on low-frequency tides like MSf and Mm is poorly understood. In this contribution, we employ a numerical model to explore low-frequency tidal behavior under varying river flow. MSf and Mm are locally generated by frictional mechanisms inside an estuary, and they are larger in amplitude far upstream in tidal rivers and persist landward of the point of tidal extinction. Increasing river flow nonlinearly modulates the longitudinal variations of MSf and Mm amplitudes. This is dynamically explained by flow-enhanced asymmetry in subtidal friction over the spring-neap (MSf) and perigee-apogee (Mm) cycles, respectively. Estuaries act as frequency filters, where low-frequency waves decay at a smaller rate and propagate more inland than high-frequency waves. Strong inland penetration of low-frequency tides informs compound flood management.

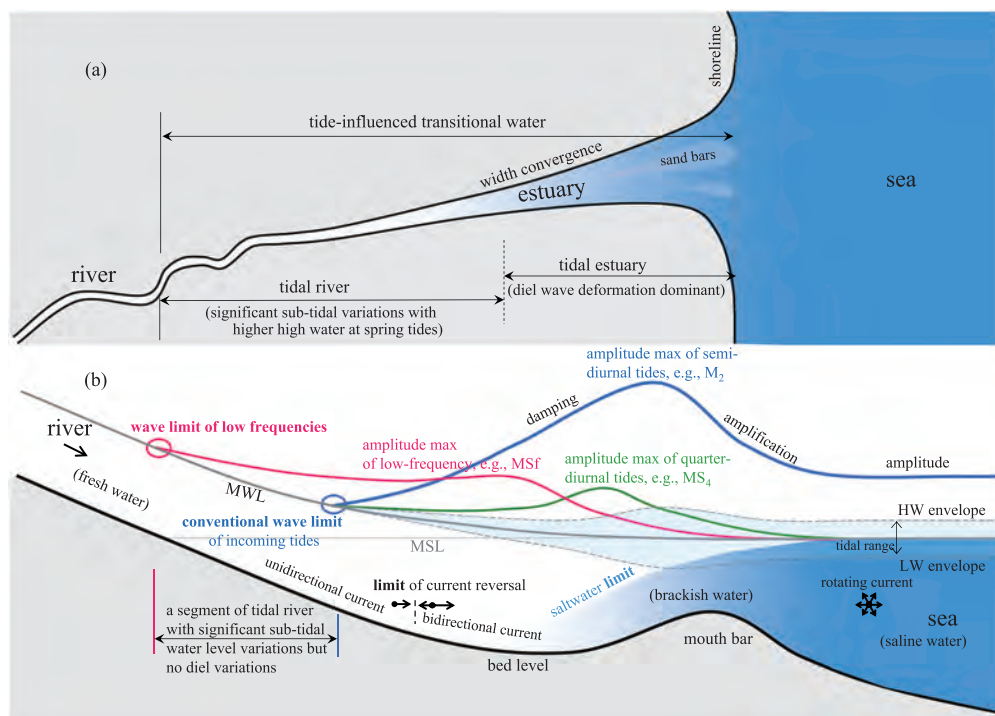


Figure 4. Sketches showing the river-to-ocean transition water in terms of tidal wave properties: (a) the planform and (b) the along-river side view. MSL and MWL indicate mean sea level and mean water level, respectively. HW and LW indicate high water and low water, respectively. The amplitude variations in panel (b) are conceptual and thus are not to the scale.

潮汐是河口水沙输移和地貌演变的关键动力之一。前人研究已经系统给出了海洋潮波进入河口后发生的潮差和分潮振幅等变化特征，给出了地形和径流的影响。然而已有研究主要关注天文分潮，对河口内部产生的更高或更低频率的浅水分潮的研究不足。本研究以长江河口为例，结合实测数据和潮汐河口模型，分析给出了低频浅水分潮在河口的变化特征及随径流大小变化的响应规律。认识到半月周期的MSf分潮在河口上游振幅显著，并导致大潮期间的平均水位显著高于小潮，且这种变化会收到径流增加而收到强化，表明径流和潮汐相互作用的影响。通过模型实验分析表明，大小潮期间的平均阻力的差异是导致这一半月周期分潮信号的关键。大潮期间水流强，阻力大，导致需要更大的沿程方向的水位坡度来输水入海。这一研究成果有助于进一步认识河口特高潮位的控制因素，服务相关的防洪减灾管理。

Organic geochemical variations for understanding past sediment dynamic processes: example from Holocene sedimentary records in the Changjiang River delta, China

Pan, Dadong; Wang, Zhanghua; Zhan, Qing; Saito, Yoshiki; Wu, Hui; Yang, Shouye; Cheng, Heqin. *Continental Shelf Research*, 2020, 204: 104189.

Estuarine fronts are the boundaries between different water masses at river mouths and play important roles in trapping suspended particles. Investigating the response of estuarine fronts to climate and sea-level changes during the Holocene could elucidate the evolution of complex hydro- and sediment-dynamic processes at river mouths. To assess the estuarine frontal dynamics of the Changjiang (Yangtze) River mouth, we examined organic geochemical proxies in surficial sediments to investigate the spatial distribution of terrestrial- and marine- sourced organic carbon in recent decades. To explore the Holocene migration of estuarine fronts, we analysed organic carbon compositions in seven age-constrained sediment cores collected across the onshore and offshore delta. The suspended sediment front was identified as a major boundary for trapping terrestrial organic carbon, and the landward limit of the salt wedge was found to constrain the landward spread of marine-sourced organic carbon. The temporal and spatial distribution of organic carbon compositions in the sediment cores indicated a rapid landward retreat of the estuarine fronts between ~10.0 and 6.0 ka (cal. kyr BP) in response to sea-level rise; this coincided with the retreat of the entire river mouth system. Despite significant deltaic progradation, the estuarine fronts slowly migrated seaward after ~6.0 ka in response to a weakened summer monsoon and a resultant decline in freshwater discharge or the lateral spreading of the delta. Accelerated deltaic progradation induced by both intensified human impacts and infilling of the palaeo-incised Changjiang valley resulted in the accelerated seaward migration of the estuarine fronts over the past ~1500 years. This interdisciplinary study strengthens our understanding of the links between hydro-sediment dynamic processes and sedimentary records to further elucidate the complex systemic behaviour at tide-dominated river mouths.

河口的锋面对于物质的输移、生态环境等十分重要。目前对河口锋的研究多集中在现代过程，揭示全新世河口锋对过去气候-海平面变化的响应，将十分有助于促进多学科交叉，比如恢复地质历史时期的河口水文、动力环境。本研究以长江三角洲为例，将表层沉积物有机碳来源与河口水团分布和锋面的关系应用到全新世地层，以探讨全新世河口主要界面的迁移特征，并分析其与气候波动、海平面变化的关系。研究揭示，长江口枯季盐水入侵头部以上的河口段，表层沉积物有机碳以陆源输入占绝对优势，悬沙锋向海一侧的羽状流区域，表层沉积物中的有机碳以海洋藻类为绝对优势，这两个界面之间的最大浑浊带区域，有机碳既有陆源也有海源贡献。本研究继续分析了7个钻孔泥质地层的有机碳来源，并据此推测盐水入侵界面和悬沙锋在全新世的演变过程，结果显示，在10-6 ka期间，各个主要界面都快速向陆移动，反映了对海平面上升的响应。自6 ka以来，虽然三角洲开始向海进积，但河口锋面向海的移动速度非常缓慢，推测和季风衰退导致的入海径流量减小以及河口的

侧向迁移有关。直到最近1500年以来，随着流域人类活动加剧和长江口的快速充填，河口锋面向海迁移的速率才明显加快。

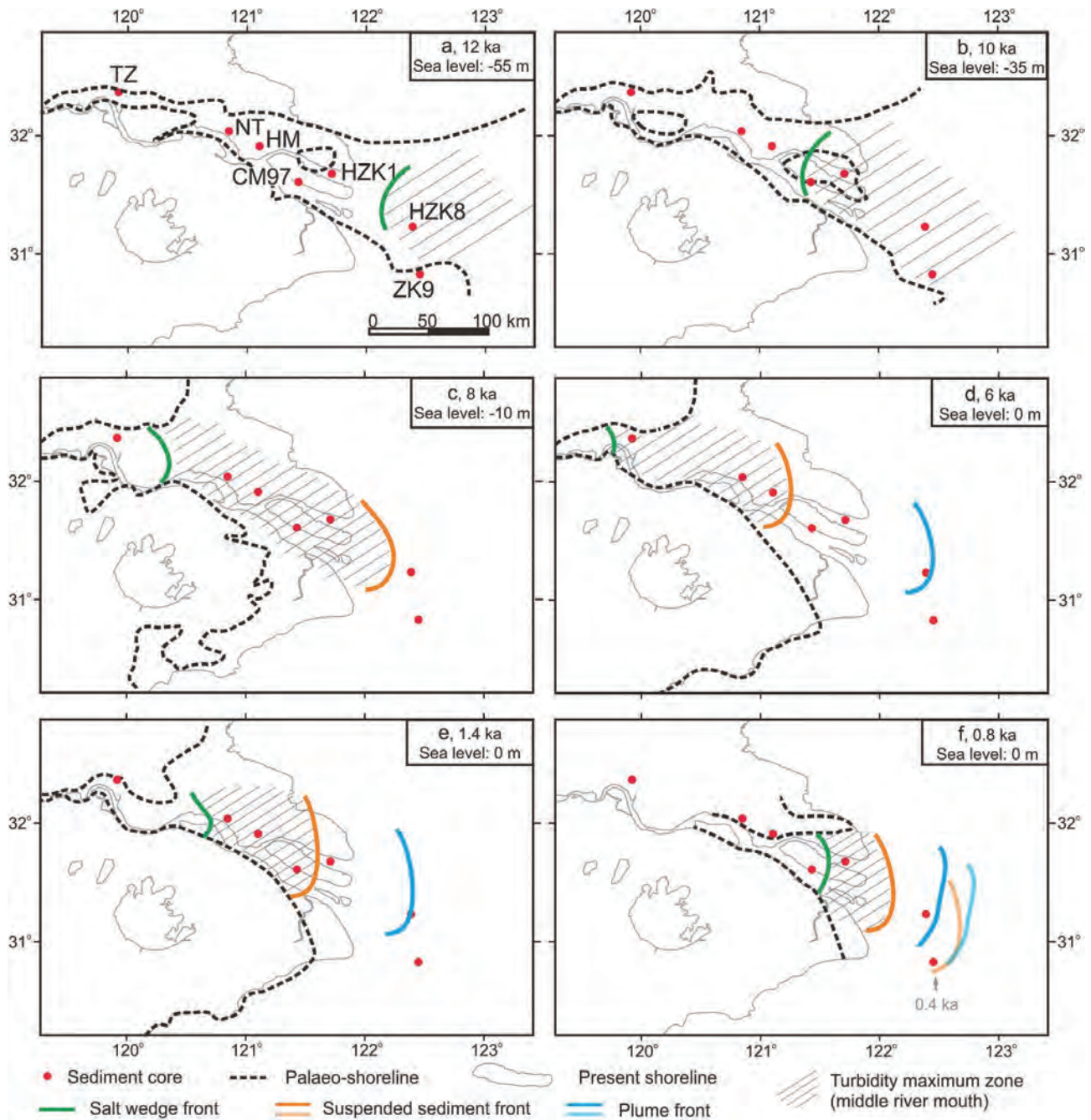


Fig. 8. Holocene evolution of the estuarine fronts and turbidity maximum zone at the Changjiang River mouth. The palaeo-shoreline was drawn from Wang et al. (2018) and Chen et al. (1988).

Mid-Holocene environmental change and human response at the Neolithic Wuguishan site in the Ningbo coastal lowland of East China

Huang, Jing; Lei, Shao; Wang, Aihua; Tang, Lliang; Wang, Zhanghua. *Holocene*, 2020, 30(II): 1591-1605.

Coastal wetlands provided a favorable settling site for Neolithic people because of their highly exploitable biomass, but were vulnerable to marine hazards such as coastal flooding. The Chinese Hemudu culture persisted for ~2000 years (7200–5300 cal. year BP) in the Ningbo coastal lowland of East China. This study explores the Hemudu people’s survival strategy using sedimentological and chronological records, and organic and acetic-acid-leachable alkaline-earth (Ca, Sr, and Ba) chemistry on a well-dated profile from the coastal Wuguishan site in the Ningbo Plain. Analyses of alkaline-earth elements in surficial sediments collected from present-day alluvial plain, tidal river, and saltmarsh/tidal flat environments in the Ningbo Plain were also undertaken to explain sedimentary environmental changes and their linkage to Hemudu activity at the Wuguishan site. Results indicate high sediment acetic-acid-leachable Ca and Sr contents with high Sr/Ba ratios, and high sediment total inorganic carbon contents at the site during 6300–6000 cal. year BP, which coincided with a marine incursion at the nearby Neolithic Yushan site. However, the increasing sediment total organic carbon contents and decreasing $\delta^{13}C$ values suggest that the Wuguishan site evolved from an upper tidal flat to a saltmarsh environment, attracting settlement by the prehistoric Hemudu people after ~6200 cal. year BP. Sr and Ca contents and Sr/Ba ratios decreased after ~6000 cal. year BP, indicating that the site developed into a low-salinity marsh in the supratidal environment after rapid accumulation caused by a storm event at ~6020 cal. year BP. Furthermore, the high Sr and Ba contents in the layers of Hemudu Culture Period III indicate the Hemudu people’s consumption of seafood and their adaption strategy for living in the vulnerable coastal wetland.

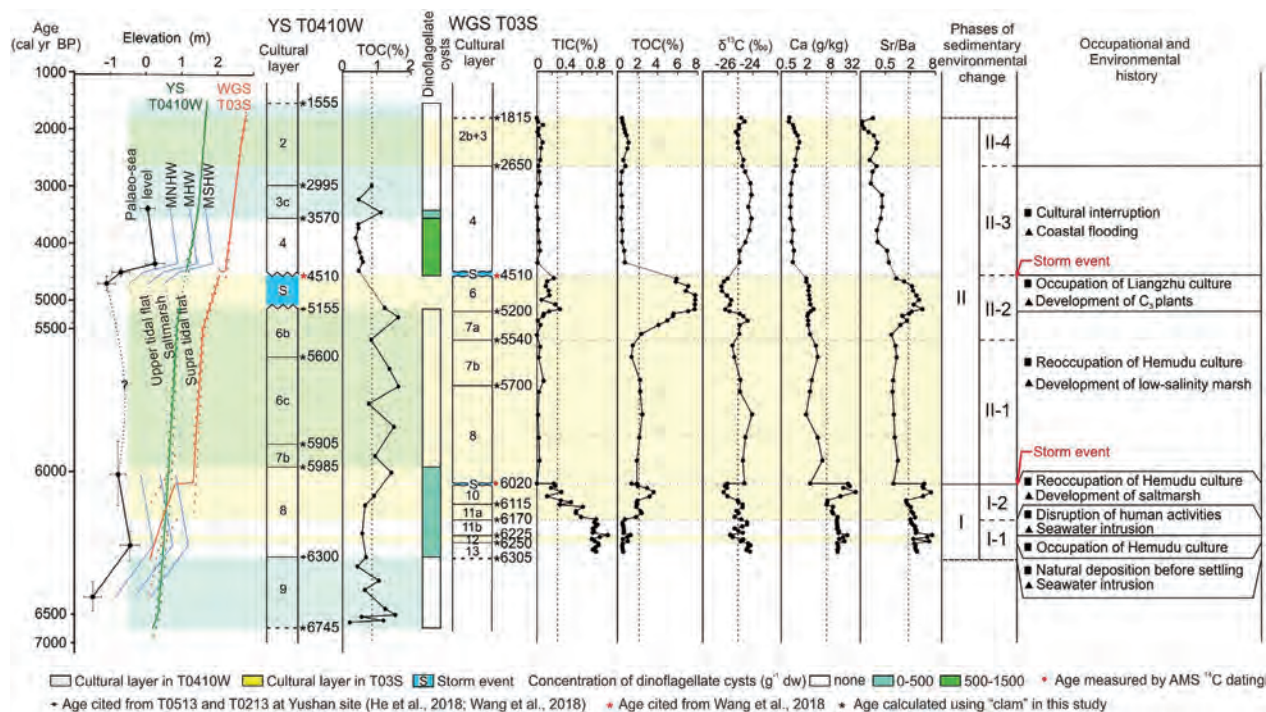


Figure 10. Temporal changes in proxies including TOC and abundance of marine dinoflagellate cysts at the Yushan site and TIC, TOC, $\delta^{13}C$, Ca, and Sr/Ba molar ratios in HAC leachates at the Wuguishan site. Also shown are: a comparison of age–depth curves of profile T03S at the Wuguishan (WGS) site and T0410W at the Yushan (YS) site with relative sea-level change in the study area (Wang et al., 2018); development of cultural layers at the two sites; environmental change stages at the Wuguishan site; an interpretation of the human–environment relationship. The tidal level curves, including MNHW (mean neap high water), MHW (mean high water), and MSHW (mean spring high water), are based on records from the nearby Zhenhai gauge station (Wang et al., 2018) and aid the interpretation of sedimentary environmental change.

河姆渡文化在宁波平原延续大约2000年，期间发生多次海水入侵。滨海低地的新石器古人如何快速响应和适应海水入侵，可以为海岸带地区应对当前的全球变暖形势提供重要科学依据。本研究在宁波平原北部乌龟山遗址获取一个地层剖面，对该剖面进行年代学、有机地球化学和碱土金属元素分析。研究显示，乌龟山遗址在距今6300-6000年间，海水入侵作用显著，但是在大约6200年前，随着盐沼的发育，古人就开始在此定居。遗址自距今约6000年前，在一次极端事件造成的快速堆积之后，成为潮上带环境，因此古人重新回归该遗址的时间早于邻近的鱼山遗址。另外，地层的碱土金属元素含量显示了河姆渡晚期食用海产品的证据，可能说明古人用调整食物结构来应对海水入侵。另外，河姆渡晚期文化层Ba含量的异常高值，可能说明古人对盐沼湿地的改造。

Role of delta-front erosion in sustaining salt marshes under sea-level rise and fluvial sediment decline

Yang, Shilun; Luo, Xiangxin; Temmerman, Stijn; Kirwan, Matthew; Bouma, Tjeerd; Xu, Kehui; Zhang, Saisai; Fan, Jiqing; Shi, Benwei; Yang, Haifei; Wang, Yaping; Shi, Xuefa; Gao, Shu. *Limnology and Oceanography*, 2020, 65 (9): 1990–2009.

Accelerating sea-level rise and decreasing riverine sediment supply are widely considered to lead to global losses of deltaic marshes and their valuable ecosystem services. However, little is known about the degree to which the related erosion of the seaward delta front can provide sediments to sustain salt marshes. Here, we present data from the mesomacrotidal Yangtze Delta demonstrating that marshes have continued to accrete vertically and laterally, despite rapid relative sea-level rise ($\sim 10 \text{ mm yr}^{-1}$) and a $> 70\%$ decrease in the Yangtze River sediment supply. Marsh progradation has decelerated at a lower rate than fluvial sediment reduction, suggesting an additional source of sediment. We find that under favorable conditions (e.g., a mesomacrotidal range, strong tidal flow, flood dominance, sedimentary settling lag/scour lag effects, and increasing high-tide level), delta-front erosion can actually supply sediment to marshes, thereby maintaining marsh accretion rates in balance with relative sea-level rise. Comparison of global deltas illustrates that the ability of sediment remobilization to sustain marshes depends on coastal processes and varies by more than an order of magnitude among the world's major deltas.

河口三角洲盐沼湿地是地球上综合生态服务功能最大的生态系统之一。然而，河口三角洲盐沼普遍面临海平面上升和河流来沙通量下降的双重风险：若没有足够的泥沙淤积抵消海平面上升淹没和海岸侵蚀，盐沼将在不久的将来消亡。三角洲及其盐沼湿地未来命运及应对策略研究受到国际学术界高度重视。已有研究很少针对河流入海泥沙通量下降后水下三角洲淤-蚀转型再悬浮向岸搬运泥沙对盐沼湿地淤积（以抵消海平面上升淹没）的“补沙功能”。本研究探讨：1) 水下三角洲淤-蚀转型能否为盐沼湿地提供丰富泥沙，以有效抵消海平面上升的影响？2) 不同三角洲之间的这种能力是否存在显著差异？关键因素是什么？

研究发现，长江和密西西比三角洲一样面临海平面快速上升和入海泥沙通量显著下降的背景，但两个三角洲出现了显著不同的命运：即长江水下三角洲出现大范围淤-蚀转变，而海岸盐沼则在继续淤涨；相比之下，密西西比水下三角洲为见淤-蚀转型报道，海岸湿地因海平面上升造成的淹没损失巨大。虽然长江三角洲海岸盐沼淤涨速率已随着河流入海泥沙通量显著下降，但前者的下降速率较后者低，反映有一个新的泥沙来源补给。

大量现场动力泥沙观测和计算表明，长江水下三角洲淤-蚀转型再悬浮的泥沙被部分搬运至盐沼，维持其淤积淤积，从而延缓盐沼衰亡。但是，随着海平面的进一步上升和三角洲前缘的持续蚀退，盐沼终将因蚀退（而非淹没）而消亡。盐沼衰亡的过程因水下三角洲和潮滩侵蚀提供的泥沙补给被推迟约100年。结论包括：1) 长江水下三角洲淤-蚀转型为盐沼湿地提供了丰富泥沙，从而使盐沼得以持续淤涨。为何长江三角洲出现淤-蚀转

型？从泥沙收支平衡角度解释：河流入海泥沙下降到远低于沿岸流从三角洲带走的泥沙通量，侵蚀必然发生。沉积动力学角度解释：中-强潮（半日潮）、风暴浪，流-浪联合剪切应力通常大于底床沉积物的临界侵蚀剪切应力，泥沙可再悬浮，高悬沙浓度；河流入海泥沙通量下降后，水下三角洲沉积通量小于侵蚀通量，发生净侵蚀。2) 密西西比三角洲盐沼泥沙补充不足，从而因淹没出现湿地损失。为何盐沼泥沙补充不足？答案是：弱潮环境（全日潮，潮差<0.5 m），流速小，虽偶受飓风、寒潮影响，但底床剪切应力通常很小，泥沙再悬浮困难，悬沙浓度低，泥沙向盐沼输运少。3) 不同三角洲之间动力环境差异显著，在海平面上升和河流入海泥沙通量下降背景下，水下三角洲淤-蚀转型为盐沼提供泥沙从而维持盐沼存在的能力存在数量级差异，应对策略应“因地制宜”。

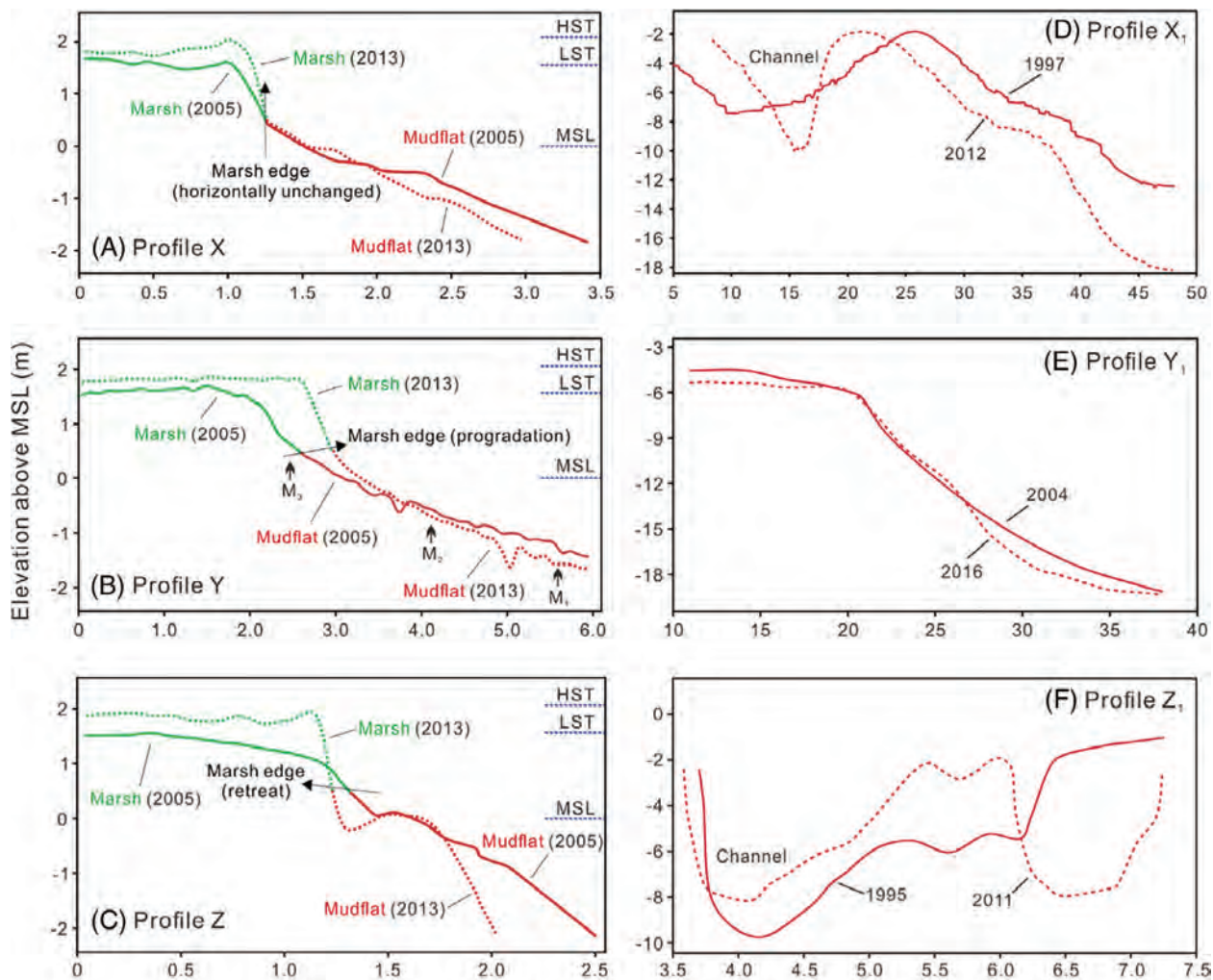


Fig. 3. Decadal changes in cross-shore elevation profiles in the Yangtze Delta. The locations of the transects are shown in Fig. 1B. (A–C) represent the intertidal wetland profiles (X, Y, and Z), whereas (D–F) represent the subaqueous delta profiles (X1, Y1, and Z1). Profiles X and X1 are located on the northeastern coast, Profiles Y and Y1 are located on the eastern coast, and Profiles Z and Z1 are located on the southeastern coast. The elevations are expressed relative to the lowest astronomical tide (LAT). HST, high spring tide; LST, low spring tide; MSL, mean sea level. Numbers within the panels represent calendar years. In each panel, the solid line represents the profile surveyed in an early stage, whereas the dotted line represents the profile surveyed in a recent stage. The green lines represent marshes, whereas the red lines represent unvegetated mudflats and subaqueous slopes.

Streamflow Decline in the Yellow River along with Socioeconomic Development: Past and Future

Yang, Shilun; Shi, Benwei; Fan, Jiqing; Luo, Xiangxin; Tian, Qing; Yang, Haifei; Chen, Shenliang; Zhang, Yingxin; Zhang, Saisai; Shi, Xuefa; Wang, Houjie. *Water*, 2020, 12: 823.

Human society and ecosystems worldwide are increasingly threatened by water shortages. Despite numerous studies of climatic impacts on water availability, little is known about the influences of socioeconomic development on streamflow and water sustainability. Here, we show that the streamflow from the Yellow River to the sea has decreased by more than 80% in total over the last 60 years due to increased water consumption by agricultural, industrial and urban developments (76% of the streamflow decrease, similarly hereinafter), decreased precipitation (13%), reservoir construction (6%) and revegetation (5%). We predict that if the past trends in streamflow will continue, year-round dry-up in the lower Yellow River will commence in the late 2020s or early 2030s, unless effective countermeasures such as water diversion from the Yangtze River are taken. These results suggest that streamflow in semiarid basins is highly vulnerable to human impacts and that streamflow decline would in turn hinder further socioeconomic development and endanger river-sea ecosystems.

对1957-2016年黄河干流唐乃亥、兰州、头道拐、龙门、潼关、花园口、利津（从源区依次向下游到达潮区界）7个测站的年径流量以及测站以上流域年降水量系列资料进行了趋势分析，发现：1）近60年7个测站径流量均呈下降趋势，越近河口，下降率越大。唐乃亥、兰州、头道拐、龙门、潼关、花园口、利津径流量变化百分比分别为-14%、-23%、-45%、-52%、-56%、-56%、-81%。2）近60年测站控制流域的降水量变化百分比分别为唐乃亥+2.6%、兰州+2.1%、头道拐-1.0%、龙门-3.3%、潼关-6.7%、花园口-7.0%、利津-7.1%，说明兰州以上流域降水量有所上升，而头道拐以下流域降水量有所下降，全流域降水量平均下降超过7%。3）在全流域尺度上，利津站径流量下降的原因76%归因于工农业和城市化发展引起的耗水增多，13%归因于降水量下降，6%归因于水土保持工程和植被重建工程，5%归因于新建水库引起的蓄水和水面蒸发。4）近60年黄河流

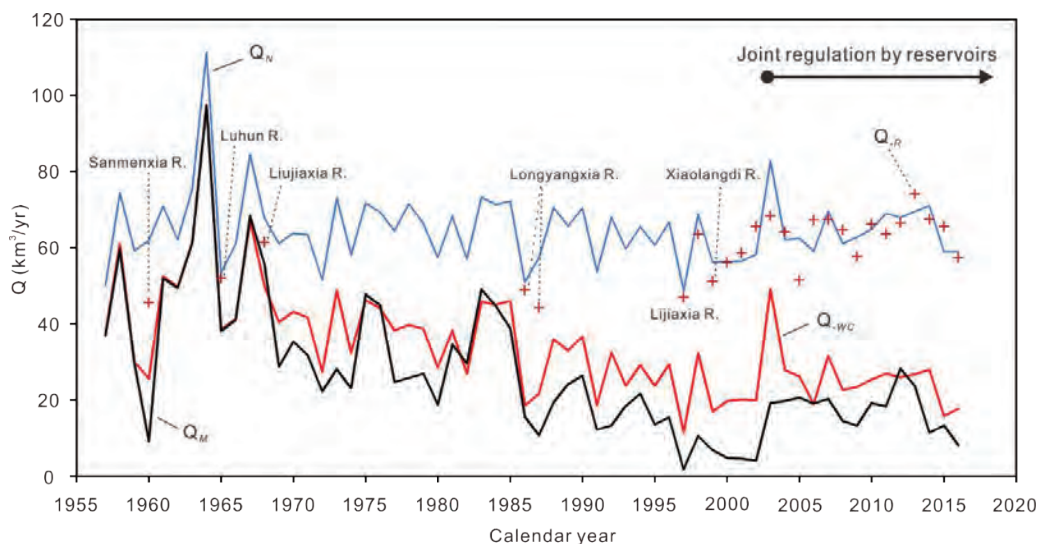


Figure 5. Human impacts on annual streamflow (Q) to the sea in the Yellow River. Q_N : Natural Q derived from precipitation (without human impact). Q_R : Q_N deduced by the impact of a reservoir or reservoirs. Q_{WC} : Q_N deduced by water consumption. Q_M : Streamflow measured at Lijin Station (with human impacts). The difference between Q_N and Q_M reflects the total impact of human activities. Sanmenxia R., Luhun R., Liujiaxia R., Longyangxia R., Liji Xia R. and Xiaolangdi R. indicate that the major reservoirs each reduced the streamflow by $>1 \text{ km}^3$ at the initial water impoundment. Detailed information on these reservoirs is shown in Figure 1A and Table A4.

域耗水量的增多与社会经济发展密切相关；农业灌溉是耗水的主要原因，多年平均占耗水的86%，但近20年工业和城市用水的比例曾增大趋势。黄河流域人类活动对径流量的影响并非始于近几十年，而是始于两千年前的引水灌溉。这种影响在时间跨度上总体上曾加速趋势：灌溉面积从两千年前开始时的近于0增加到16世纪中叶的10,000 km²左右，到1950s的14,000 km²，再到当前的50,000 km²左右。全流域耗水量在1950s初为10 km³左右，到目前达到约43 km³。尽管近60年黄河径流量的总体下降趋势主要归因于人类活动，但降水量变化是年际和数年期径流量波动的主要原因。上世纪末至本世纪初（1997-2002年）的数年期平均入海径流量极低值与同期的降水量极低值相吻合（图2G）。2003年以来的入海径流量（相对于1997-2002年）回升尽管与流域综合调度措施有一定关系，但其主要原因是降水量的回升。鉴于社会经济发展是黄河径流量长期下降趋势的控制性因素，同时鉴于今后几十年中国社会经济持续发展的预期，在三种降水量变化趋势的假设情景（即过去几十年的降水量下降趋势延续、降水量无升降趋势、降水量呈变化速率相同的上升趋势）下，假如不采取有效控制措施，预测利津站年入海径流量将呈继续下降趋势，并将于公元2028±2年左右开始出现枯竭。降水量的年际波动会左右这种枯竭：即年径流量枯竭的起始时间可能提前（枯水年），也可能延后（丰水年）；径流量枯竭先出现在干旱年，而后逐渐扩展到丰水年。

Distance Effect Correction on TLS Intensity Data Using Naturally Homogeneous Targets

Tan, Kai; Cheng, Xiaojun. *IEEE Geoscience and Remote Sensing Letters*, 2020, 17(3): 499-503.

The intensity data recorded by a terrestrial laser scanner (TLS) are significantly influenced by the distance between the scanned point and the scanner center. In this letter, we propose a new method to estimate the TLS distance–intensity relationship by using naturally homogeneous targets (NHT). Since the original intensity data of the NHT are simultaneously influenced by the incidence angle and distance, the incidence angle effect is first eliminated to obtain a corrected intensity that merely depends on distance. Then, the distance–intensity relationship is derived by analyzing the incidence angle corrected intensity data of the NHT. Results indicate that compared with existing methods the proposed method is accurate and easily implementable. The coefficient of variation for the intensity data can be reduced by 52% after correction by the proposed method.

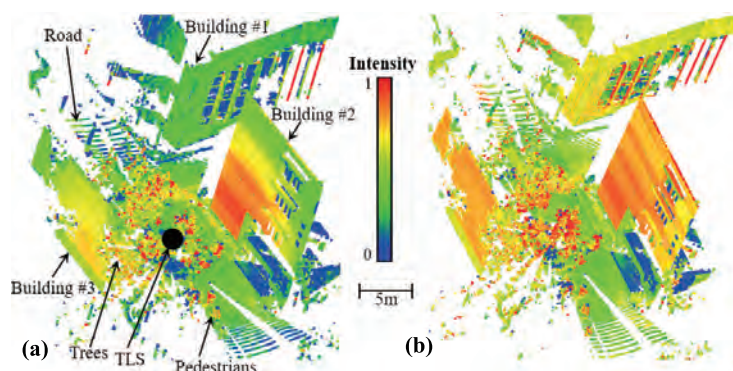


Fig. 7. Scene scanned by Faro Focus^{3D} 120. The total number of points is 453 584. (a) Point cloud colored by the incidence angle corrected data. The instrument was placed at the black solid circle. (b) Point cloud colored by the corrected intensity data of the proposed method.

Shallow gas in the Holocene mud wedge along the inner East China Sea shelf

Chen, Yufeng; Deng, Bing; Zhang, Jing. *Marine and Petroleum Geology*, 2020, 114: 104233.

High-resolution seismic surveys were carried out in the inner shelf of the East China Sea to investigate the distribution of shallow gas in Holocene sediments. Shallow gas is distributed extensively in the Holocene strata of the shelf which is dominated by the Yangtze River. Organic-rich, fine-grain sediments deposited throughout the Holocene are essential for gas generation and accumulation. The thickness of the Holocene

sediment is the main controlling factor determining the distribution of shallow gas. Gas seepages were found mostly at a water depth up to 20 m, where sediment erosion mainly occurs. Coincidence between shallow gas seepage and high methane concentration in the water column suggests that gas emission from these sediments is a potentially significant source of greenhouse gas. The interaction between shallow gas migration and coastal erosion would therefore potentially lead to increased greenhouse gas emission and accelerated sediment erosion. Such results can be applied to other coastal locations around the world.

Sedimentary transition of the Yangtze subaqueous delta during the past century: Inspiration for delta response to future decline of sediment supply

Zhan, Qing; Li, Maotian; Liu, Xiaoqiang; Chen, Jing; Chen, Zhongyuan. *Marine Geology*, 2020, 428: 106279.

How the Yangtze delta responds to riverine sediment decline has become a hot research topic and an urgent issue to be addressed, especially after the impoundment of the Three Gorges Dam in 2003. This study investigated sedimentary features through the sediment granularity of surficial samples and short cores over the entire Yangtze subaqueous delta, aiming to better understand the spatial response of the subaqueous delta to sediment supply decline and local hydrodynamic adjustment of the estuary. The results show that four sedimentary zones of estuarine sand bar (Zone I), prodelta (Zone II), delta-shelf transition zone (Zone III) and residual sand (Zone IV) are distributed from the estuary to the shelf, characterised by first fining from zone I to zone II, and then coarsening from zone II to zone IV on grain size of surficial sediments. In the past few hundred years, the subaqueous delta has been generally prograded seaward following this sedimentary system spatially, manifested by generally fining upwards in the cores of the main subaqueous delta. However, sediment coarsening occurs on the top of the cores in the delta-shelf transition zone (Zone III), implying a recent retrogradation process. Based on the results of ^{210}Pb and ^{137}Cs , the sedimentary transition from progradation to retrogradation occurred since 1950s and was intensified after 1980s in the north part of Zone III, mainly caused by channel shrinking of the North Branch and riverine sediment decline. Comparatively, such a sedimentary transition is not significant in the south part of Zone III. But it is worth noting that surficial coarsening in the core (of the south part of Zone III) is probably related to drastic sediment decline since 2003 when the Three-Gorges Dam closed, which means that the Yangtze subaqueous delta has probably been in a full sedimentary transition. The sedimentary transition of the north subaqueous delta can provide an insightful reference for the sedimentary response of the Yangtze delta to further decline of sediment supply in the future.

Magnetic evidence for Yellow River sediment in the late Holocene deposit of the Yangtze River Delta, China

Wang, Feng; Zhang, Weiguo; Nian, Xiaomei; Roberts, Andrew P.; Zhao, Xiang; Shang, Yuan; Ge, Can; Dong, Yan. *Marine Geology*, 2020, 427: 106274.

Sediment source identification is critical for understanding delta evolution processes and for managing delta sustainability, particularly for deltas experiencing significant recent fluvial sediment discharge. Sediment sources for the Yangtze River Delta (YRD) are commonly assumed to be derived from the Yangtze River, despite the fact that the YRD is a tide-dominated delta that can receive marine-sourced sediments in addition to fluvial inputs. In particular, potential contributions from the neighbouring sediment-laden Yellow River, when it dis-charged into the Yellow Sea during 1128–1855 CE, remains unclear. Here we present provenance analysis of three cores from the northern YRD using size-specific magnetic characterizations. We find that magnetic properties of sediments younger than ~400 years have large differences among the

studied cores. Comparison of magnetic properties to potential sources, including the major Yangtze River tributaries (i.e., Jinsha River, Jialing River, and Han River) and Old Yellow River (OYR), indicates that the northern core received enhanced Yellow River sediment loads over the last 400 years, while the southern core had a dominant Yangtze influence, which is most pronounced in size fractions less than 16 μm . This interpretation is supported by geochemical results. The documented spatial sediment source heterogeneity is caused by differences in tidal-fluvial interaction among delta distributary channels. Our results imply that the neighbouring OYR delta to the north exerts a remote influence on the YRD through longshore transport. This coastal connectivity between deltas should be assessed when forecasting future tide-dominated delta changes in the context of global change.

Early to middle Holocene rice cultivation in response to coastal environmental transitions along the South Hangzhou Bay of eastern China

Liu, Yan; Deng, Lanjie; He, Jin; Jiang, Ren; Fan, Daidu; Jiang, Xuezhong; Jiang, Feng; Li, Maotian; Chen, Jing; Chen, Zhongyuan; Sun, Qianli. *Palaeogeography Palaeoclimatology Palaeoecology*, 2020, 555: 109872.

South Hangzhou Bay (SHB) in eastern China is one of the regions where agriculture began in the early Holocene. To better understand how farming-based societies developed in this region, we examined pollen, charcoal, foraminifera and grain size information of a well-dated sediment core (YJ1503) in the Yaojiang Valley (YJV). Pollen assemblages show that before 8600 cal yr BP, *Pinus*, *Quercus*, *Juglans* and *Pterocarya* woodlands were dominant. During ca. 8600–8400 cal yr BP, abundant foraminifera suggest a transient marine incursion. Although the former woodland species re-established during 8400–7600 cal yr BP, freshwater algae and dino-flagellates indicate a transition to brackish environments. Two peaks of charcoal at around 8200 and 7800 cal yr BP, are possible early signs of human occupation that pre-dated the Hemudu Culture. After 7600 cal yr BP, an increase of salt-tolerant herbs including *Chenopodiaceae*, *Cyperaceae* and *Poaceae* (< 35 μm) and a decrease of dinoflagellate and foraminifera assemblages, imply a reduction in saline influence. Freshwater wetlands established around 6600 cal yr BP as indicated by increasing *Typha* and diminishing *Chenopodiaceae* pollen. This coincided with a sharp decline in *Pinus* pollen, marked increases of *Poaceae* pollen and a rise in charcoal suggesting more activity of human communities. Rice cultivation is confirmed by archaeological findings from this interval, with two distinctive periods at ca. 6600–6300 and 5500–5200 cal yr BP. The initial coastal land development started as early as 7800–7600 cal yr BP in the YJV, which was concurrent with that happened at the apex of SHB where the Kuahuqiao Culture originated, but rice farming trajectory at these two places differed. In the Kuahuqiao area, low salinity coastal settings developed, freshened by the discharge of the Qiantang River, and this area would have been especially suitable for agriculture. In contrast, in the YJV, early rice cultivation was possibly hampered by longer episodes of brackish intrusion during time of lower discharge of the Yaojiang River until a freshwater environment prevailed after ca. 7000 cal yr BP.

Stratigraphic and three-dimensional morphological evolution of the late Quaternary sequences in the western Bohai Sea, China: Controls related to eustasy, high sediment supplies and neotectonics

Liu, Shihao; Feng, Aiping; Yang, Linlong; Du, Jun; Yu, Yonggui; Feng, Wei; Wang, Yaping. *Marine Geology*, 2020, 427: 106246.

The Bohai Sea is a shallow, semi-closed gulf (basin) at the proximal position of the very wide (one to several thousand kilometers) eastern Chinese margin and was persistently impacted by tectonic frameworks. Its late Quaternary stratigraphy provides an excellent natural laboratory for research on the sedimentary processes

and evolutionary patterns on flat proximal continental margins with high sediment inputs and how these processes respond to syndepositional tectonic activity. However, due to the scarcity of comprehensive sequence stratigraphic studies, our understanding of the above processes is limited. Here, we conducted a high-resolution sequence stratigraphic study using boomer seismic data with pseudo-3D coverage. The seismic data revealed seven seismic units (SUs A-G) within the late Quaternary stratigraphy, including (1) three marine prodeltaic units (SUs A, C, G) characterized by dipping/oblique internal reflections and/or lobate structures, (2) two terrestrial (fluvial/lacus-trine) units (SUs B and E) dominated by heterogeneous reflections, (3) an erosional remnant unit (SUs D) with semitransparent reflectors and a lenticular geometry, and (4) a ravinement-attributed aggradational unit (SU F). Based on the extrapolation between the seismic stratigraphy and the onshore sedimentary architecture and well-established sequence stratigraphic models, our preferential interpretation for the four sets of SUs is that they correspond to the highstand, lowstand, falling-stage and transgressive system tracts, respectively. The seismic geomorphology suggests that the bulk of the accommodation is dominated by the former two, which is consistent with the alternative terrestrial-and-marine succession revealed by previous borehole studies. At such a proximal gulf, although the accumulation of thick highstand units is not surprising, the two thick lowstand units that are bounded above and below by two different subaerial unconformities are exceptional. Our interpretation indicates that abnormally thick accumulation occurred under subaerial environments during the lowstand period, which most likely corresponds to alluvial/floodplain progradation/aggradation given the western Bohai Sea is connected to the alluvial North China Plain. The lower subaerial unconformities of the lowstand units are associated with intensive subaerial (most likely fluvial) excavation. Erosion under SU E leads to the formation of incised and eroded areas that can be tens of kilometers wide and tens of meters deep, cutting into SU A or even into SU B, which are several times greater than the last glacial maximum incised valley at the top of SU E. Such intensive erosion appears to be a crucial contributor to the thick lowstand units, as it created

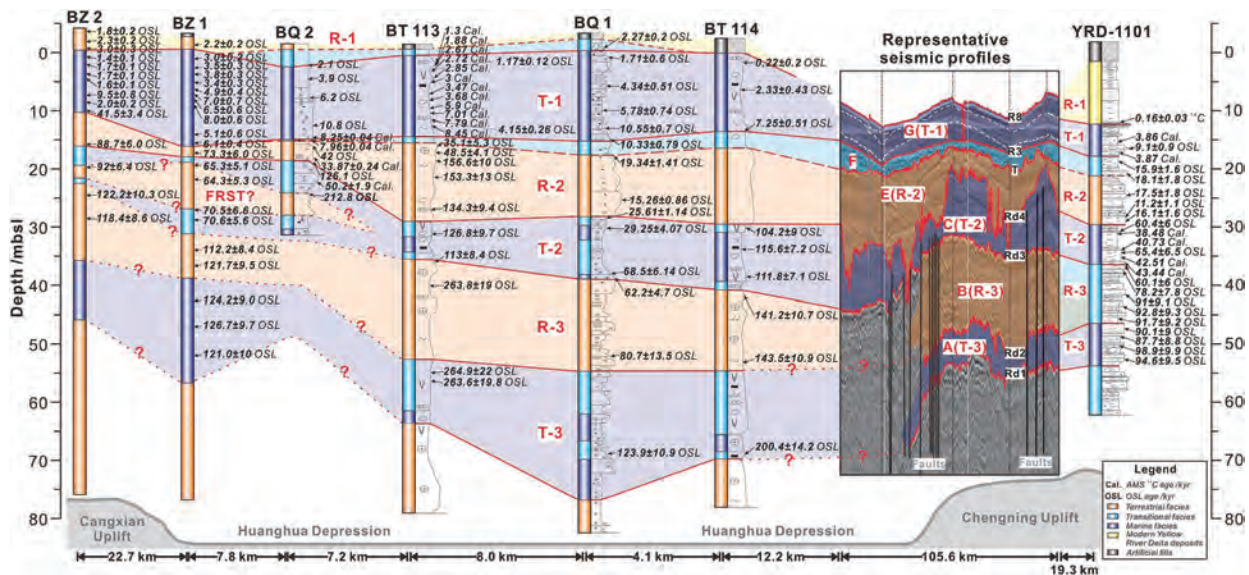


Fig. 3. Extrapolated stratigraphic correlations of the geological column of representative boreholes from the literature (Table 2) with the ^{14}C and optically stimulated luminescence (OSL) ages and the interpreted compressed seismic profiles [with all the representative seismic units (SUs) and horizons donated] acquired across the western half of the survey area (see Fig. 2 for locations and Fig. 6 for the uncompressed seismic image). The ages of the pre-LGM stratigraphy are highly controversial in these cores, and the primary hypotheses are summarized in Table 1. The orange, blue, dark blue and yellow fills denote the terrestrial, transitional, marine facies and the modern Yellow River delta deposits, respectively. Three major marine sedimentary beds (T-1 to T-3) and three terrestrial beds (R1 to R3) within the late Quaternary stratigraphy are indicated. The tectonic framework (depressions and uplifts) and distances between the cores and/or seismic profiles are denoted at the bottom. Note that the figure does not follow the horizontal scale to better exhibit the details of borehole columns. The enlarged columns of cores BQ2, BT113, BQ1, BT114, and YRD-1101 are illustrated in Supplementary Fig. 1. (For interpretation of the references to colour in this figure legend, the reader is referred to the web version of this article.)

more accommodation. The great scale of the subaerial incisions is presumably attributed to the fact that the bulk of them evolved from tectonically triggered depressions because their locations are consistent with the NE-SW- and NW-SE-striking fault populations. The tectonic forces also controlled the accumulation by resulting in high-relief basement blocks for the pre-Holocene sedimentation. However, despite such strong tectonic controls, the subsequent deposition filled and leveled the areas between the high-relief, steep-sided basement blocks and eventually resulted in a relatively flat substratum for post-LGM deposition, suggesting that the geomorphic threshold for geological control at such a proximal gulf was passed because of the high-supply environment.

Combined chronological and mineral magnetic approaches to reveal age variations and stratigraphic heterogeneity in the Yangtze River subaqueous delta

Cheng, Qinzi; Wang, Feng; Chen, Jin; Ge, Can; Chen, Yinglu; Zhao, Xuanqi; Nian, Xiaomei; Zhang, Weiguo; Liu, Kam-biu; Xu, Yijun; Lam, Nina. *Geomorphology*, 2020, 359: 107163.

Delta deposits show large spatial heterogeneity in terms of depositional rate and age, which is critical to the study of delta erosion in response to the declining fluvial sediment load observed at many river mouths in the world. In this study, we show that the magnetic susceptibility (χ) can be an indicator to reveal age variations and stratigraphic heterogeneity in the Yangtze River subaqueous delta. Ages of three short sediment cores (b2m) collected at 20–32 m water depth from the Yangtze River subaqueous delta were determined using ^{210}Pb , ^{137}Cs , and optically stimulated luminescence (OSL) dating. In addition, depth variation of χ , which is influenced by post-depositional diagenesis and hence age, was used to roughly infer sediment ages among the cores in a simple way. The profiles of ^{210}Pb , ^{137}Cs , and OSL dating results indicate the spatial variability of ages, ranging from the last 100 years to N1700 years. The cores at shallow water depths are younger than those from deeper sites. Modern deposits (i.e., b100 years old) occur primarily at water depths shallower than ca. 30 m. The core in the northern part of the subaqueous delta shows much older ages than the core at the southern site with similar water depth, which is caused by their longer distance relative to the mouth of active sediment discharge distributary. Profile of χ confirms such spatial variation of ages in terms of depth distribution pattern and χ value. Older sediments (N800 a) show lower and uniform χ values due to the reductive dissolution of ferrimagnetic minerals, while younger sediments (b350 a) show higher χ values in the top layer but they decline with increasing depth. Considering the quick way of magnetic measurement, stratigraphic correlation based on χ can be used first to screen for cores before they are subjected to more detailed dating. This study shows that the methodological approach of combining sediment dating with magnetic measurement has great potential in revealing heterogeneous deltaic deposits.

海岸动力地貌与动力沉积过程 Coastal Morphodynamics and Sedimentary Process

An integrated optic and acoustic (IOA) approach for measuring suspended sediment concentration in highly turbid environments

Lin, Jianliang; He, Qing; Guo, Leicheng; van Prooijen, Bram C.; Wang, Zheng Bing. *Marine Geology*, 2020, 421: 106062.

Accurate measurement of suspended sediment concentration (SSC) in highly turbid environments has been a problem due to optical or acoustic signal saturation and attenuation. The saturation returns a limited measurement range, and the attenuation raises an ambiguity problem that a low optical or acoustic output could mean a low or a high SSC. In this study, an integrated optic and acoustic (IOA) approach is proposed to (i) overcome the ambiguity problem; (ii) increase the measurement range to high SSC values; and (iii) obtain high-resolution SSC profiles. The IOA approach is a combination of Argus Suspension Meter (ASM), Optical Backscatter Sensor (OBS) and Acoustic Doppler Velocimeter (ADV). In this approach, the ASM-derived SSC is preferred because of its lowest relative error, followed by OBS and ADV. The ASM can produce high-resolution (1 cm interval) SSC profiles when it is not saturated (usually SSC < 9 g/L). When ASM is saturated, the SSC is recovered by OBS. Since the ambiguity problem is solved, the measurement range of OBS and ADV can be extended up to 300 g/L. The best way to use an ADV, however, is to have a rough estimation first and assist in the OBS conversion, because its estimates contain large uncertainty. To further mitigate the impact of sediment particle size on SSC retrieval, we suggest the usage of in-situ sediment samples for sensor calibration. The IOA approach was verified in the Yangtze Estuary which is a highly turbid system. Comparison of the IOA approach outputs against water sampling results demonstrates the reliability of the IOA approach with a relative error of 17–34%. The observed high SSCs were up to 63 g/L. The field data show that high SSCs were confined in the benthic layer (within 2 m above the bed) in the wet season under a high river discharge, whereas the suspension was better mixed throughout the water column in the dry season.

由于光学或声学信号的饱和及衰减，在高浊度环境中准确测量含沙量一直都是难题，制约了高含沙水体包括近底边界层泥沙运动的研究。信号的饱和限制了含沙量的测量范围，而信号的衰减则引起含沙量反演的不确定性问题，即低的光学或声学信号输出可能对应着低或高的两个含沙量（如图1a和1b）。在本研究中，我们提出了一种用多探头集成的系统观测（IOA）方法来实现：i) 克服信号反演过程的不确定性问题；ii) 扩展现场含沙量的测量范围；iii) 获取高分辨率的含沙量剖面等目标。

IOA系统集成方法，是阿格斯浊度剖面仪（ASM），光学反向散射传感器（OBS）和声学多普勒测速仪（ADV）的组合。在这种方法中，首选ASM反演的含沙量，因为它的相对误差最低（26%），其次是OBS（30%）和ADV（89%）。基于以上结果，我们提出了基于IOA方法的最佳反演模式（图1c）：步骤1，ASM未饱和时（通常含沙量 < 9 g/L），推荐使用ASM进行反演，它可以提供高分辨率（1 cm间隔）的含沙量剖面；步骤2，当ASM饱和时，ASM缺失的含沙量结果则可由OBS弥补；步骤3，ADV则协助OBS进行反演并提供高频含沙量的反演结果。

为检验和评估这一套方法，我们在长江口采用坐底三脚架系统进行了长时间的含沙量观测。结果表明，我们提出的IOA方法可以有效克服OBS和ADV信号反演过程中的不确定性问题，从而可以将OBS和ADV的测量范围扩展至 >100 g/L，并提供准确可靠的高含沙量值（相对误差为17–34%），同时可以通过ASM获得高分辨率的含沙量剖面。否则很可能低估现场的高含沙量(图1d)，甚至有可能导致得到错误的泥沙浓度剖面（图1e）。

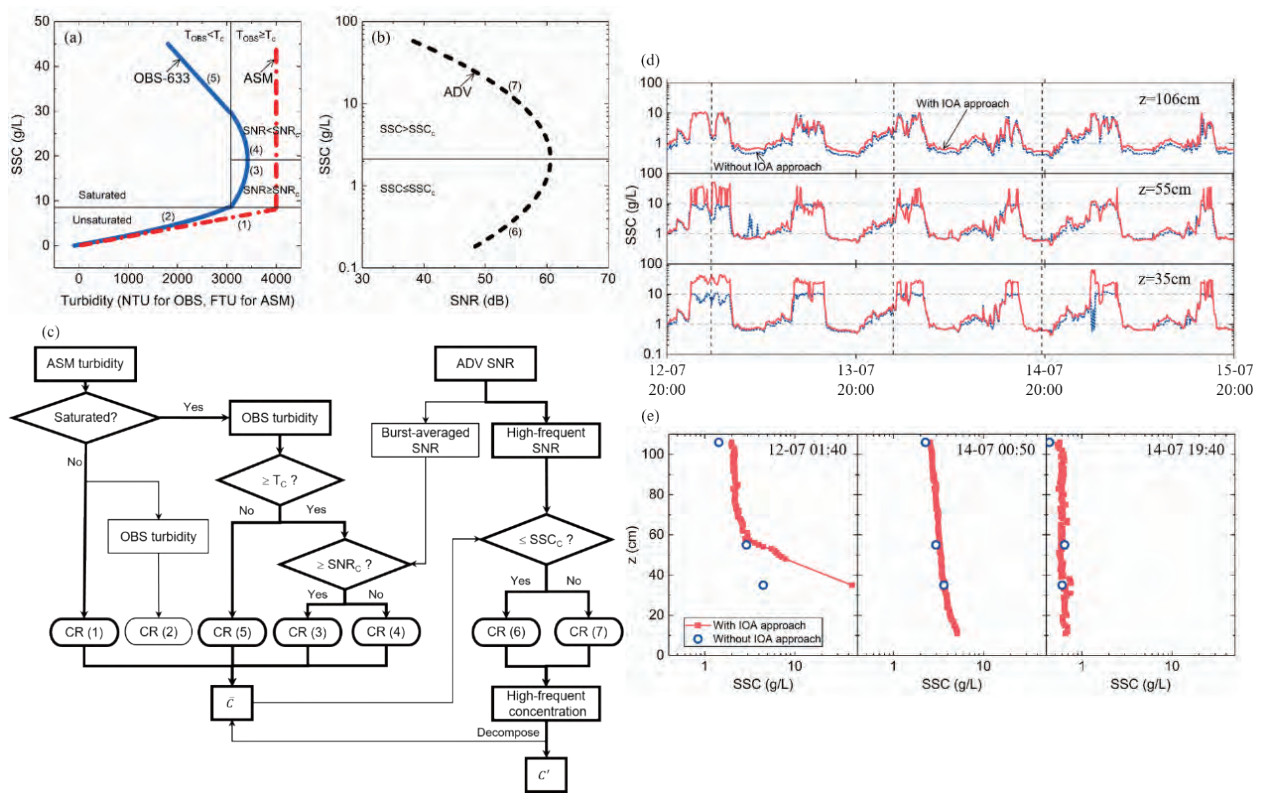


图1 高浊度河口含沙量高精度集成观测系统

Response of Stratification Processes to Tidal Current Alteration due to Channel Narrowing and Deepening

Zhu, Lei; He, Qing; Shen, Jian. *Journal of Geophysical Research-Oceans*, 2020, 125(2): 15223.

Stratification in estuaries has received much focus due to its importance in estuarine hydrodynamics and material transport. By utilizing a well-calibrated numerical model, in this work we investigate the changes in stratification in the deepened and narrowed North Passage of the Changjiang Estuary. Before channel narrowing and deepening, lateral straining, generated by the interaction between vertical shear in lateral flow and transverse salinity gradient, is the dominant factor that controls stratification. A two-layer structure of the lateral flow strains the isopycnal transversely, resulting in rapid stratification from late flood to early ebb tide. Thus, maximum stratification occurs during the early ebb. Then, the stratification was suppressed by the vertical mixing and the less stratified water advected from upstream, even the vertical shear in along-channel flow continued to strain the isopycnal. After channel deepening and narrowing, the salinity in the upper water column experienced a sharp vertical gradient during the entire tidal cycle, while the transverse salinity gradient and lateral flow are profoundly reduced. The impact of lateral straining on stratification becomes minor. The enhanced stratification results in a sharp decrease in turbulent mixing within the pycnocline. The water movement in the upper layer is in a free-stream status and the tidal current speed increases significantly. The alteration of the vertical current structure enhances the along-channel tidal straining and stratification is most vigorous on late ebb tide.

河口因其独特的地理位置，是人类生产发展及其影响和响应的敏感区域。近几个世纪以来，为满足社会经济高速发展的需求，众多河口进行航道建设、滩涂围垦，这些人类活动使河口变得日益窄深。长江口为典型案例之一。深水航道的建设使河槽由原来的7m加深到12.5m，改变了原有的潮流运动与密度场，致使河口主槽层化加剧。本文基于EFDC模型，利用工程前后的地形分别建立三维水流数值模型，系统研究水体分层对河道窄深化的响应（图1）。工程前，由于越滩流的存在，横向环流呈现表层向北底层向南的两层流结构，横向环流存在强烈的剪切($\sim 0.1 \text{ s}^{-1}$)，这种剪切作用与横向的盐度梯度相互作用产生横向潮汐应变，使垂向盐度梯度以 $1 \times 10^{-4} \text{ psu/m/s}$ 的速率增加，盐度梯度的急剧变化使得最强密度分层出现在落潮初期。在落潮中后段，上游低盐度水体进入航槽，在垂向混合的共同作用下，分层逐渐减弱。深水航道的修建使得河槽变得窄深，床面对水流的摩阻作用减小，水体底部产生的紊动被限制在密度跃层以下，因此，水体上层出现持续性的分层。与此同时，上层水体沿航槽流速在急流时刻较工程前增加近 0.1 m/s ，由此形成较大的流速剪切。工程的实施同时改变了横向的动力过程，由于层化加强，差异平流作用减小，床面附近的混合作用成为横向斜压梯度力产生的主要原因，由此产生的横向流在涨潮时仅为 0.07 m/s ，不到工程前的一半。横向流速与横向盐度梯度的减小使得横向潮汐应变对水体分层的作用减小。沿航槽流速剪切与纵向盐度梯度相互作用产生的纵向潮汐应变成为主导河口分层的因素，在落潮期间，强烈的流速剪切使垂向盐度梯度不断增加，致使最大分层时刻出现在落潮后期。

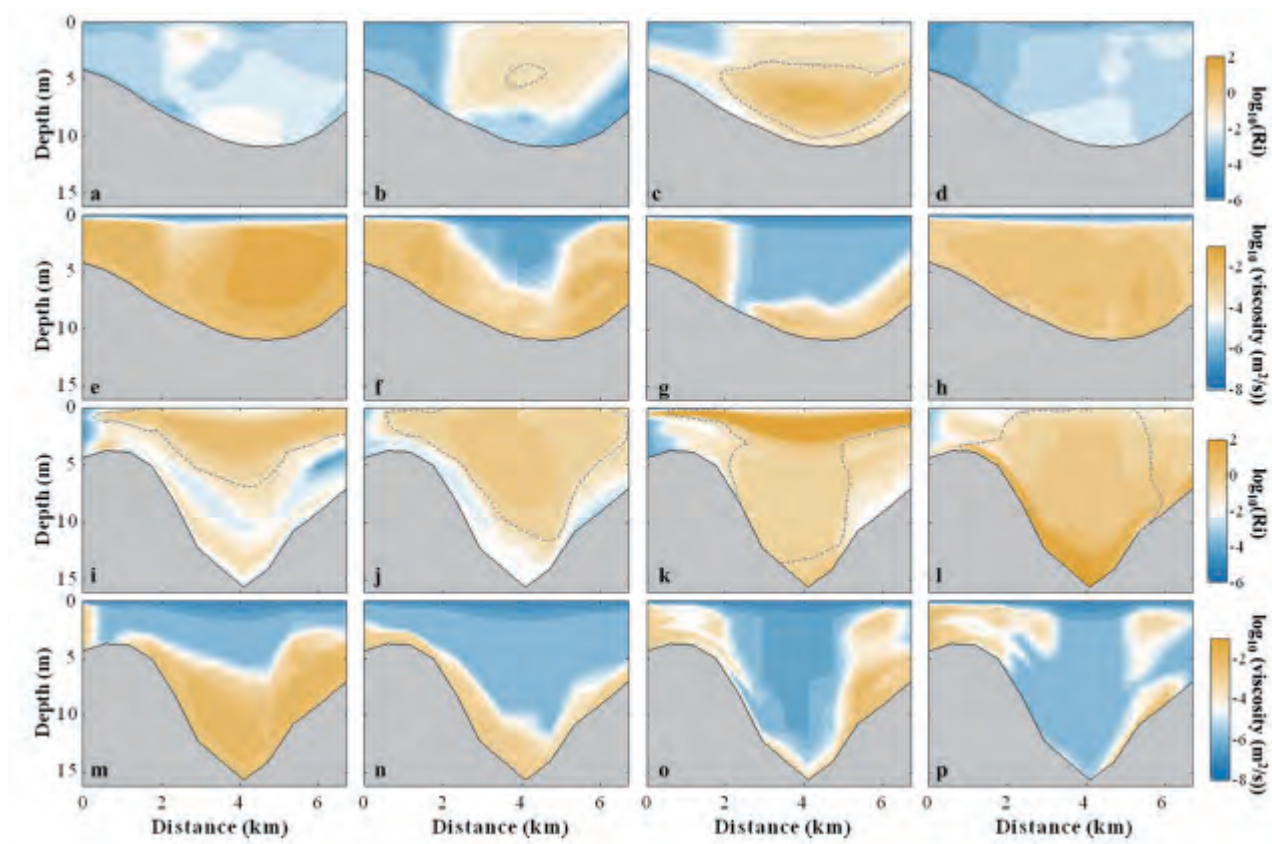


图1 浑浊带航槽核心区域Richardson数(a-d, 工程前; i-l, 工程后)与紊动粘滞系数(e-h, 工程前; m-p, 工程后)的横向分布状态, 从左至右分别为涨急、涨憩、落急与落憩时刻

Influence of Macrobenthos (*Meretrix meretrix* Linnaeus) on Erosion - Accretion Processes in Intertidal Flats: A Case Study From a Cultivation Zone

Shi, Benwei; Pratalongo, Paula; Du, Yongfen; Li, Jiasheng; Yang, Shilun; Wu, Jihua; Xu, Kehui; Wang, Ya Ping. *Journal of Geophysical Research-Biogeosciences*, 2020, 125(1): e2019JG005345.

The activity of benthic organisms can strongly influence sediment dynamics in an intertidal flat. However, few studies have conducted a quantitative assessments of the effect of benthic organisms on erosion-accretion processes under field conditions. The aim of this study was to quantify the effects of the benthic clam *Meretrix meretrix* Linnaeus (*M. meretrix*) on bed erodibility and sediment erosion-accretion processes in an intertidal flat. Within the cultivation zone at site A, *M. meretrix* is present in large numbers (up to 137 individuals per square meter). On the other hand, site B is located outside the cultivation zone. At this site, which is only 500 m away from site A alongshore, *M. meretrix* forms a sparse population with only 3.7 individuals per square meter. The results showed that the critical shear stress for erosion, denoted by τ_{ce} , was 0.22 and 0.32 N/m² at sites A and B, respectively, and the magnitudes of bed-level change were significantly higher at site A than site B. These results reveal the large effect of *M. meretrix* on decreasing τ_{ce} , augmenting the erosion rate when the bed shear stress due to combined currents and waves, denoted by τ_{cw} , was higher than τ_{ce} , and conversely enhancing the accretion rate when $\tau_{cw} < \tau_{ce}$. The changes induced in these parameters are likely to have a large impact on model predictions of bed erodibility, sedimentary processes, and morphological evolution. Thus, integrated field measurements of hydrodynamic and bed-level changes, accompanied by simultaneous biological sampling, may help to improve the parameterization of hydro-sedimentary and morphodynamic models for shallow-water environments.

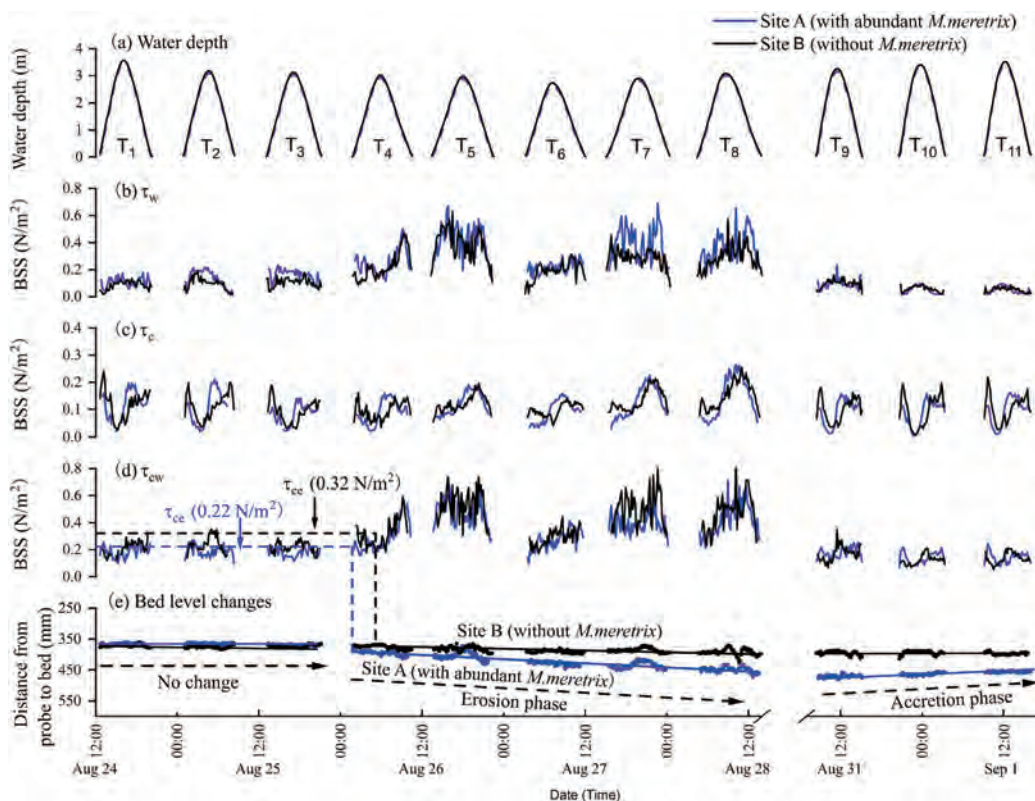


Figure 7. (a) Time series data of water depth, (b) bed shear stress due to waves (τ_w), (c) currents (τ_c), (d) combined wave-current action (τ_{cw}), and (e) bed elevation (e). Dotted lines in (d) and (e) indicate the estimated critical shear stress for the erosion of bottom sediment (τ_{ce}), which was 0.22 N/m² for site A and 0.32 N/m² for site B.

潮滩底栖生物活动对沉积动力过程有重要影响。然而，目前这方面的研究仅停留在定性研究，缺乏在现场自然环境下的定量研究。本研究针对养殖区内的文蛤对底床稳定性和侵蚀淤积过程的影响进行了量化研究。选取了两个点进行对比研究：文蛤养殖区内的测点A (文蛤密度多达137个数每平方米) 具有丰富的文蛤存在，而在文蛤养殖区外的测点B (文蛤密度仅仅3.7个数每平方米，距离测点A只有500米) 具有很少数目的文蛤。结果表明：测点A和B的底床侵蚀临界剪切应力分别为0.22和0.32 N/m²，并且测点A侵蚀淤积的幅度明显大于测点B。这些结果揭示了大型底栖动物文蛤降低了底床稳定性，当底部切应力大于底床临界侵蚀剪切应力时，加速了潮滩侵蚀过程，另一方面当底部切应力小于底床临界侵蚀剪切应力时，加速了潮滩淤积过程。本研究认为这种沉积动力学关键参数的改变(底床侵蚀临界剪切应力)会对潮滩地貌演化预测模型精度产生重要影响。因此，现场沉积动力过程观测和同步大型底栖生物收集，有助于改善浅水环境的水力-沉积和地貌动力学模型的参量化，推动生物地貌学的研究。

Characterization of longshore currents in southern East China Sea during summer and autumn

Li, Peng; Shi, Benwei; Li, Yangang; Wang, Sijian; Lv, Xin; Wang, Yaping; Tian, Qing. *Acta Oceanologica Sinica*, 2020, 39(3):1-11.

Current characteristics and vertical variations during summer and autumn in the southern East China Sea were investigated by measuring current profile, tide, wind, and wave data for 90 d from July 28 to October 25, 2015. Our results are: (1) The current was mainly a (clockwise) rotating flow, displaying reciprocating flow characteristics, and vertically the current directions were the same throughout the vertical profile. (2) The horizontal current speed was strongest during August (summer) with an average speed of 51.8 cm/s. The average current speeds during spring tides were highest in August and weakest in September, with speeds of 59.9 and 42.8 cm/s, respectively. (3) Considerable differences exist in average current speeds in different layers and seasons. The highest average current speeds were found in the middle–upper layers in August and in the middle–lower layers in September and October. (4) The residual current speed was highest in August, when the speed was 12.5–47.1 cm/s, whereas the vertical average current speed was 34.3 cm/s. The depth-averaged residual

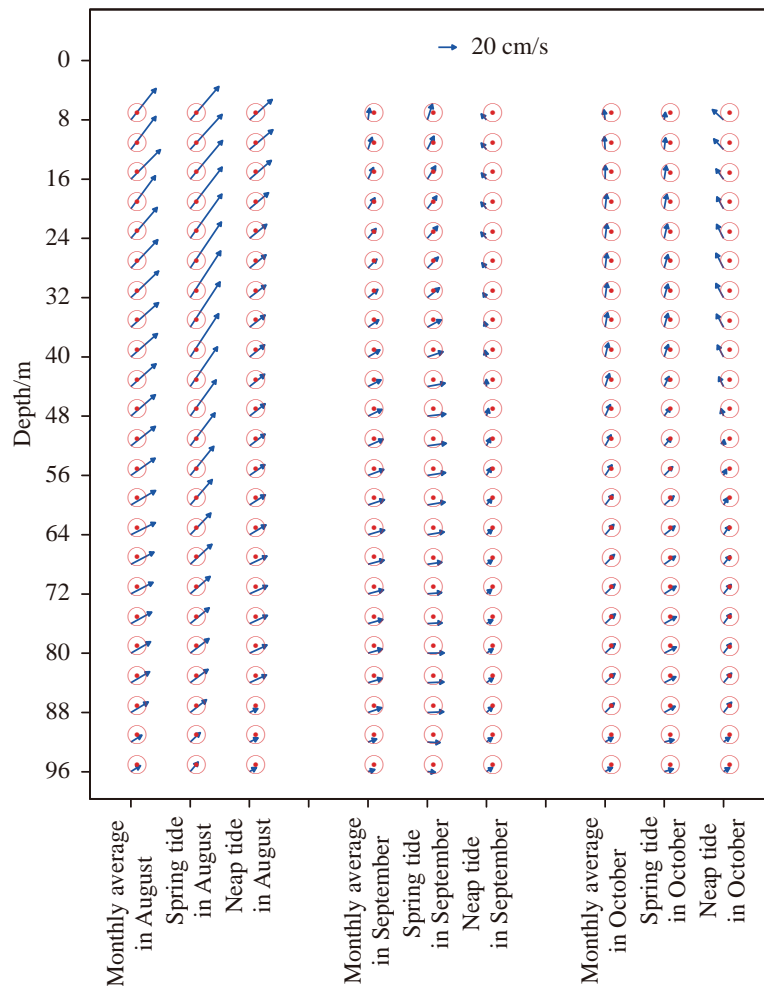


Fig. 8. Vertical variations in residual currents during the observation period.

current speeds in September and October were only 50% of that in August, and the residual current direction gradually rotated in a counter-clockwise direction from the lower to surface layers. (5) Typhoon waves had a significant influence on the currents, and even affected the middle and lower water layers at depths of >70.0 m. Our results showed that the currents are controlled by the dynamic interplay of the Taiwan Warm Current, incursion of the Kuroshio Current onto the continental shelf, and monsoonal changes.

为了揭示东海南部海域海流的夏秋季节变化特征和垂向变化规律，于2015年7月28日-10月25日在东海南部海域（平均水深105.0 m，平均潮差1.21 m）利用ADCP潜标和大型浮标进行了连续90天的剖面海流、潮汐、风速风向和波浪的观测。结果表明：（1）海流流向以旋转流为主，兼具往复流特性，涨潮流为北偏西方向，落潮流为东-东南向，旋转方向为顺时针方向，在垂向上流向分布较一致。（2）东海南部海域水平流速总体较大，8月份（夏季）的海流最强，平均流速为51.8 cm/s，各月的最大流速均大于120.0 cm/s，最大流速达202.0 cm/s，出现在8月台风期间。大潮的平均流速8月份最大（59.9 cm/s），9月份最小（42.8 cm/s），大潮平均流速为小潮的1.5~1.7倍。（3）各层和各季节平均流速垂向变化差异较大，8月份中上层水体流速最大，9和10月份中下层水体流速最大。（4）余流的流速和流向存在显著的时空变化，8月份最强，为12.5~47.1 cm/s，平均余流达34.3 cm/s，9月和10月份平均余流大小仅为8月份的50%。余流的流向从底层至表层呈逆时针方向旋转。（5）台风对海流的影响显著，台风期间，海浪甚至影响到中下层水体，深度达70.0 m以上。该海域的海流受台湾暖流、黑潮和季风等动力作用的共同制约。

Linkage between turbulent kinetic energy, waves and suspended sediment concentrations in the nearshore zone

Pang, Wenhong; Dai, Zhijun; Ma, Binbin; Wang, Jie; Huang, Hu; Li, Shushi. *Marine Geology*, 2020, 425: 106190.

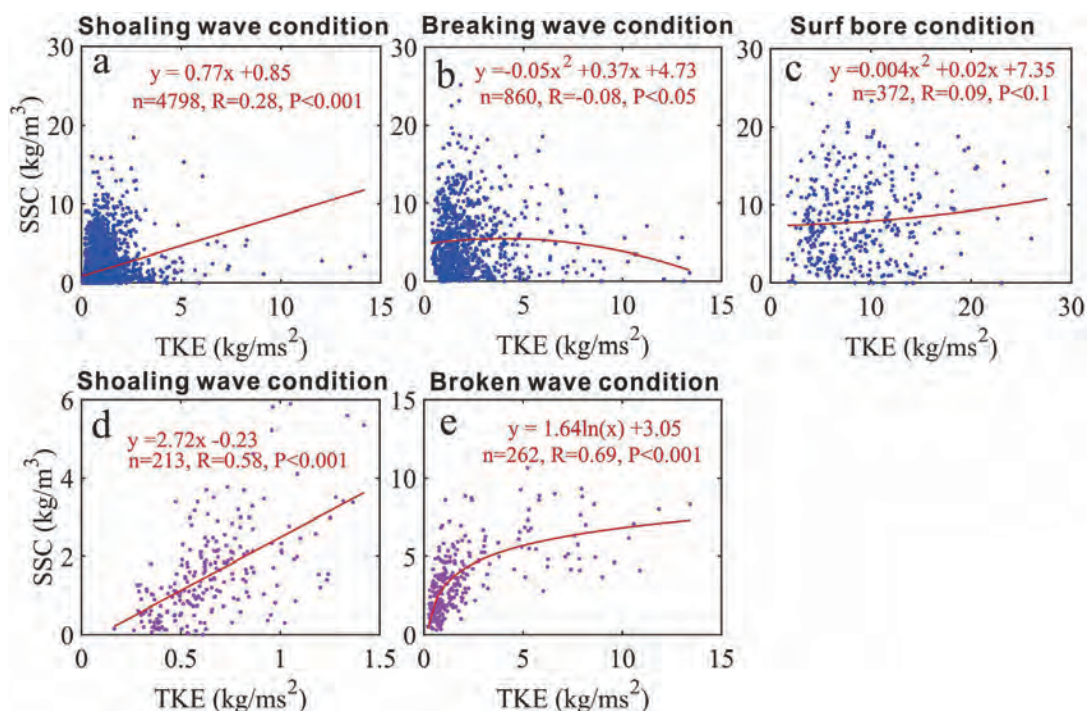


Fig. 15. Mean SSC against mean TKE in terms of incident wave time scale under (a) shoaling wave condition, (b) breaking wave condition and (c) surf bore condition. Mean SSC against TKE at the wave group time scale under (d) shoaling wave condition and (e) broken wave condition.

Knowledge about the tradeoffs among turbulent kinetic energy (TKE), waves, and suspended sediment concentrations (SSCs) in the nearshore zone is relevant for understanding beach morphodynamics at different temporal and spatial scales. A field measurement lasting for nearly three tidal cycles was conducted to holistically discern couplings between TKE, waves and SSCs, with further evaluation of the relative significance of TKE and waves on SSCs under various wave conditions over a meso-macro tidal beach, Yintan, to the north of Beibu Gulf, China. The results showed a dramatic increase in wave groupiness intensity from the shoaling wave condition to the breaking wave condition and a clear decrease further into the surf bore condition. The near-bed TKEs under the surf bore condition were an order of magnitude larger than those under the breaking and shoaling wave conditions at the measurement position. The averaged SSCs in the near-bed (approximately 10 cm) under the surf bore condition were 1.5 and 4.5 times larger than those under breaking and shoaling wave conditions, respectively. The variations in relative wave height were a decisive indicator for the differences in TKE intensities among different wave conditions, while the occurrence of peak TKEs at the wave front within the intrawave cycle was associated with flow acceleration regardless of wave conditions. Mean SSCs were well correlated with waves in terms of both incident wave scale and wave group scale, which was limited to the shoaling wave condition, and the occurrence of near-bed intrawave peak SSCs was always related to the offshore wave phase. Further, TKE contributed more effectively to sediment suspension at the wave group scale than at the incident wave scale, especially under broken wave condition. Among the hydrodynamic factors, TKE played the most important role in the variations in SSCs for all wave conditions. Flow acceleration served as the second most important factor under the broken wave condition, while wave group, single wave and advection were equivalent and less important factors for SSCs.

了解近岸区湍流动能，波浪和悬沙浓度的权衡关系对理解不同时空尺度下的海滩动力地貌过程具有重要意义。我们在中国北部湾北部的一个中强潮海滩——北海银滩进行了一次长约三个潮周期的野外监测，以整体地识别湍流动能，波浪和悬沙浓度的耦合关系，并进一步评估不同波浪带下湍流动能和波浪对悬沙浓度的相对重要性。结果表明：波群强度从浅水带到破波带有一个剧烈的增大，而进一步到碎波带后表现为明显减小。研究区域碎波带内的近底层湍流动能比破波带和浅水带内要大一个数量级。碎波带内近底层约10厘米处平均悬沙浓度比其在浅水带和破波带内大1.5倍和4.5倍。在不同波浪带内相对波高的变化都是湍流动能变化的决定性指标。入射波周期内近底层悬沙浓度峰值总是发生在波浪的离岸相位中。我们进一步对湍流动能事件和悬沙浓度事件进行条件概率统计，发现同时发生的湍流动能事件（超过 1.01 kg/ms^2 ）只占12.2%的湍流动能时间序列，却能产生42.9%的悬沙事件（超过 1.86 kg/m^3 ）。通常情况下，在所有动力因子中，无论在何种波浪状况（浅水带，破波带和碎波带），湍流动能都是影响悬沙浓度变化的最重要因素，其次是波群，水流加速度和单个波（入射波和长重力波），影响程度最弱的是平流过程（平均流）。

Impact of river discharge on hydrodynamics and sedimentary processes at Yellow River Delta

Ji, Hongyu; Pan, Shunqi; Chen, Shenliang. *Marine Geology*, 2020, 425: 106210.

During the Anthropocene, regulating river discharge by high dams may have met the need for water demands in river basins, but resulted in carrying less freshwater and sediment to the sea, inducing land degradation and shoreline retreat in worldwide mega-river deltas. In land-ocean interaction, tide response to water discharge changes plays an important role and is crucial for the river-laden sediment transfer and dispersal, affecting both nearshore and estuarine deposits. The Yellow River Delta (YRD), which is under an increasing pressure of the new discharge regime of the Yellow River, has undergone drastic changes in terms of sediment dynamics and morphologic evolution. To gain a better understanding of the overall fluvial and marine hydrodynamics and morphodynamic processes in the YRD, in this study, a full-scale

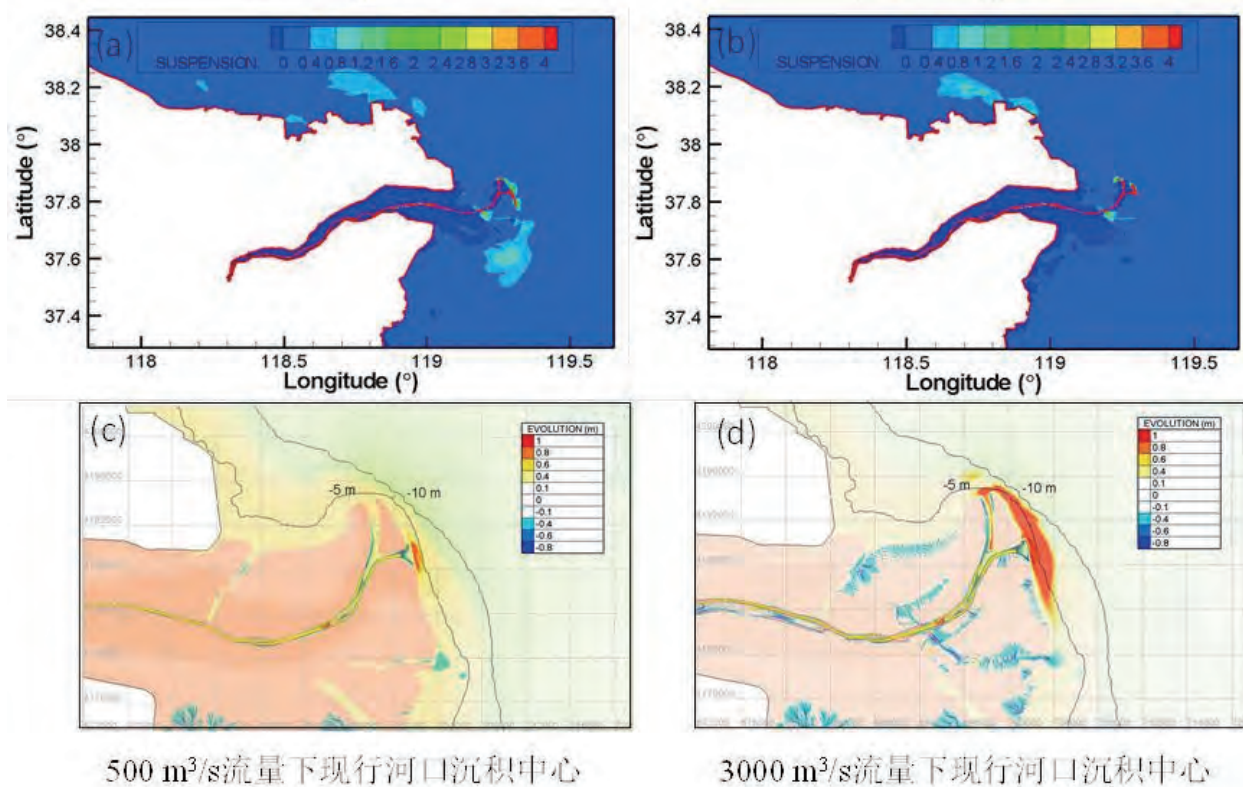


图1 不同流量下黄河入海泥沙的运输和沉积

numerical model is built to investigate the interaction and impacts of changing environmental forcing and dynamics on flow and sediment transport in the estuary of YRD and its adjacent coasts. The results show that the river discharge strongly affects the tidal dynamics and morphology of the delta, particularly in the close vicinity of the outlet and the intertidal zone. Tidal constituents M2 and K1, which are the most significant ones in the YRD, are found to be noticeably affected with a decreasing trend when the river discharge increases. The model results also indicate that river discharge affects the location and intensity of the shear front that occurs in the nearshore areas of the YRD. Increasing the river discharge can induce a seaward movement of the shear front, reduce its width and concentrate its shear intensity. It is found that the reverse of the flow direction at each side of the shear front and strong longshore tidal current can act as a barrier for the sediment dispersal process by keeping suspended sediment in the inner zone, thus to form a particular sediment deposition zone and the depo-center.

黄河素以水少沙多，含沙量高而著称，近年来为入海水沙量锐减，泥沙浓度显著降低，颗粒粗化。本研究基于 Telemac 数值模型，模拟研究了入海水沙变化对河口滨海区沉积动力过程，包括潮汐变化、切变锋、泥沙运输和沉积过程的影响。研究表明，径流量的变化显著影响黄河尾间河道及潮间带潮汐特征；潮周期内现行河口切边锋总由近岸向远岸发育，总历时 8 h 左右，且内落外涨型历时长于内涨外落型，混合潮类型内的不同潮型对切边锋发育模式无显著影响；径流量的增加减小切边锋宽度，使切边锋位置向海推进，切边锋剪切强度增加；切边锋对泥沙捕获效应明显，河流来沙不易直接扩散至外海，主要向莱州湾运输。同时，切边锋的产生对沉积中心影响较大，小径流时泥沙易在现行河口东口落淤，大流量时泥沙落淤范围扩大至从北口到东口以南，且沉积中心向海移动。

Transport Mechanism of Suspended Sediments and Migration Trends of Sediments in the Central Hangzhou Bay

Song, Zekun; Shi, Weiyong; Zhang, Junbiao; Hu, Hao; Zhang, Feng; Xu, Xuefeng. *Water*, 2020, 12(8): 2189.

Based on the 2013 field survey data of hydrology, suspended sediments and bottom sediments in the Central Hangzhou Bay, this paper explores the dynamic mechanism of suspended sediments in Hangzhou Bay by employing material flux decomposition. Meanwhile, the migration trends of bed sediments are also investigated by analyzing grain size trends. The results show that during an ebb or flood tide, the hydrograph of suspended sediment concentration of Hangzhou Bay is dominated by an M shape (bimodal), which is attributed primarily to the generation of a soft mud layer and a separate fluid mud layer. Laterally, the distribution of suspended sediment concentration is high in the south and low in the north. From a macroscopic perspective, the net sediment transport in the study area displays a “north-landward and south-seaward” trend, presenting a “C”-shaped transport mode. That is, the sediments are transported from the bay mouth to the bay head on the north side and from the bay head to the bay mouth on the south side. The sediment transports by advection and tidal pumping are predominant, while the sediment transport by vertical circulation makes little contribution to the total sediment transport. Moreover, the sediment transport in the center of the reach area is dominated by advection, whereas that near both sides of the banks is controlled by tidal pumping. The asymmetry of the tides, i.e., flood-dominance in the north and ebb-dominance in the south, is the primary cause of the dynamic mechanism for the overall “C”-shaped transport mode in Hangzhou Bay. Additionally, coupled with the narrow-head wide-mouth geomorphology, Hangzhou Bay remains evolving by south shore silting and north shore scouring.

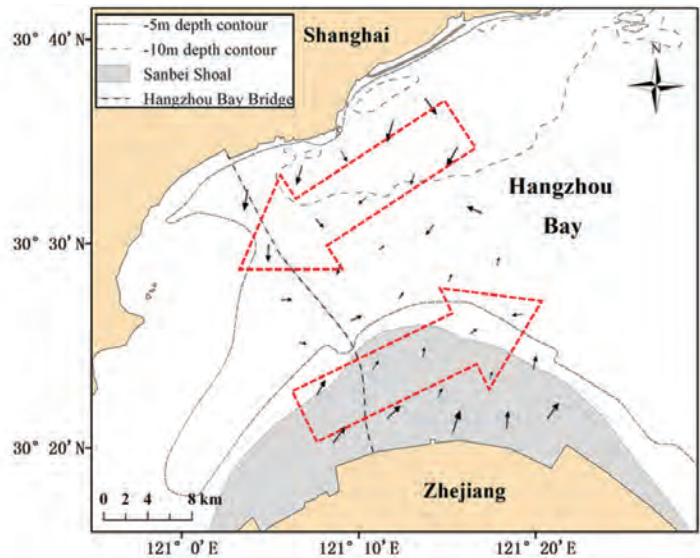


Figure 8. Distribution of sediment transport vector in the middle of Hangzhou Bay. The black arrows represent the computational results of sampling points, and the red dotted arrows are the macroscopic transport diagrams of sediments.

基于2013年杭州湾中部水文、悬沙和底部沉积物的实地调查数据，利用物质通量分解探索了杭州湾中悬浮沉积物的动力机制。同时，还通过分析颗粒大小趋势研究了河床表层沉积物的迁移趋势。结果表明，在潮退期间，杭州湾悬浮泥沙浓度的水位图以M型（双峰）为主，这主要归因于软泥层和浮泥层的产生。横向上，悬浮沉积物浓度的分布在南部较高，在北部较低。从宏观上看，研究区的净泥沙输送呈现出“北陆南海”的趋势，呈现出“C”形的输送方式。即，沉积物从湾口被运送到北侧的湾头，并从湾头被运送到南侧的湾口。平流和潮泵作用的泥沙输送占主导地位，而垂直循环的泥沙输送对总输沙量的贡献很小。而且，中心区域的泥沙运移以平流输送为主，而堤岸两侧附近的泥沙运移则由潮泵效应控制。潮汐的不对称性，即北部的涨潮优势和南部的退潮优势，是造成杭州湾总体“C”形运输方式动力机制的主要原因。此外，再加上窄头宽口地貌，杭州湾将保持南岸淤积和北岸冲刷的演变趋势。

Storm-induced hydrodynamic changes and seabed erosion in the littoral zone of Yellow River Delta: A model-guided mechanism study

Fan, Yaoshen; Chen, Shenliang; Pan, Shunqi; Dou, Shentang. *Continental Shelf Research*, 2020, 205: 104171.

Morphological evolution of large river deltas is highly vulnerable to extreme storm events due to insufficient sediment supply. As an abandoned delta lobe, the coasts along the northern Yellow River Delta (YRD) and Gudong Oil Field have recently suffered serious erosion due to extreme storm events and become increasingly vulnerable. In this study, a well validated and tested Delft 3D module by the observing hydrodynamic and sediment data to simulate the hydrodynamics and seabed erosion during a storm event in the littoral area of YRD. Observed wave, current and sediment data under both fair-weather and storm conditions were collected in the study area and used to validate the model. The results indicated that the model can reproduce well the hydro-dynamic and sediment transport processes. A series of numerical experiments were carried out to examine the hydrodynamic changes and sediment transports. In the numerical experiment of normal condition, there is hardly any sediment transport off the YRD. The numerical experiment of storm condition showed that storms enhanced tidal residual currents, weakened tidal shear front, and significant wave heights up to 2 m, considerably intensified the sediment resuspension and dispersal. The local sediment resuspension due to the increased wave-induced bottom stress promoted the sediment plume to expand to the central area of Laizhou Bay, which seemed to provide sediment source for offshore and southward transport. During the storm, the active nearshore sediment resuspension provided sediment source for offshore and southward transport. The intensive dynamics and sediment transport under storm conditions caused significant changes in seabed erosion and siltation. The main erosion occurred off the Gudong and northern YRD, while the main siltation appeared in the central area of Laizhou Bay. No significant recovery after a storm and frequent strong winds have an accumulative effect on the erosion, which is very likely to dominate the erosive states of the YRD coast in the future.

基于Delft3D模型系统构建了黄河三角洲动力地貌模型，对近岸海域水动力和泥沙过程进行数值模拟。对常态和风暴潮天气条件下水动力、泥沙输运和海床冲淤变化进行了对比研究，发现风暴潮期间在波流联合作用下，近岸海床泥沙强烈再悬浮。风暴潮期间泥沙表现为离岸、整体向南输运。风暴潮条件下近岸海床冲淤变化强烈，侵蚀区面积是常态条件下的数倍，侵蚀体积约是常态天气条件下的数十倍。秋-冬-春季频发的偏北大风是海床持续侵蚀的主要动力源。研究还发现，潮流切变锋及其剪切强度的空间分布共同限制了海床侵蚀区沉积物物源的补给；黄河三角洲近岸海床年际蚀积空间分布与海域切变锋分布高度相关。研究成果深化了黄河三角洲近岸侵蚀机制的认识。

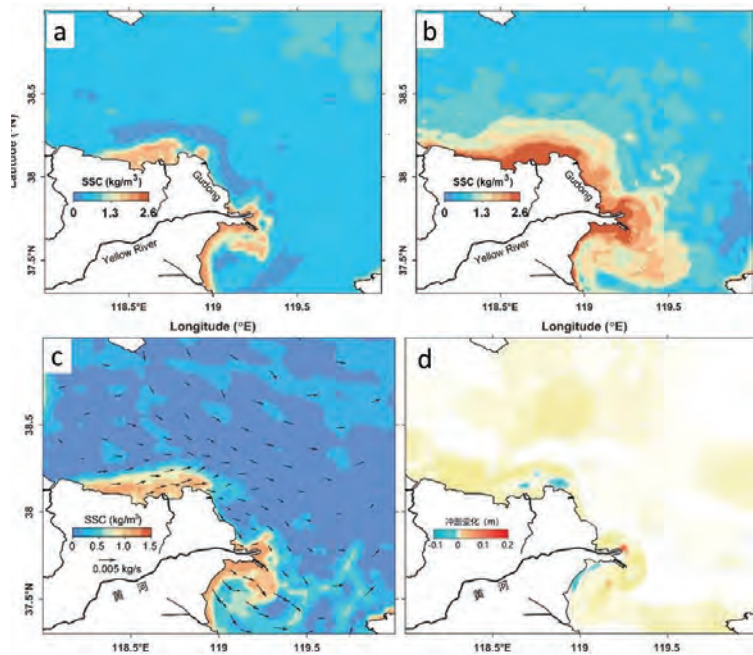


图2 黄河三角洲近岸常态(a)和风暴(b)条件下泥沙再悬浮与扩散以及风暴引起的泥沙输运(c)和海床冲淤演变(d)模拟

Monitoring and evaluation of sand nourishments on an embayed beach exposed to frequent storms in eastern China

Guo, Junli; Shi, Lianqiang; Pan, Shunqi, Ye, Qinghua; Cheng, Wufeng; Chang, Yang; Chen, Shenliang. *Ocean & Coastal Management*, 2020, 195: 105284.

Beach nourishment is a proved effective protection approach which has been widely used in recent years. An Argus video monitoring system has been set up to monitor morphological changes and effects of continuous nourishments at Dongsha beach, an embayed beach in Zhoushan Archipelago, eastern China. Video-derived shorelines along with their morphological parameters, such as dry beach width, dry beach area, beach orientation and unit width volume were analyzed during the monitoring period from June 2016 to July 2017. Analysis of video monitoring data shows that shorelines retreated during autumn and winter when storms were intensive, while advanced in spring and summer, with a lot of bulges occurred after nourishment projects. Abrupt variations in the beach orientation were always followed by gradual recoveries to the average beach orientation, while continuous counter-clockwise rotation occurred after March 2017 when storm events were sparse. Comparing the different beach responses to individual storm events, we found that small-scale and short-interval sand nourishment implemented timely after storms can compensate for sediment loss more effectively on this beach. This study can provide a reference for local beach management.

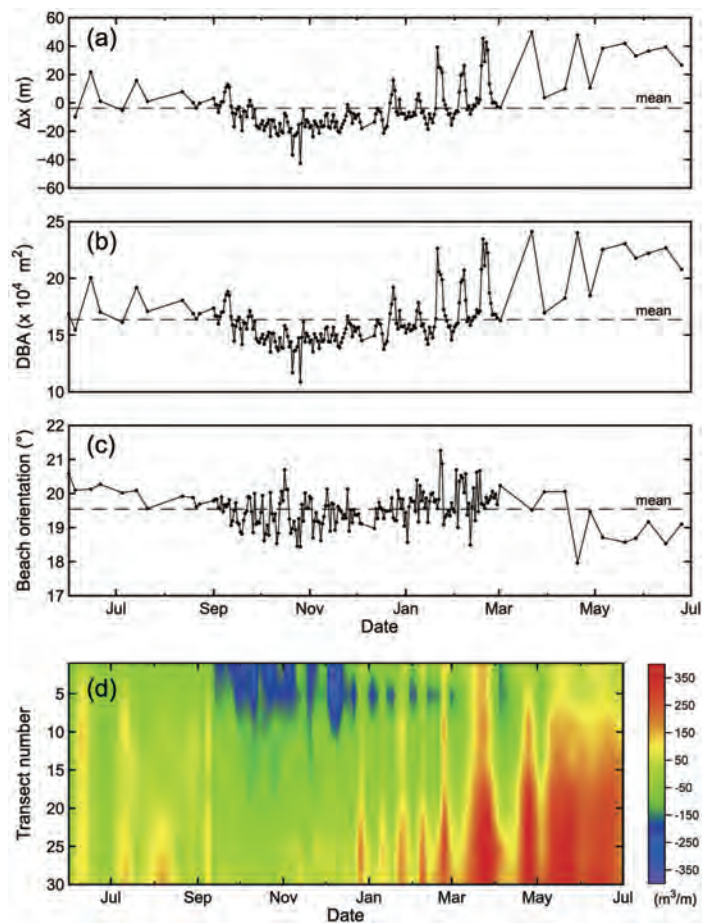


Fig. 5. Distribution of shoreline displacement (Δx) (a), dry beach area (DBA) (b), beach orientation (c) and unit width volumetric change (ΔV) (d) of Dongsha beach over the study period.

海滩养护是一种行之有效的保护手段，近年来已广泛使用。Argus视频监测系统在本研究中被用于监测舟山群岛东沙海滩的形态变化和连续养护事件的影响，在2016年6月至2017年7月的监测期内，分析了基于视频图像的海岸线、干滩宽度，干滩面积、海滩方向和单宽体积等形态参数。监测数据分析显示：海滩岸线在风暴频繁的秋冬季节发生显著地向陆后退，而在动力条件相对较弱的春季和夏季向海淤进，且在每次养护事件后岸线发生明显的向海前进；海滩方向突然变化之后，大部分情况下总是会逐渐恢复到海滩方向平均值，而在风暴事件稀少的2017年3月之后却发生了连续的逆时针旋转；通过比较海滩对单个风暴事件的不同反应，我们发现风暴后及时实施小规模和短间隔的沉积物补给可以更有效地补偿该海滩上的泥沙流失。该研究可为当地海滩管理提供参考。

Asian monsoon and oceanic circulation paced sedimentary evolution over the past 1,500 years in the central mud area of the Bohai Sea, China

Lyu, Wenzhe, Yang, Jichao; Fu, Tengfei; Chen, Yanping; Hu, Zhangxi; Tang, Ying Zhong; Lan Jianghu; Chen, Guangquan; Su, Qiao; Xu, Xingyong; Chen, Shenliang. *Geological Journal*, 2020, 55(7): 5606-5618.

Mud areas within China's marginal seas record critical information about historic environmental changes, which may have contributed to palaeoenvironmental processes and to understand their driving mechanisms. In this study, we investigated the sedimentary characteristics of a gravity core from the Bohai Sea central mud areas, to reveal the interactions between oceanic and climatic changes over the past 15 centuries. Sedimentary and mineral records indicated that the depositional environment and sediment sources were relatively stable, in which the East Asian Summer Monsoon (EASM) and Yellow Sea Warm Current (YSWC) variability can be derived. Based on these results, we found that the winter Arctic Oscillation (wAO) was negatively correlated with the coupled EASM and YSWC changes, namely, a negative (positive) relationship between EASM and YSWC during a positive (negative) wAO. We therefore suggest that over the past 15 centuries, Arctic winter climates may have modulated palaeoenvironmental changes over East Asia continental shelves, via teleconnections with the El Niño-Southern Oscillation (ENSO) and the Kuroshio Current.

中国边缘海的泥质区记录了很多古代环境变化的重要信息，可以为古环境及其驱动机制研究提供帮助。本文对取自渤海中央泥质区的钻孔沉积物进行沉积特征分析，以揭示过去1500年海洋和气候变化的内在作用机制。对沉积物的沉积学和矿物学分析发现，研究区沉积环境和物质来源相对稳定，并且从中提取出东亚夏季风和黄海暖流的变化信息。对提取的信息进行对比研究发现，东亚夏季风与黄海暖流的相关性受到冬季北极涛动的调节，东亚夏季风与黄海暖流呈正（负）相关时，冬季北极涛动为负（正）相位。研究还发现，冬季北极涛动的调节作用，是通过与ENSO和黑潮的遥相关作用实现的。

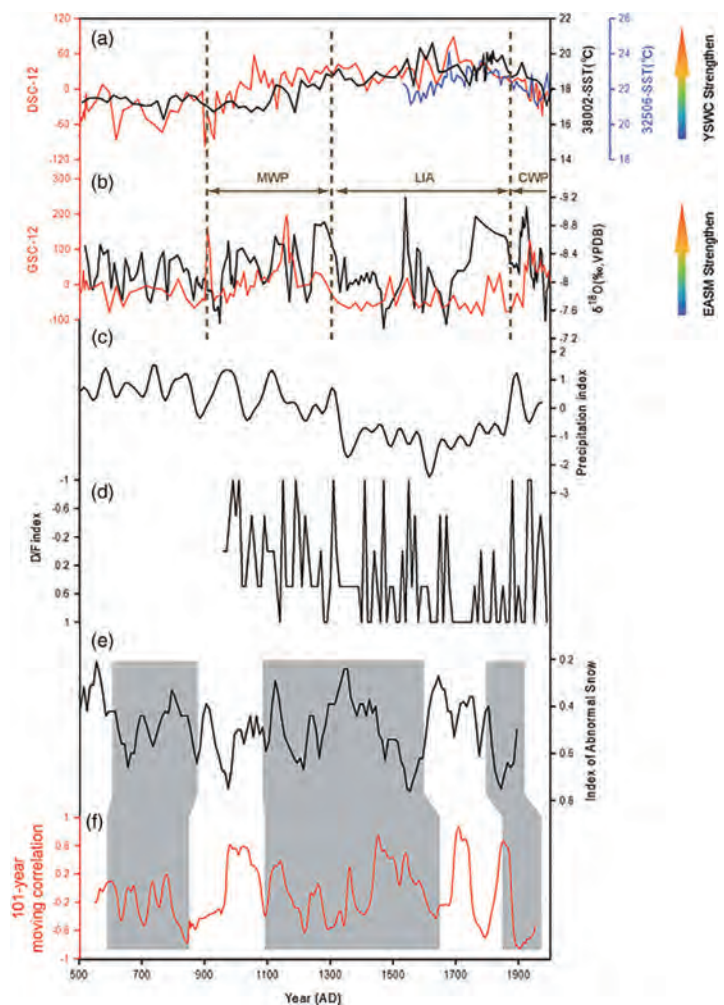


FIGURE 10 (a) Sea surface temperature (SST) records of sediment cores 32,506 (represented by the blue line) in the South Yellow Sea (He et al., 2014) and 38,002 (represented by the black line) in the North Yellow Sea (Zhang et al., 2019), the DSC-12 curve (represented by the red line), and the relationship between them; (b) stable oxygen isotope curve ($\delta^{18}\text{O}$, represented by the black line) for Heshang Cave (Hu et al., 2008), GSC-12 curve (represented by the red line), and their relationships; (c, d) the precipitation index record for north central China (Tan et al., 2011) and the drought/flood (D/F) index record of the Longxi area, with increased D/F index representing decreased precipitation (Tan et al., 2008); (e) index of abnormal snow (represented by the black line), a proxy for wAO (Chu et al., 2008); (f) 101-year moving correlations (represented by the red line) between GSC-12 and DSC-12 [Colour figure can be viewed at wileyonlinelibrary.com]

Beach management strategy for small islands: case studies of China

Zheng, Weiheng; Cai, Feng; Chen, Shenliang; Zhu, Jun; Qi, Hongshuai, Cao, Huimei; Zhao, Shaohua. *Ocean & Coastal Management*, 2020, 184: 104908.

Beaches' development on small islands has become increasingly important due to touristic appeals on their unique landscapes and natural endowments. However, compared with large islands and continental areas, the natural conditions of these islands are quite poor, their degree of development is relatively low, and they are insufficiently managed. Therefore, it is urgently necessary to undertake comprehensive management activities for tourist beaches on small islands. Three small islands in China, i.e. Meizhou, Gulang, and Weizhou, were selected as case studies to develop a preliminary beach management strategy. On the basis of a literature search, field observation, interviews with relevant officers, visits to shopkeepers and residents, tourist questionnaires and internet comment collection, this study summarizes the status of tourist beach management on small islands, analyzes tourist perceptions, and establishes a SWOT framework. A comprehensive tourist beach management system is developed with natural environmental, facility-cultural, and management sub-systems that are highly interactive and interrelated. The development pathway of tourist beach management on small islands can be subdivided into three individual stages, namely, passive, positive, and balanced development stages. Management should focus on the island's unique advantages and infrastructure building in the stage of passive development, management facilities improvement, recreational activities, policies and regulations in the stage of positive development, and balance tourist numbers against the ecological environment, the needs of residents and the tourist experience in the stage of balanced development. Moreover, the beach management being appropriate for a small island is highly correlated with its natural and/or cultural landscapes.

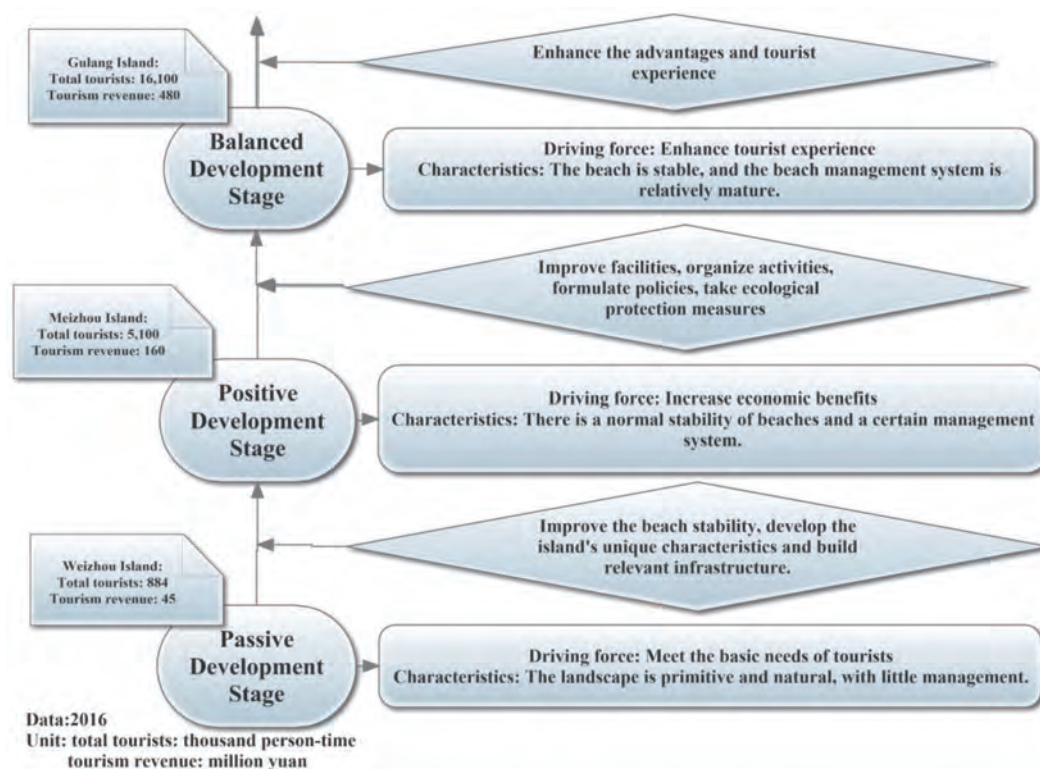


Fig. 5. Island tourist beach management developmental pathway.

由于小岛独特的风景和自然资源对旅游业的吸引力，小岛海滩的开发已变得越来越重要。但与大岛和大陆地区相比，这些岛屿自然条件较差，发展程度较低，也缺乏规范的管理。因此，对小岛旅游海滩进行综合管理研究的需求十分迫切。本文选择了中国的三个小岛（湄洲岛、鼓浪屿和涠洲岛）为例，对其旅游海滩的开发管理进行研究，以制定初步的小岛旅游海滩管理策略。本研究通过文献检索、实地勘察、相关部门访谈、店主和居民走访、游客问卷调查和网络评论收集等方法，总结出小岛旅游海滩管理现状，分析游客感知，建立SWOT框架。综合旅游海滩管理系统由自然环境、设施文化和管理子系统组成，三者相互影响、相互关联。小岛旅游海滩管理的发展路径可以细分为三个独立的发展阶段，即被动发展阶段、主动发展阶段和发展平衡阶段。在被动的发展阶段，应重点关注岛上独特的优势和基础设施建设，主动发展阶段重点关注设施改善、娱乐活动的组织、政策和法规的建立，发展平衡阶段重点关注生态环境、游客数量，以及居民和游客体验。此外，适合小岛的旅游海滩管理与其自然或人文景观高度相关。

Coastal ocean dynamics reduce the export of microplastics to the open ocean

Zhang, Zhiwei; Wu, Hui; Peng, Guyu; Xu, Pei; Li, Daoji. *Science of the Total Environment*, 2020, 713: 136634.

Huge amounts of plastic waste are dumped into the ocean every year, forming large Garbage Patches. Countless microplastics, originating from fragmentation, weathering of larger objects or primary sources, pose a wide-spread ecological risk. In this study, the dispersion of suspended and floating microplastic particles in the East China Seas (ECSs) and adjacent seas was investigated via a coupled numerical model that included a Lagrangian particle tracking module. The role of tidal dynamics was considered in transporting the microplastic particles in the ECSs and adjacent seas. The results highlighted significant differences between the transport of suspended and floating microplastic particles. Although microplastic particles originating from different source areas followed different pathways, the Taiwan Strait, the Tokara Strait and the Tsushima Strait were identified as the major delivery channels. Of these, the Taiwan Strait played the most important role in the export of near-surface floating microplastic particles from the ECSs. The results showed that only a small fraction of the microplastic particles produced from the coastal waters of China (~18%) and Korea (~14%) entered the Pacific Ocean. However, nearly all of the microplastic particles originating from the west and south coasts of Kyushu Is-land entered the Pacific Ocean.

On the cumulative dam impact in the upper Changjiang River: Streamflow and sediment load changes

Guo, Chao; Jin, Zhongwu; Guo, Leicheng; Lu, Jinyou; Ren, Shi; Zhou, Yinjun. *Catena*, 2020, 184: 104250.

Climate change and anthropogenic activities such as dam construction alter basin-scale hydrological regime of a river. The upper Changjiang River (uCR) stands out as one of the most heavily dammed rivers in the world after the construction of the Three Gorges Dam (TGD) and other large dams in its mainstem. Quantification of the cumulative dam impact is prerequisite for better river management. In this work, we provide a rigorous appraisal of the changes in streamflow, sediment load, and sediment composition at multiple time scales throughout the uCR based on data in 1950–2017. We observed that a decreasing trend in annual streamflow has emerged since 2015 at Yichang, the outlet of the uCR basin, although the changes were statistically insignificant for the first 65 years. The annual sediment load has decreased progressively and substantially, e.g., by 97% in 2010s compared to 1950s at Yichang. The Three Gorges Dam and the new large dams in the upstream mainstem accelerated the sediment load reduction in 2003 and 2014, respectively. As a result, the suspended sediment became finer, with a decrease in mean diameter from 17 μm in the 1960s to 8 μm in the 2010s at Yichang. We established a reservoir storage capacity index, which

is the ratio of the total reservoir storage capacity to annual streamflow, and identified a threshold of 4% larger than which the cumulative dam impact will induce profound sediment load reduction. We concluded that climate change and anthropogenic activities, in particular the large dams in the mainstem, have transformed the uCR system from a turbulent and muddy river to a placid one, which can affect fluvial processes as well as aquatic ecosystems by altering sediment and nutrient concentrations and ratios. These hydro-morphological changes merit the urgent attention of concerned authorities.

Variations of wave parameter statistics as influenced by water depth in coastal and inner shelf areas

Xiong, Jilian; You, Zaijin; Li, Jin; Gao, Shu; Wang, Qing; Wang, Yaping. *Coastal Engineering*, 2020, 159: 103714.

Wave height, pressure and orbital velocity statistics, as influenced by the factor of water depth, are analyzed on the basis of five data sets collected in situ from two intertidal sites with a mean water depth of 0.8–2.7 m and three inner shelf sites (water depths 14.6–27.6 m). Acoustic Doppler Velocimeters (ADV) were used to measure instantaneous wave pressure and current velocity at 0.20–0.35 m above sea bed. The zero-crossing wave analysis method was applied to analyze the wave data to determine the wave pressure amplitude P and orbital velocity amplitude U of individual waves, together with the frequency of occurrence distributions of P and U , which are compared with the three commonly-used, classic Rayleigh, modified Rayleigh and Weibull distributions. It is found that the distribution of P is almost identical to that of U for each of the five study sites. The distributions of P and U for the intertidal flat sites fit the Weibull distribution better than the classic or modified Rayleigh ones, indicating a shallowness effect which is associated with finite-banded wind-wave spectra and possible wave breaking or near-bed turbulence. On the other hand, the distributions of P and U measured at the three inner shelf sites agree almost equally with the three distributions. With increasing water depth, the distributions of P and U are shown to reduce from the two-parameter Weibull distribution at the shallow intertidal sites to the classic Rayleigh at the deep-water sites. For coastal engineering applications, an empirical formula is proposed to estimate more accurately the significant wave height in intermediate coastal waters based on the surface water elevation data.

Effect of Dikes on Saltwater Intrusion Under Various Wind Conditions in the Changjiang Estuary

Li, Linjiang; Zhu, Jianrong; Chant, Robert J.; Wang, Chuning; Pareja-Roman, L. Fernando. *Journal of Geophysical Research-Oceans*, 2020, 125(7): 43855.

To improve navigation, the deep waterway project (DWP) was implemented in the North Passage of the Changjiang Estuary in 1998, which includes a deep channel and two dikes protecting it. By altering estuarine morphology, the DWP can affect saltwater intrusion and mixing, with implications for drinking water intake and supply. In this study, we employ a numerical model to study the influence of dikes of the DWP on saltwater intrusion in the estuary under the climatic and persistent strong northerly wind conditions that occurred in February 2014. The model results show that the dikes prevent the southward transport of relatively low-salinity water at the mouth of the North Channel (NC) under climatic wind conditions, resulting in the weakening of saltwater intrusion and mixing in this channel. Under persistent strong northerly wind conditions, relatively high-salinity water is transported southward to the mouth of NC and blocked by the dikes causing a water level rise at the mouth of the NC. As a result, a large amount of high-salinity water advected into the NC and then out to the sea from the South Channel, forming a counterclockwise horizontal circulation. The salinity increases abnormally, but mixing decreases in the NC for no more salinity variance input with the implementation of the DWP. Overall, the DWP favors water intake for the reservoir in NC under climatic wind conditions and is unfavorable to water intake under persistent strong northerly winds (>9 m/s), which can lead to extremely severe saltwater intrusion.

Quantitative reconstruction of Holocene sediment sources contributing to the central Jiangsu coast, China: New insights into source - to - sink processes

Yang, Yang; Jia, Jianjun; Zhou, Liang; Gao, Jianhua; Gao, Wenhua; Shi, Benwei; Li, Zhanhai; Wang, Yaping; Gao, Shu. *Earth Surface Processes and Landforms*, 2020.

Coastal deltaic deposits are the primary locations for sediment storage on Earth, and quantifying their source contributions is a critical prerequisite for delineating S2S patterns in marginal seas. In most cases, quantification for the contribution by fine-grained sediments (i.e. particle size $< 63\mu\text{m}$) is considered to be representative to constrain the overall sediment supply. However, this approach may be inappropriate because large differences exist between the two quantities. Here we propose an approach to solve the problem, which is based on the maximum number of tracers from multiple sediment size fractions incorporating the content of all size fractions of sediment. Using this approach, absolute source contributions during the Holocene are reconstructed that provide a first-order model for the S2S pattern of the central Jiangsu coast, China. The Huanghe River is the strongest driver for the Holocene sedimentation, with a mean contribution of $\sim 72\pm 6\%$ ($1417 \times 10^8\text{t}$). The absolute contributions from the Changjiang and offshore areas were of secondary importance, (i.e. $\sim 17\pm 1\%$ ($330 \times 10^8\text{t}$) and $\sim 11\pm 5\%$ ($217 \times 10^8\text{t}$), respectively). The results show that a large difference between the relative and absolute source contributions and the assumption that the relative contribution represents the absolute contribution is invalid in a coastal setting. The impact of the Huanghe is mainly based on episodic events, such as the event of 1128-1855 AD. The model also reveals that the offshore sediments are as important as the Changjiang sediments for the central Jiangsu coast during the Holocene. Thus, the model provides both the time series and overall quantities of sediment supply during the formation and evolution of the Holocene tidal flats on the Jiangsu coast. Our findings shed new light on quantitative analysis of sediment sources applicable to future S2S studies of marginal seas.

Internal waves triggered by river mouth shoals in the Yangtze River Estuary

Wang, Jianxing; Wang, Tao; Xing, Fei; Wu, Hao; Jia, Jianjun; Yang, Zuosheng; Wang, Yaping. *Ocean Engineering*, 2020, 214: 107828.

Internal waves are widespread in oceans and play an important role in mixing. In this study, we observed some oscillations of pycnoclines that are thought to be caused by internal waves by analyzing the vertical and temporal variations of current speed and density during ebbs of the neap tides in the south channel of the Yangtze River (Changjiang) Estuary. These oscillations have an amplitude of 1–2 m and a duration of 2–3 h. To explore the mechanism of this phenomenon, topographic features of the seabed were recorded, and a huge sandbar was observed at the place where the oscillations occurred. Therefore, we infer the oscillations in the south channel were caused by the process that the stratified water flowed over the sandbar which induced internal hydraulics and led to the excitation of internal waves. Froude number was calculated according to the internal-hydraulics equations and the results verified our hypothesis that it was the interactions between the stratified water and rapidly changing topography that triggered internal hydraulics. Internal waves caused upward-directed water movement, which influenced the vertical transport of sediment and the vertical distribution of the suspended sediment. Internal waves also increased the mass diffusivity coefficient (K_z) at the interface of internal waves.

Dynamic mechanism of an extremely severe saltwater intrusion in the Changjiang estuary in February 2014

Zhu, Jianrong; Cheng, Xinyue; Li, Linjiang; Wu, Hui; Gu, Jinghua; Lyu, Hanghang. *Hydrology and Earth System Sciences*, 2020, 24: 5043-5056.

Estuarine saltwater intrusions are mainly controlled by river discharge and tides. Unexpectedly, an extremely severe saltwater intrusion event occurred in February 2014 in the Changjiang estuary under normal river discharge conditions. This intrusion cut off the freshwater input for 23 d into the Qingcaosha reservoir, which is the largest estuarine reservoir in the world, creating a severe threat to water safety in Shanghai. No similar catastrophic saltwater intrusion has occurred since records of salinity in the estuary have been kept. During the event, a persistent and strong northerly wind existed, with a maximum speed of 17.6 m s^{-1} , lasting 9 d and coinciding with a distinct water level rise. Our study demonstrates that the extremely severe saltwater intrusion was caused by this northerly wind, which drove substantial landward net water transport to form a horizontal estuarine circulation that flowed into the northern channel and out of the southern channel. This landward net water transport overpowered the seaward-flowing river runoff and transported a large volume of highly saline water into the northern channel. The mechanisms of this severe saltwater intrusion event, including the northerly wind, residual water level rise, landward water transport and resulting horizontal circulation, etc., were systematically investigated.

Frequency and magnitude variability of Yalu River flooding: numerical analyses for the last 1000 years

Sheng, Hui; Xu, Xiaomei; Gao, Jianhua; Kettner, Albert J.; Shi, Yong; Xue, Chengfeng; Wang, Ya Ping; Gao, Shu. *Hydrology and Earth System Sciences*, 2020, 24: 4743-4761.

Accurate determination of past flooding characteristics is necessary to effectively predict the future flood disaster risk and dominant controls. However, understanding the effects of environmental forcing on past flooding frequency and magnitude is difficult owing to the deficiency of observations (data available for less than 10 % of the world's rivers) and extremely short measurement time series (< 100 years). In this study, a numerical model, HYDROTREND, which generates synthetic time series of daily water discharge at a river outlet, was applied to the Yalu River to (1) reconstruct annual peak discharges over the past 1000 years and estimate flood annual exceedance probabilities and (2) identify and quantify the impacts of climate change and human activity (runoff yield induced by deforestation and dam retention) on the flooding frequency and magnitude. Climate data obtained from meteorological stations and ECHO-G climate model output, morphological characteristics (hypsometry, drainage area, river length, slope, and lapse rate), and hydrological properties (groundwater properties, canopy interception effects, cascade reservoir retention effect, and saturated hydraulic conductivity) form significant reliable model inputs. Monitored for decades, some proxies on ancient floods allow for accurate calibration and validation of numerical modeling.

Simulations match well the present-day monitored data (1958–2012) and the literature records of historical flood events (1000–1958). They indicate that flood frequencies of the Yalu River increased during 1000–1940, followed by a decrease until the present day. Frequency trends were strongly modulated by climate variability, particularly by the intensity and frequency of rainfall events. The magnitudes of larger floods, events with a return period of 50 to 100 years, increased by 19.1 % and 13.9 %, respectively, due to climate variability over the last millennium. Anthropogenic processes were found to either enhance or reduce flooding, depending on the type of human activities. Deforestation increased the magnitude of larger floods (100- and 50-year floods) by 19.2 %–20.3 %, but the construction of cascade reservoirs in 1940 significantly reduced their magnitude by 36.7 % to 41.7 %. We conclude that under intensified climate change and human activities in the future, effective river engineering should be considered, particularly for small- and medium-sized mountainous river systems, which are at a higher risk of flood disasters owing to their relatively poor hydrological regulation capacity.

Constraints of salinity- and sediment-induced stratification on the turbidity maximum in a tidal estuary

Lu, Ting; Wu, Hao; Zhang, Fan; Li, Jiasheng; Zhou, Liang; Jia, Jianjun; Li, Zhanhai; Wang, Ya Ping. *Geo-Marine Letters*, 2020, 40(5): 765-779.

The vertical density gradients of salinity and suspended sediment concentration (SSC) cause stratification in estuaries, which play a vital role in the turbulence structure, water mixing, and sediment transport. To investigate the effect of stratification, especially SSC-induced stratification, on maintaining the estuarine turbidity maximum (ETM), we conducted in situ measurements on sediment dynamics at the upper and central ETM sites in the South Passage of Changjiang Estuary in July 2018. The gradient Richardson number was estimated as a proxy for the stratification that is attributable to salinity or/and SSC. We found that salinity-induced stratification was observed mainly on the surface and in the middle layers, whereas SSC-induced stratification occurred mainly in the near-bottom layers. Furthermore, at the central ETM, the baroclinic effect was enhanced during the neap tide when the salinity-induced stratification was stronger than that during the spring tide. In the early phase of floods with minimum velocity during the neap tide, salinity-induced stratification suppressed the turbulence and vertical diffusion of sediments. Moreover, the flocculation enhanced the settling process within the water column. Consequently, high concentrations of fine-grained sediments formed near the bottom and promoted SSC-induced stratification, thereby leading to the continuous accumulation and trapping of sediments. In conclusion, the interactions among the “salinity- and SSC-induced stratification” processes served as crucial constraints of the temporal and spatial variations of the ETM in the Changjiang Estuary.

An automated procedure to calculate the morphological parameters of superimposed rhythmic bedforms

Wang, Li; Yu, Qian; Zhang, Yongzhan; Flemming, Burghard W.; Wang, Yunwei; Gao, Shu. *Earth Surface Processes and Landforms*, 2020, 45: 3496-3509.

Subaqueous dunes are often observed to be superimposed on larger dunes, sand bars and tidal ridges, while smaller dunes may also be found superimposed on larger dunes. In this study an automated method has been developed by which the geometry of superimposed rhythmic bedforms can be analysed. The method combines two-dimensional (2D) Fourier analysis, wavelet transform, zero-crossing analysis and a variety of filters. Instead of applying conventional manual procedures, the wavelength of interest can be automatically determined by a series of 2D Fourier analyses, which is a critical first step for automated analysis of dune geometries. Based on such efficient data preprocessing, the method can accurately determine dune orientation, separate target bedform profiles, and identify crests and troughs. With the input of bathymetry, the dominant regional dune orientation can be determined together with the geometric parameters of individual dunes (wavelength, height, leeside angles) and their spatial distribution. The method was applied to both synthetic and observed bathymetries of a tidal ridge off the Jiangsu coast, China, and a sand bank in the Dover Strait, UK. The results show that almost all dunes in the domain were detected and their geometric parameters accurately calculated, especially in areas of bedform superimposition.

Influence of suspended sediment front on nutrients and phytoplankton dynamics off the Changjiang Estuary: A FVCOM-ERSEM coupled model experiment

Ge, Jianzhong; Torres, Ricardo; Chen, Changsheng; Liu, Jie; Xu, Y; Bellerby, Richard; Shen, Fang; Bruggeman, Jorn; Ding, Pingxing. *Journal of Marine Systems*, 2020, 204: 103292.

High-turbidity water is a common feature in the estuary and inner shelf. Sediment suspension functions

as a modulator that directly influences the interactions among nutrients, phytoplankton and other related ecosystem variables. A physical-biological coupling model system was applied to examine the impact of sediment front on interactions among on suspended sediment, vertical mixing, nutrients and phytoplankton over the inner shelf off the high-turbidity, phosphate-limited Changjiang Estuary. The physical model was the Finite-Volume Community Ocean Model (FVCOM) and the biological model was the European Regional Seas Ecosystem Model (ERSEM). Results revealed that in the nearshore region the growth of phytoplankton over the spring-summer seasons was limited by suspended sediments and intensified vertical mixing during the autumn-winter seasons extended the sediment-induced suppression extended offshore to restrict the phytoplankton growth over the shelf. Nutrients were diluted by spreading of freshwater discharge and significantly decreased off the suspended sediment front due to the depletion by the offshore phytoplankton growth. The simulation results showed that although the diatom phytoplankton dominated the Chlorophyll a (Chl-a) concentration, the non-diatom group had a more contribution to the biomass. The relatively high phytoplankton biomass was found over the offshore deep underwater valley area as results of remote advection by the Taiwan Warm Current and weak turbulent mixing.

Interannual Variabilities of Nutrients and Phytoplankton off the Changjiang Estuary in Response to Changing River Inputs

Ge, Jianzhong; Shi, Shenyang; Liu, Jie; Xu, Yi; Chen, Changsheng; Bellerby, Richard; Ding, Pingxing. *Journal of Geophysical Research-Oceans*, 2020, 125(3): e2019JC015595.

Coastal ecosystems are strongly influenced by terrestrial inputs of freshwater, sediments, and nutrients, particularly in a megariver estuary of the Changjiang River. A remarkable increase in nutrient loading from the Changjiang River to the shelf has been observed over the period from 1999 to 2016 and turned the region into a high eutrophication condition. The Finite-Volume Community Ocean Model and the European Regional Seas Ecosystem Model were coupled to assess the impact of the nutrient loading on the interannual variability of nutrients and phytoplankton. The model was first validated via observational data, and then dynamical analysis were conducted. Singular vector decomposition analysis indicated that the rapid change of local ecosystem was highly correlated with the change in river nutrient contributions. The Changjiang estuarine ecosystem was phosphate limited. The phosphate exhibited local variation, while the abundant nitrate from the river was diluted by the low-nitrate oceanic water. The suspended sediment was significantly correlated with phytoplankton but not with nutrients. The ratio of diatom biomass to dinoflagellate biomass respected a rapid response to strong oscillations in the river nutrient input. High diatom primary production occurred near the sediment front, whereas the dinoflagellate bloom extended significantly offshore. The spring diatom and dinoflagellate blooms had major peaks in the empirical orthogonal function Modes 1 and 2, and the autumn bloom is characterized by secondary peaks from Mode 2 in the autumn.

Dynamic Response of the Fluid Mud to a Tropical Storm

Ge, Jianzhong; Chen, Changsheng; Wang, Zheng Bing; Ke, Keteng; Yi, Jinxu; Ding, Pingxing. *Journal of Geophysical Research-Oceans*, 2020, 125(3): e2019JC015419.

Fluid mud (FM) is a unique sedimentary feature in high-turbidity estuaries, where it can make a rapid contribution to morphodynamics. Insufficient field measurements and fixed-point monitoring lead to deficient understandings of the formation, transport, and breakdown of the FM under extreme weather conditions. A field survey was conducted in the Changjiang Estuary during the period of turbidity maximum, just after Typhoon Haikui. The measurements captured the formation of the FM beneath the suspended layers,

particularly around the lower reach of the North Passage. The thickness of the observed FM gradually decreased landward along the channel, with the maximum value reaching ~0.9 m. The major features of the observed storm-induced FM were simulated using the Finite-Volume Community Ocean Model. The results indicated that the initial appearance of the FM was the result of a typhoon-intensified, salinity-induced stratification in the outlet region. The subsequent landward propagation of the FM was driven by the combined effects of the FM-induced mud surface pressure gradient force and saltwater intrusion near the bottom. Weak mixing during the subsequent neap tidal period sustained the FM as it rapidly extended into the middle region of the North Passage. This produced a large velocity shear at the interface of the FM and upper suspension layer, increasing the entrainment from the FM to the upper suspension layer. As a result of the increased tidal mixing, the FM weakened and then finally broke down in the subsequent spring tidal period.

Impacts of River Engineering on Multi-Decadal Water Discharge of the Mega-Changjiang River

Ma, Binbin; Pang, Wenhong; Lou, Yaying ; Mei, Xuefei; Wang, Jie; Gu, Jinghua; Dai, Zhijun. *Sustainability*, 2020, 12(19): 8060.

Knowledge of river engineering impacts on water discharge is significant to flow guidelines and sustainable water resource managements for balancing human consumption and the natural environment. In this study, based on the collected multi-decadal discharge data at Yichang, Hankou, and Datong stations, we determined that in October, Three Gorges Dam contributed 34.4%, 24.5%, and 18.7% to the discharge decrease in the upper, middle, and lower reach, respectively, while Gezhouba Dam contributed 14.5%, 10.7%, and 10%. Danjiangkou Reservoir caused the discharge ratio of Hanjiang to Changjiang to decline from 7.2% during 1954–1973 to 6.3% during 1973–2014. Owing to growing water withdrawal and consumption, we suggest that the distribution of water diversion and consumption should be regulated to prevent the probable occurrence of the severe issue of salt water intrusion in the Changjiang Estuary in 2028.

An automated procedure to calculate the morphological parameters of superimposed rhythmic bedforms

Wang, Li; Yu, Qian; Zhang, Yongzhan; Flemming, Burghard W.; Wang, Yunwei; Gao, Shu. *Earth Surface Processes and Landforms*, 2020, 45: 3496-3509.

Subaqueous dunes are often observed to be superimposed on larger dunes, sand bars and tidal ridges, while smaller dunes may also be found superimposed on larger dunes. In this study an automated method has been developed by which the geom-etry of superimposed rhythmic bedforms can be analysed. The method combines two-dimensional (2D) Fourier analysis, wavelet transform, zero-crossing analysis and a variety of filters. Instead of applying conventional manual procedures, the wavelength of interest can be automatically determined by a series of 2D Fourier analyses, which is a critical first step for automated analysis of dune geometries. Based on such efficient data preprocessing, the method can accurately determine dune orientation, separate target bedform profiles, and identify crests and troughs. With the input of bathymetry, the dominant regional dune orientation can be deter-mined together with the geometric parameters of individual dunes (wavelength, height, leeside angles) and their spatial distribution. The method was applied to both synthetic and observed bathymetries of a tidal ridge off the Jiangsu coast, China, and a sand bank in the Dover Strait, UK. The results show that almost all dunes in the domain were detected and their geometric parameters accurately calculated, especially in areas of bedform superimposition.

Exploring records of typhoon variability in eastern China over the past 2000 years

Yang, Yang; Zhou, Liang; Normandeau Alex; Jia, Jianjun; Yin, Qijun; Wang, Yaping; Shi, Benwei; Lei Gao; Gao, Shu. *Geological Society of America Bulletin*, 2020, 13(11-12): 2243-2252.

How climate controls tropical cyclone variability has critical implications for modern human society but is not well understood due to the short length of observational records. To probe this knowledge gap, we present a synthesis of intense typhoon activity from the northwestern Pacific over the past 2000 years, which is supported by a new, well-resolved tidal flat sedimentary record from the Jiangsu coast, eastern China. The record reveals nine intervals of typhoon frequency, indicating that the frequency of intense typhoons has varied on multi-centennial scales over the past 2000 years. Our synthesis shows strong evidence for a seesaw pattern of intense typhoon frequency between south-eastern China and Japan and Korea. This pattern can be explained by the El Niño and Southern Oscillation–East Asian Monsoon–sea surface temperature hypothesis, which potentially explains the basin-wide typhoon climate in the northwestern Pacific region. A shift in typhoon activity was identified from 550–280 to 280–50 yr B.P. during the Little Ice Age, when typhoon activity changed from active to quiescent or vice versa. Centennial-scale shifts in Intertropical Convergence Zone and Western Pacific Warm Pool sea surface temperature are likely to be the primary forcing mechanisms driving this shift. Results obtained here provide links between typhoon activity and the El Niño and Southern Oscillation, the East Asian Monsoon, and the Western Pacific Warm Pool sea surface temperature, and therefore improve our ability to fully assess intense typhoon activity in future climate warming.

河口海岸生态与环境

Estuarine and Coastal Ecology and Environment

Variations of soil bacterial diversity and metabolic function with tidal flat elevation gradient in an artificial mangrove wetland

Yin, Yichen; Yan, Zhongzheng. *Science of the Total Environment*, 2020, 718: 137385.

Understanding the sensitivity of soil bacteria to environmental fluctuations can enhance the management of micro-bial ecosystem services in artificial mangrove wetlands. In this study, the variation in bacterial diversity and metabolic functions in different compartments (bulk soil, rhizosphere soil, and rhizoplane) of the soil and mangrove plant along the tidal elevation gradient was studied in Xiatanwei (Xiamen China) mangrove wetland park, a *Kandelia obovata*-dominated artificial mangrove stand. With the increase of the tidal flat elevation, the soil pH, total organic matter, and soil moisture contents decreased significantly, while the soil electric conductivity and redox potential increased significantly. The bacterial diversity in the bulk soil and the rhizosphere soil both decreased with the elevation of tidal levels. The relative abundance of the dominant phyla in the bulk and rhizosphere soils decreased with the rise of the tidal flat level. A significant rhizosphere effect was observed in the roots of *K. obovata* that the rhizosphere soil had higher bacterial diversity and richness than that in the bulk soil nearby. The rhizosphere soil of *K. obovata* at the low-tidal flat was enriched with the genera *Nitrospira* and *Planctomycetes*, which are valuable for the mangrove ecosystem. The Chao1 estimator and Shannon index of the bacterial community in the rhizoplane of *K. obovata* were much lower than that in the rhizosphere and bulk soils. Results of Biolog-Eco assay show that the bacterial groups in low tidal flat bulk soil had the highest ability in utilizing the carbon sources, which was indicated by the high values of average well color development and the high McIntosh index, and the utilization ability of carbon source decreased with the increase of tidal flat levels. The variation of the soil humidity and Eh jointly shaped the diversity and metabolic function of soil bacterial communities along the tidal flat elevation gradient.

了解土壤细菌对环境波动的敏感性有助于加强对人工红树林湿地中微生物生态系统服务功能的管理。在这项研究中，研究了在厦门红树林湿地公园中，土壤和红树林植物秋茄的不同区室细菌多样性和代谢功能沿潮汐海拔梯度的变化。随着潮滩高程的增加，土壤pH，总有机质和土壤含水量显著下降，而土壤电导率和氧化还原电

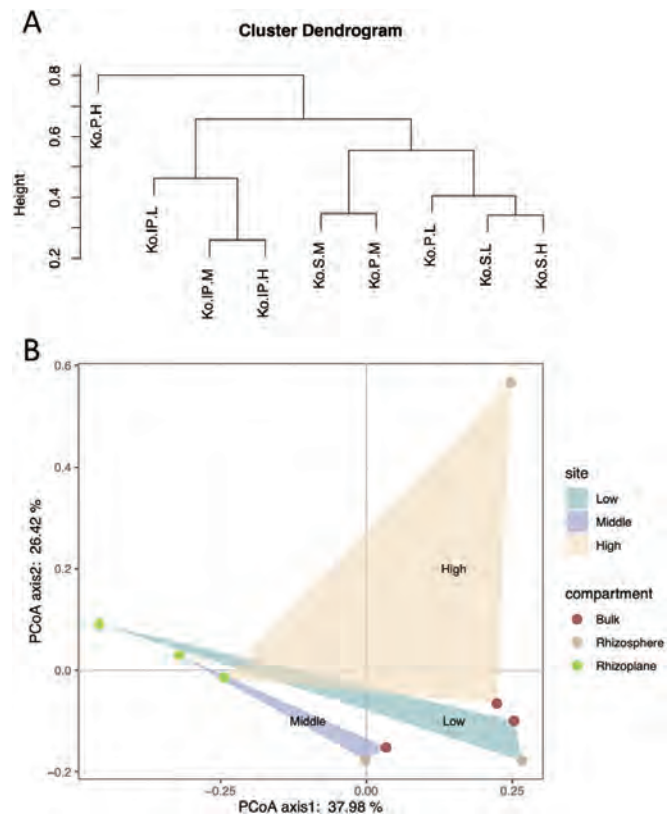


Fig. 4. (A) Principal Coordinate Analyses (PCoA) analysis of the bacterial community presented in bulk soil, rhizosphere soil and rhizoplane at different levels of tidal flat; (B) hierarchical clustering analysis of the samples (For different samples, Ko represents *K. obovata*; H, M, and L represent the high, middle and low tidal levels, respectively; S, P, and IP represent the bulk soil, rhizosphere soil, and rhizoplane, respectively).

位则显著增加。根周土壤和根际土壤中的细菌多样性都随着潮滩水平的升高而降低。随着潮滩水位的升高，根周土壤和根际土壤中优势细菌种群的相对丰度降低。在秋茄的根际中观察到明显的根际效应，即根际土壤比根周土壤具有更高的细菌多样性和丰度。低潮滩上秋茄的根际土壤富含硝化螺菌属和浮游菌属，这对红树林生态系统具有重要意义。秋茄根际平面中细菌群落的Chao1估计量和Shannon指数远低于根际和土壤中的细菌群落。Biolog-Eco分析的结果表明，低潮滩根周土壤中的细菌群落对碳源的利用能力最高，表现为显著升高的平均孔显色值（AWCD）和McIntosh指数。根周土壤细菌的碳源利用能力随着潮滩高程的升高而降低。土壤湿度和Eh的变化共同影响了沿潮滩梯度的土壤细菌群落的多样性和代谢功能。

Atmospheric microplastic over the South China Sea and East Indian Ocean: abundance, distribution and source

Wang, Xiaohui; Li, Changjun; Liu, Kai; Zhu, Lixin; Song, Zhangyu; Li, Daoji. *Journal of Hazardous Materials*, 2020, 389: 121846.

At present, microplastic (MP) is pervasive globally and has a regional difference. Recent studies have identified MP in the terrestrial atmospheric environment. However, the connection between terrigenous atmospheric MP emissions and impacts over the ocean is not well known. Here, we present the distribution of atmospheric MP abundance over the ocean based on a transoceanic survey conducted across 21 sampling transects from the Pearl River Estuary (PRE) to the South China Sea (SCS) and then to the East Indian Ocean (EIO). The abundance of atmospheric MP over the PRE (4.2 ± 2.5 items/ 100 m^3) was significantly higher than that over the EIO (0.4 ± 0.6 items/ 100 m^3). However, the abundance of atmospheric MP in the SCS (0.8 ± 1.3 items/ 100 m^3) was not significantly different from the EIO and PRE. This result revealed that MP undergoes long-range transport, more than 1000 km away, through the atmosphere, but atmospheric MP transmission as the main source of oceanic MP based on transoceanic studies is not a plausible assumption. Furthermore, backward trajectory model analysis of 21 sampling transects preliminary showed the potential sources of atmospheric MP over the PRE, SCS, and EIO.

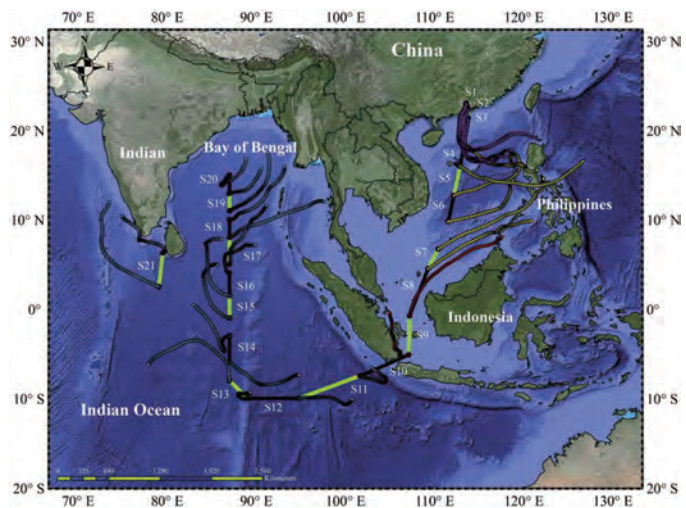


Fig. 6. The backward trajectory of the air parcel along all sampling transects. The dotted line represents the three-day backward trajectories of air parcels in different sampling areas.

在2019年3月20日至2019年4月25日期间，我们搭乘“实验3号”使用悬浮颗粒采样器对珠江口、南海、东印度洋21个连续采样断面大气悬浮微塑料进行了采样。结果发现我们发现大气中微塑料在采样横断面上呈稀疏分布，且具有不同的材质形态特征。在全部采样断面大气中微塑料的丰度为0~7.7个/ 100 m^3 ，平均为1.0个/ 100 m^3 。珠江口的大气中微塑料丰度 (4.2 ± 2.5 个/ 100 m^3) 显著大于东印度洋 (0.4 ± 0.6 个/ 100 m^3)，而南海的大气微塑料的丰度 (0.8 ± 1.3 个/ 100 m^3) 与东印度洋和珠江口无显著差异。研究结果还揭示了，微塑料可以通过大气远距离运输到一千多公里以外的地方，但大气传输是海洋微塑料的主要来源并不是一个合理的假设。目前，海洋微塑料主要是由河流向海洋输送已经被广大研究者所认知。此外，对21个采样横断面的后退轨迹模型分析初步显示了东印度洋、南海和珠江口大气中微塑料的潜在来源。其中南海大气微塑料潜在来源于菲律宾，而东印度洋大气微塑料主要来源于印度次大陆。

Influence of the herbicide haloxyfop-R-methyl on bacterial diversity in rhizosphere soil of *Spartina alterniflora*

Liang, Qiuyao; Yan, Zhongzheng; Li, Xiuzhen. *Ecotoxicology and Environmental Safety*, 2020, 194: 110365.

Haloxyfop-R-methyl (haloxyfop) can efficiently control *Spartina alterniflora* in coastal ecosystems, but its effect on soil microbial communities is not known. In the present study, the impact of the haloxyfop on rhizosphere soil bacterial communities of *S. alterniflora* over the dissipation process of the herbicide has been studied in a coastal wetland. The response of the bacterial community in the rhizosphere (iron plaque) of *S. alterniflora* subjected to haloxyfop treatment was also investigated. Results showed that the persistence of haloxyfop in the rhizosphere soil followed an exponential decay with a half-life of 2.6–4.9 days, and almost all of the haloxyfop dissipated on Day 30. The diversity of rhizosphere soil bacteria was decreased at the early stages (Days 1, 3 & 7) and recovered at late stages (Days 15 & 30) of the haloxyfop treatment. Application of haloxyfop treatment increased the relative abundance of the genera *Pseudomonas*, *Acinetobacter*, *Pontibacter*, *Shewanella* and *Aeromonas*. Strains isolated from these genera can degrade herbicides efficiently, which possibly played a role in the degradation of haloxyfop. The rhizosphere bacterial diversity was reduced on Day 15 while being vastly enhanced on Day 30. Soil variables, including the electric conductivity, redox potential, and soil moisture, along with the soil ha-loxyfop residue, jointly shape the bacterial community in rhizosphere soil.

作为我国一种主要的入侵植物，互花米草在滨海湿地的扩散严重影响了湿地生态系统的结构和功能。有效控制互花米草对于维持生物多样性和生态服务功能具有重要的意义。目前对互花米草的治理方式之一是喷洒除草剂—高效盖草能。高效盖草能比“刈割+淹水”的治理方式成本低，见效快，但是对该治理方式给湿地生态环境带来的影响还所知甚少。申报人通过野外控制实验研究高效盖草能在潮滩土壤中的消散过程及其对土壤微生物群落结构的影响，首次定量分析了高效盖草能在潮滩沉积物中的消散动态过程，发现其呈指数衰减的规律。高效盖草能处理在短期内显著降低了沉积物微生物的多样性，但长期影响不显著。这项研究成果揭示了高效盖草是一种相对环境友好的互花米草治理方式，为合理管控互花米草入侵提供了科学依据。

作为我国一种主要的入侵植物，互花米草在滨海湿地的扩散严重影响了湿地生态系统的结构和功能。有效控制互花米草对于维持生物多样性和生态服务功能具有重要的意义。目前对互花米草的治理方式之一是喷洒除草剂—高效盖草能。高效盖草能比“刈割+淹水”的治理方式成本低，见效快，但是对该治理方式给湿地生态环境带来的影响还所知甚少。申报人通过野外控制实验研究高效盖草能在潮滩土壤中的消散过程及其对土壤微生物群落结构的影响，首次定量分析了高效盖草能在潮滩沉积物中的消散动态过程，发现其呈指数衰减的规律。高效盖草能处理在短期内显著降低了沉积物微生物的多样性，但长期影响不显著。这项研究成果揭示了高效盖草是一种相对环境友好的互花米草治理方式，为合理管控互花米草入侵提供了科学依据。

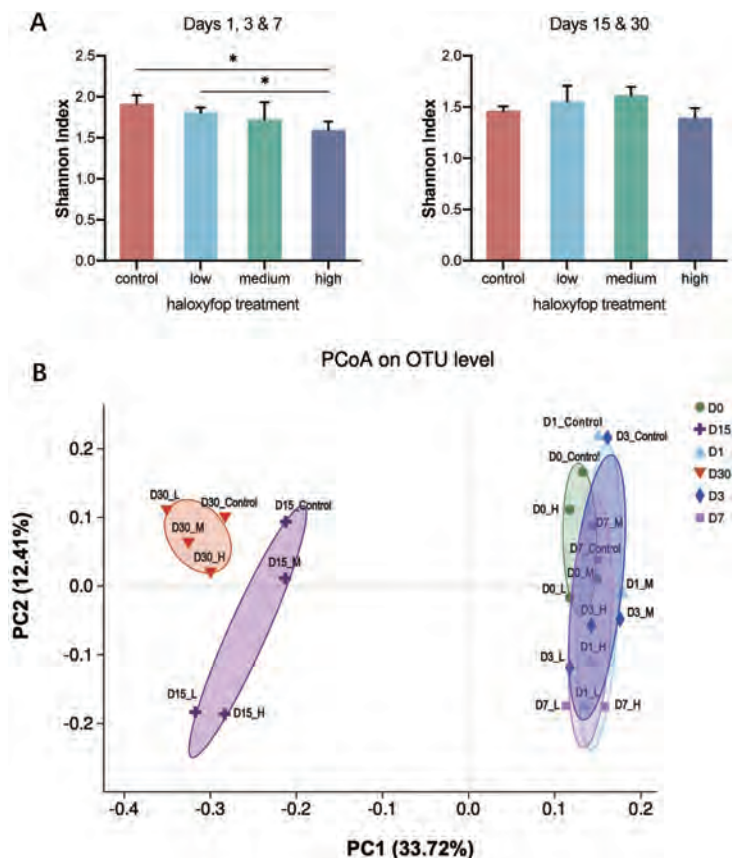


Fig. 6. The backward trajectory of the air parcel along all sampling transects. The dotted line represents the three-day backward trajectories of air parcels in different sampling areas.

Nitrogen isotopic analysis of nitrate in aquatic environment by cadmium- hydroxylamine hydrochloride reduction.

Jin, Jie; Jiang, Shan; Zhang, Jing. *Rapid Communications In Mass Spectrometry*, 2020, 34: e8804.

Rationale: The nitrogen isotopic ratio of nitrate ($\delta^{15}\text{N-NO}_3^-$ value) is a critical parameter to understand nitrogen biogeochemical cycling in aquatic systems. Current approaches to the determination of $\delta^{15}\text{N-NO}_3^-$ values involve time-intensive handling procedures, use of toxic chemicals and complicated microbial incubation.

Methods: A chemical reduction method for measuring the $\delta^{15}\text{N-NO}_3^-$ values of aquatic samples was established. Nitrate was first quantitatively reduced to nitrite in a column filled with copper-coated cadmium granules, and the produced nitrite further reduced to nitrous oxide gas with hydroxylamine hydrochloride. The nitrogen isotope ratio of the produced nitrous oxide was measured using a continuous flow isotope ratio mass spectrometer coupled with a purge and cryogenic trap system.

Results: The optimized experimental conditions were: solution acidity, H^+ concentration is 0.46 M, $\text{pH} = 0.34$; dosage of hydroxylamine, molar ratio of NH_2OH to NO_2^- is 4; reaction temperature, 45°C ; and reaction time, 14-16 h. No salt effect was found in this method. The reproducibility of the $\delta^{15}\text{N-NO}_3^-$ value for the laboratory standard was better than 0.3‰ for long-term measurements (20 nmol NO_3^- requirement). **Conclusions:** This method provides a reliable approach in the determination of $\delta^{15}\text{N-NO}_3^-$ values at natural abundance. It provides (1) high measurement accuracy, (2) ease of operation, (3) environmental-friendly procedure (less toxic reagents used), and (4) suitability for both fresh and saline water samples.

文章建立了一种天然丰度硝酸盐氮稳定同位素的测定方法。硝酸盐被 $\text{Cd-NH}_2\text{OH}$ 还原为 N_2O 气体后利用IRMS测定氮稳定同位素。该方法具有高准确度、高精密度的优点，同时操作步骤简单、减少了有毒易爆化学试剂的使用，可应用于淡水、海水等不同天然水体的硝酸盐氮稳定同位素测定。

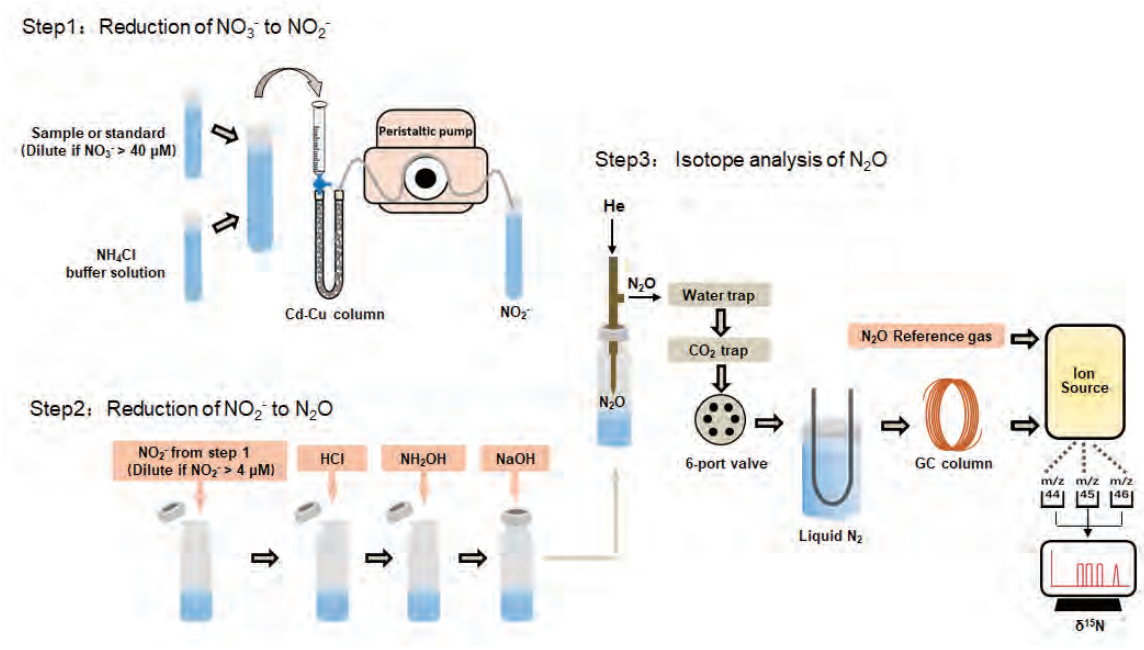


FIGURE 4 Schematic of the $\text{Cd-NH}_2\text{OH}$ method for $\delta^{15}\text{N-NO}_3^-$ analysis.

Environmental impact and recovery of the Bohai Sea following the 2011 oil spill.

Wang, Yujue; Lee, Kenneth; Liu, Dongyan; Guo, Jie; Han, Qiuying; Liu, Xihan; Zhang, Jingjing. *Environmental Pollution* (Barking, Essex : 1987), 2020, 263(Pt B): 114343.

The 2011 spill at platforms B and C of the Penglai 19-3 oil field in the Bohai Sea has been the worst oil spill accident in China. To assess long-term effects, a comprehensive monitoring program of chemical and biological variables (within a 2.2 km radius of the spill site) was conducted five years after the spill. Comparison of nutrient, Chl-a and oil concentrations in seawater, TOC, PAHs, heavy metals concentrations within the sediments, and the abundance and biomass of macrobenthic organisms to values obtained before and after the oil spill in previous studies indicate habitat recovery has occurred within the Bohai Sea following the episodic oil release. Observed elevated oil concentration in the water column and higher concentrations of two heavy metals, five PAHs, TOC, TOC/TN and lower values of $\delta^{13}\text{C}$, together with a reduction in macrobenthic biomass in near-field samples, suggest the influence of contaminants from chronic releases of oil and operational waste discharges within the vicinity of the oil platforms.

通过对渤海溢油区海水营养盐、叶绿素、油含量、沉积物TOC、PAHs、重金属以及底栖动物的分析，表明2011年蓬莱19-3 油田溢油对海区的残余影响基本消失，但在油田平台仍存在污染物和油污的慢性释放的问题，影响着周边水体和生物环境。

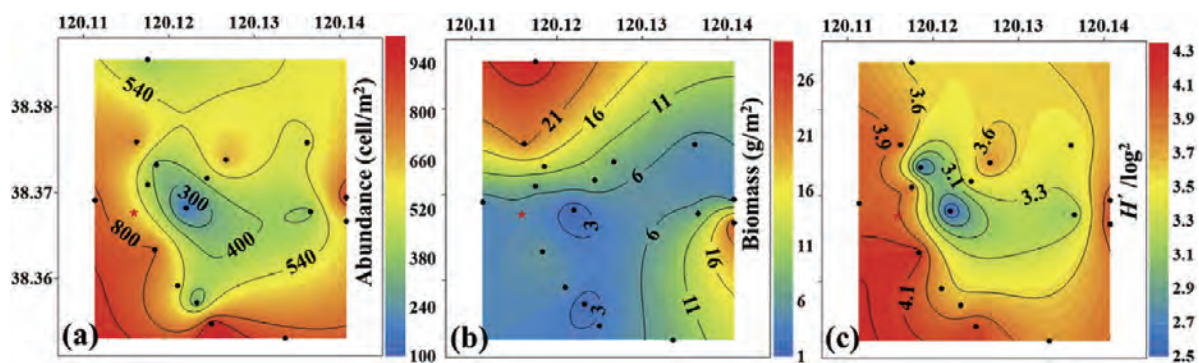
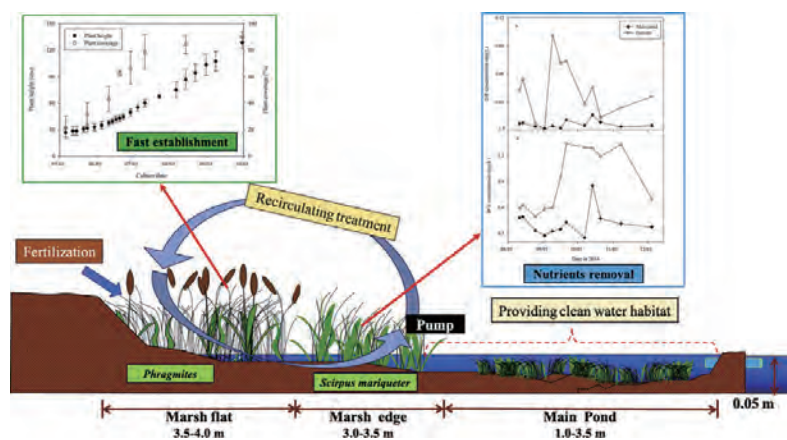


Fig. 5. Spatial distribution of macrobenthic abundance (a), biomass (b) and Shannon-Wiener index (H') (c).

Restoring wetlands outside of the seawalls and to provide clean water habitat.

Chen, Xuechu; Huang, Yingying; Yang, Hualei; Pan, Liping; Perry, Danielle C; Xu, Ping; Tang, Jianwu; You, Wenhui; He, Xiaoyan; Wen, Quan. *Science of the Total Environment*, 2020, 721: 137788.

In this study, we reported a practice at northern Hangzhou Bay, southeast China aimed at restoring coastal wetlands within the intertidal zone outside of the seawalls. The principle idea is protecting the site and helping the marsh establishment by engineering measures, and thereafter, relieving the protections to encourage the self-organization of the restored ecosystem. The results of this implementation showed the marsh reached an average



vegetation cover of 70% in the first year. The excess nitrogen was removed by an ecological recirculating treatment system, which was coupled in the wetland. The long-term performance of the wetland suggested that it could resist disturbances such as hurricanes and algal blooms, and provided clean water habitat for aquatic fauna. By presenting the case of Hangzhou Bay, we call for more novel coastal restoration implementations that aim to create new boundaries with engineering features and self-organization, which benefit both human and nature.

报道了杭州湾北岸侵蚀岸段海堤外潮滩湿地的生态恢复设计与实践，主要通过人工干预与自然演替相结合的复合技术快速恢复湿地并改善水质。在湿地植物生长期调控水位，为种苗提供适宜的非淹水生境，并待湿地植被成熟后，引入自然潮汐，达到恢复本地湿地植物、促进湿地生态系统结构和功能发育的目的。长期运行表明，该技术能够有效促进盐沼植被生长，使植被抗自然灾害能力增强，并进一步改善水质，且具有抑制藻类水华的能力。

Distribution and behaviour of dissolved selenium in tropical peatland-draining rivers and estuaries of Malaysia

Chang, Yan; Muller, Moritz; Wu, Ying; Jiang, Shan; Cao, Wan Wan; Qu, Jian Guo; Ren, Jing Ling; Wang, Xiao Na; Rao, En Ming; Wang, Xiao Lu; Mujahid, Aazani; Muhamad, Mohd Fakharuddin; Aun, Edwin Sia Sien; Jang, Faddrine Holt Ajon; Zhang, Jing. *Biogeosciences*, 2020, 17(4): 1133-1145.

Selenium (Se) is an essential micronutrient for aquatic organisms. Despite its importance, our current knowledge of the biogeochemical cycling of dissolved Se in tropical estuaries is limited, especially in Southeast Asia. To gain insights into Se cycling in tropical peat-draining rivers and estuaries, samples were collected from the Rajang, Malu-dam, Sebuyau, Simunjan, Sematan, Samunsam and Lunda rivers and estuaries in western Sarawak, Malaysia, in March and September 2017 and analysed for various forms of Se (dissolved inorganic and organic). Mean total dissolved Se (TDSe), dissolved inorganic Se (DISe) and dissolved organic Se concentrations (DOSe) were 2.2 nmol L^{-1} (range: 0.7 to 5.7 nmol L^{-1}), 0.18 nmol L^{-1} (range: less than the detection limit to 0.47 nmol L^{-1}) and 2.0 nmol L^{-1} (range: 0.42 to 5.7 nmol L^{-1}), respectively. In acidic, low-oxygen, organic-rich blackwater (peatland-draining) rivers, the concentrations of DISe were extremely low (near or below the detection limit, i.e. $0.0063 \text{ nmol L}^{-1}$), whereas those of DOSe were high. In rivers and estuaries that drained peatland, DOSe / TDSe ratios ranged from 0.67 to 0.99, showing that DOSe dominated. The positive relationship between DISe and salinity and the negative relationship between DOSe and salinity indicate marine and terrestrial origins of DISe and DOSe, respectively. The positive correlations of DOSe with the humification index and humic-like chromophoric dissolved organic matter components in freshwater river reaches suggest that peat soils are probably the main source of DOSe. The DOSe fractions may be associated with high molecu-

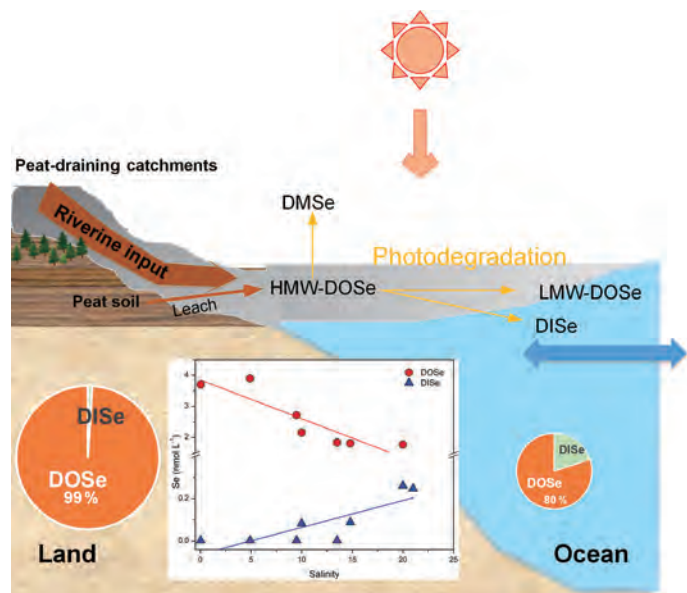


Figure 6. Conceptual diagram of the behaviour of Se species in the Maludam estuary. HMW, LMW and DMSe represent high molecular weight, low molecular weight and dimethylselenide, respectively.

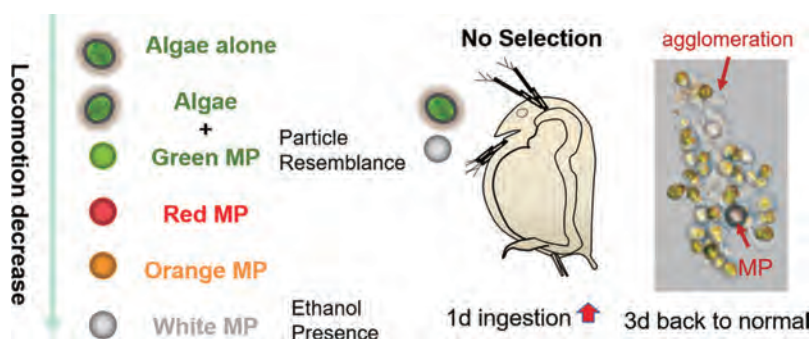
lar weight peatland-derived aromatic and black carbon compounds and may photodegrade to more bioavailable forms once transported to coastal waters. The TDSe flux delivered by the peat-draining rivers exceeded those reported for other small rivers and is quantitatively more significant than previously thought.

硒是多种生物必需的痕量营养元素。然而对热带河口硒的生物地球化学循环的认识非常有限，特别是东南亚地区。选择马来西亚沙捞越三角洲为研究区域，系统分析泥炭型河口水体中溶解态Se(IV)、Se(VI)和有机硒浓度成沿盐度梯度变化格局。在低氧酸性和富有机质的黑水河中，无机硒DISE的含量极低，主要以有机硒形态存在。在泥炭型河口，DISE浓度呈现随盐度增加的趋势，揭示了海洋是DISE的主要来源，这和其它河口的行为显著不同。DOSe浓度呈现随盐度减小的趋势，揭示了陆地是DOSe的主要来源。河流端DOSe与腐殖化参数和类腐殖质有色溶解有机质呈显著正相关性，说明泥炭土壤可能是DOSe的主要来源。DOSe可能主要和高分子量、芳香性、黑碳有机质相结合，而且易被光降解为生物可利用性强的化合物。泥炭河流向海洋输送的TDSe通量远超过其它报道的小河流，而且比较重要。

Is color a matter of concern during microplastic exposure to *Scenedesmus obliquus* and *Daphnia magna*?

Chen, Qiqing; Li, Yue; Li, Bowen. *Journal of Hazardous Materials*. 2020, 383: 121224.

Toxicities of microplastics (MPs) on aquatic organisms have been widely investigated often by using white or transparent MPs. However, various colored MPs scatter in the real aquatic environment. Here we investigated four colored MPs' effects on *Scenedesmus obliquus* algal growth first. Under the light condition, algal growth increased initially due to hormesis stimulation and then decreased gradually at higher MP concentrations. Green colored MPs exhibited the lowest inhibition effect, probably due to their resemblance to algae; white MPs inhibited the algal growth significantly, which was attributed to the presence of ethanol. Turbulence condition seemed to diminish algal growth differences among groups, but it led to slight oxidative stress. Furthermore, we also tested MP effects on *Daphnia magna* feeding ability. Results indicated that daphnids were probably not able to distinguish colored MPs from algae. But their algae ingestion amounts increased when MPs reached to 40% of algal cells, probably because daphnids could widen their filtering gapes when food quality decreases. However, this phenomenon did not last until the 3rd day, as the agglomeration of MPs and algae made them settle down. Overall, our results highlighted the color may alter some MP effects and is necessary to be considered in (eco) toxicological studies.



Under the light condition, algal growth increased initially due to hormesis stimulation and then decreased gradually at higher MP concentrations. Green colored MPs exhibited the lowest inhibition effect, probably due to their resemblance to algae; white MPs inhibited the algal growth significantly, which was attributed to the presence of ethanol. Turbulence condition seemed to diminish algal growth differences among groups, but it led to slight oxidative stress. Furthermore, we also tested MP effects on *Daphnia magna* feeding ability. Results indicated that daphnids were probably not able to distinguish colored MPs from algae. But their algae ingestion amounts increased when MPs reached to 40% of algal cells, probably because daphnids could widen their filtering gapes when food quality decreases. However, this phenomenon did not last until the 3rd day, as the agglomeration of MPs and algae made them settle down. Overall, our results highlighted the color may alter some MP effects and is necessary to be considered in (eco) toxicological studies.

本文主要考察了不同色彩的微塑料是否会导致不同的水生态毒性效应。通过对斜生栅藻的影响研究发现，在光照条件时，当微塑料浓度较低时会刺激藻类的生长，而当微塑料的浓度逐渐升高后，则表现出生长抑制现象。其中，绿色的微塑料产生的抑制效应最弱，这可能是由于它们与藻类的相似性所致；而白色的微塑料的生长抑制效应最显著，这归因于其中少量添加剂的存在。当我们在系统中引入湍流条件时，可以减少不同颜色微塑料暴露组之间的差异，但是藻类产生了轻微的氧化应激反应。同时，我们还测试了微塑料对大型蚤摄食能力的影

响。研究结果显示，大型蚤无法有效区分有色微塑料和藻类颗粒。当微塑料比例达到藻类数量的40%时，由于食物质量的下降，大型蚤还会通过扩大其滤过口径而增加对藻类的摄入。

Photochemical dissolution of buoyant microplastics to dissolved organic carbon: Rates and microbial impacts

Zhu, Lixin; Zhao, Shiye; Bittar, Thais B.; Stubbins, Mon; Li, Daoji. *Journal of Hazardous Materials*, 2020, 383: 121065.

Trillions of plastic fragments are afloat at sea, yet they represent only 1–2% of the plastics entering the ocean annually. The fate of the missing plastic and its impact on marine life remains largely unknown. To address these unknowns, we irradiated post-consumer microplastics (polyethylene, PE; polypropylene, PP; and expanded polystyrene, EPS), standard PE, and plastic-fragments collected from the surface waters of the North Pacific Gyre under a solar simulator. We report that simulated sunlight can remove plastics from the sea surface. Simulated sunlight also fragmented, oxidized, and altered the color of the irradiated polymers. Dissolved organic carbon (DOC) is identified as a major byproduct of sunlight-driven plastic photodegradation. Rates of removal depended upon polymer chemistry with EPS degrading more rapidly than PP, and PE being the most photo-resistant polymer studied. The DOC released as most plastics photodegraded was readily utilized by marine bacteria.

海洋中微塑料的归宿问题是当前微塑料研究的难点问题，根据估算，目前已知的海洋中塑料的储存量仅不到年入海输出量的1%，超过99%进入海洋的最终归宿尚不明确，这是海洋塑料和微塑料污染的生态风险评估中的主要障碍之一。本文探究了光照对于不同种类的海微塑料的降解动力过程。研究发现，微塑料的光降解动力过程与微塑料的种类密切相关，聚苯乙烯和聚丙烯光降解速率最快，而聚乙烯降解速率最慢。经过估算，光照是海洋表层漂浮微塑料的主要的汇，其产物会对海洋生态系统的物质循环产生较大的影响。

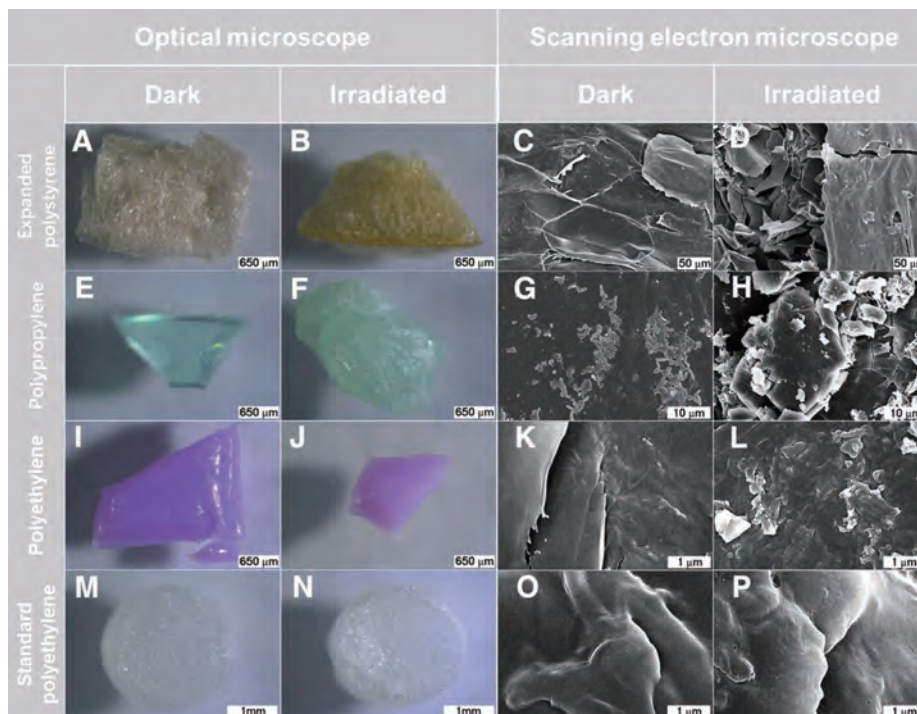


Fig. 2. Optical and scanning electron microscopic photographs of dark and irradiated microplastic samples.

Variation in microplastics composition at small spatial and temporal scales in a tidal flat of the Yangtze Estuary, China

Wu, Fengrun; Pennings, Steven C.; Tong, Chunfu; Xu, Yutian. *Science of the Total Environment*, 2020, 699: 134252.

Microplastics are small, degrade slowly, and easily persist in the water column because they are close to neutrally buoyant. Understanding the distribution of microplastics is fundamental to evaluating the ecological risks that they cause and to identifying ways to control microplastics pollution. Most of the existing research on the distribution of microplastics in the coastal zone has focused on large spatial and temporal scales. To build on past work, we investigated variation in microplastics in a tidal flat of the Yangtze Estuary on small spatial (sediment depth, mudflat vs. vegetation zone) and temporal (fortnightly and semidiurnal) scales. Microplastics were more abundant in surface (0–2 cm) sediments during neap versus spring tide cycles, likely indicating increased deposition during periods with calm waters and increased suspension when water was more turbulent, but did not vary at greater depths in the sediment. Individual microplastics particles were also larger during neap versus spring tide periods. In contrast to the variation between spring and neap tide periods, we found no variation in the abundance of microplastics on the semidiurnal scale. Microplastics were also more abundant in the transect in the vegetation than at slightly lower elevations in the adjacent mudflat. Across all samples, the abundance of microplastics was negatively correlated with the strength of hydrological processes such as submergence time and flow velocity. Our results showed that sampling of microplastics in the intertidal environment needs to consider variation among spring and neap tide cycles, and also among different intertidal habitats that may differ only slightly in elevation. We encourage coupling sampling with direct measures of hydrological processes so that variation in microplastics abundance and size can be rigorously linked to hydrological processes.

在已有工作基础上，我们研究了长江口潮滩微塑料在较小空间尺度（沉积物深度，光滩与植被带）和较小时间尺度（半日潮和半月潮）的变化。相对于大潮期，小潮期表层（0-2 cm）沉积物中的微塑料丰度更高，这可能表明在水文过程强度较弱的情况下微塑料的沉积增加，而在水文过程强度增强时微塑料的悬浮会增加，但这种变化在更深层的沉积物中不显著。微塑料颗粒的粒径在小潮期相比大潮期更大。与大、小潮期之间的变化特征不同，半日潮尺度上沉积物的微塑料含量没有变化。与邻近较低高程的光滩断面相比，植被带中的微塑料含量更高。微塑料的丰度与水文过程的强度（例如淹没时间和流速）呈负相关。我们的结果表明，河口湿地沉积环境中的微塑料采样需要考虑大潮和小潮之间水文过程的差异，以及高程可能有所不同的生境之间的差异。

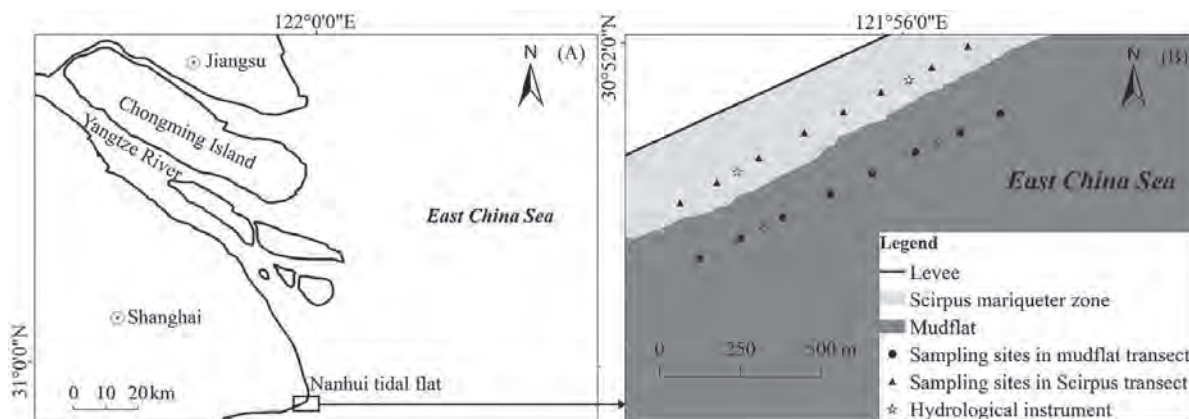


Fig. 1. A) location of the study area at the southern side of the Yangtze Estuary. B) Layout of the two transects in the Nanhui tidal flat.

Conversion of coastal wetlands, riparian wetlands, and peatlands increases greenhouse gas emissions: A global meta-analysis

Tan, Lishan; Ge, Zhenming; Zhou, Xuhui; Li, Shihua; Li, Xiuzhen; Tang, Jianwu *Global Change Biology*. 2020, 26(3): 1638-1653.

Land-use/land-cover change (LULCC) often results in degradation of natural wetlands and affects the dynamics of greenhouse gases (GHGs). However, the magnitude of changes in GHG emissions from wetlands undergoing various LULCC types remains unclear. We conducted a global meta-analysis with a database of 209 sites to examine the effects of LULCC types of constructed wetlands (CWs), croplands (CLs), aquaculture ponds (APs), drained wetlands (DWs), and pastures (PASs) on the variability in CO₂, CH₄, and N₂O emissions from the natural coastal wetlands, riparian wetlands, and peatlands. Our results showed that the natural wetlands were net sinks of atmospheric CO₂ and net sources of CH₄ and N₂O, exhibiting the capacity to mitigate greenhouse effects due to negative comprehensive global warming potentials (GWPs; -0.9 to -8.7 t CO₂-eq ha⁻¹ year⁻¹). Relative to the natural wetlands, all LULCC types (except CWs from coastal wetlands) decreased the net CO₂ uptake by 69.7%–456.6%, due to a higher increase in ecosystem respiration relative to slight changes in gross primary production. The CWs and APs significantly increased the CH₄ emissions compared to those of the coastal wetlands. All LULCC types associated with the riparian wetlands significantly decreased the CH₄ emissions. When the peatlands were converted to the PASs, the CH₄ emissions significantly increased. The CLs, as well as DWs from peatlands, significantly increased the N₂O emissions in the natural wetlands. As a result, all LULCC types (except PASs from riparian wetlands) led to remarkably higher GWPs by 65.4%–2,948.8%, compared to those of the natural wetlands. The variability in GHG fluxes with LULCC was mainly sensitive to changes in soil water content, water table, salinity, soil nitrogen content, soil pH, and bulk density. This study highlights the significant role of LULCC in increasing comprehensive GHG emissions from global natural wetlands, and our results are useful for improving future models and manipulative experiments.

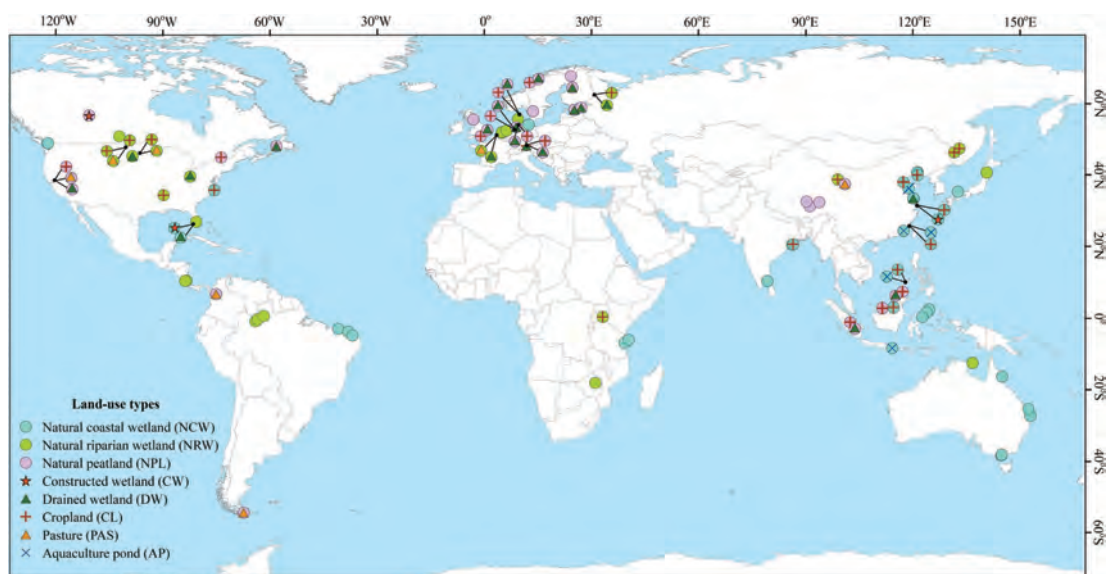


FIGURE 1 Location of the study sites. Natural coastal wetlands (NCWs) include tidal salt marshes, mangroves, and tidal freshwater marshes; natural riparian wetlands (NRWs) include undisturbed freshwater marshes and swamps in the riparian zones of rivers or shallow lakes; and natural peatlands (NPLs) include undisturbed fens, bogs, and swamps. The symbols of LULCC types of constructed wetland (CW), cropland (CL), aquaculture pond (AP), drained wetland (DW), and pastures (PAS) were overlapped on the symbols of natural wetlands (details in Tables S1–S3)

全球土地利用变化是影响自然生态系统服务功能的首要因素。本研究表明了全球范围内，自然湿地是大气中CO₂的汇，其全球增温潜势为-0.9—-8.7 t CO₂-eq ha⁻¹ yr⁻¹，具有显著缓解温室效应的能力。然而，通过研究全球主要土地利用变化类型（人工湿地、农田、养殖塘、排干湿地和牧场）对自然滨海和内陆湿地温室气体CO₂、CH₄和N₂O通量的影响，发现土地利用变化削弱了湿地的CO₂吸收能力，而且人工湿地、养殖塘、农田和排干湿地的转化显著增加了CH₄和N₂O排放。使得区域的增温潜势增幅达65.4—2948.8%。研究同时发现，土地利用变化主要是通过土壤含水量、水位、盐度、土壤氮含量、土壤pH和土壤容重的变化对温室气体通量产生影响。

The ocean's ultimate trashcan: Hadal trenches as major depositories for plastic pollution

Peng, Guyu; Bellerby, Richard; Zhang, Feng; Sun, Xuerong; Li, Daoji. *Water Research*, 2020, 168: 115121.

Plastic debris and marine microplastics are being discharged into the ocean at an alarming scale and have been observed throughout the marine environment. Here we report microplastic in sediments of the Challenger Deep, the deepest known region on the planet, abyssal plains and hadal trenches located in the Pacific Ocean (4900 m to 10,890 m). Microplastic abundance reached 71.1 items per kg dry weight sediment. That high concentrations are found at such remote depths, knowing the very slow sinking speed of microplastics, suggests that supporting mechanisms must be at-play. We discuss cascading processes that transport microplastics on their journey from land and oceanic gyres through intermediate waters to the deepest corners of the ocean. We propose that hadal trenches will be the ultimate sink for a significant proportion of the microplastics disposed in the ocean. The build-up of microplastics in hadal trenches could have large consequences for fragile deep-sea ecosystems.

塑料碎片和海洋微塑料正以惊人的规模排入海洋，并在整个海洋环境中被观察到。本文报告了地球上最深的已知区域——挑战者深渊，及深海平原和位于太平洋海底海沟（4900 m至10890 m）的沉积物中的微塑料赋存特征。每千克干重沉积物的微塑料丰度达到71.1个。在人类活动如此罕至的海洋深度中发现的高浓度微塑料分布，并且已知微塑料的沉降速度很慢，这表明有其他帮助沉降的机制在此过程中发挥作用。我们讨论了微塑料从海洋表面沉降到海底的一系列过程，这些过程将微塑料从陆地和大洋环流中，通过中层水运送到海洋最深处。我们建议，深渊海沟将是大量塑料及微塑料的重要的储存库及最终的汇。深渊海沟中微塑料的积累可能对脆弱的深海生态系统产生重大影响。

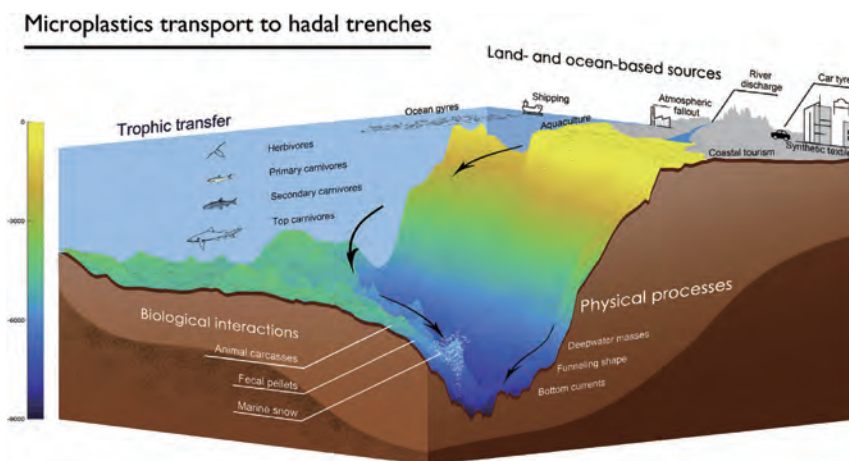


Fig. 4. A schematic of pathways of microplastics from various sources entering the hadal trenches (taking the New Britain Trench as an example), making the deepest spots on Earth the ultimate sink and depository for microplastics. Microplastics from land and ocean sources may enter the marine environments and transfer through the food chains. Through biological interactions (e.g., marine snow), microplastics increase density and sink to deeper layers. Once entering the hadal zone, physical processes facilitate microplastics to deposit in the hadal trenches and bioavailable for benthic organisms.

Wave effects on seedling establishment of three pioneer marsh species: survival, morphology and biomechanics.

Cao, Haobing; Zhu, Zhenchang; James, Rebecca; Herman, Peter M J; Zhang, Liquan; Yuan, Lin; Bouma, Tjeerd J. *Annals of Botany*, 2020, 125: 345-352.

• **Background and Aims** It is important to have an in-depth mechanistic understanding of tidal marsh establishment and dynamics to ensure the long-term persistence of these valuable ecosystems. As wave forcing may be expected to impact seedling establishment, we studied the effect of water-imposed drag forces on seedling survival, morphology and biomechanical properties of three marsh pioneer species that are dominant along the salinity gradient in many areas around the world: *Spartina anglica* (salt to brackish), *Scirpus maritimus* (brackish) and *Phragmites australis* (brackish to fresh).

• **Methods** Using a newly developed plant-shaking mesocosm (PSM) that mimicked water-imposed wave drag forces, the effect of wave stress on seedling survival was examined, together with impacts on morphology and biomechanical properties.

• **Key Results** After 7 weeks of exposure to wave stress, lowered seedling survival and growth for all species was revealed. Wave treatments increased the root/shoot biomass ratio to enhance anchorage and made seedlings more flexible (i.e. reduced flexural rigidity), which might be regarded as a mixed outcome between a stress avoidance and stress tolerance strategy.

• **Conclusions** The different biomechanical responses between the three dominant marsh pioneer species, overall, make them less resistant to external stress. Therefore, our results indicate that the likelihood of marshes becoming established is reduced if wave energy increases. Despite the different biomechanical response of these three pioneer species to waves, the seedlings of all species were found to have low resistance to external stresses.

以世界广泛分布的盐沼物种为研究对象，结合盐沼实生苗定居的“机会窗口”理论，探讨了盐沼实生苗定居对沉积动态干扰的响应，对理解盐沼定居的普遍机制和指导修复实践具有重要意义。

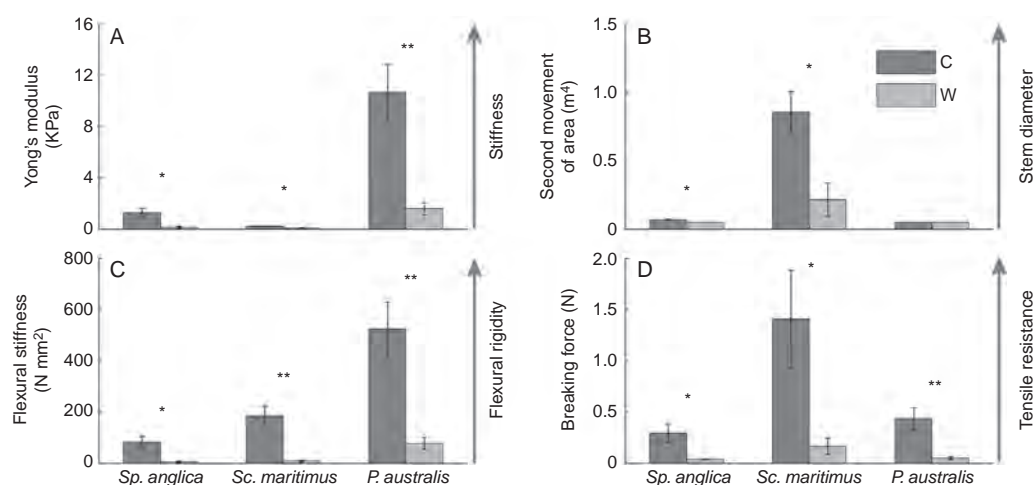


Fig. 3. Biomechanical traits of survived seedlings showing more flexibility after the continuous wave exposure: (A) Young's modulus; (B) second moment of area; (C) flexural stiffness; and (D) breaking force of three pioneer marsh seedlings (data are means \pm s.e.; C and W indicate control and wave treatment groups separately; * $P < 0.5$, ** $P < 0.01$).

Re-invasion of *Spartina alterniflora* in restored saltmarshes: Seed arrival, retention, germination, and establishment

Zhao, Zhiyuan; Yuan, Lin; Li, Wei; Tian, Bo; Zhang, Liqun. *Journal of Environmental Management*, 2020, 266: 110631.

The invasive plant *Spartina alterniflora* presents a serious threat to the saltmarsh ecosystems in the Yangtze Es-tuary. Various measures have been implemented to control *S. alterniflora* and restore the natural saltmarshes in this area. However, many saltmarsh restoration activities often fail partly because of recursions of this invasive plant. In this study, we investigated the re-invasion of *S. alterniflora* in a restored saltmarsh in the Chongming Dongtan National Nature Reserve by analysing the aspects of seed arrival, retention, germination, and establishment, to better understand the potential factors that may influence the re-invasion of restored saltmarshes. The results showed that 1) tidal currents dispersed the seeds from the possible source area to the restored saltmarsh and adjacent mudflat. The spatio-temporal dynamics of arrived seeds were shown to vary greatly depending on the intertidal geomorphology, vegetation, and hydrodynamic processes. 2) Seed retention in the re-invaded area was shown to be greatly influenced by burial depth, and moderate sedimentation rates provided safe sites for the retention of arrived seeds. 3) Only when both the burial depth and inundation duration below certain thresholds, the retained seeds could germinate and establish in the recipient habitats successfully. The results from this study highlight that control efforts and the management of *S. alterniflora* should not only focus on the re-invaded areas of restored saltmarshes, but also on the possible source areas of re-invasive species.

针对互花米草治理后二次入侵，从多阶段种子生态过程探讨了其发生机制，并量化提取了关键过程的生态阈值。研究结果强调了管控外来物种二次入侵的必要性，为进一步优化海岸地区外来物种管理策略提供了新思路。

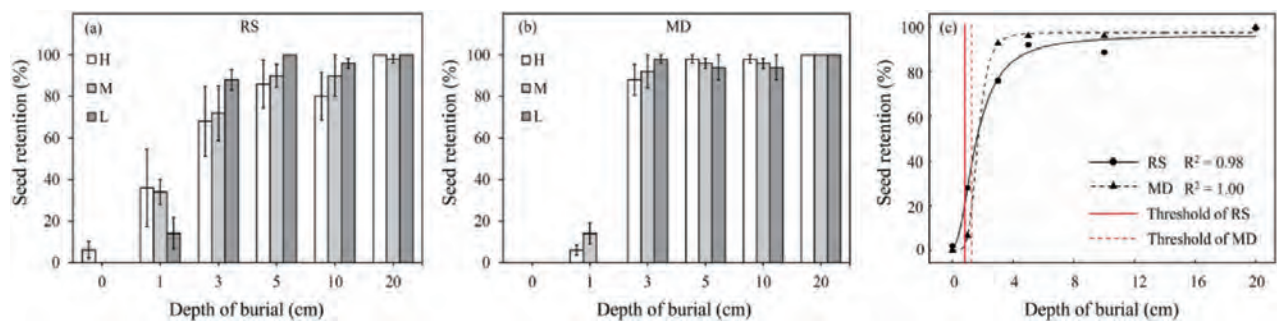


Fig. 5. (a and b) Seed retention rates of *Spartina alterniflora* under different burial depths at the high-elevation (H), intermediate-elevation (M), and low-elevation (L) sites in a restored saltmarsh (RS) and mudflat (MD). (c) Fitted curves of *S. alterniflora* seed retentions to burial depth, showing the thresholds.

Emergency control of *Spartina alterniflora* re-invasion with a chemical method in Chongming Dongtan, China

Zhao, Zhiyuan; Xu, Yuan; Yuan, Lin; Li, Wei; Zhu, Xiaojing; Zhang, Liqun. *Water Science and Engineering*, 2020, 13(1): 24-33.

The exotic species *Spartina alterniflora* (*S. alterniflora*) seriously threatens the stability and functioning of saltmarsh ecosystems in the Yangtze Estuary. Ambitious efforts have been undertaken to control this species, but subsequent re-invasion is frequent, presenting a significant barrier to restoration. The complexity and high cost of integrated physical control programs has necessitated a shift in focus, leading to considerable attention being paid to the potential of herbicides to control *S. alterniflora*. To find a strategy for emergency control of small and scattered patches of re-invading *S. alterniflora*, an in situ field experiment using Gallant

(Haloxyfop-R-methyl) herbicide was conducted. The growth parameters of plant density and height were used to evaluate the control efficiency of different treatment dosages and times and sediment samples were taken for environmental toxicity analysis. The results show the following: (1) the control efficacy of the maximum proposed application dose (2.70 g/m^2) was 92% for continuous swards and 100% for small patches, while those of other dosages (0.45 g/m^2 , 0.90 g/m^2 , and 1.35 g/m^2) were lower than 40%; (2) the appropriate implementation time was July to August with 100% mortality resulting from a single application, while *S. alterniflora* was shown to be capable of recovering rapidly after treatment in May; and (3) there were no significant differences in the community structure of meiofauna among the herbicide treatments and the control, and no herbicide residues were detected in sediment samples collected from treatment areas. This chemical control method was implemented in the Shanghai Chongming Dongtan National Bird Nature Reserve (CDNR). The results of this study indicate that Gallant is an environmentally friendly herbicide with high efficiency, which can be adopted for emergency control of re-invading *S. alterniflora*.

该研究结合滨海湿地水文变化特征，通过两轮小区实验，探索盖草能治理互花米草零星斑块的最佳喷施浓度与最适施用时间，同时评估该化学防控方法对当地底栖动物的影响及其环境残留。研究结果可应用于互花米草残留小斑块的补救性治理和二次入侵零星斑块的应急处置。

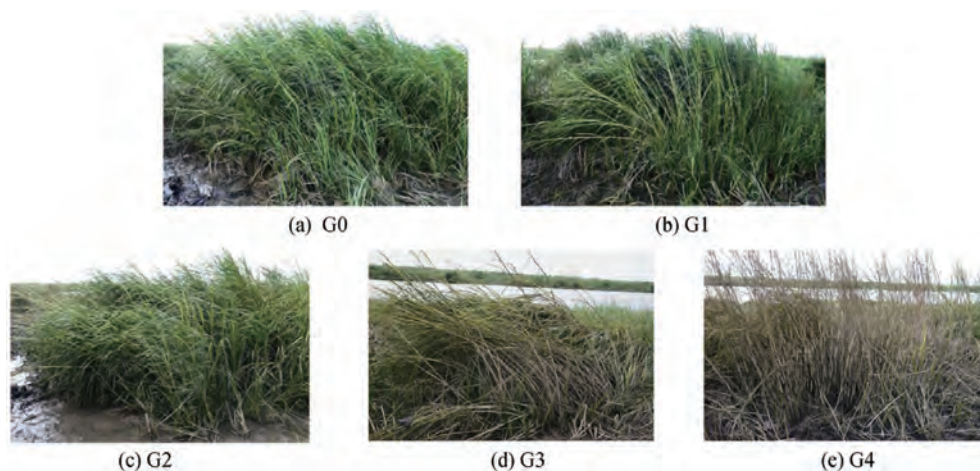


Fig. 3. Control efficacy after application of Gallant herbicide for one month with different dosages.

Sources and preservation dynamics of organic matter in surface sediments of Narmada River, India – Illustrated by amino acids

Fernandes, Dearlyn; Wu, Ying; Shirodkar, Prabhaker Vasant; Pradhan, Umesh Kumar; Zhang, Jing; Limbu, Samwel Mchele. *Journal of Marine Systems*, 2020, 201: 103239.

The preservation process of organic matter (OM) in estuarine environments determines the recycling and sinking of nutrients. This process requires the identification of sources, degradation states and the main processes affecting OM transformations. Unfortunately, our understanding of the sources, degradation and factors affecting OM distribution in tropical rivers experiencing strong seasonality and monsoonal influence is still limited. This study examined the sources, degradation and factors affecting OM distribution along the Narmada River and its estuary during different seasons. Surface waters and sediments were analyzed seasonally for selected physico-chemical parameters and bulk compositions of sediments, together with amino acids (AA, including the bacterial

biomarker, D-AA). The sources of OM were soils containing detrital terrestrial plant material, with C_4 and C_3 plants dominating the estuarine and riverine stations, respectively. The other sources of OM were in-situ production, together with bacteria and their remnants. Strong seasonality and monsoonal conditions control the sources and distribution of OM in the river. Higher concentrations of total hydrolysable amino acids (THAA) were observed in riverine stations, suggesting the presence of relatively fresher OM. The lower OC:SA ratios recorded in the estuarine sediments indicated a limited OM preservation in the studied river. Positive de-gradation index (DI) values were obtained during the pre-monsoon season, suggesting seasonal changes in OM diagenesis. Physical (strong tidal currents, rainfall, reduced water flow due to seasonal variations and shallow water depth within the estuary) and geochemical (mineral surface adsorption processes) factors control the distribution and transport of OM. Taken together, the sources, preservation and diagenesis of terrestrial OM along the Narmada River was controlled differentially by the strong seasonal variability of the region. Thus, under variable temporal conditions, tropical estuaries and rivers form important realms for examining, de-termining, evaluating and assessing OM in order to better interpret nutrient budgets of the seas and oceans.

人们对季节性强和受季风影响的热带河流中有机物分布的来源，降解和影响因素的了解仍然十分有限。我们选择印度NAMADA河流的颗粒物和沉积物进行了氨基酸（AA，包括细菌生物标志物D-AA）的季节部分特征和受控因素分析的研究。其有机物来源主要是含有碎屑陆生植物的土壤，其中 C_4 和 C_3 植物分别在河口站和河道站占主导地位。其次来自细菌等原位生产。强烈的季节性和季风条件控制着河流中有机物的来源和分布，其中有机物的保存能力十分有限。物理因素（强潮流，降雨等）和地球化学因素（矿物表面吸附过程）控制着有机物的分布和运输。综上所述，NAMADA河流的有机物的来源，保存和成岩作用受到该地区强烈的季节性变化的控制。

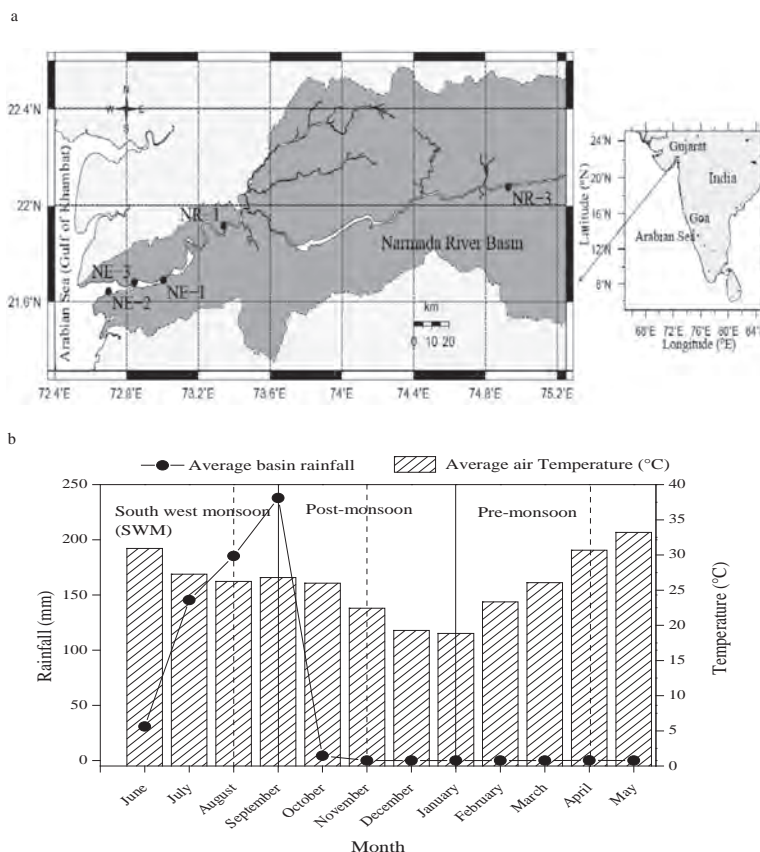


Fig. 1. a: Map of Narmada River and its basin, India surface water and sediment sampling locations are marked as solid circles; b: monthly average rainfall (mm) and air temperature (°C) for the year 2011–2012 (the solid lines demarcate the season and the dashed lines the sampling month).

An important biogeochemical link between organic and inorganic carbon cycling: Effects of organic alkalinity on carbonate chemistry in coastal waters influenced by intertidal salt marshes

Song, Shuzhen; Wang, Zhaohui Aleck; Gonnee, Meagan Eagle; Kroeger, Kevin D. ; Chu, Sophie N.; Li, Daoji; Liang, Haorui. *Geochimica Et Cosmochimica Acta*, 2020, 275: 123-139.

Dissolved organic carbon (DOC) contains organic acid charge groups that contribute organic alkalinity (OrgAlk) to total alkalinity (TA). These effects are often ignored or treated as a calculation uncertainty in many aquatic CO₂ studies. This study evaluated OrgAlk variability, sources, and characteristics in estuarine waters exchanged tidally with a groundwater-influenced salt marsh in the northeast USA. OrgAlk provided a biogeochemical link between organic and inorganic carbon cycling through its direct effects on pH, and thus CO₂ system speciation and buffer capacity. Two main charge groups were identified including carboxylic and phenolic or amine groups. Terrestrial groundwater and in-situ production within salt marsh peat contributed OrgAlk to the tidal creek, with the former being a more significant source. Groundwater entering the marsh complex contained exceptionally high OrgAlk (> 150 mmol kg⁻¹), and these compounds were preferentially preserved within the DOC pool during groundwater transport and mixing with coastal water. OrgAlk:DOC ratios in groundwater and marsh-influenced water varied across space and time. This highlights the insufficiency of using a fixed proportion of DOC to account for organic acid charge groups. Accounting for OrgAlk altered H⁺ concentrations by ~1–41 nmol kg⁻¹ (equivalent to a pH change of ~0.03–0.26), pCO₂ by ~30–1600 latm and buffer capacity by ~0.00–0.14 mmol kg⁻¹ at the relative OrgAlk contributions of 0.9–4.3% of TA observed in the marsh-influenced tidal water. Thus, OrgAlk may have a significant influence on coastal inorganic carbon cycling. Further theoretical calculations confirm that these concentrations of OrgAlk would have sizable impacts on both carbonate speciation and, ultimately, air-sea CO₂ fluxes in different coastal environments, ranging from estuarine to shelf waters. A new conceptual model linking organic and inorganic carbon cycling for coastal waters is proposed to highlight the sources and sinks of organic acid charge groups, as well as their biogeochemical behaviors and mechanistic control on the CO₂ system.

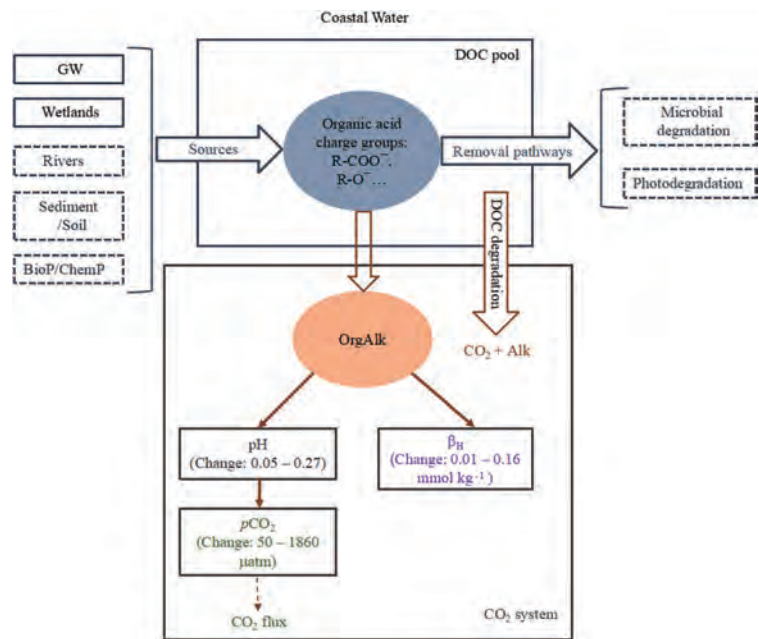


Fig. 10. A conceptual model of OrgAlk cycling in coastal systems. Alk indicates alkalinity. BioP and ChemP represent in-situ biological production and chemical production of organic acid charge groups, respectively. Boxes with dashed lines indicate processes that were not studied in the present study. The values in the boxes of pH, pCO₂, and buffer capacity (β_H) represent the magnitude of OrgAlk effects on pH, pCO₂, and β_H in the range of OrgAlk% in TA observed in this study (0.9–4.3%) in coastal waters.

有机碱同时是有机碳库和无机碳系统的一部分，是链接有机碳和无机碳循环的桥梁。以往的研究大多集中于忽略有机碱引起的二氧化碳系统各参数计算误差的角度。本研究评估了有机碱的潮周期和季节变化，主要来源以及组成特征。有机碱主要由羧酸根和酚类或胺类有机酸离子组成。地下水和湿地间隙水是有机碱的主要来源。湿地有机碱的存在可以使pH改变约0.03-0.26个单位，pCO₂变化30-1600μatm,海水缓冲能力变化0.00-0.14mmol kg⁻¹。因此，湿地有机碱在近岸海域无机碳循环中可能具有重要作用。进一步理论评估证实，有机碱可能对近岸海域不同类型海水二氧化碳系统中碳酸盐组分以及pCO₂具有重要影响，进而影响海气界面CO₂交换通量。基于本文以及前任研究建立了近岸海域有机碱模型，以阐明有机碱的来源，移除途径以及对二氧化碳的影响。

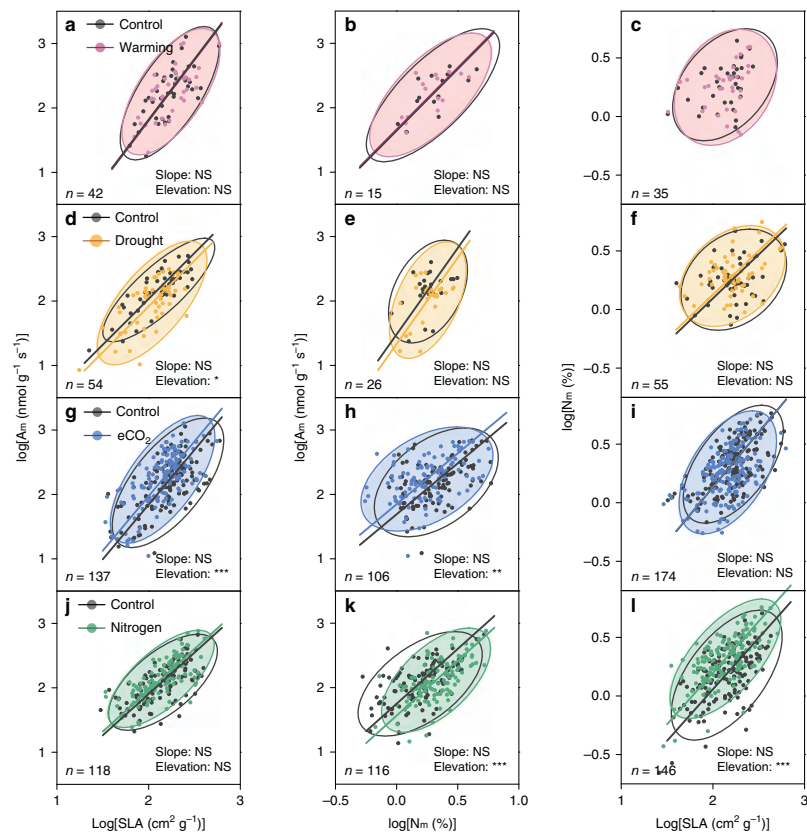
ARobust leaf trait relationships across species under global environmental changes.

Cui, Erqian; Weng, Ensheng; Yan, Enrong; Xia, Jianyang. *Nature Communications*, 2020, 11(1): 2999.

Recent studies show coordinated relationships between plant leaf traits and their capacity to predict ecosystem functions. However, how leaf traits will change within species and whether interspecific trait relationships will shift under future environmental changes both remain unclear. Here, we examine the bivariate correlations between leaf economic traits of 515 species in 210 experiments which mimic climate warming, drought, elevated CO₂, and nitrogen deposition. We find divergent directions of changes in trait-pairs between species, and the directions mostly do not follow the interspecific trait relationships. However, the slopes in the logarithmic transformed interspecific trait relationships hold stable under environmental changes, while only their elevations vary. The elevation changes of trait relationship are mainly driven by asymmetrically interspecific responses contrary to the direction of the leaf economic spectrum. These findings suggest robust interspecific trait relationships under global changes, and call for linking within-species responses to inter-specific coordination of plant traits.

基于叶片经济型谱，生态学家们陆续尝试利用植物功能性状的协同变化，优化光合作用的模拟机制，以期改进全球碳循环模型对生态系统生产力的模拟，然而其预测能力受到环境变化下性状间关系稳定性的制约。本研究系统地分析了全球210个生态学实验中 515个植物物种的叶片功能性状观测数据，发现物种间成对性状对增温、干旱、CO₂富集和氮素添加的响应方向存在较大差异，并且大部分不遵循叶片经济型谱的指示方向。同时，物种之间的叶片功能性状权衡关系在环境变化下维持较高的稳健性。

Fig. 4 Robustness of leaf trait relationships under different global environmental changes. The panels show the effects of warming (a–c), drought (d–f), eCO₂ (g–i) and nitrogen addition (j–l), respectively. The bold lines represent SMA regressions of leaf trait relationships. The ellipses show the 95% confidence level of the original scatter. The homogeneity among SMA slopes via a permutation test and for differences in SMA elevation via the SMA analog of standard ANCOVA. The statistics information is shown in Supplementary Table 3. The number of species under treatments of warming, drought, eCO₂, and nitrogen addition are 42, 54, 137, and 118 for A_m-SLA, 15, 26, 106, and 116 for N_m-SLA, and 35, 55, 174, and 146 for N_m-SLA (i.e., the numbers shown near the ellipses). The Significance of changes in slopes and elevations: NS: P > 0.05; *P < 0.05; **P < 0.01; ***P < 0.001.



Invasive *Spartina alterniflora* can mitigate N₂O emission in coastal salt marshes

Yang, Bin; Li, Xiuzhen; Lin, Shiwei; Xie, Zuolun; Yuan, Yiquan; Espenberg, Mikk; Parn, Jaan; Mander, Ulo. *Ecological Engineering*, 2020, 147: 105758.

Although there are studies on nitrous oxide (N₂O) fluxes in coastal salt marshes, temporal and spatial variations of this greenhouse gas are still uncertain. Especially salt marshes of the East China Sea coast covered by invasive *Spartina alterniflora* have shown controversial results. To analyse seasonal patterns of N₂O fluxes and their re-relationship with environmental factors, three plots dominated by *S. alterniflora*, and differing in sediment salinity and vegetation history (P1, P2, P3), and one bare mudflat (P0) in a salt marsh of Nanhui shore in the southern fringe of Yangtze River estuary have been established. Monthly studies from March 2017 to January 2018 using a chamber technique showed that average N₂O fluxes from all four plots ranged from -41.9 to 39.3 μg N₂O·m⁻²·h⁻¹, whereas average flux (4.2 μgN₂O·m⁻²·h⁻¹) in P1, P2 and P3 was not significantly different from that measured in P0 (1.3 μgN₂O·m⁻²·h⁻¹). There was a clear seasonal difference: in spring and summer, all the sites showed slight emission while consumption prevailed in autumn and winter. In vegetated sites this trend was more remarkable than in the bare mudflat. N₂O flux showed positive correlation (p < .05) with air and se-diment temperature, and plant development (height of vegetation). Nitrate was not the limiting factor of N₂O emission in the Yangtze estuary. In the salt marsh where vegetation community was mature, higher sediment salinity reduced N₂O emission (P1 < P2) by influencing other environmental factors such as total carbon (TC), total nitrogen (TN) content and sediment texture. In comparison with other tidal macrophytes *S. alterniflora* showed relatively low N₂O emission. Therefore, it can be considered as a species for tidal zone stabilisation.

为分析互花米草入侵河口湿地氧化亚氮 (N₂O) 时空排放规律和环境因子对其排放的影响, 我们在上海南汇边滩选择三个不同沉积物盐度和不同植被定植年限的互花米草群落样地 (P1, P2, P3) 和一个光滩样地(P0)。从2017年3月到2018年1月, 通过静态箱法监测N₂O排放情况。研究发现N₂O排放量在4个样地的排放范围为-41.9 to 39.3 μg N₂O·m⁻²·h⁻¹。三个植被样地的N₂O平均排放速率和光滩相比没有显著差异。所有样地N₂O排放通量都显示了季节差异, 春、夏两季为排放, 秋、冬两季均以吸收为主。N₂O排放通量和气温, 植被发育成正相关。硝酸盐在富营养化的长江口不是N₂O排放的限制因素。在植被定植年限较接近的样地, 较高的沉积物盐度通过影响其他环境因素, 如总碳、总氮和土壤粒径等, 降低了N₂O的排放通量。与其他湿地植物群落相比, 互花米草群落的盐沼湿地表现出相对较低的N₂O排放通量。

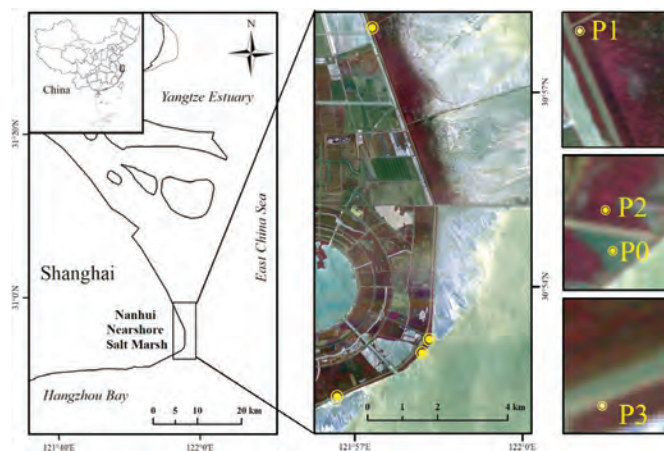


Fig. 1. Location of the four sampling plots in the Nanhui shore salt marsh of the Yangtze estuary, Shanghai, China (Photo by RapidEye Satellite).

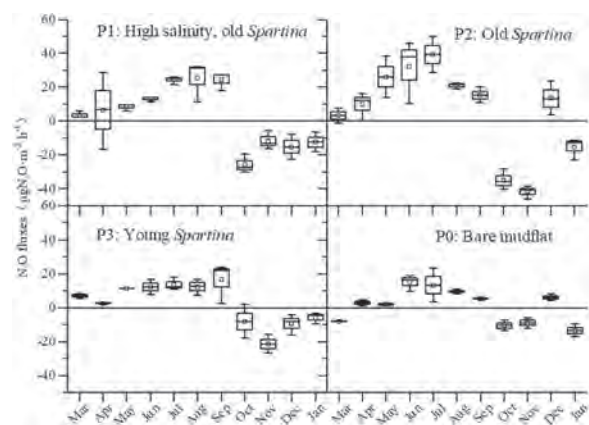


Fig. 5. Dynamics of N₂O fluxes in the study plots. The central line is the median and the dot is the mean, the edges of the box are the 25th and 75th percentiles, and the whiskers represent the 95% confidence interval.

Tidal effects on ecosystem CO₂ exchange in a Phragmites salt marsh of an intertidal shoal

Huang, Ying; Chen, Zihan; Tian, Bo; Zhou, Cheng; Wang, Jiangtao; Ge, Zhenming; Tang, Jianwu. *Agricultural and Forest Meteorology*, 2020, 292-293: 108108.

Understanding the mechanisms and controlling factors of ecosystem CO₂ exchange in tidal wetlands is of great benefit for research concerning the global carbon cycle and climate change. In spite of this, the multiple controls of ecosystem-atmosphere CO₂ exchange in coastal wetlands subject to subdaily tidal flooding have yet to be adequately addressed. In this study, we investigated the tidal influence on ecosystem CO₂ exchange in a Phragmites salt marsh of an intertidal shoal in the Changjiang estuary, based on eddy covariance (EC) measurements. The results revealed that the study area acted as a strong sink for atmospheric CO₂ (net ecosystem exchange, NEE = -901 g C m⁻²) in 2018. Photosynthetically active radiation (PAR), air

temperature (T_a), and vapor pressure deficit (VPD) were major drivers of NEE on both diel and multi-day scales. The tides, along with the bio-meteorological variables, strongly affect ecosystem photosynthesis (gross primary production, GPP) and ecosystem respiration (R_{eco}) in the tidal wetland, especially on the multi-day scale. Regardless of which flux partitioning method was utilized, tidal inundation generally imposed inhibitory effects on GPP, which were directly attributed to tidal water level (TWL) and salinity. The daytime data-based estimates of R_{eco} was also suppressed on average under the tidal inundation condition when T_a was higher relative to the non-inundation condition, reflecting the influence of TWL on R_{eco} and the reduced sensitivity of R_{eco} to T_a . We observed that NEE responded positively or negatively to tidal flooding, depending on the magnitude of tidal suppression on GPP and R_{eco} . When T_a was roughly between 28 and 32°C and PAR was > 1200 $\mu\text{mol m}^{-2} \text{s}^{-1}$, GPP was suppressed by tides more than R_{eco} during the early and rapid vegetative stage, while during the peak vegetative stage, the opposite was true. This study not only shows the unique impact of tidal salt marsh wetlands on carbon uptake, but it also represents an example of a coastal wetland in which tidal inundation promotes the net uptake of CO₂.

明晰潮汐盐沼湿地生态系统CO₂通量的控制要素与机理，在全球碳循环和气候变化方面具有重要意义。潮汐盐沼湿地地处海-陆-气三相交最为明显的河口海岸地区，盐沼生态系统—大气间CO₂通量交换受潮汐动态淹水与气象要素的共同作用，其作用机制还有待明确。

本研究选择长江河口最靠外海、受潮汐影响较大的江心沙洲—九段沙盐沼湿地为研究对象，基于涡度相关通量野外观测，运用信息论模型，深度挖掘了多时间尺度上潮汐盐沼—大气间CO₂通量交换过程的（非）线性及时间（同）异步性，定量分析了环境因子对盐沼生态系统CO₂通量变化的相对控制程度，定量甄别出光合有效辐射（PAR）、空气温度（ T_a ），以及蒸汽压亏缺（VPD）是每日、多天尺度上盐沼生态系统CO₂通量变化的主

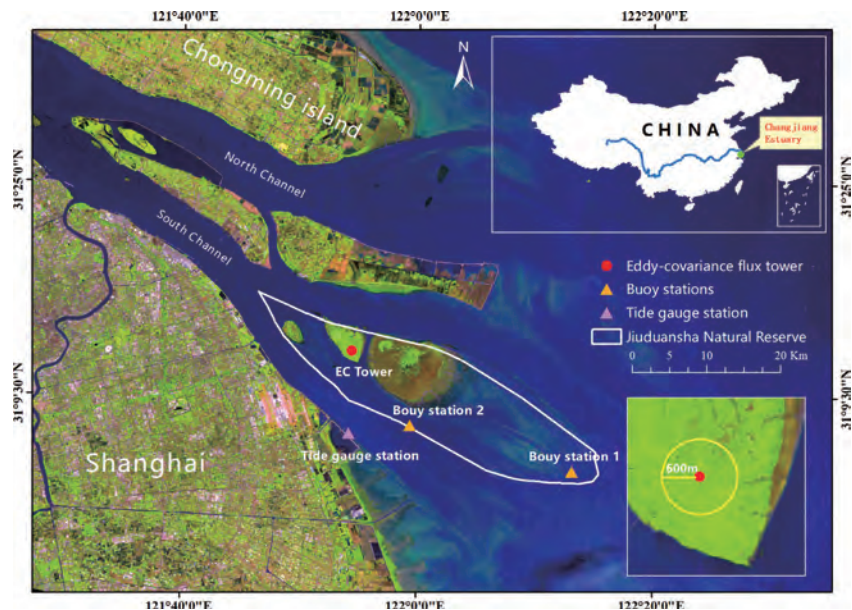


Fig. 1. Locations of the EC flux tower (red dot) in the Jiuduansha Nature Reserve, the tide gauge (purple triangle), and the buoy stations (orange triangle) in the Changjiang estuary of China. A Landsat 7 ETM+ image (RGB = bands 6, 5, and 2, respectively) acquired on June 8, 2018 provides the background. (For interpretation of the references to colour in this figure legend, the reader is referred to the web version of this article.)

控因素，而潮高和盐度是重要的影响因子。研究表明潮高和盐度是导致潮汐淹水抑制盐沼生态系统总初级生产力（GPP）的直接影响因素；潮汐淹水也对呼吸作用（Reco）起抑制作用，并降低Reco对Ta的敏感性；潮汐淹水对GPP、Reco抑制的相对程度决定其对盐沼净生态系统碳交换量（NEE）起增进或抑制作用。此外，潮汐淹水的影响和植被物候期相关：在植被快速生长期，当Ta在28—32°C之间且PAR大于1200 $\mu\text{mol m}^{-2} \text{s}^{-1}$ 时，潮汐淹水对GPP的抑制程度大于Reco，而在植被生长旺盛期，潮汐淹水对GPP的抑制程度小于Reco。

研究成果展现了潮汐淹水对盐沼湿地NEE可起正面或负面影响的新范例，揭示了潮汐动态淹水对盐沼湿地生态系统CO₂通量的影响及机理，是全球碳循环研究的重要补充，有利于提出合理刻画潮汐湿地生态系统碳交换的参数化方案，提高潮汐湿地对气候变化响应的预测精度。

Plutonium in Southern Yellow Sea sediments and its implications for the quantification of oceanic-derived mercury and zinc

Wang, Jinlong; Du, Jinzhou; Zheng, Jian; Bi, Qianqian; Ke, Yu; Qu, Jianguo. *Environmental pollution*, 2020, 266(Pt3): 115262.

The spatial distributions of mercury (Hg) and zinc (Zn) concentration and the isotopic composition of plutonium (Pu) were investigated in surface sediments and sediment cores collected from the Southern Yellow Sea (SYS) during May 2014. The variation of the ²⁴⁰Pu/²³⁹Pu atom ratio (0.18-0.31) in the surface sediments of the SYS clearly indicated a signal of close-in fallout input from the Pacific Proving Ground (PPG). The buried ²³⁹⁺²⁴⁰Pu in the sediment of the SYS was estimated to be $(4.7 \pm 0.5) \times 10^{10} \text{ Bq y}^{-1}$ during the period from 2011 to 2014, of which ~33% ($1.5 \times 10^{10} \text{ Bq y}^{-1}$) was derived from the PPG by long-range transport via ocean currents (e.g., the North Equatorial Current and Kuroshio Current). The concentrations of Hg and Zn varied from 0.003 to 0.067 mg kg^{-1} and from 43.9 to 137 mg kg^{-1} , respectively, and exhibited positive correlations with the ²³⁹⁺²⁴⁰Pu activity both in the surface sediments (0-1 cm) and upper layers (7 cm) of the sediment cores. Therefore, by using Pu as a tracer, we estimated that the oceanic input contributed 2.0 tons y^{-1} of Hg and $1.0 \times 10^3 \text{ tons y}^{-1}$ of Zn to the SYS sediments between 2011 and 2014, which accounted for 33% and 3% of total buried Hg and Zn, respectively. These findings indicate that environmental pollution control should also consider the oceanic contribution of some pollutants. The results of the present work help to elucidate the biogeochemical cycling of trace metals in marginal seas, and are helpful for managing environmental pollution in marine environments.

创新性地使用Pu同位素作为示踪剂，首次评估了外海输入对近海重金属的贡献，并指出对Hg的贡献不可忽视。本研究对于重新评估大陆边缘海区域金属元素的上午地球化学循环具有重要指示意义。

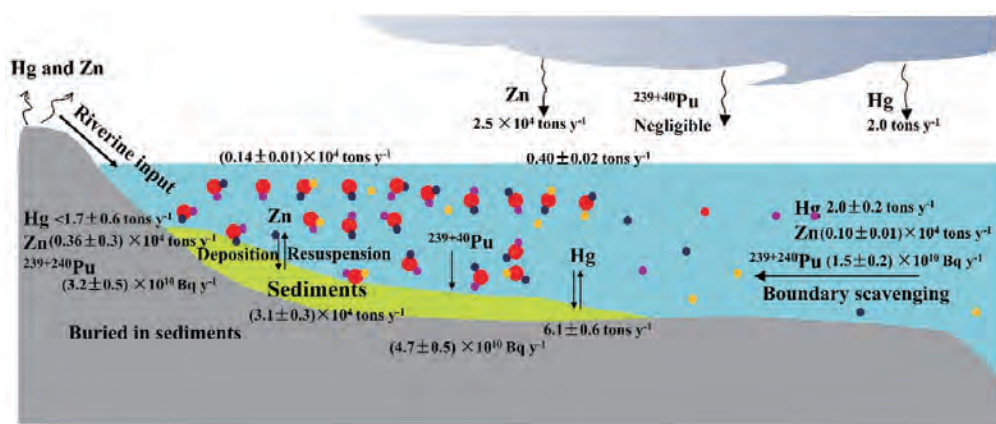


Fig. 6. Cycling of ²³⁹⁺²⁴⁰Pu Hg and Zn in the sediments of the SYS.

Salinity Affects Topsoil Organic Carbon Concentrations Through Regulating Vegetation Structure and Productivity

Xue, Lian; Jiang, Junyan; Li, Xiuzhen; Yan, Zhongzheng; Zhang, Qian; Ge, Zhenming; Tian, Bo; Craft, Christopher. *Journal of Geophysical Research-Biogeosciences*, 2020, 125(1): e2019JG005217.

Estuarine salt marshes have been recognized as one of the most efficient carbon sinks in the biosphere, with considerable potential for climate change mitigation. However, there are still uncertainties about the response of soil carbon stocks to enhanced soil salinization caused by accelerated sea-level rises and aggravated saltwater intrusion. We therefore conducted both field investigations in the Chongming Dongtan salt marsh of the Yangtze River Estuary, China, and manipulative experiments on marsh soils occupied, *respectively*, by the invasive *Spartina alterniflora*, and the native *Phragmites australis* and *Scirpus mariqueter*, to identify the effects of elevated soil salinity on top soil organic carbon (SOC) concentration. Our field data showed that SOC concentrations were significantly positively associated with soil salinity concentrations, annual net primary productivity, and marsh surface elevation but showed a significant negative relationship with median grain size. Compared with the two native species, *S. alterniflora* preferred more saline conditions and had a higher SOC concentration. Although raised flooding salinities (0–35 ppt) did not strongly affect SOC concentrations, elevated soil salinities significantly corresponded with low SOC concentrations and plant biomass in manipulative experiments. These findings indicated that soil salinity, plant species, and soil texture were key factors controlling SOC concentrations in the studied salt marsh. Moreover, soil salinity could affect SOC concentrations through regulating vegetation spatial structure and plant biomass production. The further invasion of the *S. alterniflora* community will exert a positive influence on SOC concentrations in the Chongming Dongtan salt marsh.

河口盐沼是生物圈中最有效的“碳汇”之一，具有缓解气候变化的巨大潜力。但海平面上升、盐水入侵等因素对盐沼土壤有机碳（soil organic carbon, SOC）含量的影响仍不明确。本研究通过野外采样分析了长江口崇明

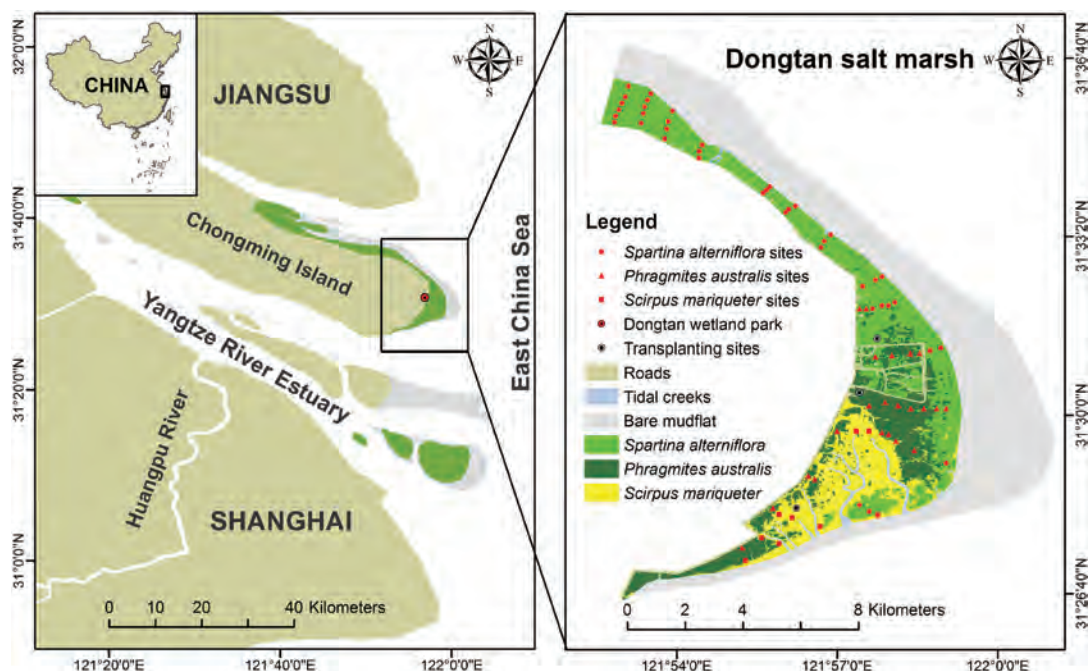


Figure 1. Location of the sampling sites for invasive *Spartina alterniflora* ($n = 39$) and native *Phragmites australis* ($n = 22$) and *Scirpus mariqueter* ($n = 9$) in the Chongming Dongtan salt marsh of the Yangtze River Estuary, China, and location of the transplanting sites where seedlings and topsoil samples were taken for pot experiments.

东滩入侵种互花米草 (*Spartina alterniflora*) 和本地种芦苇 (*Phragmites australis*)、海三棱藨草 (*Scirpus mariqueter*) 分布区域表层土壤 (0-30 cm) 盐度和SOC含量的关系, 并采用控制实验模拟淹水盐度 (0-35 ppt) 增加对3种植物SOC含量的影响。结果表明, SOC含量与土壤盐度、年净初级生产力显著正相关, 互花米草分布区SOC含量和植物生物量较高; 淹水盐度增加对SOC含量影响不显著, 但土壤盐度升高可致SOC含量与植物生物量显著降低。因此, 土壤盐度是影响盐沼SOC含量的关键因素, 可通过调节植被空间分布和植物生物量影响SOC含量, 互花米草入侵可增加长江口盐沼碳储量。

Plutonium Isotopes Research in the Marine Environment: A synthesis

Wang, Jinglong; Du, Jinzhou; Zheng, Jian. *Journal of Nuclear and Radiochemical Sciences*, 2020, 20: 1-11.

Plutonium (Pu) isotopes are one of most important artificial radionuclides. Recent advances in analytical methodology of Pu have enabled Pu to play a vital role in tracing biogenic elements and pollutants transport, sediment deposition/resuspension and other marine process. The various ratios of Pu isotopes (^{238}Pu , ^{239}Pu , ^{240}Pu and ^{241}Pu), which are dependent on the Pu sources, are useful for identifying the contributions from different sources, and these ratios can be utilized to indicate the marine processes. The aim of this manuscript is to provide an overview of the applications of Pu for studying various processes in the marine environment, such as the determination of recent sedimentation rate, to assess sediment transport and deposition/resuspension, water mass transport, etc, based on the knowledge and advances in the analytical methodology and the geochemical behavior of Pu. Furthermore, this work is expected to provide new insights for broadening the application of Pu in the marine environment and to help better understand land-sea interactions and global climate change.

全面总结了海洋环境中Pu同位素的来源、检测方法、分布、地球化学行为, 以及在示踪颗粒物动力过程和水团运输等方面的研究进展, 并指出了未来相关的研究方向。

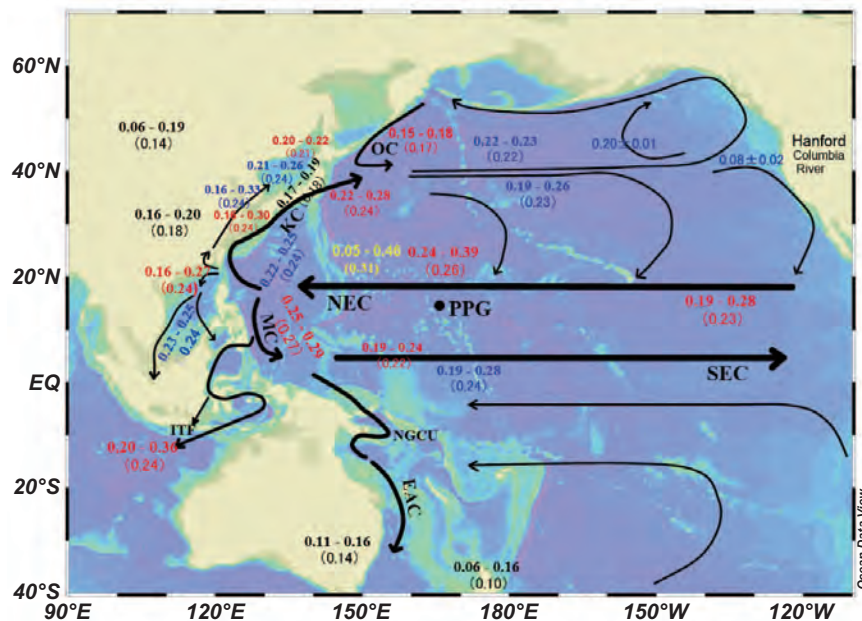


Figure 6. The synthesis of $^{240}\text{Pu}/^{239}\text{Pu}$ atom ratios in the areas surrounding the Pacific: Soil (black color),^{32,139,140,142-145} sediment (red color),^{18,22,83-90,130,140,146-148} seawater (blue color)¹⁴⁹⁻¹⁵⁷ and a coral (yellow color).^{23,117,129} NEC: North Equatorial Current; SEC: South Equatorial Current; KC: Kuroshio Current; OC: Oyashio Current; MC: Mindanao Current; NGCU: New Guinea Coastal Undercurrent; EAC: East Australian Current; ITF: Indonesian Throughflow.

Terrestrial plants as a potential temporary sink of atmospheric microplastics during transport.

Liu, Kai; Wang, Xiaohui; Song, Zhangyu; Wei, Nian; Li, Daoji. *Science of the Total Environment*, 2020, 742: 140523.

Atmospheric transport is an important pathway by which terrestrial microplastics (MPs, with sizes less than 5 mm) can move long distances to remote areas. However, little is known about the environmental behaviors of atmospheric MPs during movement. To address this issue, deposits of MPs on the leaves of plants were studied in two regions, with abundance ranging from 0.07 n/cm² (pieces per area of leaves) to 0.19 n/cm². The attached substances were mainly natural materials, but 28% of the total substances were plastics. There was a similar physical-chemical composition of the attached MPs in the two regions suggesting a similar origin. Leaves, regard-less of plant species, can indiscriminately retain atmospheric MPs. About 0.13 trillion pieces of MPs are estimated to be attached to leaf surfaces in the top 11 green countries. Leaves of terrestrial plants could be a temporal sink and a source of MPs pollution to remote areas. This is not fully recognized and merits further study.

大气输运是陆地微塑料向偏远地区的迁移重要途径，然而，人们对其环境行为知之甚少。为了解决这一问题，我们研究了两个区域陆生植物叶片上的微塑料附着，其丰度从0.07 n/cm² (叶片面积)到0.19 n/cm²。附着物质以天然材料为主，而塑料仅占总物质的28%。叶片上附着微塑料相似的物化特征表明其来源相似。此外，植物种类并不会影响微塑料的附着。初步统计显示，大约有0.13万亿个微塑料附着在叶子表面。陆生植物的叶子可能是暂时的“汇”也是偏远地区MPs的污染源。这一点尚未得到充分认识，值得进一步研究。

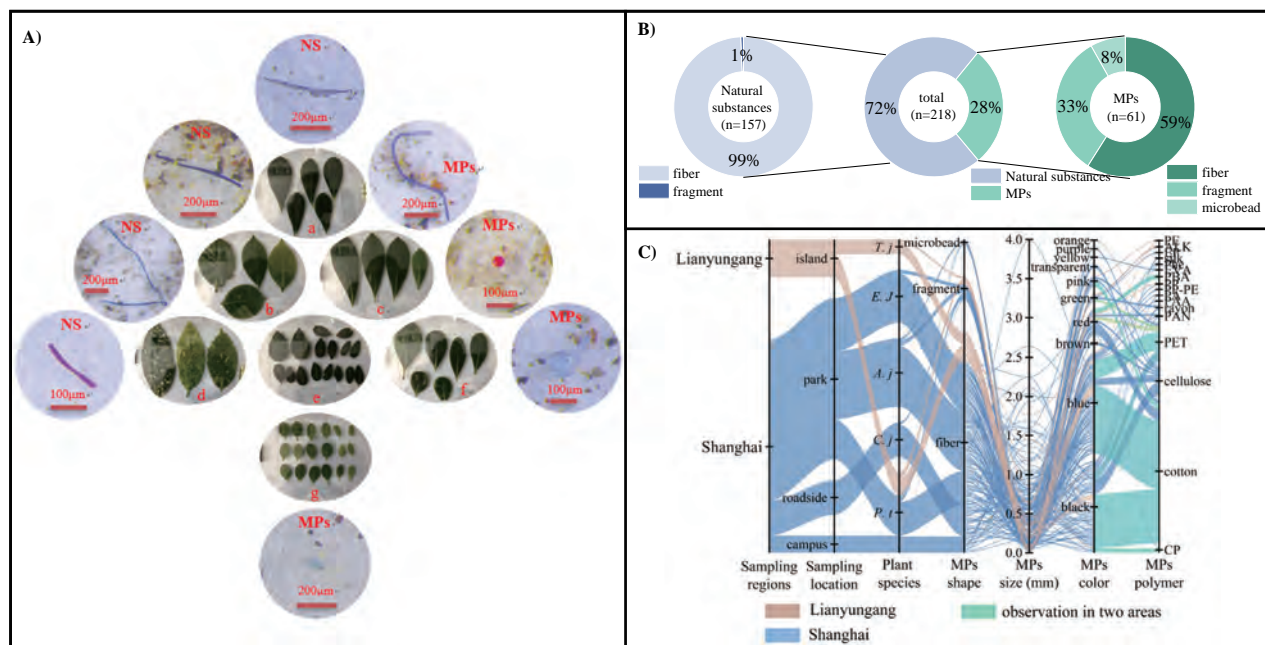


Fig. 4. Sampled leaves from LY and SH regions. a: *Pittosporum tobira* (SH, campus); b: *Camellia japonica* (SH, roadside); c: *Pittosporum tobira* (SH, park); d: *Aucuba japonica* (SH, park); e: *Trachelospermum jasminoides* (LY, island); f: *Pittosporum tobira* (LY, island); g: *Euonymus japonicus* (SH, park); NS: natural substances. Polymer composition and the shape of verified particles adhering to sampled leaves (B). Mapping interrelationship among physicochemical properties of adhered substances, sampling regions and plant species (C). Labeled abbreviations and dataset are available in supporting information.

Sea-level rise will reduce net CO₂ uptake in subtropical coastal marshes.

Li, Yalei; Guo, Haiqiang; Ge, Zhenming; Wang, Dongqi; Liu, Wenliang; Xie, Lina; Li, Shihua; Tan, Lishan; Zhao, Bin; Li, Xiuzhen; Tang, Jianwu. *Science of the Total Environment*, 2020, 747: 141214.

Coastal marshes have a significant capacity to sequester carbon; however, sea-level rise (SLR) is expected to result in prolonged flooding and saltwater intrusion in coastal regions. To explore the effects of SLR projections on net CO₂ uptake in coastal marshes, we conducted a “double-check” investigation, including the eddy covariance (EC) measurements of the CO₂ fluxes in subtropical coastal marshes along inundation and salinity gradients, in combination with a mesocosm experiment for analyzing CO₂ flux components under waterlogging and increased salinity conditions. During the same measurement periods, the net ecosystem CO₂ exchange (NEE_{EC} based on the EC dataset) in an oligohaline marsh was higher than that in a low-elevation mesohaline marsh, whereas the NEE_{EC} was lower than that in a high-elevation freshwater marsh. The declines in NEE_{EC} between the marshes could be attributed to a greater decrease in gross primary production relative to ecosystem respiration. Waterlogging slightly increased the NEE_{ms} (NEE based on the mesocosms) because of inhibited soil respiration and slight changes in plant photosynthesis and shoot respiration. However, the NEE_{ms} measured during the drainage period decreased significantly due to the stimulated soil respiration. The NEE_{ms} decreased with increasing salinity (except under mild salinity), and waterlogging exacerbated the adverse impacts of salinity. The amplificatory effect of decreases in both leaf photosynthesis and growth under hydrological stresses contributed more to reduce the NEE_{ms} than to respiratory effluxes. Both waterlogging and increased salinity reduced the root biomass, soil microbial biomass, and activities of assayed soil enzymes (except for cellulase under waterlogging conditions), leading to limited soil respiration. The declines in plant growth, photosynthesis, and soil respiration

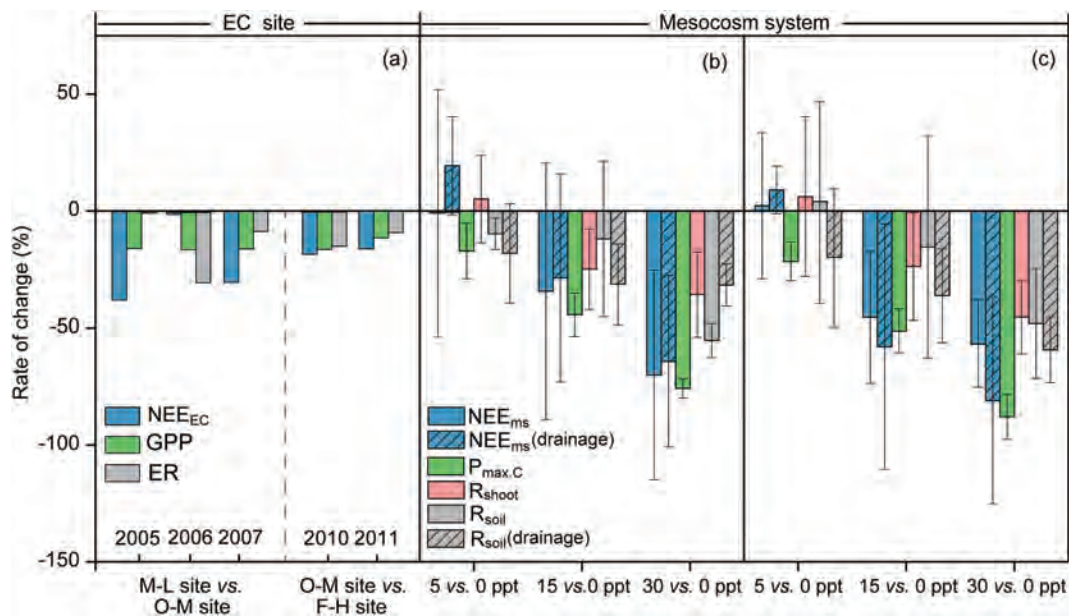


Fig. 4. (a) Rate of change in the net ecosystem exchange based on eddy covariance dataset (NEE_{EC}) [with components of gross primary production (GPP) and ecosystem respiration (ER)] by eddy covariance (EC) measurement sites and NEE based on a mesocosm (NEE_{ms}) [with components of maximum photosynthesis rate at the canopy scale ($P_{max,C}$), shoot respiration (R_{shoot}), and soil respiration (R_{soil})] based on the mesocosm with increasing saline treatments under (b) non-waterlogging and (c) waterlogging conditions during the growing season (April–October). ‘M-L (mesohaline marsh with low elevation) site vs. O-M (oligohaline marsh with high elevation) site’ indicates the rate of change in the NEE_{EC} at the M-L site relative to the O-M site from 2005 to 2007; ‘O-M site vs. F-H (freshwater marsh with high elevation) site’ indicates the rate of change in the average monthly NEE_{EC} at the O-M site relative to the F-H site from 2010 to 2011. ‘5 vs. 0 ppt’, ‘15 vs. 0 ppt’, and ‘30 vs. 0 ppt’ indicate the rates of change in the CO₂ flux components under salinities treatments of 5, 15, and 30 ppt, respectively, relative to the 0 ppt groups. Bars indicate the seasonal deviation.

全球气候变暖已经引起了海平面上升 (SLR) 和盐水入侵这些突出的区域环境变化问题。SLR将显著影响滨海湿地对温室气体CO₂的吸收能力。我们进行了两个不同尺度的研究：(1) 利用涡度相关Eddy covariance 碳通量观测系统，观测了不同淹水和盐度梯度下滨海湿地的CO₂通量；(2) 并通过中宇宙实验Mesocosm system，分析了CO₂通量组分对不同水-盐条件的响应。结果表明，低潮滩高盐度湿地的净CO₂吸收量 (NEE) 显著低于低盐度湿地和高潮滩淡水湿地。NEE的降低可以归结于初级生产力的降幅高于生态系统呼吸。淹水抑制了土壤呼吸从而增大NEE，但周期性落潮排水会加剧土壤呼吸使NEE降低。淹水条件增强了盐胁迫对湿地NEE的抑制效应。水-盐耦合胁迫交互作用于湿地的固碳能力和碳排放作用。本研究指出，SLR引起的水文过程耦合变化会显著削弱亚热带地区滨海湿地对CO₂的净吸收能力。

Ferrous iron facilitates the formation of iron plaque and enhances the tolerance of *Spartina alterniflora* to artificial sewage stress

Zhang, Qiqiong; Yan, Zhongzheng; Li, Xiuzhen. *Marine Pollution Bulletin*, 2020, 157: 111379.

The ferrous iron (Fe²⁺) facilitates the formation of root Fe plaque of wetland plants, but its effect on the tolerance of wetland plants to artificial sewage stress has been seldom reported. In this study, the influences of Fe²⁺ on the formation of Fe plaque and its effects on the tolerance of *Spartina alterniflora* to artificial sewage stress were investigated. The artificial sewage stress decreased the plant height and chlorophyll content and significantly increased the MDA content in leaves. The symptoms of these stresses were alleviated with increasing Fe²⁺ concentration accompanied by significant increase in leaf alcohol dehydrogenase activity. The increase of Fe²⁺ concentration significantly increased the root Fe plaque content and reduced the accumulation of toxic metals in leaves of *S. alterniflora*. These results support our hypothesis that the exogenous Fe²⁺ supply may enhance the stress resistance of *S. alterniflora* to artificial sewage containing heavy metals.

湿地植物根部铁膜通过吸附和共沉淀作用影响营养元素及重金属在植物中的吸收和转运，而潮滩周期性潮汐所带来的沉积物氧化还原电位变异深刻影响了湿地植物铁膜的形成及其功能。本论文研究了Fe(II)浓度对湿地植物根表铁膜形成、重金属累积转运以及植物抗逆性的影响。发现互花米草根表铁膜含量与外源Fe(II)浓度呈剂量依赖性正相关，铁膜含量的增加，显著降低了重金属元素 (Cu, Zn, Pb和Cr) 向植物地上部分的转运，从而提高了植物的抗逆性，表现为叶片主要抗氧化酶活性的提升，叶片膜脂损伤的降低，以及叶片叶绿素含量的显著增加。这项成果从机制上揭示了铁膜形成多少与植物抗逆性之间的关系。

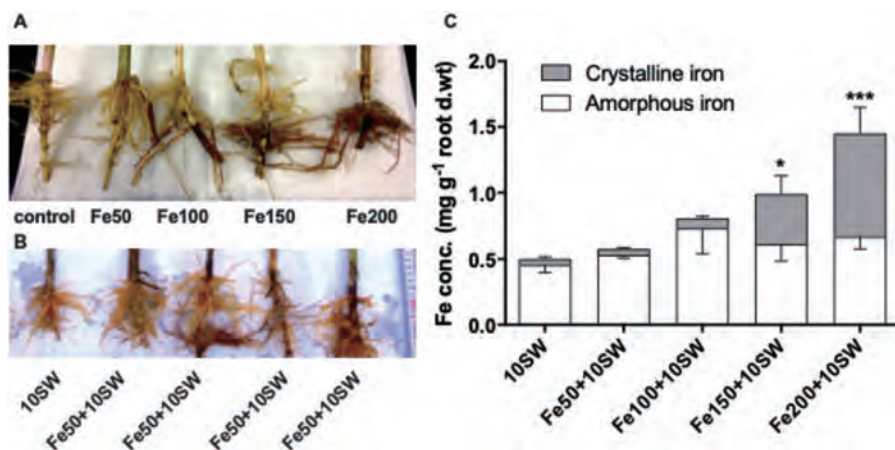


Fig. 3. The appearance of Fe plaque formed on roots of *S. alterniflora* under (A) different levels of Fe²⁺ treatments and (B) different levels of Fe²⁺ treatments with SW; (C) changes in the amorphous and crystalline Fe plaque content on roots of *S. alterniflora* along different levels of Fe²⁺ treatment with synthetic wastewater (values are mean and SD; for each parameter, significant difference between treated and control group is indicated by the asterisk, * and *** indicate significant at p < 0.05 and 0.001, respectively).

Estimation of soil surface water contents for intertidal mudflats using a near-infrared long-range terrestrial laser scanner

Tan, Kai; Chen, Jin; Zhang, Weiguo; Liu, Kunbo; Tao, Pengjie; Cheng, Xiaojun. *ISPRS Journal of Photogrammetry And Remote Sensing*, 2020, 159: 129-139.

Estimations of the soil surface water contents and distributions play a key role in the ecological, environmental, and topographical investigations for intertidal mudflats. However, existing techniques have limitations. Long-range terrestrial laser scanners (TLSs) can record the co-located intensity value which refers to a measure of the backscattered laser from each scanned point. Most long-range TLSs emit near-infrared lasers that can be strongly absorbed by water. Thus, the intensity values can be used as proxies for water contents. In this study, the intensity data of long-range TLSs are corrected for the incidence angle and distance effects to quantitatively estimate the soil surface water contents of intertidal mudflats. A case study for a mudflat in Chongming Island, Shanghai, China, is conducted. Results indicate that compared with traditional techniques, the corrected in-tensity data of long-range TLSs are extremely effective data sources for a quick, accurate, and detailed estimation of water contents for large-area mudflats. The estimation root mean square error is approximately 3%. Furthermore, the 3D distributions of the water contents can be accurately mapped by combining the point cloud of the mudflats to potentially analyze the intrinsic association among water contents and topography, vegetation coverage, and habitation of creatures in mudflats.

潮滩含水量的分布与变化对研究海岸生物、地形地貌、物质传输等具有非常重要的意义，现有方法和技术存在较大的局限性。本课题利用长距离地面三维激光雷达技术（TLS）进行大范围潮滩三维点云数据和回波强度数据的同步获取。研究长距离TLS强度数据的影响机理及改正方法，对影响强度数据的入射角和距离等因素进行改正，获取仅与目标反射率相关的改正后强度数据。探索基于改正后强度数据和点云几何信息的植被滤波方法，提取潮滩点云数据。采集潮滩样本数据，分析样本数据的含水量与改正后强度数据之间的关系，根据水对近红外激光的强吸收特性，建立改正后强度数据与潮滩含水量之间的定量函数关系，进而利用改正后强度数据对大范围潮滩的含水量进行高精度反演。结合几何数据，确定潮滩含水量的整体分布情况。研究成果为揭示潮滩含水量的变化趋势和地形地貌、泥沙冲淤、生物生长习性等之间的内在关联提供理论依据，为潮滩区域的资源利用、水文调查、生态修复、环境保护等研究提供技术支撑。

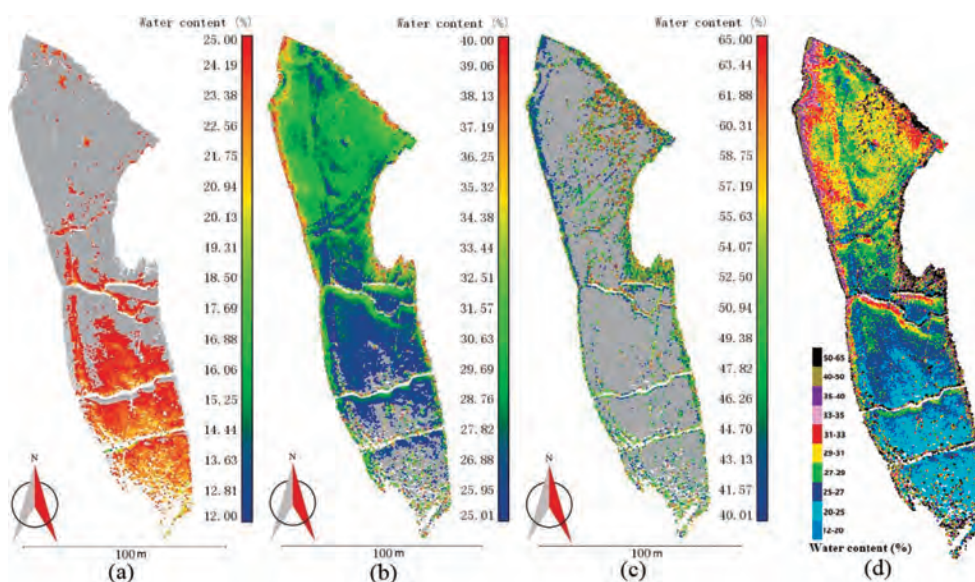


Fig. 6. Water contents estimated by corrected intensity data. (a) 12–25% (low), (b) 25–40% (middle). (c) 40–65% (high). (d) Water contents segmented into 10 sections.

Effects of waterlogging and increased salinity on microbial communities and extracellular enzyme activity in native and exotic marsh vegetation soils

Xie, Lina; Ge, Zhenming; Li, Yalei; Li, Shihua; Tan, Lishan; Li, Xiuzhen. *Soil Science Society of America Journal*, 2020, 84(1): 82-98.

Coastal ecosystems are vulnerable to plant invasion and expected sea level rise in China. This study explored the responses of microbial communities and extracellular enzyme activity in the marsh soils of native *Phragmites australis* and exotic *Spartina alterniflora* to waterlogging and increasing salinity (to

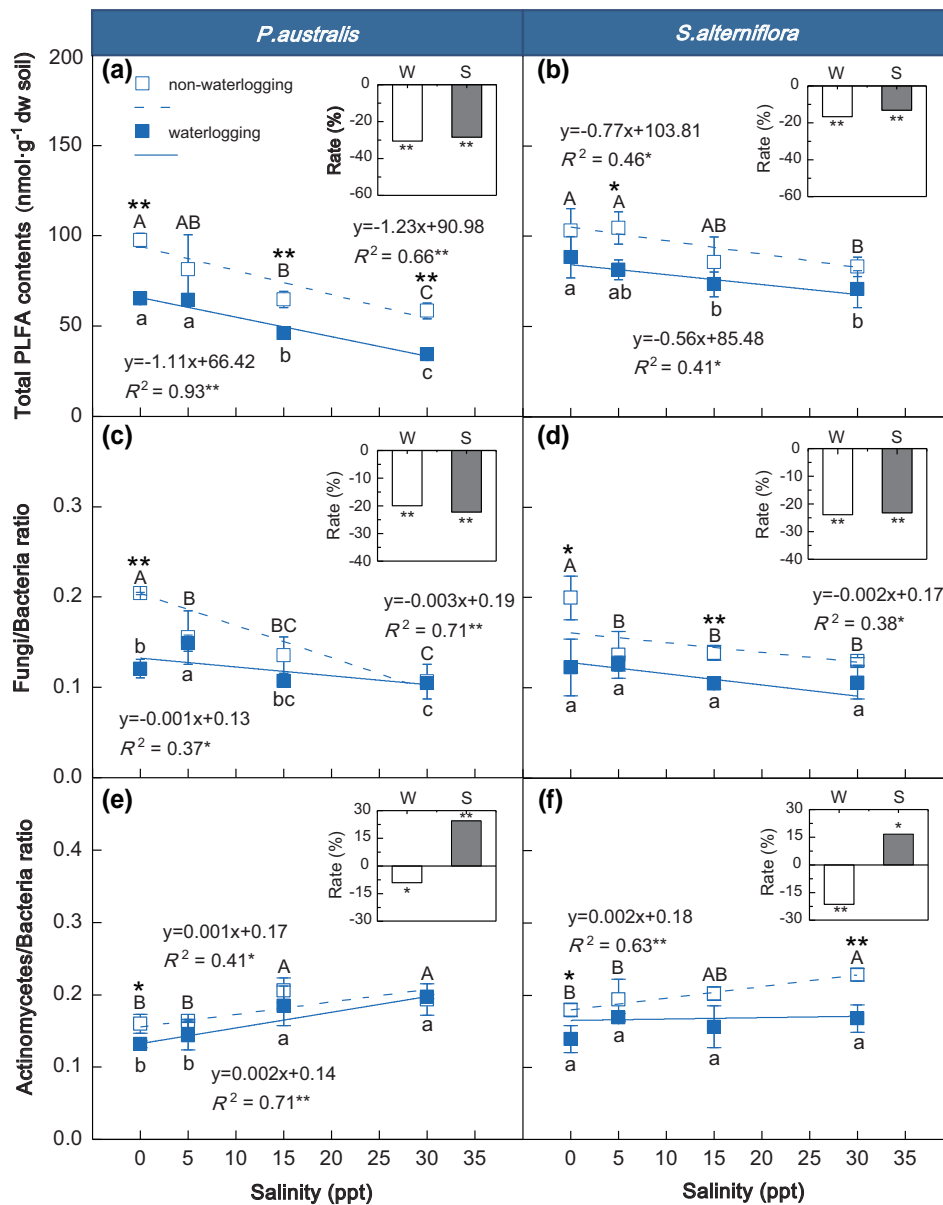


FIGURE 2 Changes in total phospholipid fatty acid (PLFA) contents, and fungi/bacteria and actinomycetes/bacteria ratios in the *Phragmites australis* (a, c, e) and *Spartina alterniflora* soils (b, d, f) under waterlogging and salinity treatments. Asterisks indicate the significant differences ($P < .05$) of variables between non-waterlogging and waterlogging conditions (within the same salinity level). Different capital and lowercase letters indicate the significant differences ($P < .05$) of the variables among salinity levels under nonwaterlogging and waterlogging conditions, respectively. Only the valid fitting functions ($P < .05$) are presented. Insets: relative change rates of the variables under waterlogging (W) and salinity (S) treatments. *Significant at $P < .05$; **significant at $P < .01$.

mimic prolonged inundation and saltwater intrusion) based on the determination of phospholipid fatty acids and analysis of enzyme kinetics. The results showed that waterlogging and increased salinity treatments decreased the soil microbial biomass in both *P. australis* and *S. alterniflora* soils, with waterlogging exacerbating the negative effects of salinity. Fungi/bacteria ratios decreased under both waterlogging and salinity treatments, whereas actinomycetes/bacteria ratios increased with increasing salinity. The degree of the adverse effects of salinity on plant growth of *S. alterniflora* and soil microbial biomass was lower than that on *P. australis*. Generally, waterlogging treatment increased the activity of sucrase, cellulase, urease, and dehydrogenase in *S. alterniflora* soil. Increased salinity decreased all the assayed extracellular enzyme activity in both *P. australis* and *S. alterniflora* soils. The synergistic effects of waterlogging and increased salinity treatments on the enzyme activities in *P. australis* soil were significant, whereas only the effect on the cellulase activity was significant in *S. alterniflora* soil. This study indicated a greater ability of the microbial community and extracellular enzyme activity of *S. alterniflora* soil to adapt to waterlogging and increased salinity compared with those of *P. australis* soil due to the lower sensitivity of *S. alterniflora* growth and soil nutrients to stress.

中国沿海湿地易受到植物入侵和海平面上升（潮汐淹水加剧和盐水入侵）的影响。本研究通过土壤微生物 PLFA测定和酶学分析，探讨了长江口滨海湿地本地种芦苇和外来种互花米草的土壤微生物群落和土壤酶活性对海平面上升效应响应。结果表明，淹水和盐度升高降低了两种植被土壤的微生物生物量，并改变土壤微生物群落结构。淹水后互花米草土壤酶活性有所升高，但芦苇土壤酶活性降低（除纤维素酶外）。盐度升高均降低了两种植被土壤酶活性。水-盐交互作用显著影响了芦苇酶活性，而互花米草仅纤维素酶活性受到显著影响。互花米草土壤微生物群落和酶活性较芦苇有更强的适应淹水和盐度升高的能力，主要是由于互花米草植物生长和土壤养分对水、盐胁迫敏感性较低。

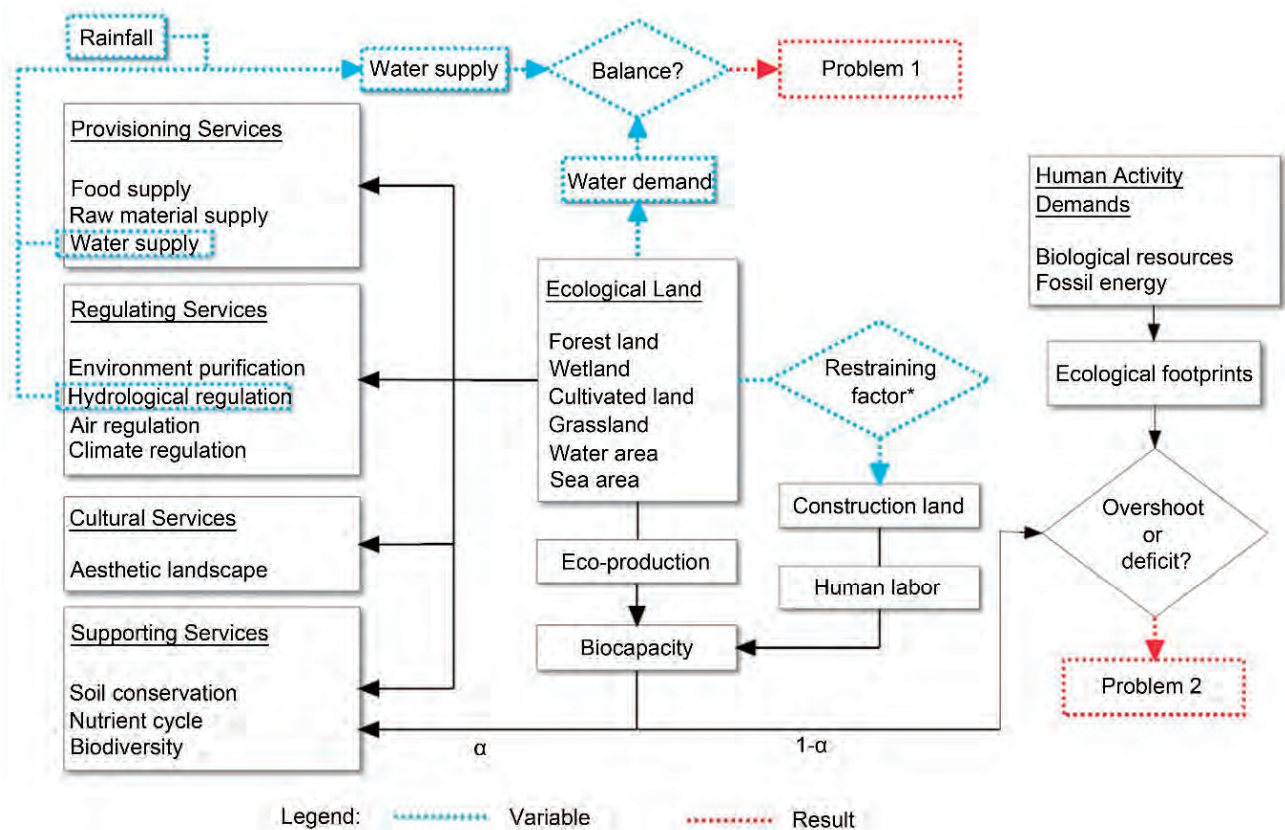
Ecological Suitability of Island Development Based on Ecosystem Services Value, Biocapacity and Ecological Footprint: A Case Study of Pingtan Island, Fujian, China

Zheng, Weiheng; Cai, Feng; Chen, Shenliang; Zhu, Jun; Qi, Hongshuai; Zhao, Shaohua; Liu, Jianhui. *Sustainability*, 2020, 12(6): 2553.

The ecological environment and resource endowment of an island are more vulnerable compared to the mainland, and special assessment and measurement of the ecological suitability for development are significant. Pingtan Island (Fujian, China) was taken as a case study. Changes in ecosystem services value and the profit-and-loss balance between ecological footprint and biocapacity were assessed using land use/cover changes based on remote-sensing images taken in 2009, 2014 and 2017, and the ecological suitability of development was measured. Results show that island development led to a decrease in the ecosystem services value and an increase in ecological footprint and biocapacity. The key ecological factors restricting the scale of island development are topography, vegetation with special functions and freshwater. Biocapacity of islands can increase not only by changing from lower-yield land types to higher-yield construction land types but also by external investment. A new measurement framework was proposed that simply and clearly reveals the ecological suitability of island development and the underlying key constraints.

海岛的生态环境和资源禀赋比大陆更为脆弱，对其开发的生态适宜性进行专门的评估和测量具有重要意义。以中国福建平潭岛为例。收集解译2009年、2014年和2017年的遥感影像，基于土地利用变化评估生态系统服务价值变化和生态足迹与生物承载力之间的盈亏平衡，并测算开发的生态适宜性。结果表明，海岛开发导致生态系统服务价值下降，生态足迹和生物承载力增加。制约海岛发展规模的关键生态因素是地形、具有特殊功能的植被和淡水。岛屿的生物承载力不仅可以通过从低产量的生态土地类型转变为高产量的建设土地类型，而且还

可以通过外部引进资源来提高。本文提出了一个新的开发生态适宜性测量框架，简单而清晰地揭示了岛屿发展的生态适宜性和潜在的关键制约因素。



α : the bio-productive land area rate which is set aside as a biodiversity conservation area to maintain ecosystem function.

Problem 1: If the water supply is deficient, there might be a decline in the water level of wetland and lakes, indicating water shortages. Once water demands of vegetation could not meet, soil desertification might occur, leading to the degradation of island ecosystem.

Problem 2: If deficient, compensation shall be made from external supplies including food, raw materials, energy or human productive labor.

Restraining factors: a) biodiversity conservation area; b) topographic elevation, slope and slope direction; c) wetland and geomorphologic characteristics that store and recharge groundwater; d) vegetation with special function.

Figure 8. Framework for measuring the ecological suitability of island development.

Composition, spatial distribution and sources of plastic litter on the East China Sea floor.

Zhang, Feng; Yao, Chenyang; Xu, Jiayi; Zhu, Lixin; Peng, Guyu; Li, Daoji. *Science of the Total Environment*, 2020, 742: 140525.

Plastics are present in all marine waters around the globe, often at high abundances and they are potentially harmful to marine organisms. In this study, we investigated the regional distribution, composition, and abundance of plastic items on the floor of the East China Sea based on 43 bottom trawl samples collected during 2019. Considerable geographical variation was detected. Polyethylene was the most abundant polymer type where it accounted for 42.83% by weight. The surface areas and lengths of the plastic items ranged from 3.43 to 2842 cm² and from 1.3 cm to 14.23 cm, respectively. The plastic density was 18.94 kg/km² in Sanmen Bay but it was significantly lower at 2.24 kg/km² in Wenzhou Bay. Fishing gear represented 23.87% of the plastic items. The plastic items found on the coastal sea bed were probably transported and moved during upwelling and downwelling processes, and finally deposited on the seafloor due to the effect of biofouling. The accumulation of macro- and mesoplastics could have detrimental impacts on seafloor ecosystems.

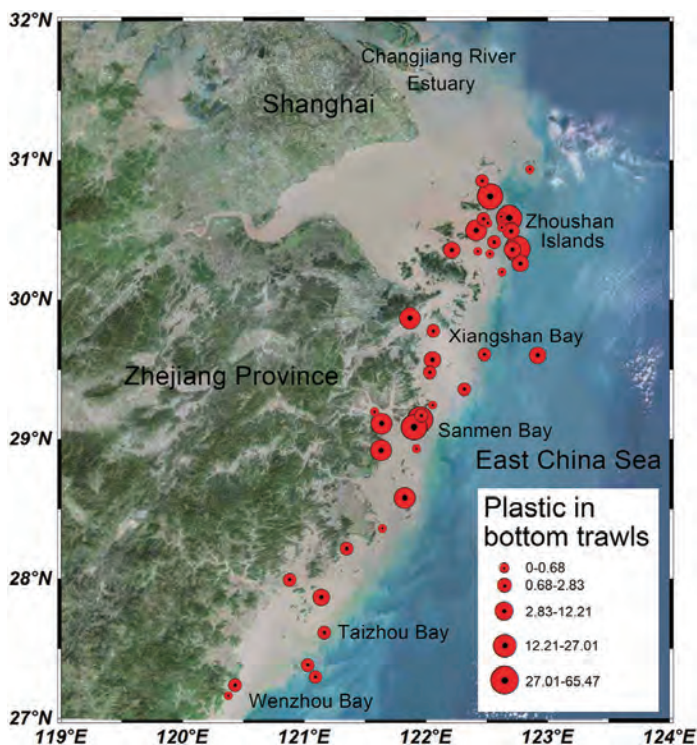


Fig. 2. Density of plastic pieces on the floor of the East China Sea (unit: kg/km²).

塑料经常以很高的含量存在于全球海洋中，并且可能对海洋生物有害。在这项研究中，我们基于2019年期间收集的43个底部拖网样本，调查了中国东海海底塑料的区域分布，组成和数量，发现了相当大的地理差异。聚乙烯是最丰富的聚合物类型，它占重量的42.83%。塑料制品的表面积和长度分别为3.43至2842 cm²和1.3 cm至14.23 cm。三门湾的塑料密度为18.94 kg / km²，而温州湾的可塑性密度则低至2.24 kg / km²。渔具占塑料制品的23.87%。在沿海海床上发现的塑料物品可能在上升流和下降流过程中被运输和移动，最后由于生物污损的影响而最终沉积在海底。大和中塑料的积累可能对海底生态系统产生不利影响。

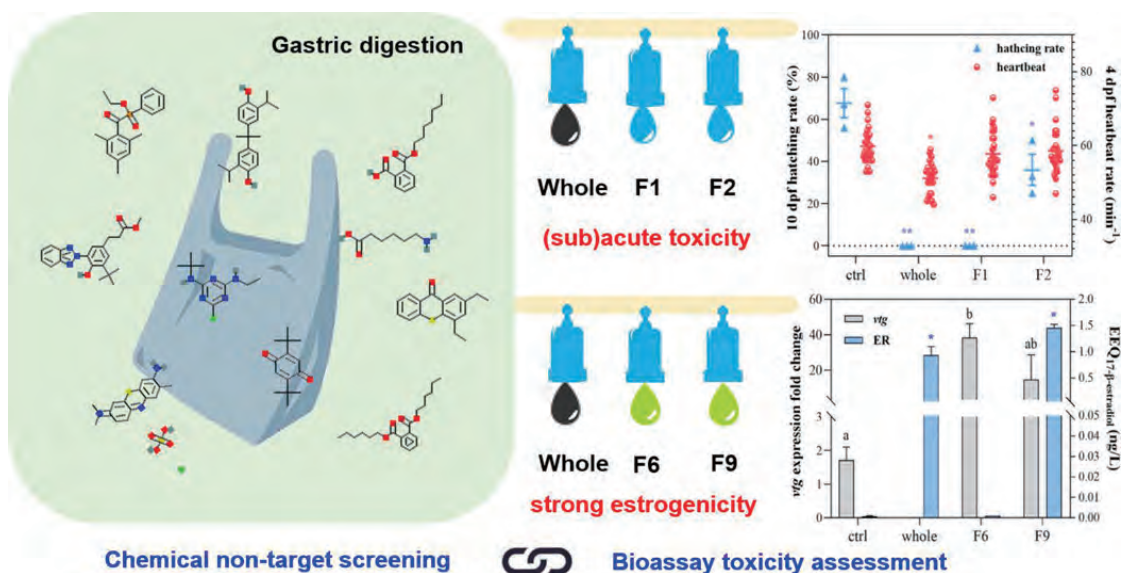
Bioassay guided analysis coupled with non-target chemical screening in polyethylene plastic shopping bag fragments after exposure to simulated gastric juice of Fish.

Chen, Qiqing; Santos, Mauricius Marques Dos; Tanabe, Philip; Harraka, Gary T; Magnuson, Jason T; McGruer, Victoria; Qiu, Wenhui; Shi, Huahong; Snyder, Shane A; Schlenk, Daniel. *Journal of Hazardous Materials*, 2020, 401: 123421.

In this study, fragments of polyethylene plastic bags were treated with simulated gastric juice of fish for 16 h. Following solid-phase extraction, methanol eluents caused acute toxicity to embryos and larvae of Japanese medaka. Chromatographic fractions (polar to more non-polar with numbers increasing) of the extract were evaluated for toxicity and estrogenic activity using medaka and an estrogen receptor (ER) cell-line. Fractions 6 and 9 had the highest estrogenic effects with relative hydrophobic chemicals. The vtg expression in fraction 6 was 22-fold higher than control,

and the ER cellular response in fraction 9 was 8.5-fold higher than controls. Following non-target screening (NTS), several novel phthalates and phenols were identified in the above two fractions. Fractions 1 and 2 appeared to be primarily responsible for the acute toxicity observed with the whole extract. The hatching rate decreased to 36 % in fraction 2, and was not observed following exposure to fraction 1. NTS of these fractions indicated 635 and 808 entities, respectively, most without toxicity information. These results indicate plastic leachates from gastric juices of fish are complex mixtures of many compounds that can have acute reproductive and sublethal endocrine impacts in fish.

在本研究中，我们用模拟的鱼体消化液萃取了聚乙烯塑料中的添加剂类物质。渗出液经固相萃取和液相组分分离（较极性至较非极性）后，发现组分1和组分2对青鳉胚胎和幼鱼产生急性毒性，孵化率和存活率显著下降。非靶标化学物质筛查（NTS）显示，这两个组分中分别含有635和808个化学物质，而这些物质大部分尚无可靠性数据。此外，我们还发现组分6和组分9可诱导青鳉幼鱼和雌激素受体细胞系产生内分泌干扰效应。通过NTS我们检出了这两个组分中存在新型邻苯二甲酸酯和酚类等物质。本研究结果表明，塑料进入鱼类消化液后渗出的添加剂是复杂的混合物，会对鱼类产生急性生长发育毒性和亚致死的内分泌干扰效应。



Role of C₄ carbon fixation in *Ulva prolifera*, the macroalga responsible for the world's largest green tides

Liu, Dongyan; Ma, Qian; Valiela, Ivan; Anderson, Donald M.; Keesing, John K.; Gao, Kunshan; Zhen, Yu; Sun, Xiyan; Wang, Yujue. *Communications Biology*, 2020, 494(3): 1.

Most marine algae preferentially assimilate CO₂ via the Calvin-Benson Cycle (C₃) and catalyze HCO₃⁻ dehydration via carbonic anhydrase (CA) as a CO₂ compensatory mechanism, but certain species utilize the Hatch-Slack Cycle (C₄) to enhance photosynthesis. The occurrence and importance of the C₄ pathway remains uncertain, however. Here, we demonstrate that carbon fixation in *Ulva prolifera*, a species responsible for massive green tides, involves a combination of C₃ and C₄ pathways, and a CA-supported HCO₃⁻ mechanism. Analysis of CA and key C₃ and C₄ enzymes, and subsequent analysis of δ¹³C photosynthetic products showed that the species assimilates CO₂ predominately via the C₃ pathway, uses HCO₃⁻ via the CA mechanism at low CO₂ levels, and takes advantage of high irradiance using the C₄ pathway. This active and multi-faceted carbon acquisition strategy is advantageous for the formation of massive blooms, as thick floating mats are subject to intense surface irradiance and CO₂ limitation.

大多数海藻通过Calvin-Benson循环 (C₃) 优先吸收CO₂，并通过碳酸酐酶 (CA) 催化HCO₃⁻脱水作为CO₂补偿

variations.

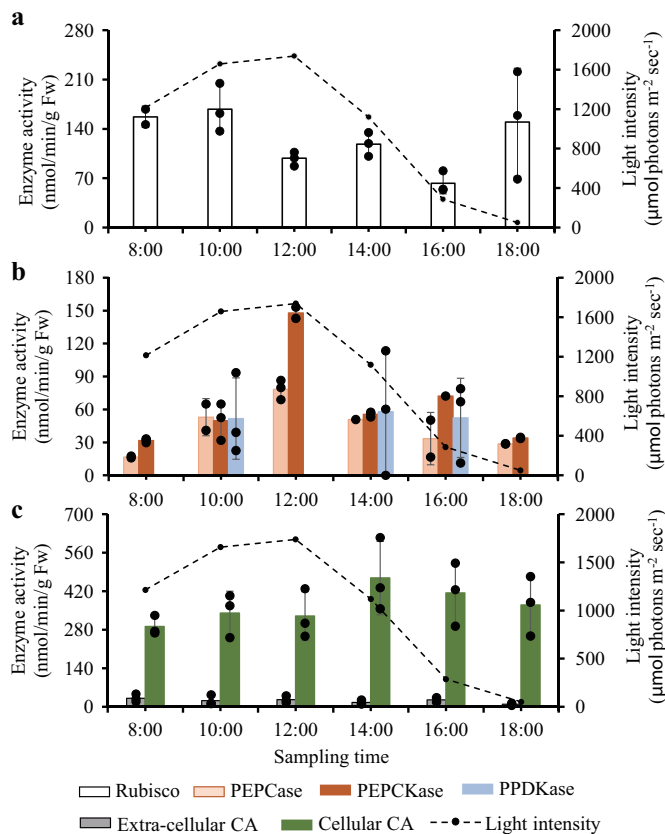


Fig. 4 Diurnal patterns of C₃ and C₄ enzymes and CA in response to sunlight variations. **a** Diurnal pattern of C₃ enzyme (Rubisco). **b** Diurnal patterns of C₄ enzyme (PEPCase, PEPCkase, and PPDkase). **c** Diurnal patterns of CA (extracellular and cellular CA). They indicate the activities of C₃ and C₄ pathways and CA mechanism, respectively, in response to diurnal sunlight variations. Each data bar is the mean of three measurements (one from each culture container) and error bars are ± 1 standard deviation from the mean; black dots in each data bar are individual data points from each culture container.

机制，但某些物种利用Hatch-Slack循环（C₄）增强光合作用。但是，C₄途径的发生和重要性仍然不确定。我们证明了物种*Ulva prolifera*中的碳固定，涉及C₃和C₄途径的组合以及CA支持的HCO₃⁻机理。

N-acyl-homoserine lactones (AHLs) in intertidal marsh: diversity and potential role in nitrogen cycling

Zhang, Zongxiao ; Zheng, Yanling; Han, Ping; Dong, Hongpo; Liang, Xia; Yin, Guoyu ; Wu, Dianming ; Yang, Yi; Liu, Sitong ; Liu, Min ; Hou, Lijun. *Plant Soil*, 2020, 454(1-2): 103-119.

Aims N-acyl-L-homoserine lactones (AHLs) based quorum sensing (QS) phenomenon is recognized as an effective agent for regulating bacterial growth and metabolism. However, diversity and biological role of AHLs in natural environments remain largely unknown. This study focuses on compositions of AHLs and their potential role in nitrogen transformation in intertidal marshes. *Methods* We investigated the levels of AHLs in rhizosphere (*Phragmites australis*, *Spartina alterniflora* and *Scirpus maritimus*) and non-rhizosphere soils from Chongming eastern intertidal wetland of the Yangtze Estuary using gas chromatography-mass spectrometry (GC/MS). Molecular techniques were employed to investigate the compositions and structure of bacterial

基于N-酰基-L-高丝氨酸内酯（AHLs）的群体感应（QS）现象被认为是调节细菌生长和代谢的有效因子。然而，AHLs在自然环境中的多样性和生物学作用仍然是未知的。为此，以长江口崇明东滩作为研究区，分析了河口潮滩湿地中AHLs的组成及其在氮素转化中的潜在作用。结果显示，潮滩植被根际沉积物中AHLs含量显著高于非根际沉积物，C₆-、C₈-、C₁₀-和C₁₂-HSLs是潮滩湿地沉积物中普遍存在的QS信号分子。实验数据显示，潮滩湿地环境中AHL的含量水平可调控微生物多样性，并在硝化、反硝化和厌氧氨氧化等氮转化过程中起重要作用。

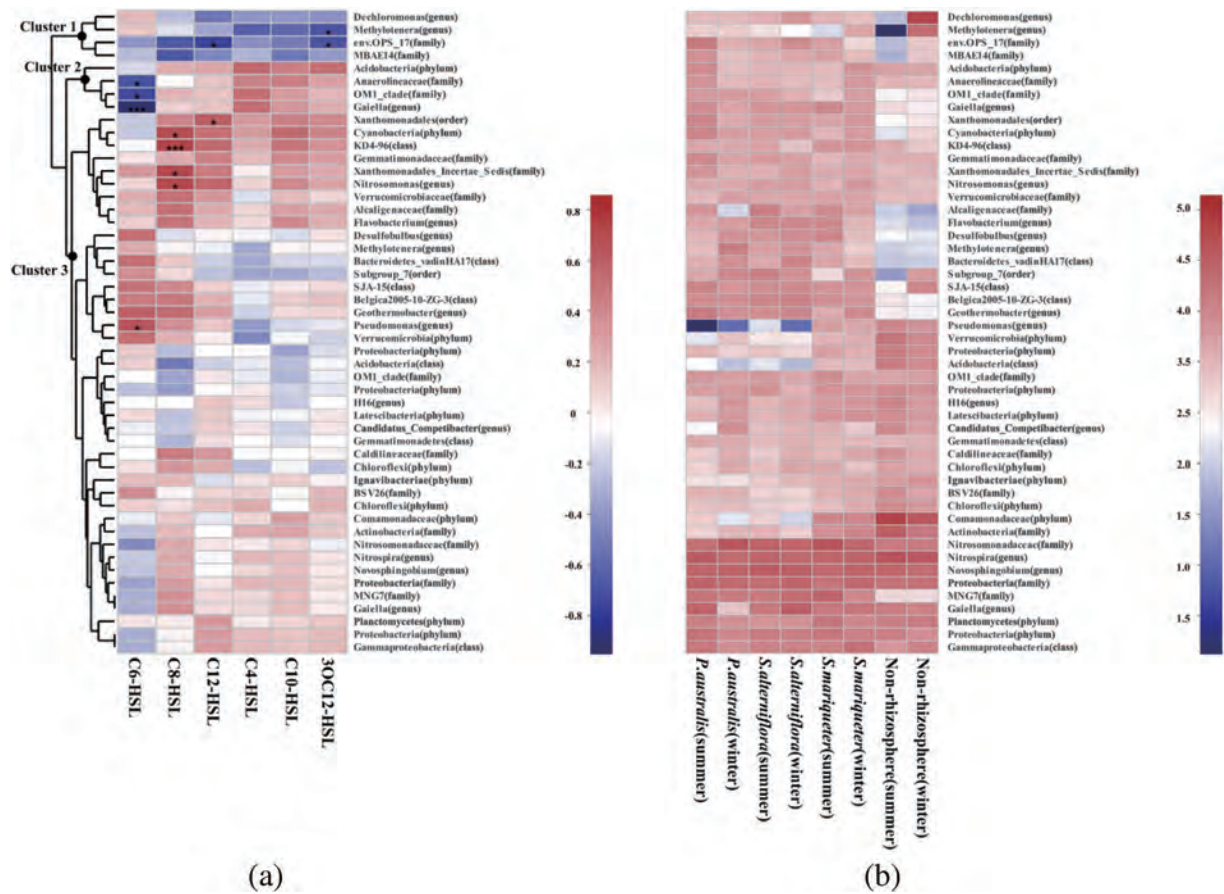


Fig. 6 Clustering of the top 50 most abundant OTUs related to concentrations of AHLs (a), and abundance of the top 50 dominant OTUs in rhizosphere and non-rhizosphere soil samples (b). Correlations of AHLs concentrations with the proportion of the top 50 OTUs were estimated on the basis of Pearson's correlation. FDR

corrections were conducted for multiple comparisons, and significant differences are shown as follows: ** $P < 0.01$ and * $P < 0.05$. The abundance is shown by a color gradient, after \log_{10} transformation

Global inventory of atmospheric fibrous microplastics input into the ocean: An implication from the indoor origin

Liu, Kai; Wang, Xiaohui; Song, Zhangyu; Wei, Nian; Ye, Haoda; Cong, Xin; Zhao, Longwei; Li, You; Qu, Liming; Zhu, Lixin; Zhang, Feng; Zong, Changxing; Jiang, Chunhua; Li, Daoji. *Journal of Hazardous Materials*, 2020, 400: 123223.

Atmospheric transport could be a significant pathway for inland microplastics (MPs, with size < 5 mm) to the ocean in addition to catchment runoff and coastal discharge. However, atmospheric input of MPs to the ocean is rarely quantified. To address this issue, transport of atmospheric MPs from source to sink was studied in the Asia-Pacific region during nine cruises from October 2018 to September 2019. Both deposited atmospheric MPs (DAMPs) and suspended atmospheric MPs (SAMPs) were collected, ranging from 23.04 n/(m²·d) to 67.54 n/(m²·d), and 0 to 1.37 n/m³, respectively. Size composition revealed that atmospheric deposition of MPs originating in terrestrial regions seems inadequate and insufficient to quantify the atmospheric input to the ocean. In addition, combined with aerodynamic modelling, for the first time, we estimated that 7.64–33.76 t of fibrous atmospheric MPs was globally generated in 2018, which is 3 % and 31 % of riverine input MPs of The Yangtze River and The Pearl River in terms of mid-point mass, respectively. The increasing load of ingestible plastics from sea air could have a far-reaching impact on marine ecosystem.

除了集水径流和沿海排放，大气输送可能是内陆微塑料进入海洋的重要途径。然而，大气微塑料向海洋输入很少被量化。为了解决这一问题，2018年10月至2019年9月，本研究揭示了大气中MPs从源头到汇在亚太地区的传输。沉积大气微塑料沉降和大气悬浮态微塑料丰度分别为23.04 - 67.54 n/(m²·d)和0 - 1.37 n/m³。粒径大小组成表明，源自陆地地区的MPs的大气沉积似乎不充分量化大气进入海洋的沉降通量。此外，结合空气动力学模型，我们估计2018年全球产生了7.64-33.76 t的大气纤维MPs。海洋空气微塑料的不断增加可能对海洋生态系统产生深远的影响。

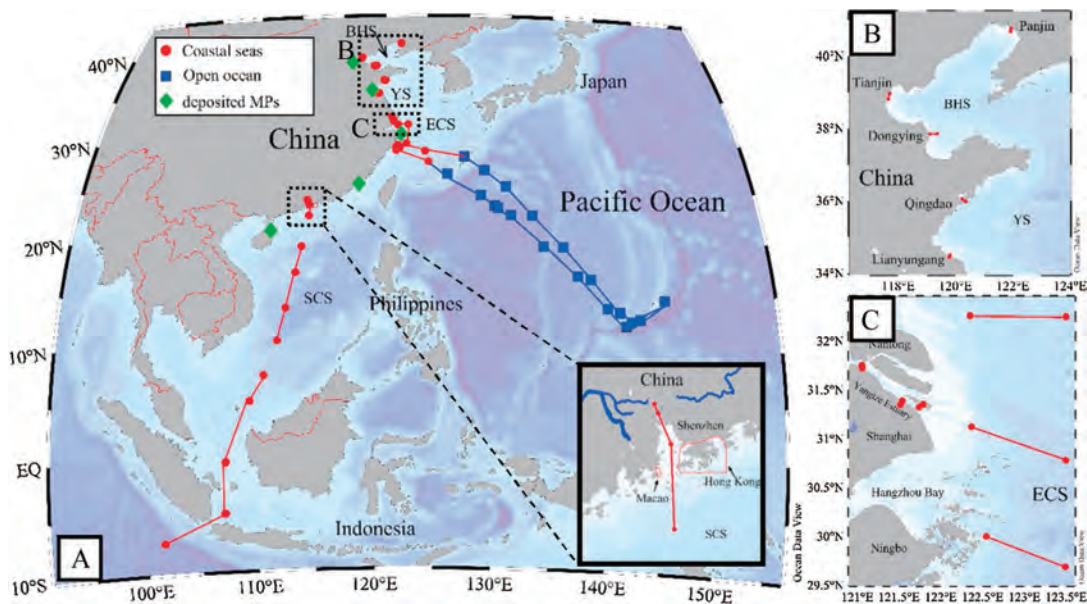


Fig. 1. Geographic locations of the general sampling track (A) and enlarged zone for northern China (B) and Yangtze Estuary (C). BHS: Bohai Sea; YS: Yellow Sea; ECS: East China Sea; SCS: South China Sea. Symbol marks (red dots and blue rectangles) indicate beginning and ending points of the suspended atmospheric microplastic (SAMP) sampling. For the sampling stations inside the Yangtze Estuary, SAMPs were continuously sampled at the fixed sites.

Elucidating the vertical transport of microplastics in the water column: a review of sampling methodologies and distributions

Liu, Kai; Courtene-Jones, Winnie; Wang, Xiaohui; Song, Zhangyu; Wei, Nian; Li, Daoji. *Water research*, 2020, 186: 116403.

There have been numerous studies that have investigated floating microplastics (MPs) in surface water, yet little data are currently available regarding the vertical distribution in the water column. This lack constrains our ability to comprehensively assess the ecological effects of MPs and develop further policy controls. In this study, we reviewed current progress of sampling methodologies, the distribution patterns, and the physiochemical properties of MPs throughout the water column. Three sampling protocols were identified in this study: bulk, net and submersible pump/in-situ sampling. In different regions, the vertical patterns of MPs in the water column varied with depth, which is possibly related to the morphological characteristics, polymeric densities, and biofouling of the MPs. The results of this review revealed that fibrous and fragmented MPs comprised over 90% of the total MPs by quantity, of which fibrous MPs constituted the majority (43%–100%). In addition, polyethylene terephthalate, polyamide, polyethylene, polyvinyl chloride, and polypropylene have been widely identified in previous studies. To minimize the impact caused by various

sampling protocols, the use of a volume gradient trail experiment and a unified mesh size of 60–100 μm for the initial concentration are recommended according to the results of this review. Given the limited knowledge regarding the vertical transport of MPs in the water column, harmonized sampling methods should first be developed. The mechanisms of this process can be separately considered for different water bodies, such as freshwater systems, coastal waters, and pelagic zones. The presence of these anthropogenic pollutants in the water column poses a threat to the largest but most vulnerable habitats of life on earth, and hence they merit further investigation.

已有许多研究对地表水中的悬浮微塑料进行了研究，但目前关于水柱垂直分布的数据很少。这种缺乏限制了我们对全面评估微塑料的生态效应和进一步制定政策控制的能力。在本研究中，我们综述了微塑料在水柱中采样方法、分布和理化性质的最新进展。本研究确定了三种采样方案：整体采样、拖网采样和潜水泵/原位采样。在不同地区，水体中微塑料的垂直形态随深度而变化，这可能与微塑料的形态特征、聚合物密度和生物附着有关。

本综述的结果显示，纤维状和碎片状微塑料的数量占总微塑料的90%以上，其中纤维状微塑料占多数(43%-100%)。此外，聚乙烯对苯二甲酸乙二醇酯、聚酰胺、聚乙烯、聚氯乙烯和聚丙烯在以往的研究中已被广泛识别。为了将各种采样方案造成的影响最小化，根据本综述的结果，建议使用体积梯度试验和统一的60-100微米

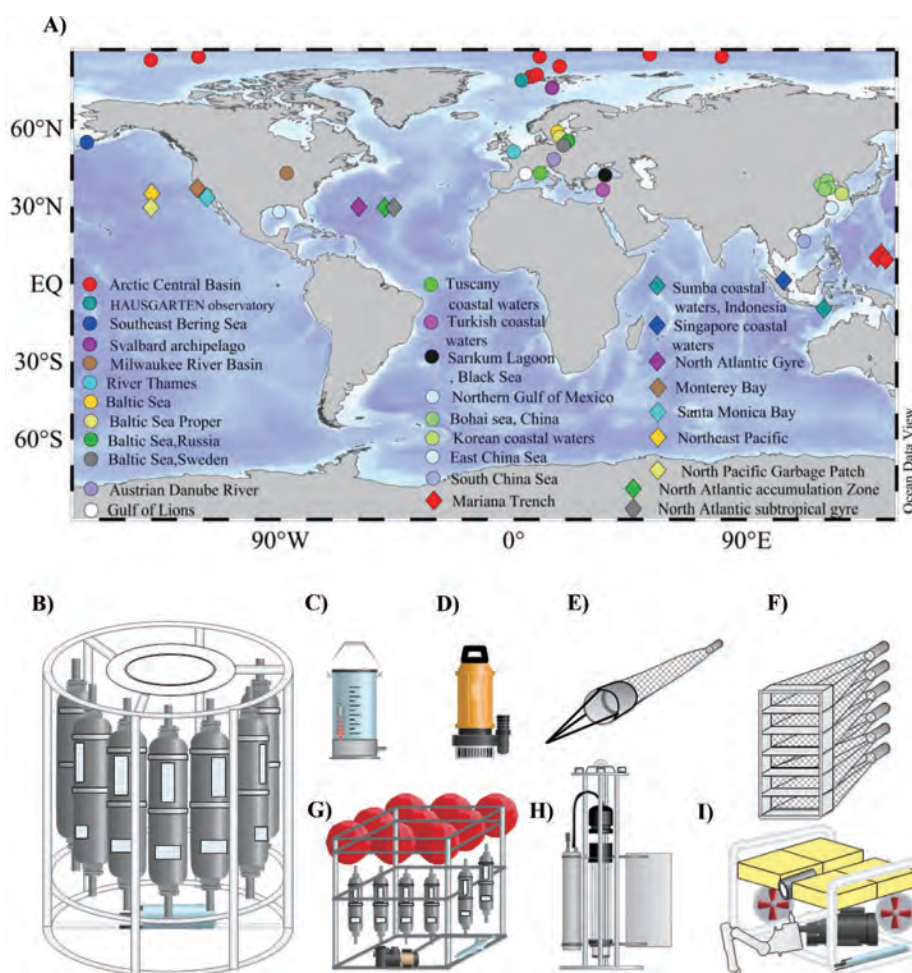


Fig 1. Geolocation of sampled water columns for MPs research (A). Red dots indicate the geographical locations of sampling sites in collected literatures except for Ryan et al., 2020 due to limited accessible information. Sampling device used for collecting MPs in the water column (B: CTD sampler; C: plexiglass water sampler; D: submersible pump; E: plankton net; F: multi-net trawls; G: lander system; H: plankton pump; I: remotely operated vehicle (ROV)).

拖网孔径。考虑到水体中微塑料的垂直运移知识有限，首先应发展统一的，可比较的采样方法。这一过程的机制可以针对不同的水体，如淡水系统、沿海水域和远洋带，分别加以考虑。水体中这些人为污染物的存在对地球上最大但最脆弱的生命栖息地构成了威胁，因此值得进一步研究。

Feeding behavior responses of a juvenile hybrid grouper, *Epinephelus fuscoguttatus* ♀ × *E. lanceolatus* ♂, to microplastics

Xu, Jiayi; Li, Daoji. *Environmental pollution*, 2020, 268(Pt A): 115648.

In recent decades, microplastic (MP) pollution has become a severe problem in aquatic environments. Yet the behavioral and selective responses of fish toward different types of MPs remain unclear. We therefore conducted laboratory-based video observations to investigate the behavioral responses of hybrid grouper juveniles (tiger grouper *Epinephelus fuscoguttatus* ♀ × giant grouper *E. lanceolatus* ♂) to eight different types of MPs. We observed four distinct feeding behaviors: (i) normal ingestion of MPs, which rarely occurred (0%-6%); (ii) pursuit, capture, and tasting of MPs, after which MPs were quickly spat out; (iii) detection and rejection of MPs without attack; and (iv) no significant response to MPs. Our results indicate that juveniles can distinguish MPs as inedible particle and behave differently between MPs with different sizes, colors, and materials, primarily using visual and gustatory senses. Notably, 50%-90% of MP rejection events occurred before capture. Juveniles spent double the time evaluating large nylon particles than they did evaluating large polyvinyl chloride particles before capture, but half the time tasting after capture. Although we observed no sub-lethal or lethal effects of MPs, we conclude that the presence of MPs can still have an impact on groupers in aquaculture. For instance, in the densely stocked conditions of an aquaculture unit, the fish could lose visibility and can inadvertently ingest MPs, thus suffering from their toxic impacts.

本文通过对珍珠龙胆石斑鱼稚鱼对食物和塑料颗粒的选择摄食行为研究，发现该鱼在稚鱼阶段已能较好识别食物与非食物颗粒，很少(几乎不)出现摄食塑料颗粒的情况，且50%-90%的选择过程发生在具有明显扑食行为之前。但通过进一步行为分析发现，即使鱼类在实验条件下未摄食塑料，其花费在分辨塑料可食与否上的时间明显高于分辨饲料颗粒的时间，并且在暴露于PVC材质的塑料颗粒时具有较长时间的咀嚼过程，推测当鱼类置身于视野较差的养殖环境中时有增加误食塑料的可能性。

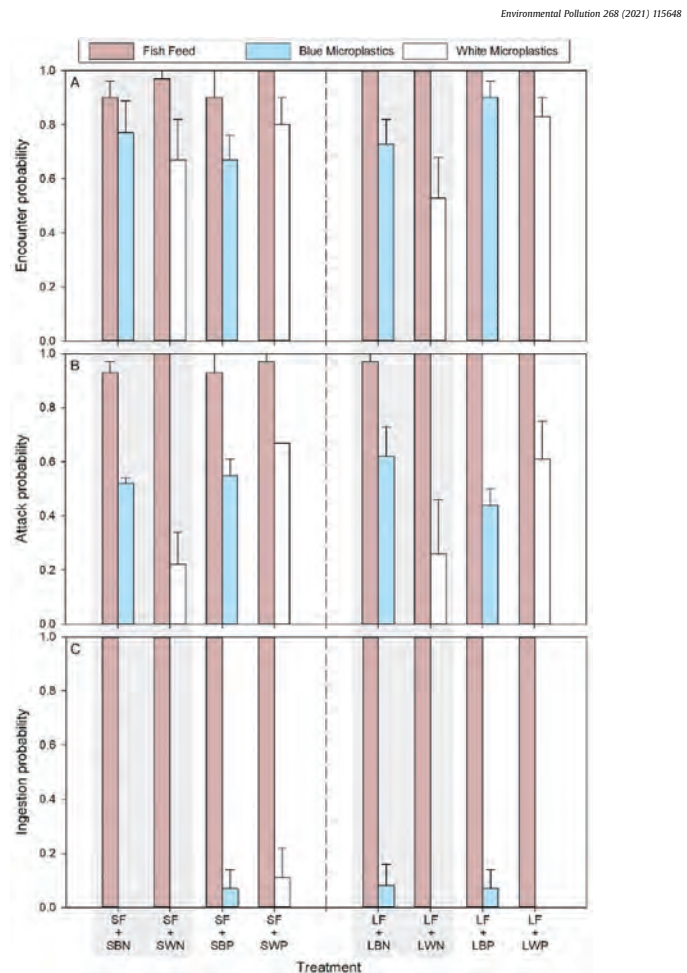


Fig. 1. Probability levels of (A) encounter, (B) attack, and (C) ingestion in treatments when hybrid grouper juveniles were supplied fish feed pellets (brown bars) or MP particles (blue and white bars). Error bars show standard error (n = 3). (For interpretation of the references to color in this figure legend, the reader is referred to the Web version of this article.)

Profiling the vertical transport of microplastics in the West Pacific Ocean and East Indian Ocean with a novel in situ filtration technique

Li, Daoji; Liu, Kai; Li, Changjun; Peng, Guyu; Andrady, Anthony L; Wu, Tianning; Zhang, Zhiwei; Wang, Xiaohui; Song, Zhangyu; Zong, Changxing; Zhang, Feng; Wei, Nian; Bai, Mengyu; Zhu, Lixin; Xu, Jiayi; Wu, Hui; Wang, Lu; Chang, Siyuan; Zhu, Wenxi. *Environmental science & technology*, 2020, 54(20): 12979-12988.

A new technique involving large-volume (10 m³) samples of seawater was used to determine the abundance of microplastics (MPs) in the water column in the West Pacific Ocean and the East Indian Ocean. Compared to the conventional sampling methods based on smaller volumes of water, the new data yielded abundance values for the deep-water column that were at least 1–2 orders of magnitude lower. The data suggested that limited bulk volumes currently used for surface sampling are insufficient to obtain accurate estimates of MP abundance in deep water. Size distribution data indicated that the lateral movement of MPs into the water column contributed to their movement from the surface to the bottom. This study provides a reliable dataset for the water column to enable a better understanding of the transport and fate of plastic contamination in the deep-ocean ecosystem.

一种涉及大体积(10立方米)样品的新技术用海水样品测定微塑料的丰度在西太平洋及东太平洋和印度洋水柱应用。与传统的抽样方法相比,在水量较小的情况下,本研究得出的丰度值至少低于有1—2个数量级。数据表明,整体采样的方法目前用不足以获得深层水微塑料的准确估计。粒径分布数据表明,微塑料在沉降过程中伴随着长距离的水平运移。本研究为深海塑料和微塑料沉降机制和归趋提供了可靠的数据集。

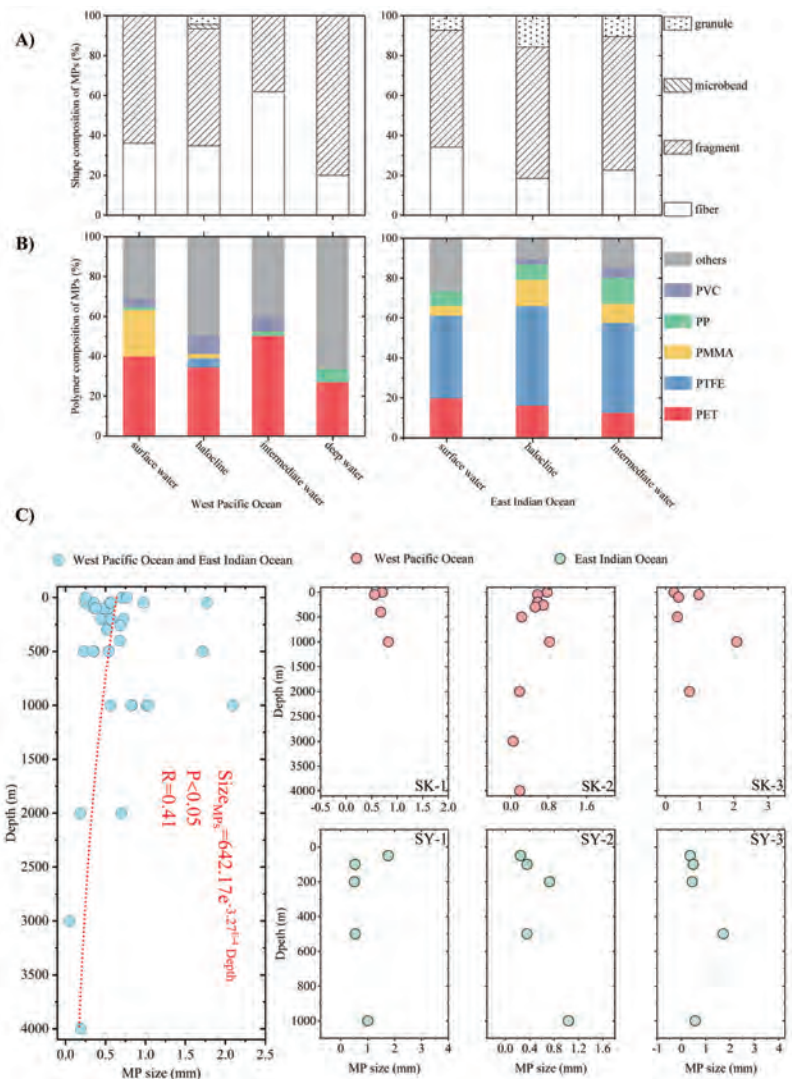


Figure 3. Shape (A), polymer (B), and size (C) compositions in different water layers of PO and IO. In (B), only the top five polymers of MPs by quantity are displayed. In (C), colored dots represent the average size of the MPs.

The nonconservative distribution pattern of organic matter in the Rajang, a tropical river with peatland in its estuary

Zhu, Zhuoyi; Oakes, Joanne; Eyre, Bradley; Hao, Youyou; Sia, Edwin Sien Aun; Jiang, Shan; Muller, Moritz; Zhang, Jing. *Biogeosciences*, 2020, 17: 2473-2485.

Southeast Asian peatland-draining rivers have attracted much attention due to their high dissolved organic carbon (DOC) yield and high CO₂ emissions under anthropogenic influences. In August 2016, we carried out a field investigation of the Rajang River and its estuary, a tropical system located in Sarawak, Malaysia. The Rajang has peatland in its estuary, while the river basin is covered by tropical rainforest. DOC-δ¹³C in the Rajang ranged from -28.7 ‰ to -20.1 ‰, with a U-shaped trend from river to estuary. For particulate organic carbon (POC), δ¹³C ranged between -29.4 ‰ and -31.1 ‰ in the river, and there was a clear increasing trend towards more enriched δ¹³C values with higher salinity. In the estuary, there was a linear conservative dilution pattern for dissolved organic matter composition (as quantified by D- and L-amino acid enantiomers) plotted against DOC-δ¹³C, whereas when plotted against salinity, dissolved D- and L-amino acid enantiomer values were higher than the theoretical dilution value. Together, these data indicate that the addition of DOC to the estuary (by peatland) not only increased the DOC concentration but also altered its composition, by adding more biodegraded, ¹³C-depleted organic matter into the bulk dissolved organic matter. Alteration of organic matter composition (addition of a more degraded subpart) was also apparent for the particulate phase, but patterns were less clear. The Rajang was characterized by DOC to DON (dissolved organic nitrogen) ratios of 50 in the river section, with loss of DON in the estuary increasing the ratio to 140, suggesting an unbalanced export of organic carbon and nitrogen. Where affected by anthropogenic activities, further assessment of organic carbon to nitrogen ratios is needed.

2480

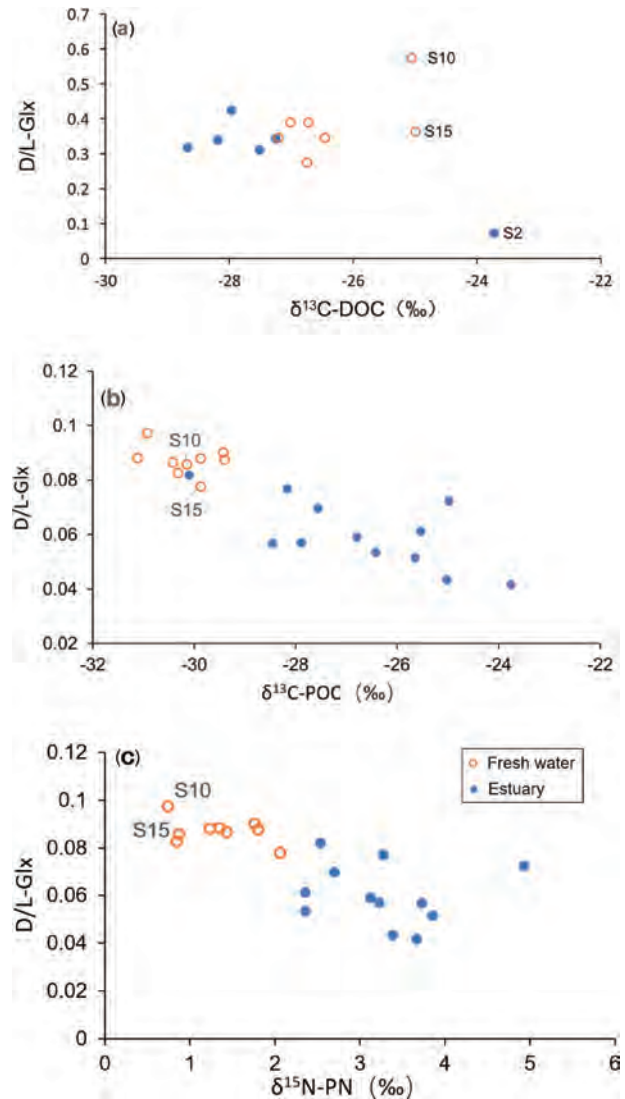


Figure 6. D / L ratio of AAs (as Glx) plotted against (a) DOC-δ¹³C (b) POC-δ¹³C, and (c) PN-δ¹⁵N.

热带泥炭地是全球碳的重要储库；在人类活动和全球变化的背景下，热带泥炭地中碳的活化和去向是重要的科学和气候问题。本文以马来西亚沙捞越的拉让河及河口为研究对象，探讨了河口泥炭地，以及人类活动（伐木、土地利用改变）对河流中有机质含量河成分的影响。主要发现如下：1）热带雨林为盆地特征的拉让河中氨基酸信号呈现很强的细菌改造信号，表现为极高的D/L比值；2）河口泥炭地对河流溶解有机质中存在显著的有机质成分改变和影响；3）以碳氮同位素和D性氨基酸二维坐标系区分的河流溶解有机质分布表明，陆源有机质在经由河流入海过程中在盐度为5的泥炭地河口区域存在陆源输入最大值，从而造成拉让河独特的倒U性陆源有机质随盐度分布型号。

Hotspot of Organic Carbon Export Driven by Mesoscale Eddies in the Slope Region of the Northern South China Sea.

Zhang, Miao; Wu, Ying; Wang, Fuqiang; Xu, Dongfeng; Liu, Sumei; Zhou, Meng. *Frontiers in Marine Science*, 2020, 7: 444.

Mesoscale eddies frequently observed in the northern slope region of the South China Sea (SCS) significantly modulate the biological and biogeochemical behavior of organic carbon (OC). There have been few comparative studies on biological and biogeochemical processes in a pair of anticyclonic eddies (ACEs) and cyclonic eddies (CEs) in continental slope. In our research, an ACE–CE pair was observed in June 2015 on the northern slope of the SCS. The surface dissolved OC (DOC) was approximately $3 \mu\text{mol L}^{-1}$ higher in the ACE than that of the CE, and particulate OC (POC) was approximately $3.9 \mu\text{mol L}^{-1}$ higher in the CE than in the ACE. Along the transect across the ACE and CE, the concentrations of DOC and fluorescent dissolved organic matter (FDOM) were coincident with the downwelling and upwelling in the eddies. In the euphotic layer, the total OC (TOC) stock in the ACE was higher than that of the CE with a lower POC/TOC ratio. There was net consumption of both DOC and POC in the upper 120 m in the ACE; however, net POC production was observed within the CE. The results also indicated that the production of fresh OC was higher in the CE while carbon export was higher in ACE. The vertical export rates of DOC and POC at 120 m in the ACE were approximately 70.2 and $1.69 \text{ mmol C m}^{-2} \text{ day}^{-1}$. Summarizing these measurements, the horizontal export of TOC across the slope to the SCS basin transported by dual eddies was estimated more than $22.1 \times 10^9 \text{ g C}$. This estimate implies that mesoscale eddies can contribute significantly to carbon sequestration in the SCS.

在南海陆坡区中经常观察到的中尺度涡旋可显著调节有机碳的生物地球化学行为。在一对反气旋涡（ACEs）和气旋涡（CEs）观测中，我们发现表明，气旋涡中新鲜OC的产量较高，而反气旋涡中的碳输出较高。反气旋涡中120 m处的DOC和POC垂向碳输送速率分别约为70.2和 $1.69 \text{ mmol C m}^{-2} \text{ d}^{-1}$ 。初步估算表明通过双涡流将TOC穿过陆坡向南海海盆的水平输出量估计大于 $22.1 \times 10^9 \text{ gC}$ 。该估计值表明，中尺度涡旋可显著促进南海的碳固存。

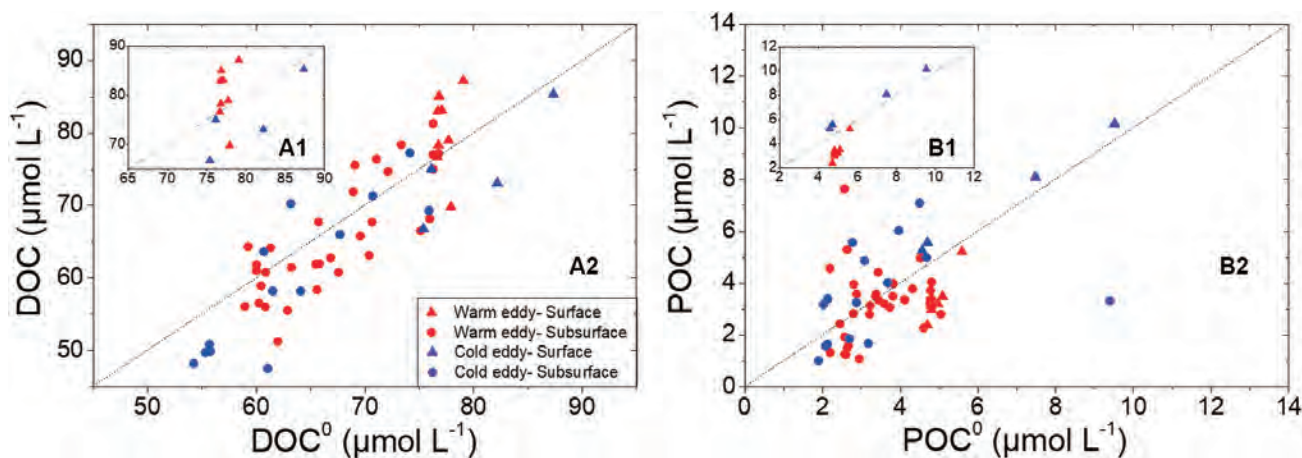


FIGURE 6 | Measured DOC vs. modeled DOC⁰ (A) and measured POC vs. modeled POC⁰ (B) derived from the mixing model. Triangles represent samples of surface, while circles represent subsurface samples. Marks in red represent samples in warm eddy and in blue represent samples influenced by cold eddy. The gray dashed line means that the modeled value was equal to measured value.

Simulation of Enhanced Growth of Marine Group II Euryarchaeota From the Deep Chlorophyll Maximum of the Western Pacific Ocean: Implication for Upwelling Impact on Microbial Functions in the Photic Zone

Dai, Jinlong; Ye, Qi; Wu, Ying; Zhang, Miao; Zhang, Jing. *Frontiers in Microbiology*, 2020, 11: 2141.

Mesoscale eddies can have a strong impact on regional biogeochemistry and primary productivity. To investigate the effect of the upwelling of seawater by western Pacific eddies on the composition of the active planktonic marine archaeal community composition of the deep chlorophyll maximum (DCM) layer, mesoscale cold-core eddies were simulated in situ by mixing western Pacific DCM layer water with mesopelagic layer (400 m) water. Illumina sequencing of the 16S rRNA gene and 16S rRNA transcripts indicated that the specific heterotrophic Marine Group IIb (MGIIb) taxonomic group of the DCM layer was rapidly stimulated after receiving fresh substrate from 400 m water, which was dominated by uncultured autotrophic Marine Group I (MGI) archaea. Furthermore, niche differentiation of autotrophic ammonia-oxidizing archaea (MGI) was demonstrated by deep sequencing of 16S rRNA, *amoA*, and *accA* genes, respectively. Similar distribution patterns of active Marine Group III (MGIII) were observed in the DCM layer with or without vertical mixing, indicating that they are inclined to utilize the substrates already present in the DCM layer. These findings underscore the importance of mesoscale cyclonic eddies in stimulating microbial processes involved in the regional carbon cycle.

大洋中的中尺度涡旋如何影响不同水层中的微生物及有机物利用过程尚不清楚，通过现场模拟实验，我们成功揭示了不同水层混合体系中微生物组成及其功能变化，研究发现，中尺度涡旋混合过程中，将储存在中下层水体中细菌及氨氧化过程产生的有机物引入叶绿素极大层。这种新的有机碳为该层异养菌提供了碳源，并迅速刺激特定MGII快速增长。有机物利用降解过程中产生的二氧化碳或通过海气交换释放到大气中或提供给叶绿素极大层的浮游生物生长。

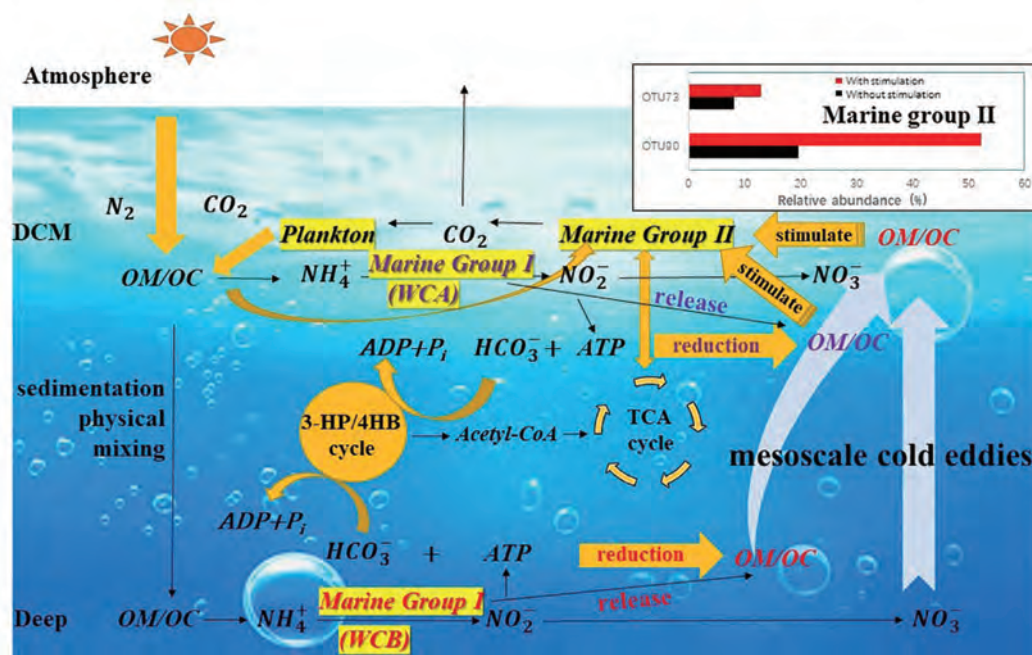


FIGURE 7 | The possible mechanism by which the growth of Marine Group II Euryarchaeota is stimulated by carbon flow affected by mesoscale eddies. Particulate organic matter (POM) produced in the upper ocean enters the ocean interior by sedimentation and physical mixing and releases NH_4^+ under the action of heterotrophic microorganisms. MGI Thaumarchaeota couples the oxidation of ammonia with carbon fixation in HCO_3^- through the 3HP/4HB pathway, and the intermediate acetyl-CoA can act as a precursor of the TCA cycle and participate in the metabolism of MGII. Much organic matter produced by ammonia-oxidizing archaea stored in mesopelagic water is brought into the DCM layer by the mesoscale process. This new organic carbon provides a carbon source for heterotrophic MGII members and rapidly stimulates the growth of specific MGII taxa. The CO_2 produced during degradation is released into the atmosphere by sea-air exchange or supplied to plankton of the DCM layer.

Bacterial-derived nutrient and carbon source-sink behaviors in a sandy beach subterranean estuary

Chen, Xiaogang; Ye, Qi; Sanders, L Christian; Du, Jinzhou; Zhang, Jing. *Marine Pollution Bulletin*, 2020, 160: 111570.

Microbial communities in subterranean estuaries play important roles in the biogeochemical cycle. However, the microorganisms associated with biogeochemical behaviors in subterranean estuaries have received little attention. Here, the bacterial communities were compared between the fresh and saline groundwater in a subterranean estuary. Correlation analysis between bacterial groups and salinity indicated that different species represented different groundwater types. The key bacterial groups found along the subterranean estuaries have been shown to influence organic pollutant degradation and nitrate utilization. These species may be potential candidates for the in situ bioremediation of subterranean estuaries that are contaminated with pollutants. The utilization of nitrate and organic pollutants by bacteria in subterranean estuaries serves as a nitrate sink and inorganic carbon source. Our results show the role of bacteria in remediating pollutants through submarine groundwater discharge (SGD) to the coastal ocean, and specific species may be helpful in selecting reasonable groundwater end-members and reducing SGD uncertainties.

在对崂泗岛沿岸井水和间隙水两种不同类型的地下水细菌多样性的研究中发现盐度是影响菌群组成的重要因素，两类地下水样品的关键细菌菌群都有降解有机污染物和利用硝酸盐的代谢功能，这些菌群可以作为清除地下河口污染物的潜在候选菌种。同时地下河口特定菌群的代谢功能有助于合理选择地下水端元，进而降低海底地下水估算的不确定性。此项研究表明地下河口细菌在驱动营养盐和碳的源汇过程中起着重要作用。

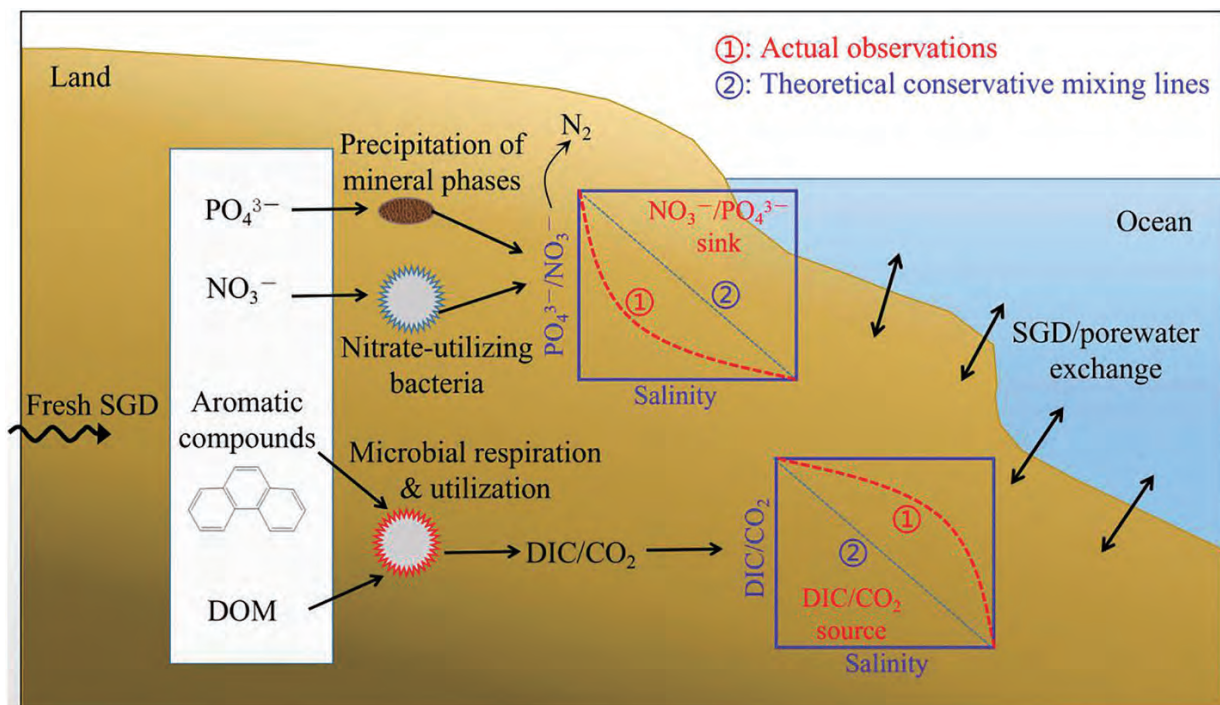


Fig. 7. Schematic diagram of biogeochemical and source-sink processes in the subterranean estuary of Shengsi Island.

Physical processes controlling chlorophyll-a variability on the Mid-Atlantic Bight along northeast United States

Xu, Yi; Travis, Miles; Oscar, Schofield. *Journal of Marine Systems*, 2020, 212: 103433.

We employed empirical orthogonal function (EOF) analysis to examine the spatial and temporal pattern changes in the surface chlorophyll a distribution (chl-a) on the Mid-Atlantic Bight (MAB) using Moderate Resolution Imaging Spectroradiometer Aqua (MODISA) chl-a data (2003–2016) and Sea-viewing Wide Field-of-view Sensor (SeaWiFS) chl-a data (1998–2007), and interpreted the underlying environmental determinants. A coupled physical-biogeochemical model was used to explore the primary physical factors determining the chl-a variability on the shelf. Model sensitivity studies identified wind mixing, net heat flux, and river discharge as the dominant factors influencing the MAB water column stability and consequent phytoplankton growth. The primary feature of chl-a indicated spring peaks on the outer shelf during the MODISA period, while fall-winter high during the SeaWiFS period in the same area. The observed increase in wind mixing and heat loss during winter and pre-spring were responsible for the delay in the phytoplankton bloom to spring on the outer shelf. The secondary chl-a peak occurred in the fall on the New Jersey shelf during MODISA period, and in the fall-winter in the Delaware Bay estuary for chl-a during SeaWiFS period. The Hudson River discharge was associated with the chl-a anomalies on the New Jersey shelf in the fall and winter during the MODISA period. Both the MODISA and SeaWiFS chl-a

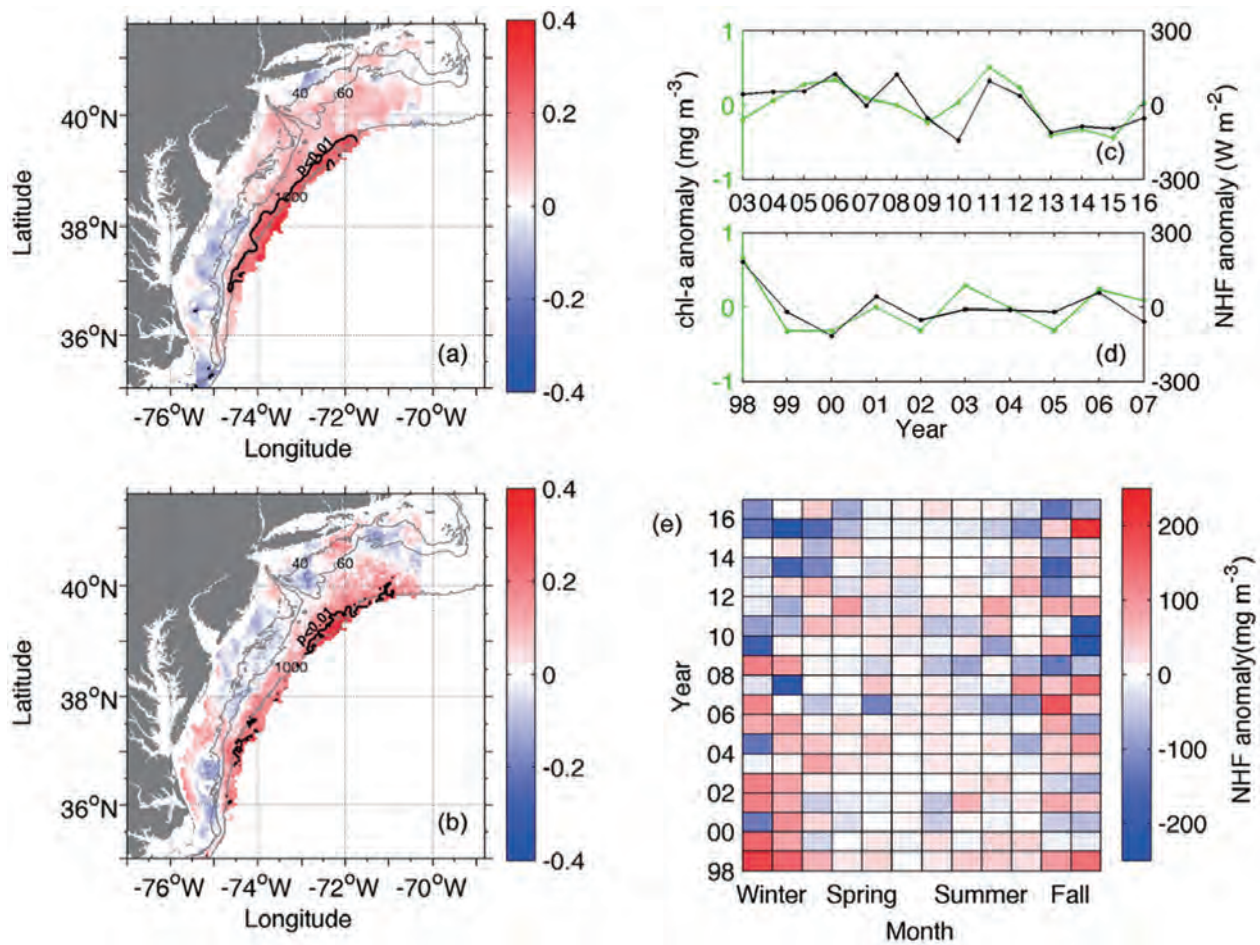


Fig. 6. Comparison of chl-a and NHF anomalies. (a) Correlation coefficients of chl-a and NHF anomalies during the MODISA period. The black lines specify the significant correlated area with $r > 0.3$ and $p < 0.01$. (b) For the SeaWiFS period. (c) Time series of the winter to pre-spring spatial mean chl-a (green line) and NHF (black line) anomalies in the significant correlated area for the MODISA period. (d) For the SeaWiFS period. (e) NHF anomaly in different seasons during 1998–2016. (For interpretation of the references to color in this figure legend, the reader is referred to the web version of this article.)

concentrations peaked during the fall-winter on the southern part of the MAB (in the EOF mode 3 region), but the MODISA chl-a peak area was north of the SeaWiFS chl-a peak area. The variation of chl-a concentration in the southern region of the MAB was most likely associated with the Chesapeake Bay rivers' discharge. In our study, the regional associations between chl-a and multiple climate-sensitive environmental parameters suggest that basin-scale forcing plays an important role in the underlying chl-a variabilities on the MAB.

利用MODISA chl-a数据（2003-2016）和SeaWiFS chl-a数据，采用经验正交函数（EOF）分析了中大西洋湾（MAB）表层叶绿素a分布的时空格局变化（1998-2007），并解释了潜在的环境决定因素。利用三维耦合的物理-生物地球化学模型，探讨了决定表层chl-a变异性的主要物理因素。模型敏感性研究发现，风混合、海表净热通量和河流输入是影响MAB水体稳定性和浮游植物生长的主要因素。chl-a的主要特征表明，同一地区在MODISA期出现春季高峰，在SeaWiFS却出现秋冬季高峰。在冬季和春季前观察到的风混合和热量损失的增加是导致浮游植物水华推迟到春季的原因。第二次chl-a峰值出现在MODISA时期的新泽西大陆架秋季，而chl-a的第二次高峰出现在特拉华湾河口的秋冬季。哈得逊河流量与MODISA期新泽西大陆架秋冬季chl-a异常有关。MODISA和SeaWiFS chl-a浓度在秋冬期间在MAB南部达到峰值（在EOF模式3区域），但MODISA chl-a峰值区域位于SeaWiFS chl-a峰值区域的北部。在MAB南部地区chl-a浓度的变化很可能与切萨皮克湾河流的排放有关。在我们的研究中，chl-a与多个气候敏感环境参数之间的区域关联表明，盆地尺度强迫在MAB潜在chl-a变化中起着重要作用。

Leaf and Wood Separation for Individual Trees Using the Intensity and Density Data of Terrestrial Laser Scanners

Tan, Kai; Zhang, Weiguo; Dong, Zhen; Cheng, Xiaolong; Cheng, Xiaojun. *IEEE Transactions on Geoscience and Remote Sensing*, 2020.

Terrestrial laser scanning (TLS) is a highly effective and noninvasive technology for retrieving the structural and biophysical attributes of trees using 3-D high-accuracy and high-density point clouds. The separation of leaf and wood points in TLS data is a prerequisite for the accurate and reliable derivation of these attributes. In this study, a new method is proposed to separate the leaf and wood points of individual trees by combining the TLS radiometric (intensity) and geometric (density) data. The leaf points are separated from the wood ones through three steps. First, the corrected intensity data are used to separate a part of the leaf points preliminarily given the differences in reflectance characteristics. Second, the density data are adopted for the further separation of another part of the leaf points because the density of the remaining leaf points is smaller than that of the wood points. Finally, a connectivity clustering algorithm is conducted to form several clusters with different sizes (points) and the remaining leaf points are separated in accordance with the cluster sizes. Eight different trees are selected to evaluate the performance of the proposed method. The averaged overall accuracy and kappa coefficient of the eight trees are approximately 95% and 0.81, respectively. The results suggest that the combination of TLS intensity and density data can perform a superior separation of leaf and wood points in terms of efficiency and accuracy, and the proposed separation method can be accurately and robustly used for various trees with different species, sizes, and structures.

植被是人类生存环境的重要组成部分，是提示自然环境特征最重要的手段。植被能进行光合作用，对环境有巨大的改造调节作用，还可改善大气污染、保持水土、涵养水源、调节气候等，对全球生态系统、物质循环和能量流动具有重要影响。地面LiDAR具有高密度、高精度、非接触测量、数据采集灵活等特点，近年来已在森林植被三维结构和生化参数高精度精细反演方面取得广泛应用，可作为光学遥感及空-天LiDAR植被产品的重要补充并为其提供精度验证。地面LiDAR获取的数据中包含植被的茎和叶两个不同部分：茎是衡量植被生长发育状况及趋势的重要指标，从点云数据中可以提取胸径、地茎等参数；叶是植被进行光合作用、呼吸作用、

蒸腾作用等物化过程的载体，从点云数据中可以提取叶面积指数、叶倾角等参数对植被的生化过程进行估算和预测。因此，从地面LiDAR点云数据中反演植被结构和生化参数的首要和关键步骤就是对茎叶点云进行分类。地面LiDAR获取的高密度植被点云是无任何拓扑关系和语义关联的，如何从海量点云数据中分离植被茎和叶是点云数据处理的一个技术难点。虽然地面LiDAR获取的植被点云是无序的，但是茎和叶在空间结构和分布上会存在较大差异。通常情况下，茎为柱状而叶为面状薄片。在点云数据中，茎呈现较为规律分布而叶则呈现散乱状，二者在曲率、法向、密度等几何特征方面会存在较大差异。本文充分利用并结合地面LiDAR几何数据和强度数据，提出了一种新的方法对植被的茎叶点云进行精确分类，为进一步的植被结构与生化参数提取奠定基础。首先，根据茎叶反射率的差异，对原始强度数据进行入射角和距离效应改正，利用改正后强度数据对叶点进行初步分离；然后，由于单株植被空间范围较小，密度不受距离的影响，利用茎和叶在密度方面的差异，再次分离叶点；最后提出了一种连通性聚类方法，对茎叶点进行聚类，根据类的点、线、面特征及类大小对茎类和叶类进行区分。实验结果表明：所提方法充分利用地面LiDAR强度数据和几何数据，与现有方法相比，运行速度快，抗差性好，普适性强，总体分类精度达到95%以上。研究成果为海岸滩涂植被结构参数与生化参数反演提供了理论基础和技术示范。

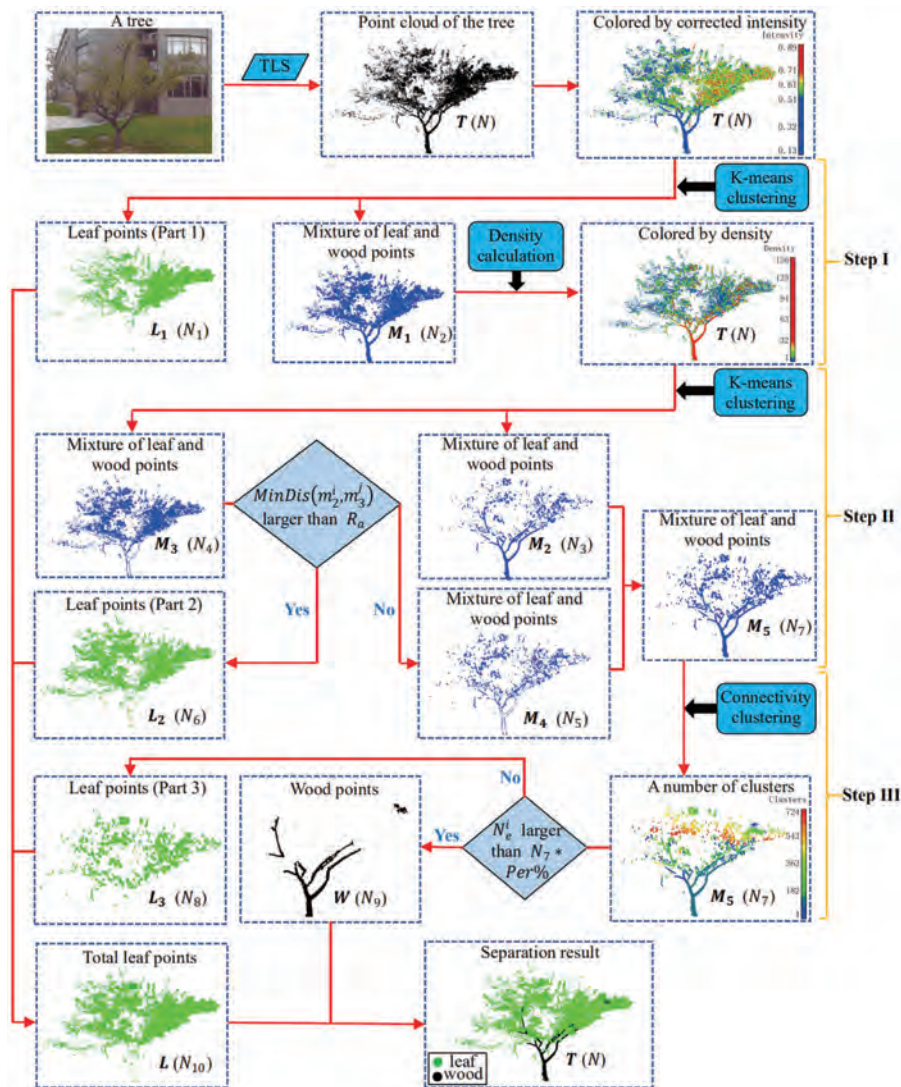


Fig. 1. Technical flow of the proposed method (Tree 1 is used as an example).

Reduced magnitude and shifted seasonality of CO₂ sink by experimental warming in a coastal wetland.

Sun, Baoyu; Yan Liming; Jiang Ming; Li Xingge; Han Guangxuan; Xia Jianyang. *Ecology*, 2020: e03236.

Coastal wetlands have the highest carbon sequestration rate per unit area among all unmanaged natural ecosystems. However, how the magnitude and seasonality of the CO₂ sink in coastal wetlands will respond to future climate warming remains unclear. Here, based on measurements of ecosystem CO₂ fluxes in a field experiment in the Yellow River Delta, we found that experimental warming (i.e., a 2.4°C increase in soil temperature) reduced net ecosystem productivity (NEP) by 23.7% across two growing seasons of 2017–2018. Such a reduction in NEP resulted from the greater decrease in gross primary productivity (GPP) than ecosystem respiration (ER) under warming. The negative warming effect on NEP mainly occurred in summer (-43.9%) but not in autumn (+61.3%), leading to a shifted NEP seasonality under warming. Further analyses showed that the warming effects on ecosystem CO₂ exchange were mainly controlled by soil salinity and its corresponding impacts on species composition. For example, warming increased soil salinity (+35.0%), reduced total aboveground biomass (-9.9%), and benefited the growth of plant species with high salt tolerance and late peak growth. To the best of our knowledge, this study provides the first experimental evidence on the reduced magnitude and shifted seasonality of CO₂ exchange under climate warming in coastal wetlands. These findings underscore the high vulnerability of wetland CO₂ sink in coastal regions under future climate change.

滨海湿地是单位面积碳封存速率最高的自然生态系统。我们不清楚的是滨海湿地二氧化碳吸收的量和季节性如何响应气候变暖。基于黄河三角洲生态系统碳交换田间测量，我们发现实验升温降低了生态系统净生产力（NEP）。增温对NEP的负效应主要发生在夏季，而不在秋季，从而导致增温条件下NEP的季节性变化。进一步分析表明，气候变暖对生态系统CO₂交换的影响主要受土壤盐分及其对物种组成的影响控制。例如，暖化使土壤盐度增加，地上总生物量减少，有利于耐盐性高、生长高峰晚的植物物种的生长。这项研究首次提供了气候变暖下沿海湿地二氧化碳交换量减少和季节性变化的实验证据。

Morphological and reproductive responses of coastal pioneer sedge vegetations to inundation intensity

Li, Shihua, Ge, Zhenming, Tan, Lishan, Hu, Mengyao, Li, Yalei, Li, Xiuzhen, Ysebaert, Tom. *Estuarine, Coastal and Shelf Science*, 2020, 244: 106945.

Coastal plants have unique adaptability to cope with strong hydrological stresses in tidal wetlands. A fundamental understanding of the establishment and maintenance of coastal plants is needed for conservation and restoration. In the Yangtze Estuary, the plasticity of the morphological and reproductive traits of a pioneer *Scirpus* species (sedge), in terms of phenotypic growth, biomass allocation, and sexual and asexual

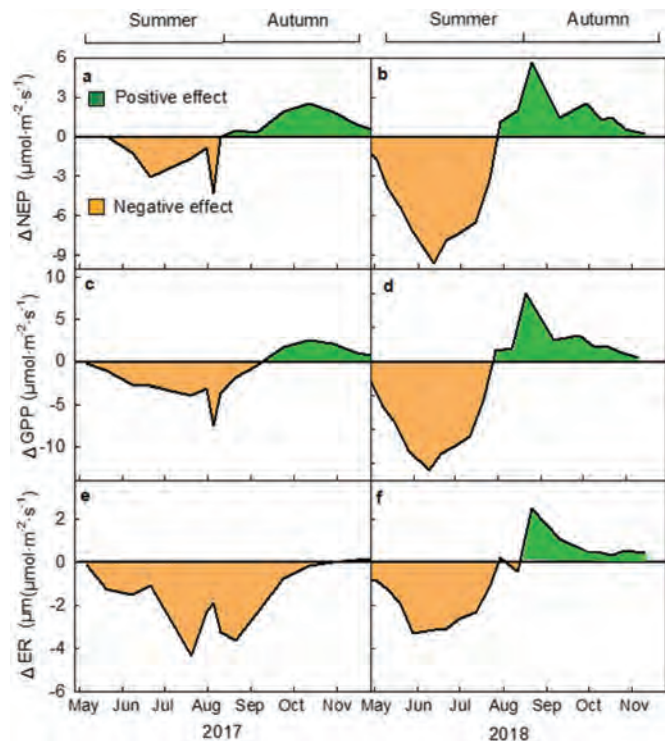


FIG. 4. Seasonal patterns of warming-induced changes in ecosystem C fluxes, net ecosystem production (DNEP), gross primary production (DGPP), and ecosystem respiration (DER).

reproductive traits, was investigated with increasing flooding intensity (elevation gradient) in a tidal flat. The varying response extents (thresholds) of plant zonation and morphological and reproductive traits to multiscale environmental heterogeneity were also assessed. Our results showed that plant colonization and performance at coastal frontiers are sensitive to the microtopography of elevation and reflect the ecological adaptability at both the landscape and individual scales. Sedge species typically exhibit morphological and reproductive flexibility across the inundation intensity. The plants allocated more biomass to belowground tissues in response to decreasing elevation. The elevation thresholds for the yield of reproductive organs were higher (2.38–2.50 m based on the local Wusong datum) than those for morphology (2.05–2.14 m). The thresholds for the yield of asexual reproductive organs shifted to a lower elevation by approximately 0.15 m relative to that of the sexual reproductive organs. The increasing corm: spike ratios of plants with longer inundation durations also indicated this reproductive plasticity. This study revealed that the combination of morphological and reproductive re-sponses of pioneer sedges contributed to survival and colonization at the foremost coastal flat. Our results are useful for developing restoration strategies for the native *Scirpus* species on China's coast.

探究滨海植物对水文胁迫的生态适应性，有助于滨海湿地的保护和恢复。本文在长江口潮滩不同高程梯度上研究了先锋莎草科蘆草属植物的生长适应性和繁殖策略可塑性。研究表明，随着潮滩高程的降低，植物密度、株高、基径均降低，植被将更多的生物量分配给地下根系组织（有利于稳定），且球茎：穗比值增大。潮滩先锋植物的生长形态高程阈值低于植物定居的高程阈值，繁殖器官生长的高程阈值高于形态适应性阈值，而无性繁殖器官（球茎）生长阈值相较于有性繁殖器官（穗和种子）更低。本研究提出潮滩前沿植被在不同空间尺度上均体现出生长形态和繁殖策略的可塑性，这对于制定滨海湿地植被恢复策略具有科学价值。

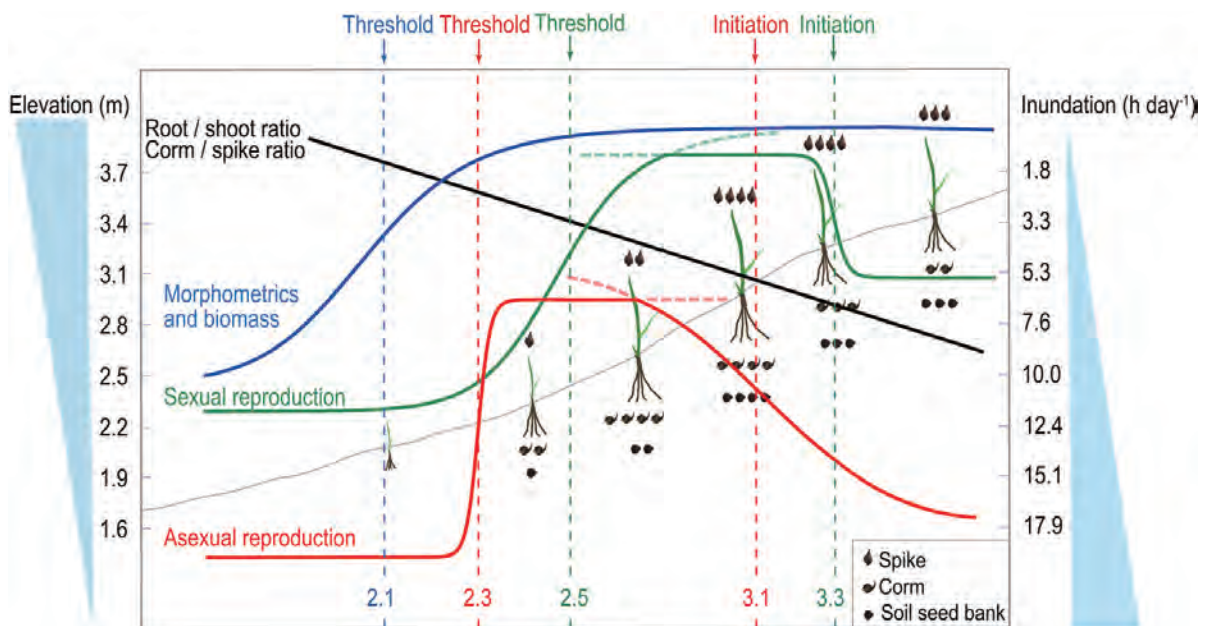


Fig. 8. Schematic diagram of the morphological and reproductive adaptations of a pioneer sedge species *S. mariqueter* to increasing inundation (or decreasing elevation). The morphological characteristics and biomass growth agreed with the unilateral 4 PL curve (blue solid line) and the reproductive characteristics (solid green lines for sexual reproductive organs and solid red lines for asexual reproductive organs) agreed with a bilateral 4 PL relationship with changes in elevation. The root:shoot and corm:spike ratios increased linearly (black solid line). The elevation threshold for the sexual reproductive organs was the highest (vertical green dashed line, data in Fig. 6), followed by the sexual reproductive organs (vertical red dashed line, data shown in Fig. 7) and morphometrics and biomass (vertical blue dashed line, data in Figs. 4 and 5). The initiation point (regarding elevation) of a steep increase in asexual reproductive organs was lower than that for sexual reproductive organs. (For interpretation of the references to colour in this figure legend, the reader is referred to the Web version of this article.)

The roles of vegetation, tide and sediment in the variability of carbon in the salt marsh dominated tidal creeks

Tan, Lishan, Ge, Zhenming, Fei, Beili, Xie, Lina, Li, Yalei, Li, Shihua, Li, Xiuzhen, Ysebaert, Tom. *Estuarine, Coastal and Shelf Science*, 2020, 239: 106752.

Combined effects of vegetation, tide and sediment on the carbon dynamics in the intertidal creek-marsh systems remain unclear. We investigated the variability of dissolved organic (DOC) and inorganic carbon (DIC), and particulate organic (POC) and inorganic carbon (PIC) in the tidal creeks within the Poaceae and Cyperaceae communities on flood-ebb cycle in a salt marsh of eastern China. In the Poaceae creek with high plant biomass and soil carbon stock, the DOC concentrations were higher by on average 1.00–1.48 times than that in the Cyperaceae creek across all seasons and spring and neap tide stages, while the difference of DIC was not notable. The POC and PIC concentrations were lower in the Poaceae creek compared to the Cyperaceae creek. Spring tides increased the carbon concentrations (except for PIC) in both creeks by on average 7–40%, relative to neap tides. Seasonal variations of sedimentary rate within the communities probably result in the discrepancy of particulate carbon loading between the creeks. The Poaceae creek functioned as a source of DOC and DIC throughout a year but as a sink of POC and PIC in summer and autumn, while it turned to a weak source of PIC in winter and spring. The Cyperaceae creek exhibited as a source of all carbon components throughout a year. We suggest that vegetation type (with soil carbon stocks), tidal regimes and sedimentary dynamics would synergistically determine the fate of carbon in the creeks. Our results are helpful in reliable estimates of carbon transport between the coastal marsh and the adjacent ocean.

滨海湿地潮沟系统是海-陆物质循环的重要传输通道。本研究对长江口滨海湿地典型生境（禾本科和莎草科盐沼）潮沟中的溶解有机碳（DOC）和溶解无机碳（DIC）、颗粒有机碳（POC）和颗粒无机碳（PIC）进行了连续观测。结果发现，湿地植被类型、潮汐类型和泥沙沉积动态对滨海盐沼潮沟中的碳浓度季节变化具有协同作用。两种植被生境潮沟内的碳含量在大潮期均高于小潮期。禾本科群落潮沟由于具有较高的植物生物量和土壤碳储量，其DOC含量高于莎草科群落潮沟。两种潮沟中POC和PIC含量的差异受泥沙沉积速率的季节变化影响。禾本科群落潮沟全年均是DOC和DIC的输出源，在夏季和秋季则是POC和PIC沉积汇，而莎草科群落潮沟的所有碳组分均显示为输出源。本研究有助于准确估算滨海盐沼湿地与邻近海洋之间的碳交换通量。

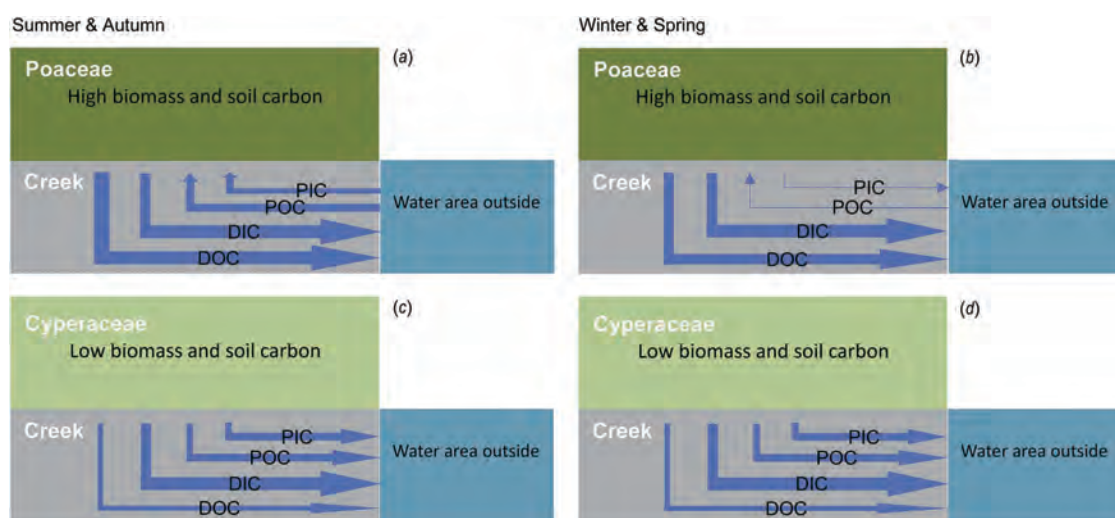


Fig. 8. Scheme of the sink (arrows from the water area outside the creek mouth to the vegetated creek) and source (arrows from the vegetated creek to the water area outside the creek mouth) processes for carbon components in the tidal creeks during a flood-ebb time scale in the seasons of summer and autumn (a for the Poaceae creek, and c for the Cyperaceae creek), and winter & spring (b for the Poaceae creek, and d for the Cyperaceae creek). The degree of fineness indicates the relative loading amount (data refer to Table 2).

Distribution of organic carbon storage in different saltmarsh plant communities: A case study at the Yangtze Estuary

Yuan, Yiquan; Li, Xiuzhen; Jiang, Junyan; Xue, Liming; Christopher B. Craft. *Estuarine, Coastal and Shelf Science*, 2020, 243: 106900.

The high carbon (C) sequestration potentials of coastal wetlands play an important role in mitigating climate change associated with the greenhouse effect. In the present study, soil samples were collected from the 0–30-cm topsoil layers and from 0 to 100-cm cores for the analysis of the spatial dynamics and vertical distribution of organic carbon (OC) and biomass in different vegetation zones in a small tidal basin in Chongming Dongtan wetland. According to the results, sediments in the region were a mixture of terrestrial and marine sources and the proportions of terrestrial components decreased with an increase in depth. In addition, soil properties were quite similar in the top-soil layer. In the study area, the OC concentration was in the 0.7–10.93 g/kg range, which was positively correlated with halophyte biomass and negatively correlated with soil salinity and particle size. Furthermore, OC content decreased with an increase in depth. The OC content in different halophyte communities was in the order of *Phragmites australis* community > Mixed community > sedge community, and was consistent with the gross biomass. The total C sequestered of 100-cm depth in the area was 31,177 ton, with the *P. australis* community, mixed community, sedge community, and water sequestering 57.7, 49.2, 25.5 t/ha, and 8 t/tidal cycle, respectively. Tidal marshes in Chongming Dongtan exhibited a high C sequestration capacity, indicating that they play a major role in the C cycle in the Yangtze Estuary.

以崇明东滩南部典型盐沼为研究对象，开展了不同植被带有机碳（Organic carbon, OC）的空间分布特征及储量的研究。结果表明，研究区土壤有机碳含量范围为0.7 ~ 10.93 g/kg。空间分布上，土壤有机碳含量与盐生植物生物量变化一致，植被带内OC储量表现为芦苇群落>混合群落>莎草群落；垂向分布上，土壤OC浓度随深度增加而降低。以2017年10月一次大潮为例，研究区内100 cm深度的“沉积物-植物-水”系统满潮时瞬时总OC储量为31177t，其中芦苇群落、混合群落、莎草群落碳密度分别为57.7 t/ha、49.2 t/ha、25.5 t/ha，潮汐水体中含有8 t OC。崇明东滩湿地表现出较强的固碳能力，证明其在长江口碳循环中的重要地位。

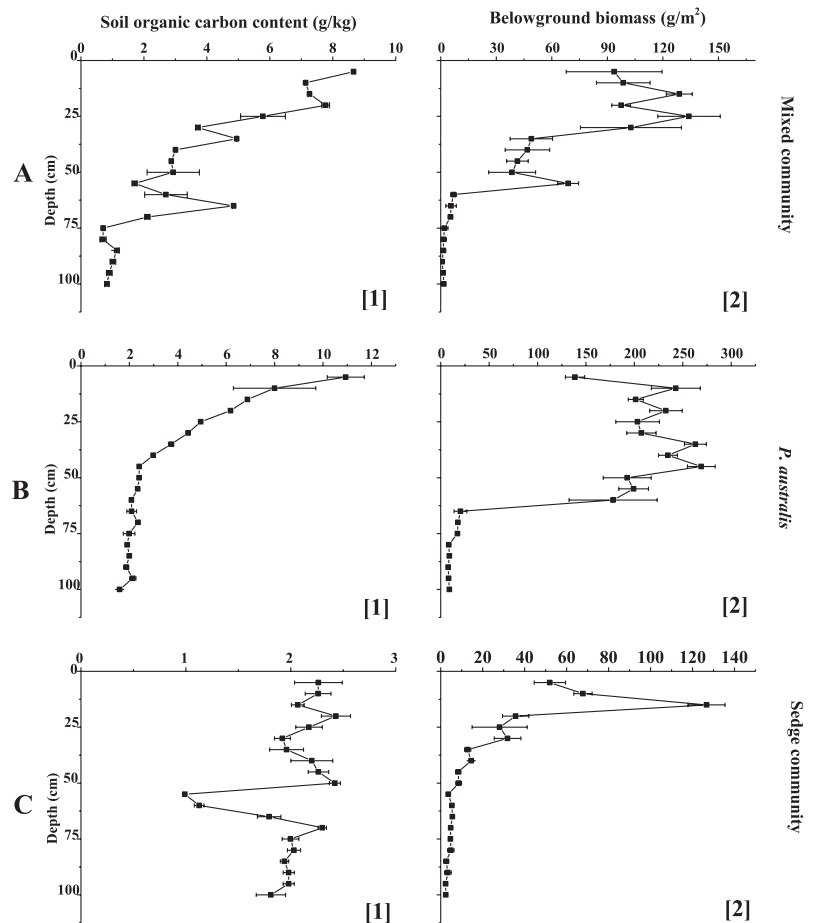


Fig. 3. Vertical distribution of organic carbon and underground biomass of: A, mixed communities; B, *P. australis*; C, Sedge community.

Spatio-Temporal Variations in the Abundance and Community Structure of Nitrospira in a Tropical Bay

Mao, Tieqiang; Li, Yanqun; Dong, Hongpo; Yang, Wenna; Hou, Lijun. *Current Microbiology*, 2020, (77): 3492-3503.

Nitrospira is the most diverse genus of nitrite-oxidizing bacteria, and its members are widely spread in various natural and engineered ecosystems. In this study, the phylogenetic diversity of *Nitrospira* and monthly changes of its abundance from Zhanjiang Bay were investigated. Phylogenetic analysis showed that among 58 OTUs with high abundance, 74% were not affiliated with any previously described *Nitrospira* species, revealing a previously unrecognized diversity of coastal *Nitrospira*. The abundances of both *Nitrospira* and *Nitrospira* exhibited a significantly monthly change. During most of the months, abundance of *Nitrospira* was greater than that of *Nitrospira*. In particle-attached communities, either abundance of *Nitrospira* or *Nitrospira* was highly correlated with that of ammonia-oxidizing archaea (AOA), whereas abundance of ammonia-oxidizing bacteria was only highly correlated with that of *Nitrospira*. In free-living communities, either abundance of *Nitrospira* or *Nitrospira* was correlated only with that of AOA. These results suggest that both *Nitrospira* and *Nitrospira* can be involved in nitrite oxidation by coupling with AOA, but *Nitrospira* may play a greater role than *Nitrospira* in this tropical bay.

硝化螺菌属是最多样化的亚硝酸氧化菌，它们在自然界分布广泛，对全球氮循环有重要影响。本研究对湛江湾水体和沉积物中硝化螺菌群落结构和丰度进行了长期的观测。进化分析表明74%的OTU为新型的硝化螺菌，意味着海洋近岸蕴含着丰富的迄今未被发现的亚硝酸氧化菌。丰度统计学分析发现，硝化螺菌属和硝化刺菌属与氨氧化古菌丰度高度相关，但硝化刺菌属仅仅与氨氧化细菌丰度相关。这些结果表明在湛江湾硝化螺菌属和硝化刺菌属均能与氨氧化古菌耦合参与了对亚硝酸盐的氧化。我们的研究改变了以前的认识，即硝化螺菌主要在陆地或湖泊氮循环中发挥作用。

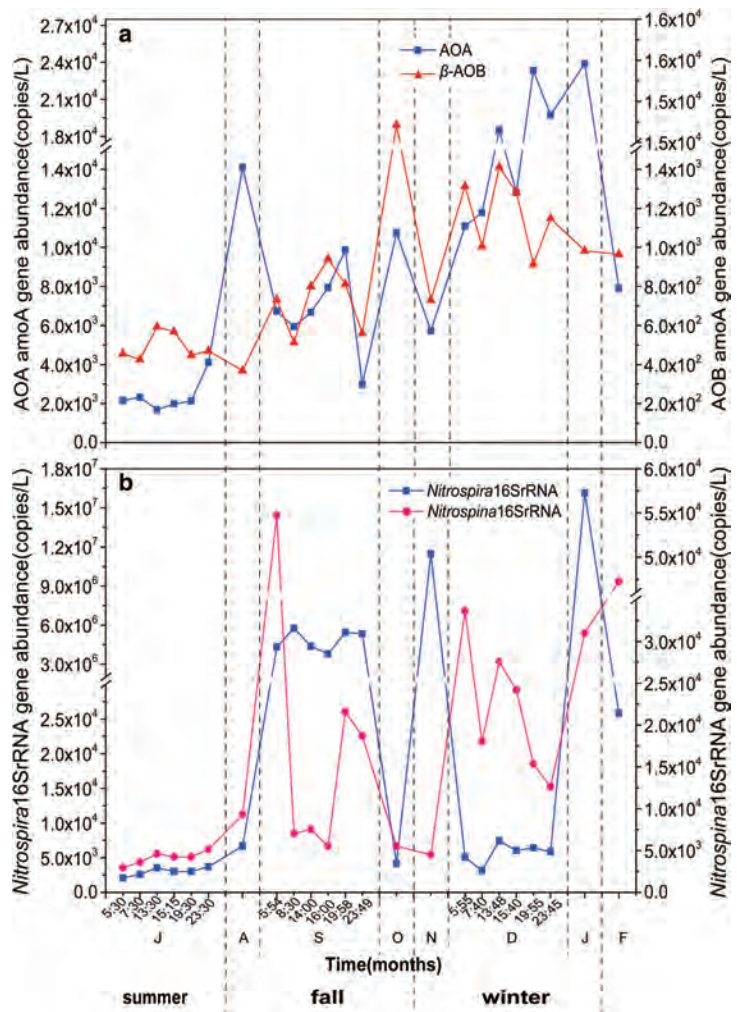


Fig. 3 Profiles of amoA genes of ammonia-oxidizing micro-organisms (a) and 16S rRNA genes of nitrite-oxidizing bacteria (b) from site Z11 between July 2018 and February 2019. J, A, S, O, N, D, J, F are initials of months. Diel observations were performed in July, September, and December

Evolution of shoals and vegetation of Jiuduansha in the Changjiang River Estuary of China in the last 30 years

Wu, Fengrun; Tong, Chunfu; Mitch Torkelson; Wang, Yan. *Acta of Oceanologica Sinica*, 2020, 39(8): 71-78.

The evolution of the shoals and vegetation plays an important role in maintaining the stability of the river regime and the estuarine ecosystem. However, the interaction between the evolution of shoals and vegetation dynamic has rarely been reported. In this study, we determined the interaction between the shoal and vegetation evolution of Jiuduansha in the Changjiang River Estuary in the last 30 years. We did this through the collection and summarization of the existing data of the regional hydrological processes, wading engineering, and vegetation, and combined it with the analysis of nautical charts and remote sensing images. During the past 30 years, the expansion of the shoals within the 0 m isobath in Jiuduansha was obvious, with an increase of 176.5%, while the expansion of the shoals within the 5 m isobath was relatively slow. The regional hydrological characteristics in the Jiuduansha area changed dramatically, especially the sediment discharges. The area of vegetation in Jiuduansha increased from 9.1 km² in 1990 to 65.68 km² in 2015, while the variations in the different vegetation types were different. The best combination of environmental factors with a significant correlation on the shoals within the 0 m isobath is the area of *Spartina alterniflora* and *Phragmites australis*. The evolution of Jiuduansha shoals was significantly affected by the variations in hydrological characteristics. Meanwhile, on a long-term scale, the expansion of the shoals could promote the regional vegetation expansions due to the suitable elevation and environmental conditions it provides. The interaction between the shoal and vegetation evolution varied in the different vegetation types and different elevations. In the future, long-term monitoring and detailed data are needed to the systematical analysis of the interaction between the hydrological processes and the evolution of the shoal and vegetation.

通过对文献资料中九段沙区域水沙变化、涉水工程、植被面积等数据的整理和总结，结合海图及遥感影像分析，归纳并分析近三十年九段沙沙体及植被的演变特征及其相互作用关系。结果显示，近三十年九段沙沙体扩张明显，特别是0m以上沙体面积增长迅速，增长了176.5%，而-5m以上沙体扩张相对缓慢。区域河口入海泥沙量、汉道分流比、分沙比、悬沙浓度等水文、泥沙要素变化显著。九段沙的植被面积从1990年的9.1 km²增加到2015年的65.68 km²，但不同植被类型的变化有所不同。非线性相关分析显示，与0m以上沙体面积具有显著相关的最佳环境因子组合是互花米草和芦苇的面积。水文特征的变化显著影响了九段沙沙体的演变。同时，从较长时间尺度来看，沙体的扩张由于能够提供适宜的高程条件可以促进区域植被的扩张。沙体与植被演变之间的相互作用因不同的植被类型和高程而异。

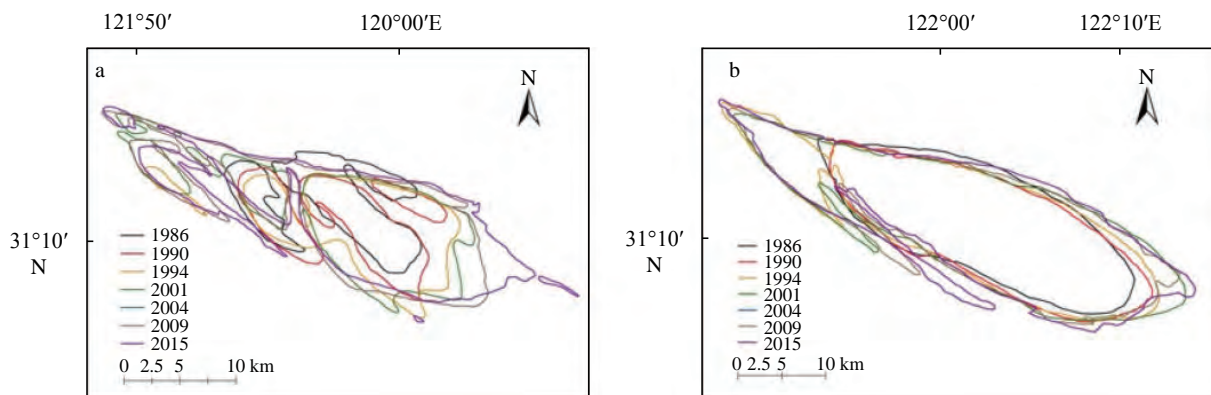


Fig. 2. Variations in the isobaths of 0 m (a) and 5 m (b) of the Jiuduansha shoals in last 30 years.

Windows of opportunity for salt marsh establishment: The importance for salt marsh restoration in the Yangtze Estuary.

Yuan, Lin; Chen, Yahui; Wang, Heng; Cao, Haobing; Zhao, Zhiyuan; Zhang, Liqun. *Ecosphere*, 2020,11: e03180.

Restoration has been promoted as an important strategy to reverse the decline of salt marsh ecosystems. Physical and biological processes limiting the colonization of bare tidal flats by pioneer salt marsh species are commonly recognized. Recently, the window of opportunity (WoO) concept has been proposed as a framework to provide an explanation for the initial establishment of biogeomorphic ecosystems on tidal flats under high physical stress. Understanding the thresholds for early seedling establishment and colonization is critical for the successful restoration and management of this threatened ecosystem. In this study, we investigated the WoOs for the establishment and colonization of a *Scirpus mariqueter* salt marsh at a large-scale restoration site in the Yangtze Estuary. A set of field monitoring and measurements were conducted to identify the potential physical and biological thresholds that could provide a mechanistic insight on the establishment and colonization of this pioneer marsh. The results showed that the successful colonization and expansion of the *S. mariqueter* marsh on the tidal flat required passing both physical and biological thresholds to open WoOs for establishment and colonization. The concurrence of WoOs, that is, propagule availability in the early growing season at a suitable tidal flat elevation with a benign sedimentary regime together with the removal of competition from invasive species, is presumed to be essential for the success

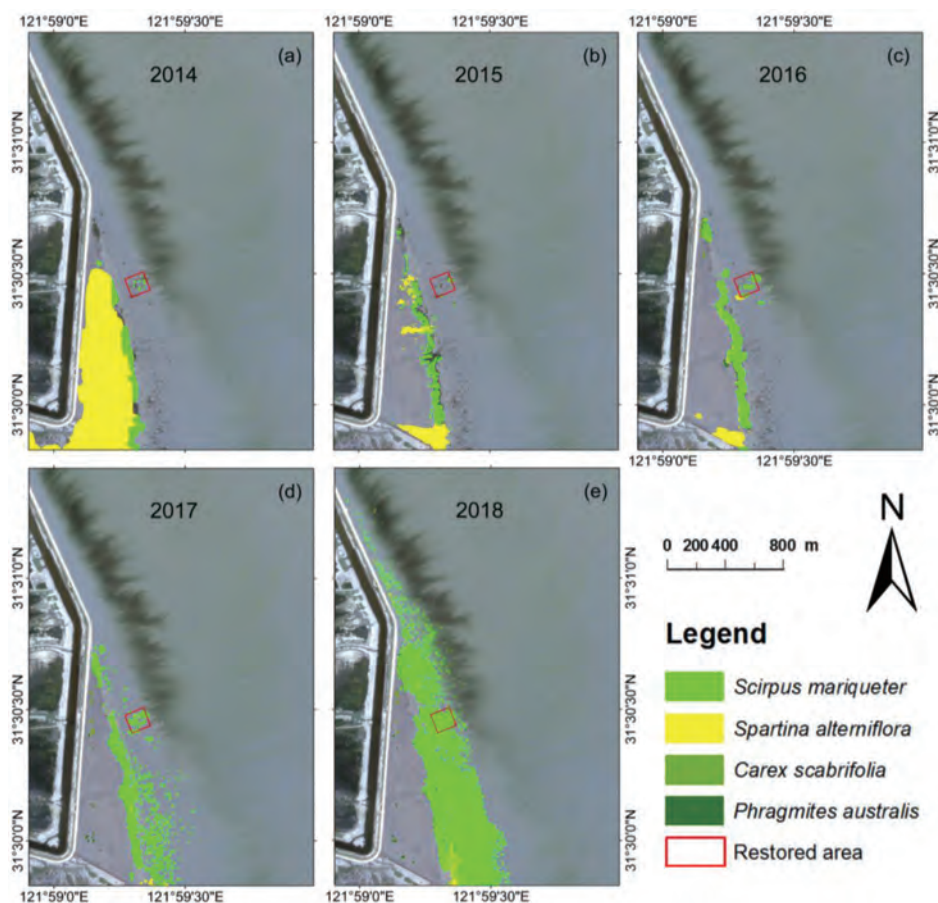


Fig. 4. Salt marsh vegetation propagation and cover changes on the study area from 2014 to 2018. Notes (a) The large area of *Spartina alterniflora* and small patches of *Scirpus mariqueter* in July 2014; (b) after applying herbicide and cutting in August 2015, *S. alterniflora* was effectively controlled; (c–e) successful propagation of *S. mariqueter* in the marsh from July 2016 to 2018. The restored area (red square) was created by outplanting corms of *S. mariqueter* in April 2014.

of *S. mariqueter* marsh establishment and colonization. In applying such eco-logical insights, the seed-sowing field experiment proved that by surpassing these thresholds, an *S. mari-queter* salt marsh can be successfully restored in a cost-effective manner. We suggest that these WoO-related establishment and colonization thresholds as well the cost-effectiveness of using these WoOs should be considered in future large-scale restorations of salt marshes.

基于机会窗口理论框架，首次阐明了与生物-物理阈值相关的机会窗口在盐沼先锋植被定居和扩散中的作用，揭示了盐沼修复所需的机会窗口条件，从理论上丰富了盐沼植被扩散过程与机制研究，为盐沼植被修复提供了重要的理论依据。

Reconstruction of Temporal Variations of Metal Concentrations using Radiochronology ($^{239+240}\text{Pu}$ and ^{137}Cs) in Sediments from Kizilirmak River, Turkey

Wang, Jinlong; Baskaran, Mark; Kumar, Anupam; Bilhan, Omer; J. Miller, Carol. *Journal of Paleolimnology*, 2020: 1-13.

Sediment cores retrieved from rivers, lakes, and coastal marine environment have been widely utilized to reconstruct historical variations of anthropogenic pollutants. A sediment core was collected in the Kizilirmak River, Turkey during 2014 and analyzed for a suite of metals (Cu, Pb, Zn, Ag, Ni, Co, Mn, As, Cd, Sb, V, Cr, Hg and Se) to reconstruct their temporal variations. Chronology was attempted using excess ^{210}Pb ($^{210}\text{Pb}_{\text{exs}}$), ^{137}Cs and $^{239,240}\text{Pu}$ in the sediment cores. The vertical profile of excess ^{210}Pb indicates that this core is not datable using excess ^{210}Pb method. The ^{137}Cs -based linear and mass.

研究了土耳其河流沉积物中 ^{210}Pb 、 ^{137}Cs 和 $^{239+240}\text{Pu}$ 的垂向分布，指出在沉积物受物理扰动影响的条件下可以使用 ^{137}Cs 和 $^{239+240}\text{Pu}$ 进行年代测量。定量估算了人为来源占有所有14种金属来源的份额，发现了金属元素在上世纪九十年代达到沉降峰值。

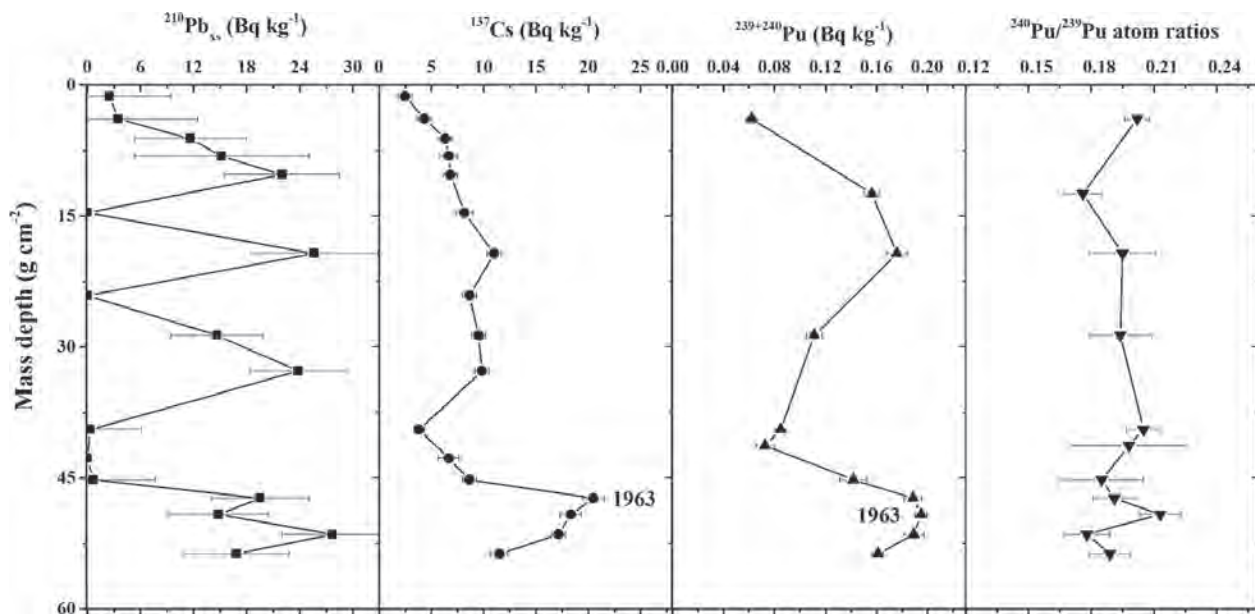


Fig. 2 Vertical profiles of $^{210}\text{Pb}_{\text{exs}}$, ^{137}Cs , $^{239+240}\text{Pu}$ activities and $^{240}\text{Pu}/^{239}\text{Pu}$ atom ratios with respect to cumulative mass depth

Sargassum blooms in the East China Sea and Yellow Sea: Formation and management

Zhuang, Minmin; Liu, Jinlin; Ding, Xiaowei; He, Jianzong; Zhao, Shuang; Wu, Lingjuan; Gao, Song; Zhao, Chunyan; Liu, Dongyan; Zhang, Jianheng; He, Peimin. *Marine Pollution Bulletin*, 2020: 111845.

Large-scale *Sargassum* blooms, known as golden tides, have been occurring along the coast of the Yellow Sea in recent years, resulting in an enormous loss of *Pyropia yezoensis* production. To locate the source of the blooms, we performed large-scale spatio-temporal sampling in the South Yellow Sea, East China Sea, and Jeju Island, South Korea. Based on morphology and molecular traits, the attached and floating *Sargassum* samples collected from the three regions were all identified as *Sargassum horneri*, although slight differences were observed in morphology among samples. Genetic distance and automatic barcode gap discovery analysis revealed very low genetic diversity among the three regions. The 33 samples from 12 sites were divided into six haplotypes, and the samples from the ECS shared more haplotypes than samples from other two regions. Our results suggested that *S. horneri* in the ECS was responsible for the formation of blooms in the Yellow Sea.

黄海和东海的金潮都被确定为 *Sargassum horneri*。 *S. horneri* 在不同的生境中表现出略微不同的形态特征。附着在东海的 *S. horneri* 是金潮的主要来源。

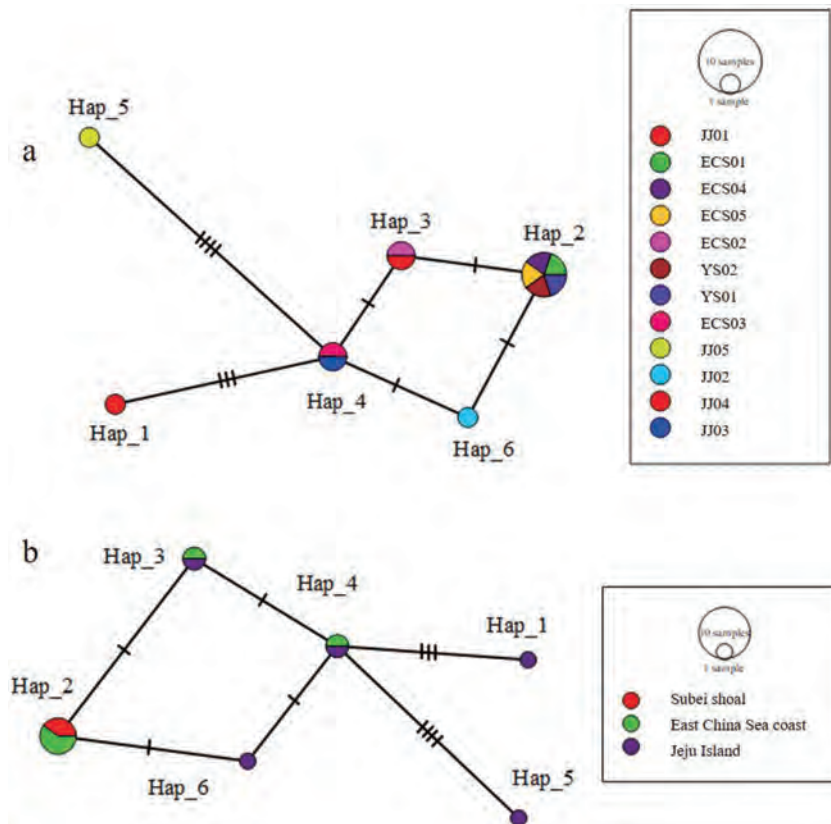


Fig. 6. Network diagram for *cox3* gene haplotypes of *S. horneri* based on samples names (a) and collection sites (b). A circle represents one haplotype, and the size of the circle reflects the number of haplotypes. Different colors indicate different geographic haplotypes, and the blank circles indicate undetected haplotypes.

Tidal Effect on Water Export Rate in the Eastern Shelf Seas of China

Lin, Lei; Liu, Dongyan; Guo, Xinyu; Luo, Chongxin; Cheng, Yao. *Journal of Geophysical Research-Oceans*, 2020, 125(5): e2019JC015863.

Water export rate of shelf seas is a pivotal factor impacting the global carbon cycle. Tides have important impacts on shelf hydrodynamics but are excluded in many climate models. To assess the effect of tides on export rates of shelf water, this study used a regional hydrodynamic model and a water residence time (WRT) adjoint model and examined model runs with and without tides for the eastern shelf seas of China. The results show that the average WRTs in the Bohai, Yellow, and East China seas were 11.60, 4.95, and 0.39 years, respectively. When tides were excluded, the WRTs decreased by >70% in the Bohai and Yellow seas and by ~10% in the East China Sea, indicating a significant acceleration in the shelf water export due to the absence of tides. The tidal effect has spatial variability associated with the water depth. Sensitivity experiments suggest that the tidal effect on the mean WRT was stronger than the effect of other dynamical factors (winds, rivers, and boundary currents). In the model with tides, tides weakened the wind-driven coastal current by intensifying the bottom resistance and thus slowed water export in the inner and middle portions of the shelf, compared to the model without tides. Parameterization of the tidal bottom friction in the model without tides could significantly improve the WRT result. This study highlights the crucial role of tides on the long-term transport of shelf seas and the significance of parameterizing the effect of tidal friction in climate models.

时间尺度上, 评估了潮汐对中国东部陆架海 (ESSC) 水输出速率的影响。ESSC中的平均水停留时间为2.12年, 如果将水动力模型中的潮汐排除在外, 则减少到0.64年。潮汐对水输出量的影响在空间上存在很大的变化, 这与水深有关。

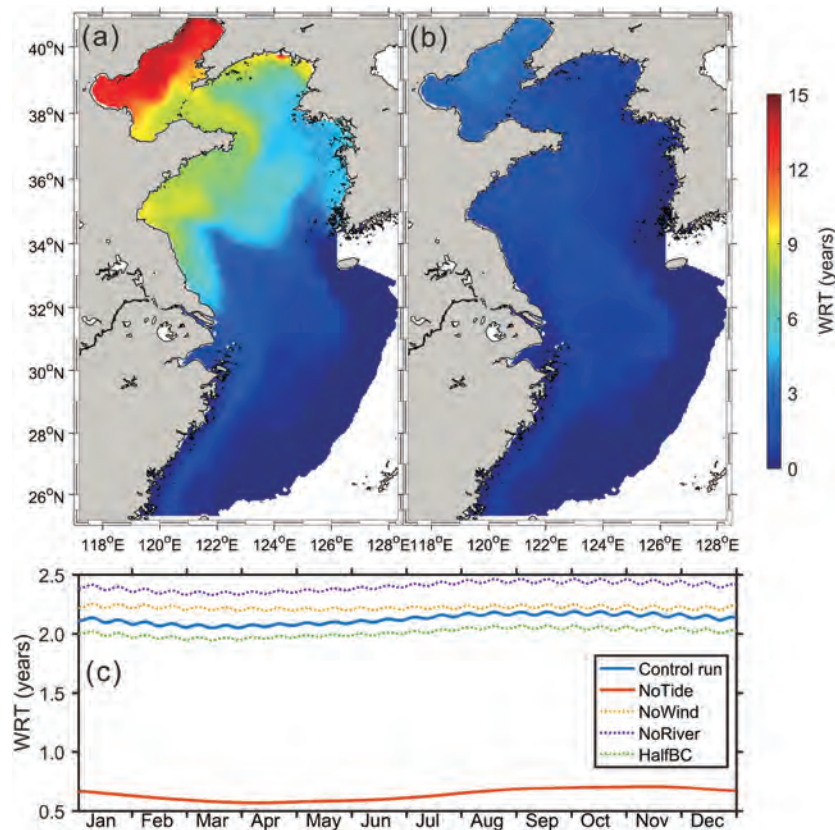


Figure 2. The annual mean of vertically averaged WRT in the ESSC for (a) the control run and (b) the NoTide case.(c) The daily mean WRTs over the ESSC for the five cases.

交流与合作 Academic Exchange & Cooperation

实验室在“111”创新引智计划2.0及科技部重点研发计划、国家自然科学基金等项目的支持下，积极开展国际交流与合作，目前承担了政府间国际科技创新合作重点专项项目“应对转型中的河口三角洲”、“中美大河三角洲侵蚀灾害与应对策略比较研究”“中美大河河口滩涂稳定性及城市安全生态防护比较研究”；国家自然科学基金重点国际（地区）合作研究项目“早-中全新世长江与尼罗河三角洲环境演变异同及早期农业文明对比研究”及“长江河口最大浑浊带的动力沉积过程对大型工程的自适应机理研究”等国家级国际合作项目5项。

在研国际合作项目进展 Progress of International Cooperation Projects

国家重点研发计划中美政府间国际科技创新合作重点专项：中美大河河口滩涂稳定性及城市安全生态防护比较研究（2018YFE0109900）（2019.09-2022.12）

受海平面上升和人类活动影响，全球已出现较大规模的河口滩涂损失，这将导致滩涂衰退且对沿海城市群海堤安全构成威胁，也放大风暴潮事件侵袭沿海城市的风险概率。基于此，针对这一世界极为关注的重大现实和科学问题，项目通过对中美两大河口滩涂的冲淤与演化格局、生态修复措施与海岸防护工程开展比较研究，以提出基于恢复与保护的河口滩涂绿色堤防技术与应用策略。该项目已开展一年，因疫情故通过视频进行了中美双边会议，工作在河口滩涂沉积、滩槽地貌稳定及河势演化等方面取得一定的突破，成果主要以论文的形式刊发于Geophysical Research Letters、Marine Geology、Sedimentary Geology、海洋学报等国内外高档次期刊9篇。同时撰写的关于崇明岛环岛绿色堤防建议获崇明区交通委员会认可，涉及长江口滩涂及河势稳定的3份专报得到中央相关部门、中央政治局委员及上海市相关领导等的肯定与重要批示。主要研究进展包括：1. 聚焦长江口滩涂响应海陆双重作用的变化行为，研究发现长江高径流造成南槽拦门沙口内泥沙大规模净侵蚀，台风过程能够将海源沉积物向陆输移，使得洪季南槽净侵蚀量降低，进而定量甄别出台风可显著缓解洪季高径流引致三角洲侵蚀的地貌效应，由此提出当上游泥沙急剧减少将导致滩涂出现冲淤转型，有效拦截台风携带的海域来沙可有利提升滩涂淤涨能力；2. 聚焦长江口南槽拦门沙这一既是盐水入侵的屏障却又是影响航运的障碍，成果揭示南槽拦门沙动力地貌演化过程可分为V型成长期（1959-1979年）、“尖端-凹陷”型局部调整期（1999-2003年）、平台型（2004-2010年）、局部调整期（2011-2017年间）以及目前的平台型稳定期。其中入海径流与悬沙通量并没有控制拦门沙的演化过程，ENSO事件通常导致拦门沙形态产生突变，局部沙坝移动、近期逐渐增强的潮流动力所导致海侧方向增多的沉积物输运以及河口局部工程，致使其展现目前独特的动力地貌形态；3. 研究揭示南支最大的扁担沙自1860年以来历经淤积-冲刷-淤积，浅滩由最初水下阴滩发育出露而形成纺锤状沙体，随后演变为细长扁担状，沙尾切滩成爪状沙体，其中扁担沙体积变化和长江入海泥沙的增减无直接联系，但与入海径流量的变化密切相关；白茆沙“南强北弱”的河势、南北港分流工程以及东风西沙水库的建立导致扁担沙向北推移，这有可能影响新桥水道的冲淤，进而危及崇明岛南沿岸滩的稳定。

**国家重点研发计划中荷（兰）政府间国际科技创新合作重点专项：应对转型中的河口三角洲
(2016YFE0133700) (2018.01-2021.12)**

由我室与荷兰代尔夫特理工大学合作的国家重点研发计划政府间国际科技创新合作重点专项“应对转型中的河口三角洲”，本年度取得了重大进展。

在入海物质通量变化机制与趋势方面，给出了长江上游干流梯级水库联合运行后的水沙变化特征。发现2011年后，上游出口断面宜昌站的输沙量减少到往年的3%，悬沙开始细化；提出水库的累积库容指数超过~4%临界阈值对下游河道水体含沙量的关键控制作用。相关研究拓展到黄河流域，量化分析给出了气候变化和人类活动对黄河流域降水、径流和输沙变化过程的控制作用和机理，认识到水坝对黄河入海泥沙通量下降的贡献超过30%。

河口水沙运动机制研究方面：a) 揭示了低频分潮在长江河口的变化特征，认识到径流增加会强化河口上游的低频信号，该低频信号可以传播到传统河口潮区界的更上游，表明河口的滤波器效应，为重新认识感潮河口区域的范围及河口特高潮位推算和防洪减灾管理提供基础。b) 探究了生物过程对泥沙絮凝的影响机制，认识到“紊动-盐度-含沙量”等三者对于生物泥沙絮凝过程的不同作用：阐明紊动是控制因素，盐度是激发因素，而含沙量因素的影响作用，取决于藻类与含沙量的比值，当含沙量相对于藻类浓度较低时，藻类本身对絮凝起主导作用，产生的絮团较大、密度较低，相反含沙量相对藻类浓度较高时，则絮团易形成体积较小、密度较大纯泥沙絮团。c) 提出了特高含沙量的多探头高精度集成观测的方法，认识到ASM可提供准确且高分辨率的泥沙浓度剖面，OBS和ADV存在信号反演的不确定性问题。多探头集成方法可以有效解决信号反演的不确定性问题并扩展含沙量测量范围 (>100 g/L)。

河口三角洲沉积地貌演变方面，认识到水下三角洲淤-蚀转型后再悬浮泥沙对海岸盐沼湿地的补给作用，即水下三角洲侵蚀的泥沙被部分搬运至盐沼，维持其淤长并延缓盐沼衰亡。随着海平面的进一步上升和三角洲前缘的持续蚀退，盐沼可能因蚀退（而非淹没）而消亡。盐沼衰亡的过程因水下三角洲和潮滩侵蚀提供的泥沙补给，或被推迟约100年。

河口三角洲湿地生态系统结构功能与修复研究：滨海湿地是大气中CO₂的汇，研究量化认识到其消减全球增温潜能的能力约为-0.9—-8.7 t CO₂-eq ha⁻¹ yr⁻¹。植被类型、潮汐类型和泥沙沉积动态对滨海盐沼潮沟中的碳浓度和交换通量均具有协同影响作用；海平面上升引起的水文过程耦合变化会显著削弱亚热带地区滨海湿地对CO₂的净吸收能力；土地利用变化类型也会对湿地温室气体CO₂、CH₄和N₂O的排放通量产生影响，表明受损滨海湿地功能恢复的紧迫性。进而研究提出植被在不同空间尺度的生长形态和繁殖策略的可塑性，识别了长江口盐沼植物海三棱藨草定居和扩散过程中的生物与物理阈值，创新识别和强调了与生物与物理阈值相关的机会窗口在长江口盐沼先锋植被定居和扩散中的至关重要作用，提出了海三棱藨草在光滩成功定居和扩散需要超越潮滩上的生物与物理阈值以打开幼苗的定居机会窗口。研发了一种经济有效的海三棱藨草盐沼修复新技术，并在崇明东滩鸟类自然保护区进行应用，形成修复示范区1000亩以上。系统研究了互花米草治理后的二次入侵过程，揭示了潮滩动力过程对互花米草种子到达、保留、萌发和定居等阶段的影响机制，丰富了外来物种入侵机制的理论研究。研发了精准、安全、高效的互花米草二次入侵综合防控技术，在崇明东滩完成1500亩示范，为我国开展生物入侵防控提供了技术支撑和成功案例。

**国家重点研发计划中美政府间国际科技创新合作重点专项：中美大河三角洲侵蚀灾害与应对策略比较研究
(2017YFE0107400) (2018.01-2020.12)**

由我室与美国路易斯安那州立大学合作的国家重点研发计划政府间国际创新合作专项项目“中美大河三角洲侵蚀灾害与应对策略比较研究”，本年度中方研究人员三人访问了美国，期间双方合作召开了“US-China Forum on Mississippi-Yangtze River Deltas”研讨会，共有9位研究人员交流了在长江和密西西比河三角洲开展的研究工作；中方研究人员访问了路易斯安那州立大学河流研究中心，并赴密西西比河三角洲进行了野外考察，实地考察三角洲分洪工程和湿地保护状况。根据前期研究工作的进展，双方骨干正在准备系列合作论文，并向国际优秀期刊Geomorphology提交了两大三角洲地貌对比研究的专辑“Environmental and Human Dynamics of the Yangtze River and Mississippi River Deltas: Temporal and Geographical Perspectives”申请，得到了批准，预计该专辑明年见刊。

国家自然科学基金重点国际（地区）合作研究项目：早-中全新世长江与尼罗河三角洲环境演变异同及早期农业文明对比研究 (41620104004) (2017.01-2021.12)

在国家自然科学基金委国际合作重点项目的资助下，陈中原团队开展了早-中全新世长江与尼罗河三角洲环境演变异同及早期农业文明对比研究。主要探索两地三角洲全新世沉积地貌的成因，流域水文泥沙波动对三角



洲建造的意义，以及海平面上升对三角洲环境演变的控制作用；在此基础上挖掘两地三角洲早期农业文明的起源、发展，探讨农业文明对气候海平面波动响应，以及人类活动如何适应三角洲环境演变。项目团队成员经过3年的努力，已经在以下几个方面取得足有成效的成果：1) 圆满地完成了两地三角洲项目设计的钻孔、考古遗址沉积物采样工作，尤其是尼罗河三角洲的样品，并成功地带回我们实验室，为项目完成打下了厚实的基础；2) 建立了扎实的两地三角洲沉积地貌数据库，全新世钻孔达近千个，收集了上千个关键层位的碳十四测年数据；3) 完成了2400多个沉积环境代指标的分析，以及代表性钻孔地层、考古遗址剖面高分辨率测年（50-100a）；在此基础上，我们在国际核心期刊上（如，PPP；MG；QSR；ESR等）发表了一系列有科学创新的成果：建立了两地三角洲全新世地貌演变的模式，提出长江口单一下切河谷发育的新模式和尼罗河三角洲扇形网状式河谷的发育，以及它们对三角洲建造的控制作用；提出了气候-海平面共同驱动下的长江三角洲农业文明发展模式，以及非洲高原季风摆动下的尼罗河三角洲旱作农业模式；提出赤道热复合带（ITCZ）的迁移对尼罗河三角洲早期农业文明的“控制性”意义，以及长江三角洲季风带对农业文明“催化性”意义；在高分辨率测年和孢粉分析基础上，可将尼罗河三角洲农业起源的时间提前约700年，并提出外来农业迁入的证据；发掘并建立了两地三角洲早期农业起源和气候演变的有效指标体系，以及入海物源指标，为三角洲环境重建提供了科学依据。本项目与合作方（埃方和法方）保持了紧密的合作研究，尤其是成立了两地三角洲研究中心，培养或正在培养多名中埃法硕博博士生、博士后，项目负责人陈中原教授受邀担任国际著名刊物地貌学主编。

国家自然科学基金委员会与荷兰科学研究组织、英国研究理事会合作研究项目：长江河口最大浑浊带的动力沉积过程对大型工程的自适应机理研究（2017.06-2021.04）

由我室牵头的中荷英国际合作项目“长江河口最大浑浊带的动力沉积过程对大型工程的自适应机理研究”，本年度共组织3次野外测量，使用河口海岸智能移动观测系统、浅地层剖面仪、OBS、ADCP、CTD等仪器获取北港长江口青草沙水库北沿高分辨率全覆盖水下地形、水动力、浅层沉积结构，以及南槽下段流速、悬沙浓度、盐度等多站位同步实测数据；收集了黄浦江上中游两个站点的长系列潮位资料。项目荷方负责人乌特勒支大学 Huib E. de Swart 发起并组织欧洲 EGU2020 Ocean Science 2.1: Open session on coastal and shelf seas，项目组中荷英三方全员参加口头报告。本年度已发表英文论文1篇，中文论文5篇；提交英文论文修改稿5篇，中文论文修改稿2篇，已投稿英文论文8篇，中文论文1篇。而且，在这些成果基础上，受交通运输部东海航海保障中心上海海事测绘中心委托，开发了“重点港口航道水深变化监测系统”，实现了水深变化数据的导入、水下地形构建、交互式断面生成、冲淤分析和成果数据导出等功能，并初步应用于长江口深水航道(北槽)监测。主要成果如下：

1 长江口最大浑浊带形成机制

基于北槽上、中、下段及外海四个典型站点实测洪枯季大小潮的水沙盐数据，分析北槽潮周期内垂向平均应变、对流、非平均应变和潮汐搅动等混合层化主要贡献项随潮相的变化过程。该成果已完成中文论文初稿1篇，正在修改。

使用扫描电镜和多种先进仪器现场观测长江口细颗粒泥沙絮凝特征。认为絮凝体大小形态具有明显的潮汐变化，憩流时刻絮凝体平均粒径（94.8 μm ）明显大于涨、落急时刻（24.1 μm ），涨憩时刻平均絮凝体粒径（105.6 μm ）大于落憩时刻（83.9 μm ），小潮汛平均絮凝体平均粒径（74.7 μm ）大于大潮汛（44.3 μm ）。分析认为紊流剪切应力是泥沙絮凝过程主控因子之一。该成果已投稿英文论文1篇。

根据长江口深水航道2010~2016年15次风暴潮和3次常规天气条件下的实测资料，研究长江口北槽风暴潮浮泥

的时空分布特征、发育规律及其影响。结果显示台风或寒潮大风造成的大浪掀扬巨量长江口浅滩沉积的细颗粒泥沙积聚在最大浑浊带，是长江口巨量风暴潮浮泥事件发生的主要原因；风暴潮波浪累积波能强度决定了风暴潮浮泥发育规模的大小；陡坡异重流和盐度、悬沙浓度层化导致的湍动抑制作用造成了风暴潮浮泥最终积聚于浚深的主槽内；风暴潮浮泥，长江口浮泥规模在主槽纵向上可以达到长10~60 km，厚0.5~4 m，对于航槽的回淤不可忽视。该成果已投稿英文论文1篇。

基于长江口潮流界水域洪季和枯季野外观测数据，研究河口非恒定流作用下低角度沙波（LADs）形态演变及其对水动力影响。结果表明，复合沙丘存在于洪水后期，经过5个月的衰变，枯季后期仅观察到简单沙波；潮汐作用增强了推移质输移，进而加速了复合沙丘的衰变；洪水末期的叠加沙波和枯季末期简单沙波的发育和演变，受半月潮的控制，反过来床面叠加沙波的形态会影响河槽水流结构。此外，基于geomorphons方法，实现了沙波、平床及局部冲刷坑的自动识别与统计分析。该成果已发表英文论文1篇，已提交英文论文修改稿2篇。

对湍流模型进行了改进，即假设在每个谐波分量中，由恒定湍流粘滞系数所产生的能量耗散与依赖于时空的湍流闭合模型产生的能量耗散相同，其系Lorentz线性化方法的扩展。基于该改进模型的分析结果表明，从枯季到洪季潮汐（潮位和潮流）作用的减少不仅是本项目荷方负责人前期认为的底部剪切应力增强的结果(Alebregtse and de Swart, 2016)，更重要的是由径/潮流相互作用产生的内部剪切应力增强所致。潮汐河道间串沟（横沙通道）减少了相邻河道间潮位、潮流、径流的差异，但这种影响较小，且在局域内。该模型的解析揭示了径流产生的水面梯度与水深立方呈反比，导致海平面上升时由径流产生的余水位减小。而且，还考虑了由密度梯度与湍流粘滞协方差产生的余流对长江河口各河道净输水分布的影响，并将其应用到南港—北槽/南槽系统的悬沙输移。初步分析结果显示，随着枯季径流量的减少，北槽最大浑浊带上边界向南槽迁移。此外，在iFlow河网模块开发中，我们研制了将单一河槽的任意线性水沙模型扩展到河网水沙模型的通用方法，为iFlow模型实现了河口网络扩展包。该成果已投稿英文论文1篇，完成英文论文初稿1篇，正在修改。

2 最大浑浊带水动力及悬沙浓度空间分布对人类活动的自适应机理

收集了北港历史地形数据、余山水文站潮汐、大通水文站径流流量数据、长江口历年遥感影像以及流速、悬沙浓度定点实测资料。分析河口最大浑浊带空间分布对围垦工程的自适应机制。分析结果表明，围垦工程导致河道束窄和固定，造成深槽侵蚀，两侧边滩淤积。由此引起最大浑浊带的宽度减小，大潮最大浑浊带上边界向海移动6 km，小潮期间最大浑浊带向海移动5 km，下边界受潮汐强度影响，在3 km范围内移动。小潮时刻最大浑浊带位置更偏向下游。该成果已投稿英文论文1篇。

历史实测水沙数据和地形数据分析结果表明，深水航道整治工程引起南槽最大浑浊带呈向海迁移趋势，南槽上口段的最大浑浊带和河口拦门沙消失；北槽上口段落潮量的减少导致低流量时最大浑浊带较工程前呈向陆迁移趋势，而中下河段落潮量增加则导致高流量时最大浑浊带呈向海迁移趋势。分析认为长江来沙量的减少导致了河口最大浑浊带核心区悬沙浓度在洪季呈下降趋势。尽管北槽拦门沙主体在航道疏浚工程和航道整治建筑物共同作用下已近乎消失，但事实上仍旧以高回淤强度的形式隐形存在。实测资料表明，北槽、南槽最大浑浊带迁移引起南港深槽淤积。该成果已投稿英文论文2篇，已提交英文论文修改稿1篇。

学术会议 Workshop & Conference

华东师大与海洋生物圈整合研究科学计划合作备忘录签约仪式暨战略合作伙伴研讨会

1月16日，华东师大与海洋生物圈整合研究（Integrated Marine Biosphere Research, IMBeR）科学计划合作备忘录签约仪式暨战略合作伙伴研讨会在中山北路校区举行。双方约定自签约之日起，华东师大将承办IMBeR国际项目办公室（IMBeR IPO-China）。未来五年，该办公室将负责推进《IMBeR科学计划与实施战略2016-2025》的执行，重点关注亚太地区、中东和非洲；支持并协调IMBeR区域项目和工作组的学术活动，包括气候对海洋顶级捕食者的影响研究区域项目，印度洋生物地球化学与生态系统可持续发展研究区域项目，陆架边缘海工作组和东部边界上升流系统研究工作组；组织开展一系列IMBeR的学术交流活动、科教推广活动和能力建设活动等。



华东师范大学 2020 年度青年科学家（学者）在线国际论坛—海洋科学分论坛举行

6月1日，华东师范大学2020年度青年科学家（学者）在线国际论坛-海洋科学分论坛举行。本次海洋科学分论坛由河口海岸学国家重点实验室、河口海岸科学研究院、海洋科学学院、崇明生态研究院联合承办。来自德国马克思普朗克化学研究所、美国缅因大学、特拉华大学、澳大利亚墨尔本大学、荷兰代尔夫特理工大学、自然资源部第三海洋研究所、长江水利委员会水文局长江口水文水资源勘测局等国内外高校和研究机构的13名青年学者以ZOOM视频平台相聚云端，进行了精彩的学术报告，介绍了自己的学术经历、研究领域、最新科研进展以及未来发展计划。与会专家和教授就学科热点、未来合作契合点等与青年学者进行了详细交流，并给青年学者提出了积极建议。



2020 河口三角洲动力与沉积地貌综合青年学者论坛

10月18-20日，“2020河口三角洲动力与沉积地貌综合青年学者论坛”，为青年学者搭建学术交流平台，促进河口三角洲动力-沉积-地貌综合研究的理论和方法进步。论坛以“河口三角洲动力与沉积地貌综合研究领域前



沿与发展”为主题，围绕“变化条件下的河口及近海动力过程、多尺度沉积过程与地貌演变、动力地貌观测与模拟技术、河口三角洲资源保护中的应用”四个方面，采用口头报告与现场讨论相结合的方式展开。邀请领域内的专家学者与青年学者约50人出席，共同就当前研究领域内的前沿和热点问题进行讨论交流。

第 106 次中国科学院学部科学与技术前沿论坛 “中 - 欧海洋科学与技术进展”

2020年10月20日至21日，中国科学院学部第106次科学与技术前沿论坛“中-欧海洋科学与技术进展”在上海举行。论坛由中国科学院地学部张经院士、欧洲科学院地学部Paul Tréguer院士和欧洲科学院地学部Louis Legendre院士共同召集，为分析近期中国与欧洲双方在海洋科学与技术领域的主要进展情况，聚焦制约学科发展的关键瓶颈，凝练在21世纪影响海洋科学发展的重大科学问题，寻求双方在海洋科学与技术方面进行深入合作的优先领域。论坛由中国科学院学部主办，中国科学院地学部常委会、中国科学院学部学术与出版工作委员会、欧洲科学院地球与环境科学学部共同承办，华东师范大学、《中国科学》杂志社协办。论坛议题包括：全球变化背景下海洋的作用、海洋科学与技术的前沿问题，海洋可持续发展以及中欧海洋科学与技术领域的合作四个方面。论坛采用线上线下相结合的形式，来自中国和欧洲科学院地学部12位嘉宾分享了主题报告，相关领域海内外43所科研院所的46位专家学者围绕主题进行了自由讨论。会议以视频直播方式面向公众开放，约有400名观众观看了会议。



开放基金

SKLEC Research Fund

2020年，实验室在研开放基金课题35项，合计资助241万元，其中，新增开放基金课题11项，合计资助53万元。

2020年河口海岸学国家重点实验室设立开放基金课题

姓名 Name	课题名称 Title	单位 Affiliation
禹定峰	数值模拟与遥感定量反演耦合的黄河口悬浮泥沙运移规律研究	山东省科学院海洋仪器仪表研究所
李 鹏	多源SAR 遥感湿地相干性变化探测及驱动因素研究	中国海洋大学
陈大可	不同组分的沙泥混合物冲刷率研究	河海大学
武国相	崇明东滩盐沼湿地演变的植被-地貌耦合模拟研究	中国海洋大学
张 帆	尼罗河三角洲全新世沉积物中GDGTs的古环境意义	南方科技大学
苏 敏	基于沙源突变的沙脊群地貌自适应机制研究	河海大学
Neven Cukrov	Eco-environmental impacts of submarine groundwater discharge-derived nutrients, carbon and metal in oligotrophic karstic estuary of the Krka River (Adriatic Sea, Croatia)	Ruđer Bo kovi Institute, Croatia
Sheikh Aftab Uddin	Nutrient and organic carbon dynamics in the Ganges-Brahmaputra-Meghna (GBM) river system discharging to the tropical sea Bay of Bengal, Bangladesh	Institute of Marine Sciences, University of Chittagong, Bangladesh
王宝利	九段沙湿地微生物群落构建与温室气体释放	天津大学
刘 森	莱州湾南岸地下咸水赋存区微生物多样性及其在碳循环中的驱动机制	山东大学
苏应龙	纳米材料和微塑料对河口沉积物关键生态功能反硝化过程的联合影响效应	华东师范大学

论文专著 List of Peer Reviewed Publication

2020年，实验室在国内外重要刊物上发表学术论文255篇，其中国际刊物207篇，中文重要刊物48篇（数据统计截止2020年11月）。

国外刊物发表论文列表

List of International Peer Reviewed Publications

- [1] Akoueson, Fleurine; Sheldon, Lisa M; Danopoulos, Evangelos; Morris, Steve; Hotten, Jessica; Chapman, Emma; Li, Jiana; Rotchell, Jeanette M. A preliminary analysis of microplastics in edible versus non-edible tissues from seafood samples[J]. Environmental Pollution (Barking, Essex : 1987), 2020, 263(Pt A): 114452.
- [2] Bi, Qianqian; Zhang, Fenfen; Deng, Bing; Du, Jinzhou. SPM control on the partitioning and balance of 210Po and 210Pb in high-turbidity surface waters of the East China Sea[J]. Journal of Environmental Radioactivity, 2020, 222: 106367.
- [3] Borja, Angel; Andersen, Jesper H.; Arvanitidis, Christos D.; Basset, Alberto; Buhl-Mortensen, Lene; Carvalho, Susana; Dafforn, Katherine A.; Devlin, Michelle J.; Escobar-Briones, Elva G.; Grenz, Christian; Harder, Tilmann; Katsanevakis, Stelios; Liu, Dongyan; Metaxas, Anna; Moran, Xose Anxelu G.; Newton, Alice; Piroddi, Chiara; Pochon, Xavier; Queiros, Ana M.; Snelgrove, Paul V. R.; Solidoro, Cosimo; John, Michael A.; Teixeira, Heliana. Past and Future Grand Challenges in Marine Ecosystem Ecology[J]. Frontiers in Marine Science, 2020, 7: 362.
- [4] Cai, Huiwen; Chen, Mengdi; Chen, Qiqing; Du, Fangni; Liu, Jingfu; Shi, Huahong. Microplastic quantification affected by structure and pore size of filters[J]. Chemosphere, 2020, 257: 127198.
- [5] Cai, Mingqi; Liu, Zhiquan; Chen, Minghai; Zhang, Meng; Jiao, Yang; Chen, Qiang; Zhao, Yunlong. Comparative proteomic analysis of senescence in the freshwater cladoceran *Daphnia pulex*[J]. Comparative Biochemistry and Physiology B-Biochemistry & Molecular Biology, 2020, 239: 110352.
- [6] Cai, Mingqi; Liu, Zhiquan; Yu, Ping; Jiao, Yang; Chen, Qiang; Jiang, Qichen; Zhao, Yunlong. Circadian rhythm regulation of the oxidation-antioxidant balance in *Daphnia pulex*[J]. Comparative Biochemistry and Physiology B-Biochemistry & Molecular Biology, 2020, 240: 110387.
- [7] Cao, Haobing; Zhu, Zhenchang; James, Rebecca; Herman, Peter M J; Zhang, Liquan; Yuan, Lin; Bouma, Tjeerd J. Wave effects on seedling establishment of three pioneer marsh species: survival, morphology and biomechanics[J]. Annals of Botany, 2020, 125: 345-352.
- [8] Chang, Yan; Muller, Moritz; Wu, Ying; Jiang, Shan; Cao, Wan Wan; Qu, Jian Guo; Ren, Jing Ling; Wang, Xiao Na; Rao, En Ming; Wang, Xiao Lu; Mujahid, Aazani; Muhamad, Mohd Fakhruddin; Aun, Edwin Sia Sien; Jang, Faddrine Holt Ajon; Zhang, Jing. Distribution and behaviour of dissolved selenium in tropical peatland-draining rivers and estuaries of Malaysia[J]. Biogeosciences, 2020, 17(4): 1133-1145.

- [9] Chen, Dezhi; Li, Mingliang; Zhang, Yiyi; Zhang, Longhui; Tang, Jieping; Wu, Hao; Wang, Yaping. Effects of diatoms on erosion and accretion processes in saltmarsh inferred from field observations of hydrodynamic and sedimentary processes[J]. *Ecohydrology*, 2020: e2246.
- [10] Chen, Feiyang; Zheng, Yanling; Hou, Lijun; Zhou, Jie; Yin, Guoyu; Liu, Min. Denitrifying anaerobic methane oxidation in marsh sediments of Chongming eastern intertidal flat[J]. *Marine Pollution Bulletin*, 2020, 150: 110681.
- [11] Chen, Qiang; Lv, Weiwei; Jiao, Yang; Liu, Zhiquan; Li, Yiming; Cai, Mingqi; Wu, Donglei; Zhou, Wenzong; Zhao, Yunlong. Effects of exposure to waterborne polystyrene microspheres on lipid metabolism in the hepatopancreas of juvenile redclaw crayfish, *Cherax quadricarinatus*[J]. *Aquatic Toxicology*, 2020, 224: 105497.
- [12] Chen, Qiqing; Lackmann, Carina; Wang, Weiye; Seiler, Thomas-Benjamin; Hollert, Henner; Shi, Huahong. Microplastics Lead to Hyperactive Swimming Behaviour in Adult Zebrafish[J]. *Aquatic Toxicology*, 2020, 224: 105521.
- [13] Chen, Qiqing; Li, Yue; Li, Bowen. Is color a matter of concern during microplastic exposure to *Scenedesmus obliquus* and *Daphnia magna*?[J]. *Journal of Hazardous Materials*, 2020, 383: 121224.
- [14] Chen, Qiqing; Santos, Mauricius Marques Dos; Tanabe, Philip; Harraka, Gary T; Magnuson, Jason T; McGruer, Victoria; Qiu, Wenhui; Shi, Huahong; Snyder, Shane A; Schlenk, Daniel. Bioassay guided analysis coupled with non-target chemical screening in polyethylene plastic shopping bag fragments after exposure to simulated gastric juice of Fish[J]. *Journal of Hazardous Materials*, 2020, 401: 123421.
- [15] Chen, Xiaogang; Cukrov, Neven; Santos, Isaac R.; Rodellas, Valenti; Cukrov, Nusa; Du, Jinzhou. Karstic submarine groundwater discharge into the Mediterranean: Radon-based nutrient fluxes in an anchialine cave and a basin-wide upscaling[J]. *Geochimica et Cosmochimica Acta*, 2020, 268: 467-484.
- [16] Chen, Xiaogang; Ye, Qi; Sanders, L Christian; Du, Jinzhou; Zhang, Jing. Bacterial-derived nutrient and carbon source-sink behaviors in a sandy beach subterranean estuary[J]. *Marine Pollution Bulletin*, 2020, 160: 111570.
- [17] Chen, Xuechu; Huang, Yingying; Yang, Hualei; Pan, Liping; Perry, Danielle C; Xu, Ping; Tang, Jianwu; You, Wenhui; He, Xiaoyan; Wen, Quan. Restoring wetlands outside of the seawalls and to provide clean water habitat[J]. *Science of the Total Environment*, 2020, 721: 137788.
- [18] Chen, Yufeng; Deng, Bing; Zhang, Jing. Shallow gas in the Holocene mud wedge along the inner East China Sea shelf[J]. *Marine and Petroleum Geology*, 2020, 114: 104233.
- [19] Chen, Yuru; Guo, Xingpan; Niu, Zuoshun; Lu, Dapei; Sun, Xiaoli; Zhao, Sai; Hou, Lijun; Liu, Min; Yang, Yi. Antibiotic resistance genes (ARGs) and their associated environmental factors in the Yangtze Estuary, China: From inlet to outlet[J]. *Marine pollution bulletin*, 2020, 158: 111360.
- [20] Cheng, Gaolei; Wang, Yaping; Voulgaris, George; Du, Jiabi; Sheng, Jinyu; Xiong, Jillian; Xing, Fei. Sediment exchange between channel and sand ridges in the southern Yellow Sea: the importance of tidal asymmetries[J]. *Continental Shelf Research*, 2020, 205: 104169.
- [21] Cheng, Qinzi; Wang, Feng; Chen, Jin; Ge, Can; Chen, Yinglu; Zhao, Xuanqi; Nian, Xiaomei; Zhang, Weiguo; Liu, Kam-biu; Xu, Yijun; Lam, Nina. Combined chronological and mineral magnetic

- approaches to reveal age variations and stratigraphic heterogeneity in the Yangtze River subaqueous delta[J]. *Geomorphology*, 2020, 359: 107163.
- [22] Cui, Erqian; Weng, Ensheng; Yan, Enrong; Xia, Jianyang. Robust leaf trait relationships across species under global environmental changes[J]. *Nature Communications*, 2020, 11(1): 2999.
- [23] Cui, Lifang; Yuan, Lin; Ge, Zhenming; Cao, Haobing; Zhang, Liquan. The impacts of biotic and abiotic interaction on the spatial pattern of salt marshes in the Yangtze Estuary, China[J]. *Estuarine Coastal and Shelf Science*, 2020, 238: 106717.
- [24] Dai, Jinlong; Ye, Qi; Wu, Ying; Zhang, Miao; Zhang, Jing. Simulation of Enhanced Growth of Marine Group II Euryarchaeota From the Deep Chlorophyll Maximum of the Western Pacific Ocean: Implication for Upwelling Impact on Microbial Functions in the Photic Zone[J]. *Frontiers in Microbiology*, 2020, 11: 2141.
- [25] Deng, Hua; Wei, Ren; Luo, Wenya; Hu, Lingling; Li, Bowen; Di, Ya'nan; Shi, Huahong. Microplastic pollution in water and sediment in a textile industrial area[J]. *Environmental Pollution*, 2020, 258: 113658.
- [26] Du, Fangni; Cai, Huiwen; Zhang, Qun; Chen, Qiqing; Shi, Huahong. Microplastics in take-out food containers[J]. *Journal of Hazardous Materials*, 2020, 399: 122969.
- [27] Du, Juan; Baskaran, Mark; Du, Jinzhou. Atmospheric deposition of Be-7, Pb-210 and Po-210 during typhoons and thunderstorm in Shanghai, China and global data synthesis[J]. *Science China-Earth Sciences*, 2020, 63(4): 602-614.
- [28] Fan, Yaoshen; Chen, Shenliang; Pan, Shunqi; Dou, Shentang. Storm-induced hydrodynamic changes and seabed erosion in the littoral zone of Yellow River Delta: A model-guided mechanism study[J]. *Continental Shelf Research*, 2020, 205: 104171.
- [29] Feng, Jingnan; Guo, Xingpan; Chen, Yuru; Lu, Dapei; Niu, Zuoshun; Tou, Feiyun; Hou, Lijun; Xu, Jiang; Liu, Min; Yang, Yi. Time-dependent effects of ZnO nanoparticles on bacteria in an estuarine aquatic environment[J]. *Science of the Total Environment*, 2020, 698: 134298.
- [30] Feng, Zhihua; Zhang, Tao; Shi, Huahong; Gao, Kunshan; Huang, Wei; Xu, Juntian; Wang, Jiaxuan; Wang, Rui; Li, Ji; Gao, Guang. Microplastics in bloom-forming macroalgae: Distribution, characteristics and impacts[J]. *Journal of Hazardous Materials*, 2020, 397: 122752.
- [31] Fernandes, Dearlyn; Wu, Ying; Shirodkar, Prabhaker Vasant; Pradhan, Umesh Kumar; Zhang, Jing. Sources and implications of particulate organic matter from a small tropical river-Zuari River, India[J]. *Acta Oceanologica Sinica*, 2020, 39(4): 18-32.
- [32] Fernandes, Dearlyn; Wu, Ying; Shirodkar, Prabhaker Vasant; Pradhan, Umesh Kumar; Zhang, Jing; Limbu, Samwel Mchele. Sources and preservation dynamics of organic matter in surface sediments of Narmada River, India – Illustrated by amino acids[J]. *Journal of Marine Systems*, 2020, 201: 103239.
- [33] Fozia; Zheng, Yanling; Hou, Lijun; Zhang, Zongxiao; Chen, Feiyang; Gao, Dengzhou; Yin, Guoyu; Han, Ping; Dong, Hongpo; Liang, Xia; Yang, Yi; Liu, Min. Anaerobic ammonium oxidation (anammox) bacterial diversity, abundance, and activity in sediments of the Indus Estuary[J]. *Estuarine, Coastal and Shelf Science*, 2020, 243: 106925.

- [34] Fozia; Zheng, Yanling; Hou, Lijun; Zhang, Zongxiao; Gao, Dengzhou; Yin, Guoyu; Han, Ping; Dong, Hongpo; Liang, Xia; Yang, Yi; Liu, Min. Community dynamics and activity of nirS-harboring denitrifiers in sediments of the Indus River Estuary[J]. *Marine Pollution Bulletin*, 2020, 153: 110971.
- [35] Galdies, Charles; Bellerby, Richard; Canu, Donata; et al. European policies and legislation targeting ocean acidification in European waters - Current state[J]. *Marine Policy*, 2020, 118: 103947.
- [36] Gao, Dengzhou; Hou, Lijun; Liu, Min; Li, Xiaofei; Zheng, Yanling; Yin, Guoyu; Wu, Dianming; Yang, Yi; Han, Ping; Liang, Xia; Dong, Hongpo. Mechanisms responsible for N₂O emissions from intertidal soils of the Yangtze Estuary[J]. *Science of the Total Environment*, 2020, 716: 137073.
- [37] Ge, Jianzhong; Chen, Changsheng; Wang, Zheng Bing; Ke, Keteng; Yi, Jinxu; Ding, Pingxing. Dynamic Response of the Fluid Mud to a Tropical Storm[J]. *Journal of Geophysical Research-Oceans*, 2020, 125(3): e2019JC015419.
- [38] Ge, Jianzhong; Shi, Shenyang; Liu, Jie; Xu, Yi; Chen, Changsheng; Bellerby, Richard; Ding, Pingxing. Interannual Variabilities of Nutrients and Phytoplankton off the Changjiang Estuary in Response to Changing River Inputs[J]. *Journal of Geophysical Research-Oceans*, 2020, 125(3): e2019JC015595.
- [39] Ge, Jianzhong; Torres, Ricardo; Chen, Changsheng; Liu, Jie; Xu, Y; Bellerby, Richard; Shen, Fang; Bruggeman, Jorn; Ding, Pingxing. Influence of suspended sediment front on nutrients and phytoplankton dynamics off the Changjiang Estuary: A FVCOM-ERSEM coupled model experiment[J]. *Journal of Marine Systems*, 2020, 204: 103292.
- [40] Gu, Huaxin; Wei, Shuaishuai; Hu, Menghong; Wei, Huang; Wang, Xinghuo; Shang, Yueyong; Li, Li'ang; Shi, Huahong; Wang, Youji. Microplastics aggravate the adverse effects of BDE-47 on physiological and defense performance in mussels[J]. *Journal of Hazardous Materials*, 2020, 398: 122909.
- [41] Guo, Chao; Jin, Zhongwu; Guo, Leicheng; Lu, Jinyou; Ren, Shi; Zhou, Yinjun. On the cumulative dam impact in the upper Changjiang River: Streamflow and sediment load changes[J]. *Catena*, 2020, 184: 104250.
- [42] Guo, Junli; Shi, Lianqiang; Pan, Shunqi, Ye, Qinghua; Cheng, Wufeng; Chang, Yang; Chen, Shenliang. Monitoring and evaluation of sand nourishments on an embayed beach exposed to frequent storms in eastern China[J]. *Ocean & Coastal Management*, 2020, 195: 105284.
- [43] Guo, Leicheng; Zhu, Chunyan; Wu, Xuefeng; Wan, Yuanyang; David, A. Jay; Ian, Townend; Wang, Zheng Bing; He, Qing. Strong inland propagation of low-frequency long waves in river estuaries[J]. *Geophysical Research Letters*, 2020, 47: e, 2020GL089112.
- [44] Guo, Xingpan; Sun, Xiaoli; Chen, Yuru; Hou, Lijun; Liu, Min; Yang, Yi. Antibiotic resistance genes in biofilms on plastic wastes in an estuarine environment[J]. *Science of the Total Environment*, 2020, 745: 140916.
- [45] Guo, Xingpan; Zhao, Sai; Chen, Yuru; Yang, Jing; Hou, Lijun; Liu, Min; Yang, Yi. Antibiotic resistance genes in sediments of the Yangtze Estuary: From 2007 to 2019[J]. *Science of the Total Environment*, 2020, 744: 140713.
- [46] Hong, Bo; Liu, Zhonghui; Shen, Jian; Wu, Hui; Gong, Wenping; Xu, Hongzhou; Wang, Dongxiao. Potential physical impacts of sea-level rise on the Pearl River Estuary, China[J]. *Journal of Marine Systems*, 2020, 201: 103245.

- [47] Hu, Junfa; Sha, Zhanjiang; Wang, Jinlong; Du, Jinzhou; Ma, Yujun. Atmospheric deposition of ^7Be , ^{210}Pb in Xining, a typical city on the Qinghai-Tibet Plateau, China[J]. *Journal of Radioanalytical and Nuclear Chemistry*, 2020, 324: 1141-1150.
- [48] Hu, Lingling; Chernick, Melissa; Lewis, Anna M; Ferguson, P Lee; Hinton, David E. Chronic microfiber exposure in adult Japanese medaka (*Oryzias latipes*)[J]. *Plos One*, 2020, 15(3): e0229962.
- [49] Huang, Dekun; Lin, Jing; Du, Jinzhou; Yu, Tao. The detection of Fukushima-derived radiocesium in the Bering Sea and Arctic Ocean six years after the nuclear accident[J]. *Environmental Pollution*, 2020, 256: 113386.
- [50] Huang, Jing; Lei, Shao; Wang, Aihua; Tang, Liliang; Wang, Zhanghua. Mid-Holocene environmental change and human response at the Neolithic Wuguishan site in the Ningbo coastal lowland of East China[J]. *Holocene*, 2020, 30(II): 1591-1605.
- [51] Huang, Xing; Wang, Xueping; Li, Xiuzhen; Yan, Zhongzheng; Sun, Yonggang. Occurrence and transfer of heavy metals in sediments and plants of *Aegiceras corniculatum* community in the Qinzhou Bay, southwestern China[J]. *Acta Oceanologica Sinica*, 2020, 39(2): 79-88.
- [52] Huang, Ying; Chen, Zihan; Tian, Bo; Zhou, Cheng; Wang, Jiangtao; Ge, Zhenming; Tang, Jianwu. Tidal effects on ecosystem CO₂ exchange in a *Phragmites* salt marsh of an intertidal shoal[J]. *Agricultural and Forest Meteorology*, 2020, 292-293: 108.
- [53] Huang, Youhui; Wu, Donglei; Li, Yiming; Chen, Qiang; Zhao, Yunlong. Characterization and expression of arginine kinase 2 from *Macrobrachium nipponense* in response to salinity stress[J]. *Developmental And Comparative Immunology*, 2020, 113: 103804.
- [54] Ji, Hongyu; Pan, Shunqi; Chen, Shenliang. Impact of river discharge on hydrodynamics and sedimentary processes at Yellow River Delta[J]. *Marine Geology*, 2020, 425: 106210.
- [55] Jiang, Shan; Zhang, Yixue; Jin, Jie; Wu, Ying; Wei, Yongjun; Wang, Xiaolu; Rocha, Carlos; Ibanhez, Juan Severino Pino; Zhang, Jing. Organic carbon in a seepage face of a subterranean estuary: Turnover and microbial interrelations[J]. *Science of the Total Environment*, 2020, 725: 138220.
- [56] Jiang, Yamei; Saito, Yoshiki; Thi Kim Oanh Ta; Wang, Zhanghua; Gugliotta, Marcello; Van Lap Nguyen. Spatial and seasonal variability in grain size, magnetic susceptibility, and organic elemental geochemistry of channel-bed sediments from the Mekong Delta, Vietnam: Implications for hydro-sedimentary dynamic processes[J]. *Marine Geology*, 2020, 420: 106089.
- [57] Jin, Jie; Jiang, Shan; Zhang, Jing. Nitrogen isotopic analysis of nitrate in aquatic environment by cadmium- hydroxylamine hydrochloride reduction[J]. *Rapid Communications In Mass Spectrometry*, 2020, 34: e8804.
- [58] Kun, Zhao; Gong, Zheng; Zhang, Kaili; Wang, Keyu; Jin, Chuang; Zhou, Zeng; Xu, Fan; Coco, Giovanni. Laboratory experiments of bank collapse: the role of bank height and near-bank water depth[J]. *Journal of Geophysical Research:-Earth Surface*, 2020, 125(5): e2019JF005281.
- [59] Lambertini, Carla; Guo, Wenyong; Ye, Siyuan; Eller, Franziska; Guo, Xiao; Li, Xiuzhen; Sorrell, Brian K.; Speranza, Maria; Brix, Hans. Phylogenetic diversity shapes salt tolerance in *Phragmites australis* estuarine populations in East China[J]. *Scientific Reports*, 2020, 10(1): 17645.

- [60] Laura J. Falkenberg; Richard G.J. Bellerby; Sean D. Connell; Lora E. Fleming; Bruce Maycock; Bayden D. Russell; Francis J. Sullivan; Sam Dupont. Ocean acidification and human health[J]. *International Journal of Environmental Research and Public Health*, 2020, 17(12): 4563.
- [61] Li, Bowen; Su, Lei; Zhang, Haibo; Deng, Hua; Chen, Qiqing; Shi, Huahong. Microplastics in fishes and their living environments surrounding a plastic production area[J]. *Science of the Total Environment*, 2020, 727: 138662.
- [62] Li, Cheng; Yu, Junkun; Ai, Kete; Li, Huiying; Zhang, Yu; Zhao, Tianyu; Wei, Xiumei; Yang, Jialong. I kappa B alpha phosphorylation and associated NF-kappa B activation are essential events in lymphocyte activation, proliferation, and anti-bacterial adaptive immune response of Nile tilapia[J]. *Developmental and Comparative Immunology*, 2020, 103: 103526.
- [63] Li, Daoji; Liu, Kai; Li, Changjun; Peng, Guyu; Andrady, Anthony L; Wu, Tianning; Zhang, Zhiwei; Wang, Xiaohui; Song, Zhangyu; Zong, Changxing; Zhang, Feng; Wei, Nian; Bai, Mengyu; Zhu, Lixin; Xu, Jiayi; Wu, Hui; Wang, Lu; Chang, Siyuan; Zhu, Wenxi. Profiling the vertical transport of microplastics in the West Pacific Ocean and East Indian Ocean with a novel in situ filtration technique[J]. *Environmental science & technology*, 2020, 54(20): 12979-12988.
- [64] Li, Jiana; Chapman, Emma C.; Shi, Huahong; Rotchell, Jeanette M PVC. Does Not Influence Cadmium Uptake or Effects in the Mussel (*Mytilus edulis*)[J]. *Bulletin of Environmental Contamination and Toxicology*, 2020, 104(3): 315-320.
- [65] Li, Jun; Shang, Songyang; Fang, Na; Zhu, Yubo; Zhang, Junpeng; Irwin, David M.; Zhang, Shuyi; Wang, Zhe. Accelerated Evolution of Limb-Related Gene *Hoxd11* in the Common Ancestor of Cetaceans and Ruminants (Cetruminantia)[J]. *G3-Genes Genomes Genetics*, 2020, 10(2): 515-524.
- [66] Li, Linjiang; Zhu, Jianrong; Chant, Robert J.; Wang, Chuning; Pareja-Roman, L. Fernando. Effect of Dikes on Saltwater Intrusion Under Various Wind Conditions in the Changjiang Estuary[J]. *Journal of Geophysical Research-Oceans*, 2020, 125(7): 43855.
- [67] Li, Peng; Shi, Benwei; Li, Yangang; Wang, Sijian; Lv, Xin; Wang, Yaping; Tian, Qing. Characterization of longshore currents in southern East China Sea during summer and autumn[J]. *Acta Oceanologica Sinica*, 2020, 39(3): 1-11.
- [68] Li, Qipei; Feng, Zhihua; Zhang, Tao; Ma, Cuizhu; Shi, Huahong. Microplastics in the commercial seaweed nori[J]. *Journal of Hazardous Materials*, 2020, 388: 122060.
- [69] Li, Shihua, Ge, Zhenming, Tan, Lishan, Hu, Mengyao, Li, Yalei, Li, Xiuzhen, Ysebaert, Tom. Morphological and reproductive responses of coastal pioneer sedge vegetations to inundation intensity[J]. *Estuarine, Coastal and Shelf Science*, 2020, 244: 106945.
- [70] Li, Xiaofei; Hou, Lijun; Liu, Min; Tong, Chuan. Biogeochemical controls on nitrogen transformations in subtropical estuarine wetlands[J]. *Environmental Pollution*, 2020, 263(A): 114379.
- [71] Li, Xiaofei; Jordi Sardans, Hou, Lijun; Liu, Min; Xu, Chaobin; Josep Peñuelas. Climatic temperature controls the geographical patterns of coastal marshes greenhouse gases emissions over China[J]. *Journal of Hydrology*, 2020, 590: 125378.
- [72] Li, Xiaofei; Qian, Wei; Hou, Lijun; Liu, Min; Chen, Zhibiao; Tong, Chuan. Soil organic carbon controls dissimilatory nitrate reduction to ammonium along a freshwater-oligohaline gradient of Min River

- Estuary, Southeast China[J]. *Marine Pollution Bulletin*, 2020, 160: 111696.
- [73] Li, Xiaoshuang; Bellerby, Richard G. J.; Ge, Jianzhong; Wallhead, Philip; Liu, Jing; Yang, Anqiang. Retrieving monthly and interannual pHT in the East China Sea shelf using an artificial neural network: ANN-pHT-v1[J]. *Geophysical Model Development*, 2020, 13(10): 5103-5117.
- [74] Li, Xiaoshuang; Bellerby, Richard G. J.; Wallhead, Philip; Ge, Jianzhong; Liu, Jie; Liu, Jing; Yang, Anqiang. A Neural Network-Based Analysis of the Seasonal Variability of Surface Total Alkalinity on the East China Sea Shelf[J]. *Frontiers in Marine Science*, 2020, 7: 219.
- [75] Li, Yalei; Guo, Haiqiang; Ge, Zhenming; Wang, Dongqi; Liu, Wenliang; Xie, Lina; Li, Shihua; Tan, Lishan; Zhao, Bin; Li, Xiuzhen; Tang, Jianwu. Sea-level rise will reduce net CO₂ uptake in subtropical coastal marshes[J]. *Science of the Total Environment*, 2020, 747: 141214.
- [76] Li, Yiming; Liu, Zhiquan; Li, Maofeng; Jiang, Qichen; Wu, Donglei; Huang, Youhui; Jiao, Yang; Zhang, Meng; Zhao, Yunlong. Effects of nanoplastics on antioxidant and immune enzyme activities and related gene expression in juvenile *Macrobrachium nipponense*[J]. *Journal of Hazardous Materials*, 2020, 398: 122990.
- [77] Li, Yiming; Liu, Zhiquan; Yang, Yuan; Jiang, Qichen; Wu, Donglei; Huang, Youhui; Jiao, Yang; Chen, Qiang; Huang, Yinying; Zhao, Yunlong. Effects of nanoplastics on energy metabolism in the oriental river prawn (*Macrobrachium nipponense*)[J]. *Environmental Pollution*, 2020: 115890.
- [78] Li, Zhongqiao; Wu, Ying; Yang, Liyang; Du, Jinzhou; Deng, Bing; Zhang, Jing. Carbon isotopes and lignin phenols for tracing the floods during the past 70 years in the middle reach of the Changjiang River[J]. *Acta Oceanologica Sinica*, 2020, 39(4): 33-41.
- [79] Liang, Qiuyao; Yan, Zhongzheng; Li, Xiuzhen. Influence of the herbicide haloxyfop-R-methyl on bacterial diversity in rhizosphere soil of *Spartina alterniflora*[J]. *Ecotoxicology and Environmental Safety*, 2020, 194: 110365.
- [80] Lin, Jianliang; He, Qing; Guo, Leicheng; van Prooijen, Bram C.; Wang, Zheng Bing. An integrated optic and acoustic (IOA) approach for measuring suspended sediment concentration in highly turbid environments[J]. *Marine Geology*, 2020, 421: 106062.
- [81] Lin, Lei; Liu, Dongyan; Guo, Xinyu; Luo, Chongxin; Cheng, Yao. Tidal Effect on Water Export Rate in the Eastern Shelf Seas of China[J]. *Journal of Geophysical Research-Oceans*, 2020, 125(5): e2019JC015863.
- [82] Liu, Cheng; Hou, Lijun; Liu, Min; Zheng, Yanling; Yin, Guoyu; Dong, Hongpo; Liang, Xia; Li, Xiaofei; Gao, Dengzhou; Zhang, Zongxiao. In situ nitrogen removal processes in intertidal wetlands of the Yangtze Estuary[J]. *Journal of Environmental Sciences*, 2020, 93: 91-97.
- [83] Liu, Dongyan; Ma, Qian; Valiela, Ivan; Anderson, Donald M. ; Keesing, John K.; Gao, Kunshan; Zhen, Yu; Sun, Xiyan; Wang, Yujue. Role of C₄ carbon fixation in *Ulva prolifera*, the macroalga responsible for the world's largest green tides[J]. *Communications Biology*, 2020, 494(3): 1.
- [84] Liu, Jian; Qiu, Jiandong; Saito, Yoshiki; Zhang, Xin; Nian, Xiaomei; Wang, Feifei; Xu, Gang; Xu, Taoyu; Li, Meina. Formation of the Yangtze Shoal in response to the post-glacial transgression of the paleo-Yangtze (Changjiang) estuary, China[J]. *Marine Geology*, 2020, 423: 106080.

- [85] Liu, Kai; Wang, Xiaohui; Song, Zhangyu; Wei, Nian; Li, Daoji. Terrestrial plants as a potential temporary sink of atmospheric microplastics during transport[J]. *Science of the Total Environment*, 2020, 742: 140523.
- [86] Liu, Kai; Wang, Xiaohui; Song, Zhangyu; Wei, Nian; Ye, Haoda; Cong, Xin; Zhao, Longwei; Li, You; Qu, Liming; Zhu, Lixin; Zhang, Feng; Zong, Changxing; Jiang, Chunhua; Li, Daoji. Global inventory of atmospheric fibrous microplastics input into the ocean: An implication from the indoor origin[J]. *Journal of Hazardous Materials*, 2020, 400: 123223.
- [87] Liu, Kai; Courtene-Jones, Winnie; Wang, Xiaohui; Song, Zhangyu; Wei, Nian; Li, Daoji. Elucidating the vertical transport of microplastics in the water column: a review of sampling methodologies and distributions[J]. *Water research*, 2020, 186: 116403.
- [88] Liu, Shihao; Feng, Aiping; Yang, Linlong; Du, Jun; Yu, Yonggui; Feng, Wei; Wang, Yaping. Stratigraphic and three-dimensional morphological evolution of the late Quaternary sequences in the western Bohai Sea, China: Controls related to eustasy, high sediment supplies and neotectonics[J]. *Marine Geology*, 2020, 427: 106246.
- [89] Liu, Yan; Deng, Lanjie; He, Jin; Jiang, Ren; Fan, Daidu; Jiang, Xuezhong; Jiang, Feng; Li, Maotian; Chen, Jing; Chen, Zhongyuan; Sun, Qianli. Early to middle Holocene rice cultivation in response to coastal environmental transitions along the South Hangzhou Bay of eastern China[J]. *Palaeogeography Palaeoclimatology Palaeoecology*, 2020, 555: 109872.
- [90] Liu, Zhiquan; Cai, Mingqi; Wu, Donglei; Yu, Ping; Jiao, Yang; Jiang, Qichen; Zhao, Yunlong. Effects of nanoplastics at predicted environmental concentration on *Daphnia pulex* after exposure through multiple generations[J]. *Environmental Pollution*, 2020, 256: 113506.
- [91] Liu, Zhiquan; Huang, Youhui; Jiao, Yang; Chen, Qiang; Wu, Donglei; Yu, Ping; Li, Yiming; Cai, Mingqi; Zhao, Yunlong. Polystyrene nanoplastic induces ROS production and affects the MAPK-HIF-1/NF kappa B-mediated antioxidant system in *Daphnia pulex*[J]. *Aquatic Toxicology*, 2020, 220: 105420.
- [92] Liu, Zhiquan; Jiao, Yang; Chen, Qiang; Li, Yiming; Tian, Jiangtao; Huang, Yinying; Cai, Mingqi; Wu, Donglei; Zhao, Yunlong. Two sigma and two mu class genes of glutathione S-transferase in the waterflea *Daphnia pulex*: Molecular characterization and transcriptional response to nanoplastic exposure[J]. *Chemosphere*, 2020, 248: 126065.
- [93] Long L H, Ji D B, Yang Z Y, Cheng H Q, Yang Z Liu J, D F, Liu L, Lorke A. Tributary oscillations generated by diurnal discharge regulation in Three Gorges Reservoir[J]. *Environmental Research Letters*, 2020, 15: 84011.
- [94] Lou, Yaying; Dai, Zhijun; He, Yuying; Mei, Xuefei; Wei, Wen. Morphodynamic couplings between the Biandan Shoal and Xinqiao Channel, Changjiang (Yangtze) Estuary[J]. *Ocean and Coastal Management*, 2020, 183: 105036.
- [95] Lu, Hongfang; Zhang, Huanshi; Qin, Pei; Li, Xiuzhen; Campbell, Daniel E..Integrated emergy and economic evaluation of an ecological engineering system for the utilization of *Spartina alterniflora*[J]. *Journal of Cleaner Production*, 2020, 247: 119592.
- [96] Lu, Shibo; Qiu, Rong; Hu, Jiani; Li, Xinyu; Chen, Yingxin; Zhang, Xiaoting; Cao, Chengjin; Shi, Huahong; Xie, Bing; Wu, Wei-Min; He, Defu. Prevalence of microplastics in animal-based traditional medicinal materials: Widespread pollution in terrestrial environments[J]. *Science of the Total Environment*, 2020, 742: 140523.

- Environment, 2020, 709: 136214.
- [97] Lu, Ting; Wu, Hao; Zhang, Fan; Li, Jiasheng; Zhou, Liang; Jia, Jianjun; Li, Zhanhai; Wang, Ya Ping. Constraints of salinity- and sediment-induced stratification on the turbidity maximum in a tidal estuary[J]. *Geo-Marine Letters*, 2020, 40(5): 765-779.
- [98] Lv, Min; Luan, Xiaolin; Liao, Chunyang; Wang, Dongqi; Liu, Dongyan; Zhang, Gan; Jiang, Guibin; Chen, Lingxin. Human impacts on polycyclic aromatic hydrocarbon distribution in Chinese intertidal zones[J]. *Nature Sustainability*, 2020, 3(10): 878-884.
- [99] Lyu, Wenzhe, Yang, Jichao; Fu, Tengfei; Chen, Yanping; Hu, Zhangxi; Tang, Ying Zhong; Lan Jianghu; Chen, Guangquan; Su, Qiao; Xu, Xingyong; Chen, Shenliang. Asian monsoon and oceanic circulation paced sedimentary evolution over the past 1,500 years in the central mud area of the Bohai Sea, China[J]. *Geological Journal*, 2020, 55(7): 5606-5618.
- [100] Ma, Binbin; Pang, Wenhong; Lou, Yaying ; Mei, Xuefei; Wang, Jie; Gu, Jinghua; Dai, Zhijun. Impacts of River Engineering on Multi-Decadal Water Discharge of the Mega-Changjiang River[J]. *Sustainability*, 2020, 12(19): 8060.
- [101] Mao, Tiegang; Li, Yanqun; Dong, Hongpo; Yang, Wenna; Hou, Lijun. Spatio-Temporal Variations in the Abundance and Community Structure of *Nitrospira* in a Tropical Bay[J]. *Current Microbiology*, 2020, (77): 3492-3503.
- [102] Nan, Bingxu; Su, Lei; Kellar, Claudette; Craig, Nicholas J; Keough, Michael J; Pettigrove, Vincent. Identification of microplastics in surface water and Australian freshwater shrimp *Paratya australiensis* in Victoria, Australia[J]. *Environmental Pollution (Barking, Essex : 1987)*, 2020, 259: 113865.
- [103] [Pan, Dadong; Wang, Zhanghua; Zhan, Qing; Saito, Yoshiki; Wu, Hui; Yang, Shouye; Cheng, Heqin. Organic geochemical variations for understanding past sediment dynamic processes: example from Holocene sedimentary records in the Changjiang River delta, China[J]. *Continental Shelf Research*, 2020, 204: 104189.
- [104] Pang, Wenhong; Dai, Zhijun; Ma, Binbin; Wang, Jie; Huang, Hu; Li, Shushi. Linkage between turbulent kinetic energy, waves and suspended sediment concentrations in the nearshore zone[J]. *Marine Geology*, 2020, 425: 106190.
- [105] Park, Jun Chul; Choi, Beom-Soon; Kim, Min-Sub; Shi, Huahong; Zhou, Bingsheng; Park, Heum Gi; Lee, Jae-Seong. The genome of the marine rotifer *Brachionus koreanus* sheds light on the antioxidative defense system in response to 2-ethyl-phenanthrene and piperonyl butoxide[J]. *Aquatic Toxicology*, 2020, 221: 105443.
- [106] Peng, Guyu; Bellerby, Richard; Zhang, Feng; Sun, Xuerong; Li, Daoji. The ocean's ultimate trashcan: Hadal trenches as major depositories for plastic pollution[J]. *Water Research*, 2020, 168: 115121.
- [107] Peng, Yun; Yu, Qian; Yang, Yang; Wang, Yunwei; Wang, Yaping; Gao, Shu. Flow structure modification and drag reduction induced by sediment stratification in coastal tidal bottom boundary layers[J]. *Estuarine, Coastal and Shelf Science*, 2020, 241: 106829.
- [108] Pradhan, U K; Wu, Y; Shirodkar, P V; Kumar, H Shiva; Zhang, J. Connecting land use-land cover and precipitation with organic matter biogeochemistry in a tropical river-estuary system of western peninsular India[J]. *Journal of Environmental Management*, 2020, 271: 110993.

- [109] Pradhan, U. K.; Wu, Ying; Shirodkar, P. V.; Kumar, H. Shiva; Zhang, Jing. Connecting land use-land cover and precipitation with organic matter biogeochemistry in a tropical river-estuary system of western peninsular India. [J]. *Journal of environmental management*, 2020, 271: 110993.
- [110] Qiang, Liyuan; Arabeyyat, Zeinab H.; Xin, Qi; Paunov, Vesselin N.; Dale, Imogen J. F.; Mills, Richard I. Lloyd; Rotchell, Jeanette M.; Cheng, Jinping. Silver Nanoparticles in Zebrafish (*Danio rerio*) Embryos: Uptake, Growth and Molecular Responses[J]. *International Journal of Molecular Sciences*, 2020, 21(5): 1876.
- [111] Qiu, Wenhui; Fang, Meijuan; Magnuson, Jason T; Greer, Justin B; Chen, Qiqing; Zheng, Yi; Xiong, Ying; Luo, Shusheng; Zheng, Chunmiao; Schlenk, Daniel. Maternal exposure to environmental antibiotic mixture during gravid period predicts gastrointestinal effects in zebrafish offspring[J]. *Journal of Hazardous Materials*, 2020, 399: 123009.
- [112] Qiu, Wenhui; Hu, Jiaqi; Magnuson, Jason T.; Greer, Justin; Yang, Ming; Chen, Qiqing; Fang, Meijuan; Zheng, Chunmiao; Schlenk, Daniel. Evidence linking exposure of fish primary macrophages to antibiotics activates the NF- κ B pathway[J]. *Environment International*, 2020, 138: 105624.
- [113] Shao, Da; Mei, Yanjun; Yang, Zhongkang; Wang, Yuhong; Yang, Wenqing; Gao, Yuesong; Yang, Lianjiao; Sun, Liguang. Holocene ENSO variability in the South China Sea recorded by high-resolution oxygen isotope records from the shells of *Tridacna* spp[J]. *Scientific Reports*, 2020, 10(1): 3921
- [114] Sheng, Hui; Xu, Xiaomei; Gao, Jianhua; Kettner, Albert J.; Shi, Yong; Xue, Chengfeng; Wang, Ya Ping; Gao, Shu. Frequency and magnitude variability of Yalu River flooding: numerical analyses for the last 1000 years[J]. *Hydrology and Earth System Sciences*, 2020, 24: 4743-4761.
- [115] Shi, Benwei; Pratolongo, Paula; Du, Yongfen; Li, Jiasheng; Yang, Shilun; Wu, Jihua; Xu, Kehui; Wang, Ya Ping. Influence of Macrobenthos (*Meretrix meretrix* Linnaeus) on Erosion/Accretion Processes in Intertidal Flats: A Case Study From a Cultivation Zone[J]. *Journal of Geophysical Research-Biogeosciences*, 2020, 125(1): e2019JG005345.
- [116] Song, Shuzhen; Wang, Zhaohui Aleck; Gonnee, Meagan Eagle; Kroeger, Kevin D.; Chu, Sophie N.; Li, Daoji; Liang, Haorui. An important biogeochemical link between organic and inorganic carbon cycling: Effects of organic alkalinity on carbonate chemistry in coastal waters influenced by intertidal salt marshes[J]. *Geochimica et Cosmochimica Acta*, 2020, 275: 123-139.
- [117] Song, Zekun; Shi, Weiyong; Zhang, Junbiao; Hu, Hao; Zhang, Feng; Xu, Xuefeng. Transport Mechanism of Suspended Sediments and Migration Trends of Sediments in the Central Hangzhou Bay[J]. *Water*, 2020, 12(8): 2189.
- [118] Su, Lei; Nan, Bingxu; Craig, Nicholas J.; Pettigrove, Vincent. Temporal and spatial variations of microplastics in roadside dust from rural and urban Victoria, Australia: Implications for diffuse pollution[J]. *Chemosphere*, 2020, 252: 126567.
- [119] Su, Lei; Sharp, Simon M.; Pettigrove, Vincent J.; Craig, Nicholas J.; Nan, Bingxu; Du, Fangni; Shi, Huahong. Superimposed microplastic pollution in a coastal metropolis[J]. *Water Research*, 2020, 168: 115140.
- [120] Sun, Baoyu; Yan Liming; Jiang Ming; Li Xingge; Han Guangxuan; Xia Jianyang. Reduced magnitude and shifted seasonality of CO₂ sink by experimental warming in a coastal wetland[J]. *Ecology*, 2020: e03236.

- [121] Sun, Dongyao; Tang, Xiufeng; Zhao, Mengyue; Zhang, Zongxiao; Hou, Lijun; Liu, Min; Wang, Baozhan; Klumper, Uli; Han, Ping. Distribution and Diversity of Comammox Nitrospira in Coastal Wetlands of China[J]. *Frontiers in Microbiology*, 2020, 11: 589268.
- [122] Sun, Shengxiang; Wu, Junlin; Lv, Hongbo; Zhang, Haiyang; Zhang, Jing; Limbu, Samwel Mchele; Qiao, Fang; Chen, Liqiao; Yang, Yi; Zhang, Meiling; Du, Zhenyu. Environmental estrogen exposure converts lipid metabolism in male fish to a female pattern mediated by AMPK and mTOR signaling pathways[J]. *Journal of Hazardous Materials*, 2020, 394: 122537.
- [123] Tan, Kai; Chen, Jin; Zhang, Weiguo; Liu, Kunbo; Tao, Pengjie; Cheng, Xiaojun. Estimation of soil surface water contents for intertidal mudflats using a near-infrared long-range terrestrial laser scanner[J]. *ISPRS Journal of Photogrammetry And Remote Sensing*, 2020, 159: 129-139.
- [124] Tan, Kai; Cheng, Xiaojun. Distance Effect Correction on TLS Intensity Data Using Naturally Homogeneous Targets[J]. *IEEE Geoscience and Remote Sensing Letters*, 2020, 17(3): 499-503.
- [125] Tan, Kai; Zhang, Weiguo; Dong, Zhen; Cheng, Xiaolong; Cheng, Xiaojun. Leaf and Wood Separation for Individual Trees Using the Intensity and Density Data of Terrestrial Laser Scanners[J]. *IEEE Transactions on Geoscience and Remote Sensing*, 2020.
- [126] Tan, Lishan, Ge, Zhenming, Fei, Beili, Xie, Lina, Li, Yalei, Li, Shihua, Li, Xiuzhen, Ysebaert, Tom. The roles of vegetation, tide and sediment in the variability of carbon in the salt marsh dominated tidal creeks[J]. *Estuarine, Coastal and Shelf Science*, 2020, 239: 106752.
- [127] Tan, Lishan; Ge, Zhenming; Zhou, Xuhui; Li, Shihua; Li, Xiuzhen; Tang, Jianwu. Conversion of coastal wetlands, riparian wetlands, and peatlands increases greenhouse gas emissions: A global meta-analysis[J]. *Global Change Biology*, 2020, 26(3): 1638-1653.
- [128] Wang, Bo; Xu, Y.Jun; Xu, Wei; Cheng, Heqin; Chen, Zhongyuan; Zhang, Weiguo. Riverbed changes of the uppermost atchafalaya river, usa-a case study of channel dynamics in large man-controlled alluvial river [J]. *Water*, 2020,12: 2139.
- [129] Wang, Feng; Zhang, Weiguo; Nian, Xiaomei; Roberts, Andrew P.; Zhao, Xiang; Shang, Yuan; Ge, Can; Dong, Yan. Magnetic evidence for Yellow River sediment in the late Holocene deposit of the Yangtze River Delta, China[J]. *Marine Geology*, 2020, 427: 106274.
- [130] Wang, Hui; Wang, Yonghao; Zhuang, Wan-E; Chen, Wei; Shi, Weixin; Zhu, Zhuoyi; Yang, Liyang. Effects of fish culture on particulate organic matter in a reservoir-type river as revealed by absorption spectroscopy and fluorescence EEM-PARAFAC[J]. *Chemosphere*, 2020, 239: 124734.
- [131] Wang, Jianxing; Wang, Tao; Xing, Fei; Wu, Hao; Jia, Jianjun; Yang, Zuosheng; Wang, Yaping. Internal waves triggered by river mouth shoals in the Yangtze River Est[J]. *Ocean Engineering*, 2020, 214: 107828.
- [132] Wang, Jie; Dai, Zhijun; Mei, Xuefei; Fagherazzi, Sergio. Tropical cyclones significantly alleviate mega-deltaic erosion induced by high riverine flow[J]. *Geophysical Research Letters*, 2020, 47(19): e:2020GL089065.
- [133] Wang, Jingjing; Wang, Yun; Wang, Wei; Peng, Tong; Liang, Jianjun; Li, Ping; Pan, Duoqiang; Fan, Qiaohui; Wu, Wangsuo. Visible light driven Ti^{3+} self-doped TiO_2 for adsorption-photocatalysis of aqueous U(VI)[J]. *Environmental Pollution*, 2020, 262: 114373.

- [134] Wang, Jinglong; Du, Jinzhou; Zheng, Jian. Plutonium Isotopes Research in the Marine Environment: A synthesis[J]. *Journal of Nuclear and Radiochemical Sciences*, 2020, 20: 1-11.
- [135] Wang, Jinlong; Baskaran, Mark; Kumar, Anupam; Bilhan, Omer; J. Miller, Carol. Reconstruction of Temporal Variations of Metal Concentrations using Radiochronology ($^{239+240}\text{Pu}$ and ^{137}Cs) in Sediments from Kizilirmak River, Turkey[J]. *Journal of Paleolimnology*, 2020: 1-13.
- [136] Wang, Jinlong; Du, Jinzhou; Zheng, Jian; Bi, Qianqian; Ke, Yu; Qu, Jianguo. Plutonium in Southern Yellow Sea sediments and its implications for the quantification of oceanic-derived mercury and zinc[J]. *Environmental pollution*, 2020, 266(Pt3): 115262.
- [137] Wang, Li; Yu, Qian; Zhang, Yongzhan; Flemming, Burghard W.; Wang, Yunwei; Gao, Shu. An automated procedure to calculate the morphological parameters of superimposed rhythmic bedforms[J]. *Earth Surface Processes and Landforms*, 2020, 45: 3496-3509.
- [138] Wang, Ming; Li, Yaping; Jiang, Xuefeng. Recent Advances in Sulfuration Chemistry Enabled by Bunte Salts[J]. *Aldrich. Acta*, 2020, 53(1)(SI): 19-35.
- [139] Wang, Ning; Wang, Ya Ping; Duan, Xiaoyong; Wan, Jianqiang; Xie, Yongqing; Dong, Chao; Gao, Jianhua; Yin, Ping. Controlling factors for the distribution of typical organic pollutants in the surface sediment of a macrotidal bay[J]. *Environmental Science and Pollution Research*, 2020.
- [140] Wang, Qiugui; Sha, Zhanjiang; Wang, Jinlong; Zhong, Qiangqiang; Fang, Penggao; Ma, Yujun; Du, Jinzhou. Vertical distribution of radionuclides in Lake Qinghai, Qinghai-Tibet Plateau, and its environmental implications[J]. *Chemosphere*, 2020, 259: 127489.
- [141] Wang, Shuo; Ge, Jianzhong; Kilbourne, K. Halimeda; Wang, Zhanghua. Numerical simulation of mid-Holocene tidal regime and storm-tide inundation in the south Yangtze coastal plain, East China[J]. *Marine Geology*, 2020, 423: 106134.
- [142] Wang, Xianye; Sun, Jianwei; Zhao, Zhonghao. Effects of river discharge and tidal meandering on morphological changes[J]. *Estuarine, Coastal and Shelf Science*, 2020, 234: 106635.
- [143] Wang, Xiaohui; Li, Changjun; Liu, Kai; Zhu, Lixin; Song, Zhangyu; Li, Daoji. Atmospheric microplastic over the South China Sea and East Indian Ocean: abundance, distribution and source[J]. *Journal of Hazardous Materials*, 2020, 389: 121846.
- [144] Wang, Xinghuo; Huang, Wei; Wei, Shuaishuai; Shang, Yueyong; Gu, Huaxin; Wu, Fangzhu; Lan, Zhaohui; Hu, Menghong; Shi, Huahong; Wang, Youji. Microplastics impair digestive performance but show little effects on antioxidant activity in mussels under low pH condition[J]. *Environmental Pollution*, 2020, 258: 113691.
- [145] Wang, Yameng; Zhang, Lixia; Wang, Jining; Lv, Jianshu. Identifying quantitative sources and spatial distributions of potentially toxic elements in soils by using three receptor models and sequential indicator simulation[J]. *Chemosphere*, 2020, 242: 125266.
- [146] Wang, Yaping; Sun, Fasheng; Xu, Hongquan. On Design Orthogonality, Maximin Distance, and Projection Uniformity for Computer Experiments[J]. *Journal of the American Statistical Association*, 2020: 1782221.
- [147] Wang, Yujue; Lee, Kenneth; Liu, Dongyan; Guo, Jie; Han, Qiuying; Liu, Xihan; Zhang, Jingjing.

- Environmental impact and recovery of the Bohai Sea following the 2011 oil spill[J]. *Environmental Pollution (Barking, Essex : 1987)*, 2020, 263(Pt B): 114343.
- [148] Wei, Wen; Dai, Zhijun; Pang, Wenhong; Wang, Jie; Gao, Shu. Sedimentary zonation shift of tidal flats in a meso-tidal estuary[J]. *Sedimentary Geology*, 2020, 407: 105749.
- [149] Wei, Xiumei; Li, Huiying; Zhang, Yu; Li, Cheng; Li, Kang; Ai, Kete; Yang, Jialong. Ca^{2+} -Calcineurin Axis-Controlled NFAT Nuclear Translocation Is Crucial for Optimal T Cell Immunity in an Early Vertebrate[J]. *Journal of Immunology*, 2020, 204(3): 569-585.
- [150] Wei, Xiumei; Zhang, Yu; Li, Cheng; Ai, Kete; Li, Kang; Li, Huiying; Yang, Jialong. The evolutionarily conserved MAPK/Erk signaling promotes ancestral T-cell immunity in fish via c-Myc-mediated glycolysis[J]. *Journal of Biological Chemistry*, 2020, 295(10): 3000-3016.
- [151] Wu, Donglei; Liu, Zhiquan; Yu, Ping; Huang, Youhu; Cai, Mingqi; Zhang, Meng; Zhao, Yunlong. Cold stress regulates lipid metabolism via AMPK signalling in *Cherax quadricarinatus*[J]. *Journal of Thermal Biology*, 2020, 92: 102693.
- [152] Wu, Fengrun; Pennings, Steven C.; Tong, Chunfu; Xu, Yutian. Variation in microplastics composition at small spatial and temporal scales in a tidal flat of the Yangtze Estuary, China[J]. *Science of the Total Environment*, 2020, 699: 134252.
- [153] Wu, Fengrun; Tong, Chunfu; Mitch Torkelson; Wang, Yan. Evolution of shoals and vegetation of Jiuduansha in the Changjiang River Estuary of China in the last 30 years[J]. *Acta of Oceanologica Sinica*, 2020, 39(8): 71-78.
- [154] Xiao, Rui; Wu, Xiuning; Du, Jinzhou; Deng, Bing; Xing, Lei. Impacts of anthropogenic forcing on source variability of sedimentary organic matter in the Yellow River estuary over the past 60 years[J]. *Marine Pollution Bulletin*, 2020, 151: 110818.
- [155] Xie, Lina; Ge, Zhenming; Li, Yalei; Li, Shihua; Tan, Lishan; Li, Xiuzhen. Effects of waterlogging and increased salinity on microbial communities and extracellular enzyme activity in native and exotic marsh vegetation soils[J]. *Soil Science Society of America Journal*, 2020, 84(1): 82-98.
- [156] Xiong, Jilian; You, Zaijin; Li, Jin; Gao, Shu; Wang, Qing; Wang, Xiping. Variations of wave parameter statistics as influenced by water depth in coastal and inner shelf areas[J]. *Coastal Engineering*, 2020, 159: 103714.
- [157] Xu, Fan; Coco, Giovanni; Zhou, Zeng; Townend, Ian; Guo, Leicheng; He, Qing. A Universal Form of Power Law Relationships for River and Stream Channels[J]. *Geophysical Research Letters*, 2020, 47(20): e2020GL090493.
- [158] Xu, Jiang; Liu, Xue; Cao, Zhen; Bai, Weiliang; Shi, Qingyang; Yang, Yi. Fast degradation, large capacity, and high electron efficiency of chloramphenicol removal by different carbon-supported nanoscale zerovalent iron[J]. *Journal of Hazardous Materials*, 2020, 384: 121253.
- [159] Xu, Jiayi; Li, Daoji. Feeding behavior responses of a juvenile hybrid grouper, *Epinephelus fuscoguttatus*♀ × *E. lanceolatus*♂ to microplastics[J]. *Environmental pollution*, 2020, 268(Pt A): 115648.
- [160] Xu, Qibin; Chu, Zhuding; Gao, Yuesong; Mei, Yanjun; Yang, Zhongkang; Huang, Yikang; Yang,

- Lianjiao; Xie, Zhouqing; Sun, Liguang. Levels, sources and influence mechanisms of heavy metal contamination in topsoils in Mirror Peninsula, East Antarctica[J]. *Environmental Pollution*, 2020, 257: 113552.
- [161] Xu, Y; Yao, S; Soetaert, K; Fan, X. Effects of salt marsh restoration on eukaryotic microbenthic communities in the Yangtze Estuary[J]. *Marine Ecology Progress Series*, 2020, 638: 39-50.
- [162] Xu, Yi; Travis, Miles; Oscar, Schofield. Physical processes controlling chlorophyll-a variability on the Mid-Atlantic Bight along northeast United States[J]. *Journal of Marine Systems*, 2020, 212: 103433.
- [163] Xue, Lian; Jiang, Junyan; Li, Xiuzhen; Yan, Zhongzheng; Zhang, Qian; Ge, Zhenming; Tian, Bo; Craft, Christopher. Salinity Affects Topsoil Organic Carbon Concentrations Through Regulating Vegetation Structure and Productivity[J]. *Journal of Geophysical Research-Biogeosciences*, 2020, 125(1): e2019JG005217.
- [164] Yan, Ge; Cheng, Heqin; Teng, LiZhi; Xu, Wei; Jiang, Yuehua; Yang, Guoqiang; Zhou, Quanping. Analysis of the Use of Geomorphic Elements Mapping to Characterize Subaqueous Bedforms Using Multibeam Bathymetric Data in River System[J]. *Applied Sciences*, 2020, 10: 7692.
- [165] Yang, Bin; Li, Xiuzhen; Lin, Shiwei; Xie, Zuolun; Yuan, Yiquan; Espenberg, Mikk; Parn, Jaan; Mander, Ulo. Invasive *Spartina alterniflora* can mitigate N₂O emission in coastal salt marshes[J]. *Ecological Engineering*, 2020, 147: 105758.
- [166] Yang, Guosheng; Zheng, Jian; Tagami, Keiko; Uchida, Shigeo; Zhang, Jing; Wang, Jinlong; Du, Jinzhou. Simple and sensitive determination of radium-226 in river water by single column-chromatographic separation coupled to SF-ICP-MS analysis in medium resolution mode[J]. *Journal of environmental radioactivity*, 2020, 220-221: 106305.
- [167] Yang, Hualei; Tang, Jianwu; Zhang, Chunsong; Dai, Yuhang; Zhou, Cheng; Xu, Ping; Perry, Danielle C.; Chen, Xuechu. Enhanced Carbon Uptake and Reduced Methane Emissions in a Newly Restored Wetland[J]. *Journal of Geophysical Research-Biogeosciences*, 2020, 125(1): e2019JG005222.
- [168] Yang, Shaobo; Fan, Linlin; Duan, Shanhua; Zheng, Chongwei; Li, Xingfei; Li, Hongyu; Xu, Jianjun. Long-term assessment of wave energy in the China Sea using 30-year hindcast data[J]. *Energy Exploration & Exploitation*, 2020, 38(1): 37-56.
- [169] Yang, Shilun; Luo, Xiangxin; Temmerman, Stijn; Kirwan, Matthew; Bouma, Tjeerd; Xu, Kehui; Zhang, Saisai; Fan, Jiqing; Shi, Benwei; Yang, Haifei; Wang, Yaping; Shi, Xuefa; Gao, Shu. Role of delta-front erosion in sustaining salt marshes under sea-level rise and fluvial sediment decline[J]. *Limnology and Oceanography*, 2020, 65 (9): 1990–2009.
- [170] Yang, Shilun; Shi, Benwei; Fan, Jiqing; Luo, Xiangxin; Tian, Qing; Yang, Haifei; Chen, Shenliang; Zhang, Yingxin; Zhang, Saisai; Shi, Xuefa; Wang, Houjie. Streamflow Decline in the Yellow River along with Socioeconomic Development: Past and Future[J]. *Water*, 2020, 12: 823.
- [171] Yang, Yang; Jia, Jianjun; Zhou, Liang; Gao, Jianhua; Gao, Wenhua; Shi, Benwei; Li, Zhanhai; Wang, Yaping; Gao, Shu. Quantitative reconstruction of Holocene sediment sources contributing to the central Jiangsu coast, China: New insights into source-to-sink processes[J]. *Earth Surface Processes and Landforms*, 2020, <https://doi.org/10.1002/esp.4891>.
- [172] Yang, Yang; Zhou, Liang; Normandeau Alex; Jia, Jianjun; Yin, Qijun; Wang, Yaping; Shi, Benwei; Lei

- Gao; Gao, Shu. Exploring records of typhoon variability in eastern China over the past 2000 years[J]. Geological Society of America Bulletin, 2020, 13(11-12): 2243-2252.
- [173] Yang, Zhongyong; Zhu, Yingying; Ji, Daobin; Yang, Zhengjian; Tan, Junjun; Hu, Hao; Andreas, Lorkeac. Discharge and water level fluctuations in response to flow regulation in impounded rivers: An analytical study[J]. Journal of Hydrology, 2020, 590: 125519.
- [174] Yang, Yang; Maselli, Vittorio , Normandeau, Alexandre; Piper, J.W. David; Li, Michael Z; Campbell, D. Calvin; Gregory, Taylor; Gao, Shu. Latitudinal Response of Storm Activity to Abrupt Climate Change During the Last 6,500 Years[J]. Geophysical Research Letters, 2020, 47(19): e2020GL089859.
- [175] Yin, Yichen; Yan, Zhongzheng. Variations of soil bacterial diversity and metabolic function with tidal flat elevation gradient in an artificial mangrove wetland[J]. Science of the Total Environment, 2020, 718: 137385.
- [176] Yuan, Lin; Chen, Yahui; Wang, Heng; Cao, Haobing; Zhao, Zhiyuan; Zhang, Liquan. Windows of opportunity for salt marsh establishment: The importance for salt marsh restoration in the Yangtze Estuary[J]. Ecosphere, 2020, 11: e03180
- [177] Yuan, Yiquan; Li, Xiuzhen; Jiang, Junyan; Xue, Liming; Christopher B. Craft. Distribution of organic carbon storage in different saltmarsh plant communities: A case study at the Yangtze Estuary[J]. Estuarine, Coastal and Shelf Science, 2020, 243: 106900.
- [178] Zhan, Qing; Li, Maotian; Liu, Xiaoqiang; Chen, Jing; Chen, Zhongyuan. Sedimentary transition of the Yangtze subaqueous delta during the past century: Inspiration for delta response to future decline of sediment supply[J]. Marine Geology, 2020, 428: 106279.
- [179] Zhang, Feng; Yao, Chenyang; Xu, Jiayi; Zhu, Lixin; Peng, Guyu; Li, Daoji. Composition, spatial distribution and sources of plastic litter on the East China Sea floor[J]. Science of the Total Environment, 2020, 742: 140525.
- [180] Zhang, Miao; Wu, Ying; Wang, Fuqiang; Xu, Dongfeng; Liu, Sumei; Zhou, Meng. Hotspot of Organic Carbon Export Driven by Mesoscale Eddies in the Slope Region of the Northern South China Sea[J]. Frontiers in Marine Science, 2020, 7: 444.
- [181] Zhang, Qiqiong; Yan, Zhongzheng; Li, Xiuzhen. Ferrous iron facilitates the formation of iron plaque and enhances the tolerance of *Spartina alterniflora* to artificial sewage stress[J]. Marine Pollution Bulletin, 2020, 157: 111379.
- [182] Zhang, Qun; Xu, Elvis Genbo; Li, Jiana; Chen, Qiqing; Ma, Liping; Zeng, Eddy Y.; Shi, Huahong. A Review of Microplastics in Table Salt, Drinking Water, and Air: Direct Human Exposure[J]. Environmental Science & Technology, 2020, 54(7): 3740-3751.
- [183] Zhang, Qun; Zhao, Yaping; Du, Fangni; Cai, Huiwen; Wang, Gehui; Shi, Huahong. Microplastic Fallout in Different Indoor Environments[J]. Environmental Science & Technology, 2020, 54(11): 6530-6539.
- [184] Zhang, Shaozeng; Zhao, Bo; Tian, Yuanyuan; Chen, Shenliang. Stand with #StandingRock: Envisioning an epistemological shift in understanding geospatial big data in the “post-truth” era[J]. Annals of the American Association of Geographers, 2020: doi:10.1080/24694452., 2020.1782166.
- [185] Zhang, Weiguo; Ge, Zhenming; Baskaran, Mark Mahalingam. Where land meets ocean: The

- vulnerable interface[J]. *Estuarine, Coastal and Shelf Science*, 2020, 243: 106893.
- [186] Zhang, Xiaohua; Lin, Senjie; Liu, Dongyan. Transcriptomic and physiological responses of *Skeletonema costatum* to ATP utilization[J]. *Environmental Microbiology*, 2020, 22(5): 1861-1869.
- [187] Zhang, Xiaohui; Mueller, Moritz; Jiang, Shan; Wu, Ying; Zhu, Xunchi; Mujahid, Aazani; Zhu, Zhuoyi; Muhamad, Mohd Fakharuddin; Sia, Edwin Sien Aun; Jang, Faddrine Holt Ajon; Zhang, Jing. Distribution and flux of dissolved iron in the peatland-draining rivers and estuaries of Sarawak, Malaysian Borneo[J]. *Biogeosciences*, 2020, 17(6): 1805-1819.
- [188] Zhang, Yushuang; Xiao, Xiaotong; Liu, Dongyan; Wang, Enhui; Liu, Ke; Ding, Yang; Yao, Peng; Zhao, Meixun. Spatial and seasonal variations of organic carbon distributions in typical intertidal sediments of China[J]. *Organic Geochemistry*, 2020, 142: 103993.
- [189] Zhang, Zhiwei; Wu, Hui; Peng, Guyu; Xu, Pei; Li, Daoji. Coastal ocean dynamics reduce the export of microplastics to the open ocean[J]. *Science of the Total Environment*, 2020, 713: 136634.
- [190] Zhang, Zongxiao; Zheng, Yanling; Han, Ping; Dong, Hongpo; Liang, Xia; Yin, Guoyu; Wu, Dianming; Yang, Yi; Liu, Sitong; Liu, Min; Hou, Lijun. N-acyl-homoserine lactones (AHLs) in intertidal marsh: diversity and potential role in nitrogen cycling[J]. *Plant Soil*, 2020, 454(1-2): 103-119.
- [191] Zhao, Yiyi; Bu, Cuina; Yang, Houling; Qiao, Zhuangming; Ding, Shaowu; Ni, Shou-Qing. Survey of dissimilatory nitrate reduction to ammonium microbial community at national wetland of Shanghai, China[J]. *Chemosphere*, 2020, 250: 126195.
- [192] Zhao, Zhiyuan; Xu, Yuan; Yuan, Lin; Li, Wei; Zhu, Xiaojing; Zhang, Liquan. Emergency control of *Spartina alterniflora* re-invasion with a chemical method in Chongming Dongtan, China[J]. *Water Science and Engineering*, 2020, 13(1): 24-33.
- [193] Zhao, Zhiyuan; Yuan, Lin; Li, Wei; Tian, Bo; Zhang, Liquan. Re-invasion of *Spartina alterniflora* in restored saltmarshes: Seed arrival, retention, germination, and establishment[J]. *Journal of Environmental Management*, 2020, 266: 110631.
- [194] Zheng, Weiheng; Cai, Feng; Chen, Shenliang; Zhu, Jun; Qi, Hongshuai; Cao, Huimei; Zhao, Shaohua. Beach management strategy for small islands: case studies of China[J]. *Ocean & Coastal Management*, 2020, 184: 104908.
- [195] Zheng, Weiheng; Cai, Feng; Chen, Shenliang; Zhu, Jun; Qi, Hongshuai; Zhao, Shaohua; Liu, Jianhui. Ecological Suitability of Island Development Based on Ecosystem Services Value, Biocapacity and Ecological Footprint: A Case Study of Pingtan Island, Fujian, China[J]. *Sustainability*, 2020, 12(6): 2553.
- [196] Zheng, Yanling; Hou, Lijun; Chen, Feiyang; Zhou, Jie; Liu, Min; Yin, Guoyu; Gao, Juan; Han, Ping. Denitrifying anaerobic methane oxidation in intertidal marsh soils: Occurrence and environmental significance[J]. *Geoderma*, 2020, 357: 113943.
- [197] Zhong, Qiangqiang; Puigcorbe, Viena; Sanders, Christian; Du, Jinzhou. Analysis of ^{210}Po , ^{210}Bi , and ^{210}Pb in atmospheric and oceanic samples by simultaneously auto-plating ^{210}Po and ^{210}Bi onto a nickel disc[J]. *Journal of Environmental Radioactivity*, 2020, 220-221: 106301.
- [198] Zhou, Bianying; Wang, Jiaqing; Zhang, Haibo; Shi, Huahong; Fei, Yufan; Huang, Shunying; Tong, Yazhi;

- Wen, Dishu; Luo, Yongming; Barcelo, Damia. Microplastics in agricultural soils on the coastal plain of Hangzhou Bay, east China: Multiple sources other than plastic mulching film[J]. *Journal of Hazardous Materials*, 2020, 388: 121814.
- [199] Zhou, Xiaoyan; Dai, Zhijun; Mei, Xuefei. The multi-decadal morphodynamic changes of the mouth bar in a mixed fluvial-tidal estuarine channel[J]. *Marine Geology*, 2020, 429: 106311.
- [200] Zhou, Zeng; Chen, Luying; Tao, Jianfeng; Gong, Zheng; Guo, Leicheng; Mick van der Wegen; Ian, Townend; Zhang, Chuankuan. The role of salinity in fluvio-deltaic morphodynamics: A long-term modelling study[J]. *Earth Surface Processes and Landforms*, 2020, 45(3): 590-604.
- [201] Zhu, Jianrong; Cheng, Xinyue; Li, Linjiang; Wu, Hui; Gu, Jinghua; Lyu, Hanghang. Dynamic mechanism of an extremely severe saltwater intrusion in the Changjiang estuary in February 2014[J]. *Hydrology and Earth System Sciences*, 2020, 24: 5043-5056.
- [202] Zhu, Lei; He, Qing; Shen, Jian. Response of Stratification Processes to Tidal Current Alteration due to Channel Narrowing and Deepening[J]. *Journal of Geophysical Research- Oceans*, 2020, 125(2): 15223.
- [203] Zhu, Lei; Zhang, Heng; Guo, Leicheng; Huang, Weihao; Gong, Wenping. Estimation of riverine sediment fate and transport timescales in a wide estuary with multiple sources[J]. *Journal of Marine Systems*, 2020: 103488.
- [204] Zhu, Lixin; Zhao, Shiye; Bittar, Thais B.; Stubbins, Mon; Li, Daoji. Photochemical dissolution of buoyant microplastics to dissolved organic carbon: Rates and microbial impacts[J]. *Journal of Hazardous Materials*, 2020, 383: 121065.
- [205] Zhu, Xiaotong; Qiang, Liyuan; Shi, Huahong; Cheng, Jinping. Bioaccumulation of microplastics and its in vivo interactions with trace metals in edible oysters[J]. *Marine Pollution Bulletin*, 2020, 154: 111079.
- [206] Zhu, Zhuoyi; Oakes, Joanne; Eyre, Bradley; Hao, Youyou; Sia, Edwin Sien Aun; Jiang, Shan; Muller, Moritz; Zhang, Jing. The nonconservative distribution pattern of organic matter in the Rajang, a tropical river with peatland in its estuary[J]. *Biogeosciences*, 2020, 17: 2473-2485.
- [207] Zhuang, Minmin; Liu, Jinlin; Ding, Xiaowei; He, Jianzong; Zhao, Shuang; Wu, Lingjuan; Gao, Song; Zhao, Chunyan; Liu, Dongyan; Zhang, Jianheng; He, Peimin. Sargassum blooms in the East China Sea and Yellow Sea: Formation and management[J]. *Marine Pollution Bulletin*, 2020: 111845.

中文期刊发表论文列表

List of Chinese Peer Reviewed Publications

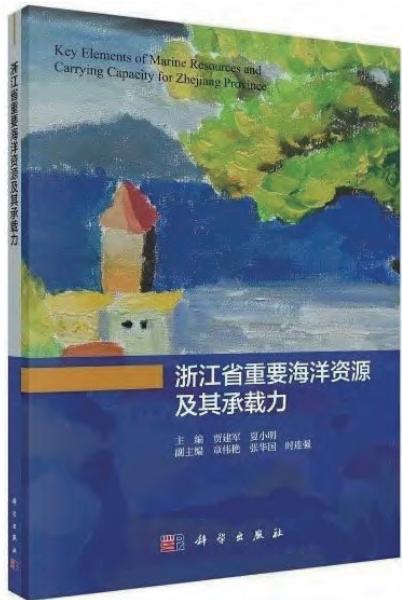
- [1] 陈锦, 谭凯, 张卫国. 基于地面三维激光扫描强度数据的潮滩表层含水量估算[J]. 地球信息科学学报, 2020, 22(2): 290-297.
- [2] 陈思明, 王宪业, 孙健伟, 何青. 粉砂淤泥质潮滩表层沉积物可侵蚀性研究[J]. 泥沙研究, 2020, 45(1): 45-51.
- [3] 顾靖华, 葛振鹏, 王杰. 河口海岸环境监测技术研究进展[J]. 华东师范大学学报(自然科学版), 2020, 1: 159-170.
- [4] 何钰滢, 戴志军, 楼亚颖, 王杰. 长江口扁担沙动力地貌变化过程研究[J]. 海洋学报, 2020, 42(5): 104-116.
- [5] 华凯, 程和琴, 颜阁, 滕立志. 近期长江口南支扁担沙洲演变特性[J]. 泥沙研究, 2020, 45(6): 33-39.
- [6] 贾建军. 海面变化: 驱动因素、现状与低地海岸风险[J]. 《科学》杂志, 2020, 72(4): 1-6.
- [7] 姜泽宇, 程和琴, 华凯, 石天, 唐明, 滕立志, 颜阁. 长江口横沙北侧岸坡冲刷特征与趋势分析[J]. 海洋通报, 2020, 39(2): 249-256.
- [8] 李道季. 海洋塑料污染及应对[J]. 世界环境, 2020, 171-73.
- [9] 李道季. 海洋微塑料研究焦点及存在的科学认知误区[J]. 科技导报, 2020, 38(14): 46-53.
- [10] 李道季. 消减海洋塑料垃圾保护海洋环境[J]. 民主与科学, 2020, 182 32-34.
- [11] 李玲, 杨平, 谭立山, 仝川. 闽江河口短叶茳芩湿地及围垦养虾塘的沉积物 CH_4 和 N_2O 产生潜力[J]. 生态学杂志, 2020, 39(2): 645-654.
- [12] 李亚, 陈海峰, 黄明毅, 杨立文, 姜立志, 王宪业. 新型聚氨酯碎石空心块体生态堤结构构建[J]. 水运工程, 2020, 575(11): 132-137.
- [13] 刘毛亚, 童春富, 吴逢润. 太浦河水体叶绿素a纵向演变特征及主要影响因子[J]. 生态学报, 2020, 40(19): 7084-7092.
- [14] 刘西汉, 王玉珏, 石雅君, 刘东艳, 王艳霞, 田海兰, 程林. 曹妃甸近海营养盐和叶绿素a的时空分布及其影响因素研究[J]. 海洋环境科学, 2020, 39(1): 89-98.
- [15] 刘晓彤, 李秀珍, 闫中正, 谢作轮, 林世伟. 海三棱藨草对极端高温的生长与生理响应[J]. 生态学杂志, 2020, 39(1): 110-119.
- [16] 鲁佩仪, 朱建荣, 钱伟伟, 袁琳. 崇明东滩鸟类栖息地优化工程区海堤水闸外侧引水渠冲淤数值模拟[J]. 华东师范大学学报(自然科学版), 2020, 3: 43-54.
- [17] 鲁佩仪, 朱建荣, 袁琳, 田波, 潘家琳. 崇明东滩保护区生态修复工程区的调水方案[J]. 华东师范大学学报(自然科学版), 2020, 1: 139-149.
- [18] 马茜, 王玉珏, 孙西艳, 刘东艳. 光和温度对两种绿潮藻光合途径及抗氧化功能的影响[J]. 海洋学报, 2020, 42(08): 21-29.

- [19] 毛铁墙, 董宏坡, 陈法锦, 侯庆华, 朱庆梅, 阳雯娜, 张家伟, 纪梓晗, 凌炜琪. 湛江湾沉积物中反硝化和厌氧氨氧化细菌的丰度、多样性及分布特征[J]. 海洋与湖沼, 2020, 51(1): 59-74.
- [20] 潘大东, 王张华. 东亚和南亚典型大河三角洲晚第四纪地层结构及成因对比[J]. 海洋地质与第四纪地质, 2020, 40(1): 12-21.
- [21] 彭子源, 蒋雪中, 侯立军, 何青. 1982和2012年枯季长江口最大浑浊带悬浮泥沙和盐度垂向剖面特征对比[J]. 海洋地质前沿, 2020, 36(1): 7-18.
- [22] 乔立新, 张国安, 何青, 张卫国, 李茂田. 长江分汊河口涨、落潮悬沙不对称特征及季节性差异[J]. 海洋学报, 2020, 42(3): 107-117.
- [23] 乔宇, 何青, 王宪业, 孟翊. 长江口表层沉积物含水量影响因素分析[J]. 泥沙研究, 2020, 45(1): 29-36.
- [24] 曲莹雪, 金杰, 徐文琦, 刘素美. 中国近岸海域优势藻种吸收利用磷的过程[J]. 中国环境科学, 2020, 40(3): 1257-1265.
- [25] 任剑波, 何青, 沈健, 徐凡, 郭磊城, 谢卫明, 朱磊. 远区台风“三巴”对长江口波浪动力场的作用机制[J]. 海洋科学进展, 2020, 44(5): 12-23.
- [26] 石天, 程和琴, 华凯, 滕立志, 唐明, 姜泽宇, 颜阁, 姜月华, 周权平. 工程影响下长江口涨潮槽演变特征研究 - 以北港六淤涨潮槽为例[J]. 海洋通报, 2020, 39(1): 134-142.
- [27] 唐川敏, 朱建荣. 长江河口水位上升对流场和盐水入侵的影响[J]. 华东师范大学学报(自然科学版), 2020, 3: 23-31.
- [28] 唐明, 程和琴, 陈钢, 李九发. 基于ADCP的长江口感潮河段床面稳定性分析[J]. 泥沙研究, 2020, 45(1): 37-44.
- [29] 唐玥, 童春富, 刘毛亚, 朱宜平, 陈蓓蓓. 上海金泽水库典型挺水植物碳、氮、磷化学计量特征的季节变化[J]. 生态学报, 2020, 40(13): 4528-4537.
- [30] 王日明, 戴志军, 黄鹤, 梁喜幸, 黎树式, 胡宝清, 周晓妍, 吴天亮. 北部湾大风江与南流江河口红树林空间分布格局研究[J]. 海洋学报, 2020, 42(12): 63-70.
- [31] 王珊珊, 刘东艳, 王玉珏, 袁子能. 渤海3个河口区底栖硅藻群落的时空变化特征[J]. 海洋学报, 2020, 42(08): 101-114.
- [32] 王晓峰, 刘东艳, 吴辉, 王玉珏. 2016年夏季长江口及其邻近海域表层沉积物中有机质的分布特征与来源分析[J]. 海洋湖沼通报, 2020, 165-74.
- [33] 王鑫, 吴莹, 曹梦莉, 齐丽君, 张经. 沉积记录中脂类生物标志物对琼东上升流强度的指示及其影响因素初探[J]. 海洋学报, 2020, 42(10): 28-36.
- [34] 王琰, 童春富, 汤琳, 吴阿娜, 吴逢润. 崇明东滩盐沼湿地大型底栖动物功能群分布特征及其影响因子[J]. 生态学杂志, 2020, 39(3): 880-890.
- [35] 吴秋原, 史本伟, 黄远光, 杨世伦. 1979-2018年长江口及邻近海域风速和波高的分布特征与变化趋势[J]. 海

- 洋通报, 2020, 39(4): 447-455.
- [36] 吴帅虎, 程和琴, 郑树伟, 唐倩玉. 近期长江口北槽河段河槽演变对人类活动的响应[J]. 长江流域资源与环境, 2020, 29(6): 1401-1412.
- [37] 徐博, 张衡, 张瑛瑛, 冯春雷. 《南印度洋渔业协定》管理措施的新进展及我国的应对策略[J]. 中国农业科技导报, 2020, 22(4): 10-23.
- [38] 薛成凤, 盛辉, 魏东运, 杨阳, 汪亚平, 贾建军. 沉积物干容重分析及其沉积学意义: 以东海内陆架为例[J]. 海洋与湖沼, 2020, 51(5): 1093-1107.
- [39] 杨立建, 马小川, 贾建军, 阎军, 梁振东. 近百年来黄河改道及输沙量变化对山东半岛泥质楔沉积物粒度特征的影响[J]. 海洋学报, 2020, 42(1): 78-89.
- [40] 杨照祥, 薛成凤, 杨阳, 周亮, 艾乔, 高建华, 贾建军. 百年尺度东海内陆架风暴事件重建: 器测记录与沉积记录耦合[J]. 海洋学报, 2020, 42(7): 119-129.
- [41] 张家伟, 董宏坡, 毛铁墙, 欧亚飞. 湛江湾表层水体海洋类群II 古菌的基因组分析[J]. 广东海洋大学学报, 2020, 40(6): 16-26.
- [42] 张靖婷, 王宪业, 李铨, 葛建忠. 基于DISTMESH的三角形网格自适应生成方法与应用[J]. 海洋科学进展, 2020, 38(3): 412-424.
- [43] 张赛赛, 杨世伦, 李鹏, 陈沈良, 李占海, 石学法. 长江口潮差中长期变化对河口生态环境的影响[J]. 海洋科学进展, 2020, 38(2): 317-325.
- [44] 赵成建, 童春富. 九段沙湿地大型底栖动物分布特征及其影响因子[J]. 海洋学报, 2020, 42(2): 65-74.
- [45] 周细平, 吴培芳, 李贞, 吴茜, 陈逸欣, 刘康格, 刘东艳, 王玉珏, 王跃启. 福建闽江口潮间带大型底栖动物次级生产力时空特征[J]. 海洋通报, 2020, 39(03): 342-350.
- [46] 周晓妍, 戴志军, 庞文鸿, 李为华. ASM-IV 仪器在河口近底层悬沙浓度观测分析中的应用研究[J]. 应用海洋学学报, 2020, 39(2): 221-228.
- [47] 朱建荣, 鲁佩仪, 唐川敏, 陈 晴, 吕行行. 长江河口北支建闸对减轻盐水入侵的数值模拟[J]. 华东师范大学学报(自然科学版), 2020, 3: 13-22.
- [48] 朱坤, 吴莹, 齐丽君. 上海城市内河中有机碳含量的时空变化及影响因素分析[J]. 华东师范大学学报(自然科学版), 2020, 1: 150-158.

专著 Books

- [1] 贾建军, 夏小明 (主编), 浙江省重要海洋资源及其承载力, 北京: 科学出版社, 2020.06; ISBN 978-7-03-062419-2.



专利与软著

Patents & Software Copyright

发明专利

Invention Patent

2020年度，实验室获批3项发明专利。

专利名称 Patent Name	发明人 Inventor	专利号 Patent Number
一种宽量程和动态最佳分辨率测量含沙量的测量装置及方法	李为华;戴志军	ZL 2017 1 1090653.3
一种高浊度水域水下护滩结构物下滩面冲淤厚度抽样测量方法	李为华;戴志军	ZL 2017 1 1180287.0
一种潮间带海三棱藨草自然群落生态恢复方法	袁琳;陈雅慧;田波;汤臣栋;马强; 曹浩冰;赵志远;王恒;张利权	ZL 2018 1 0864917.4



实用新型专利 National Utility Model Patent

2020年度，实验室获批5项实用新型专利。

专利名称 Patent Name	发明人 Inventor	专利号 Patent Number
快拆装式便携潮滩多参数观测架	顾靖华; 戴志军; 胡高建; 王杰; 庞文鸿; 马彬彬	ZL 2019 2 2401270.4
一种高度可调用于富集分离痕量元素的工作台	瞿建国; 汤震宇	ZL 2019 2 1443223.X
一种采集湿地原状土壤的便携式采样器	李亚雷; 谢丽娜; 葛振鸣	ZL 2019 2 0807876.5
一种用于测定湿地植物茎叶呼吸的采样装置	谢丽娜; 葛振鸣; 李亚雷	ZL 2019 2 0807994.6
一种高温分析仪炉体的隔热装置	崔莹; 韩香举; 张文祥; 张丹; 毕倩倩	ZL 2019 2 1081421.6



软件著作权 Software Copyright

2020年度，实验室获得4项计算机软件著作权授权登记。

软件名称 Software Name	著作权人 Copyright Owner	登记号 Register Number
非结构四边形网格有限差分河口海岸三维水动力模拟软件V1.0	华东师范大学	2020SR0855315
一人多机状态下仪器预约管理系统V1.0	华东师范大学	2020SR0961511
总有机碳分析仪数据批量处理软件V1.0	华东师范大学	2020SR0885891
综合实验室运营台账管理系统V1.0	华东师范大学	2020SR0888877

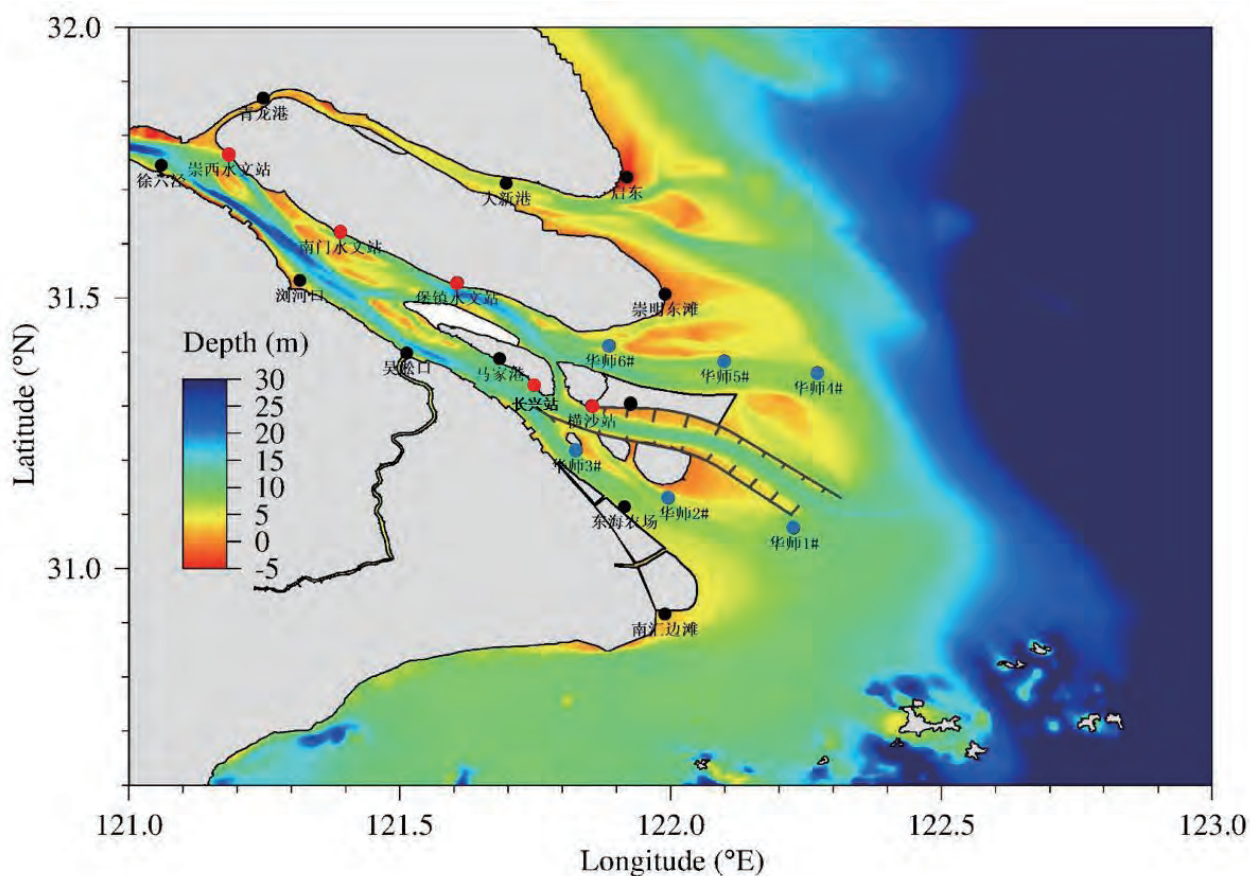


平台设施与野外观测 Facilities & Field Observations

平台与设施 Facilities

1. 水文观测站

实验室现有水文观测站包括崇西水文站、南门水文站、堡镇水文站、横沙站、长兴站和永隆沙水文站等6个水文站及南槽、北港6个浮标站。



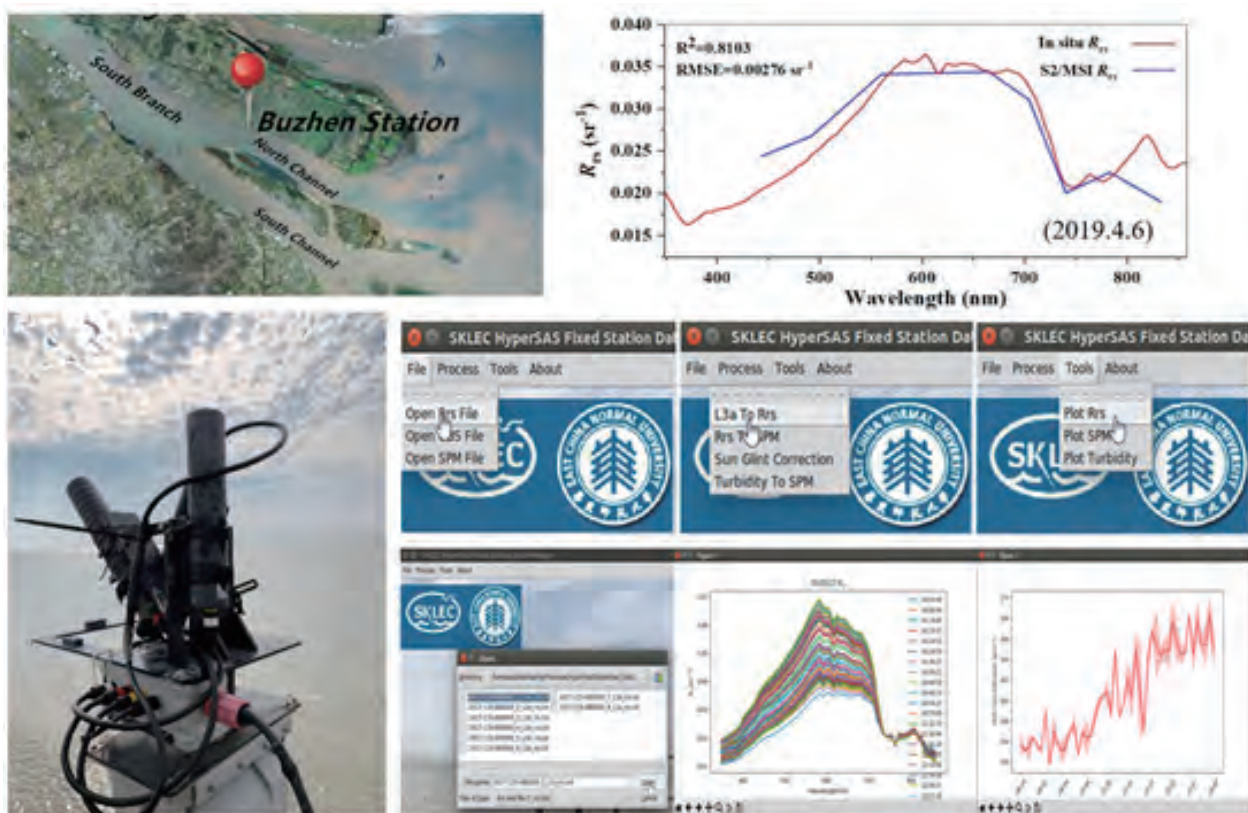
长江河口水文观测站分布图

2. 崇明遥感观测平台

我室在崇明堡镇水文站布设太阳跟踪式水面高光谱辐射自动观测及数据采集系统，采集系统由三个探测器组成的测量系统，自动跟踪装置以及计算机三部分组成。测量系统主要用于采集水体与天空光的辐射信息，自动跟踪装置用于水体光学信息采集时传感器探头与太阳相对方位的调整，计算机负责相关软件控制，数据远程传输以及处理分析。

该系统服务于卫星遥感数据、反演算法、反演产品的真实性检验。

开发的数据处理软件系统，主要功能：1. 高光谱数处理及遥感反射率计算；2. 反射率耀光校正；4. 浊度及悬浮泥沙浓度遥感反演。



3. 九段沙蓝碳监测系统

实验室在九段沙湿地国家级自然保护区建成两座自有产权含叶绿素荧光（SIF）、二氧化碳/水（CO₂/H₂O）及甲烷（CH₄）的一体化‘蓝碳’实时观测塔站。

LI-7500A开路式CO₂/H₂O涡度相关测量系统主要用于近地气层的瞬时三维风速脉动、温度脉动、H₂O脉动和CO₂脉动及CO₂通量、H₂O通量、显热通量、空气动力通量等地表与大气之间的物质与能量交换通量及磨擦风速等微气象特征量。

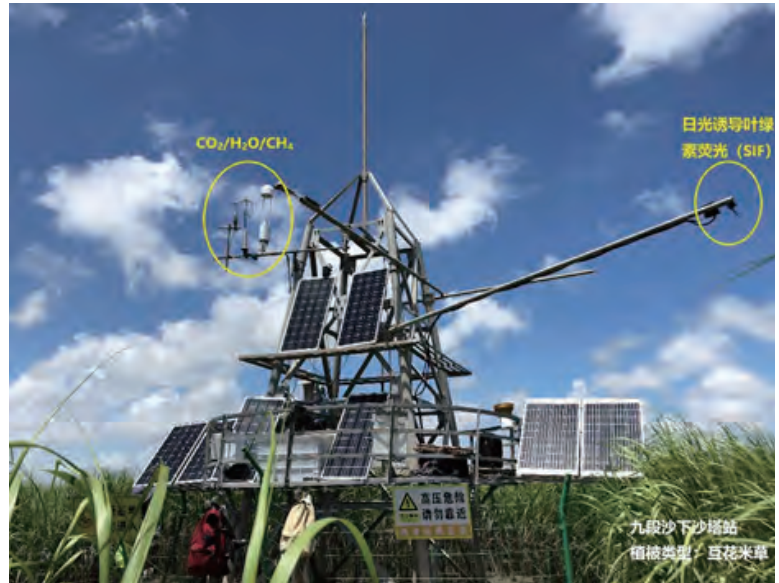
Biomet101能量平衡系统（生物气象辅助传感器系统）主要用于净辐射四分量、光合有效辐射、降雨量、空气温度、空气相对湿度、土壤温度、土壤湿度、土壤热通量。

LI-7700甲烷分析仪重量轻，功耗低，高频响应，用于获取描述生态系统CH₄通量所必需的CH₄密度数据，是美国LI-COR公司历时4年研发测试后推出的全球第一款开路式甲烷测定设备。

高性能微型光谱仪QE-PRO用于测定盐沼植被冠层日光诱导叶绿素荧光（SIF）。

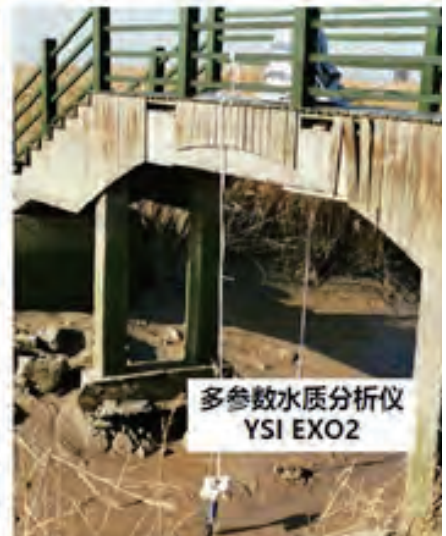


九段沙上沙野外全天候观测塔站，主要植被类型为芦苇



九段沙下沙野外全天候观测塔站，主要植被类型为互花米草

水平碳通量观测-溶解有机碳



用多参数水质分析仪YSI EXO2和自动采样器Teledyne ISCO-7300自动观测溶解有机碳水平输移

水平碳通量观测-溶解无机碳

自建pCO₂原位连续观测系统



自建pCO₂原位连续观测系统野外使用情况



用自建pCO₂原位连续观测系统观测溶解无机碳水平转移

4. 崇明东滩 Argus 视频观测系统

为了确保监测平台的稳定运行，本年度对于崇明东滩Argus海岸视频观测系统的软硬件设施进行了维护和更新，目前单景的分析数据精度可达到1920*1280分辨率。系统获取海岸带实时视频图片数据，通过计算机视觉算法自动拼接多景数据并获取水边线、波浪、地貌和植被等关键参数,实现海岸线变化、潮滩宽度和植被类型的定量监测，为地貌学、水动力学及生态学等学科提供高精度的基础数据，也为潮滩演化模型的构建提供数据支撑。



5. 河口海岸智能移动观测系统

河口海岸智能移动观测系统由实验室和珠海云洲智能科技有限公司共同开发。其主要以无人船为载体，集成多波束测深系统、声学多普勒流速剖面仪、三维激光扫描仪、车载海洋反射信号处理系统、磁力仪等多种观测设备。无人船可通过观测设备反馈的水深、位置、姿态参数信息，自主规划测量路径，实时修正路径偏差，无需人工干预，实现对重点观测区域的安全、高效测量。通过各观测设备的协同工作及数据融合，可实现河口海岸浅水、极浅水地区的水陆一体化地形、水动力、人工建构筑物形态的智能同步获取。该系统可为河口、海岸及河流临水区域的风险监测预警提供信息支撑。



河口海岸智能移动观测系统



河口海岸智能移动观测系统载荷

6. 滨海湿地生态物联网定位观测系统

在上海崇明东滩国家级自然保护区进行长期在线的综合定位监测，物联网系统实时自动采集湿地生态系统水-土-气-生等多种生态环境要素数据，通过大数据技术分析湿地环境变化及演变趋势。系统对滨海湿地的生态环境现状状态进行持续测定，为监测与评估湿地长期变化提供基础性科学数据。



7. 长江河口观测计数值成果展示系统

系统基于GIS地理空间数据库及WebGIS技术建立，通过连接浮标、水文站点等监控数据实现对河口水温，盐度，浊度，流速，水深等数据的实时监测及动态显示；通过接入及集成长江口潮汐潮流预报平台和长江口盐水入侵预报平台，对指定边界条件（径流、潮汐、风应力）及初始条件（盐度初始场）模型实现自动化预报及数据分析后处理，并动态展示预报成果。



主要新增科研设备（20万元以上）

Major New Instruments

设备名称 Equipment	型号 Type	管理人员 Manager
流式细胞摄像系统	FlowCAM8400	刘东艳
滩涂监测船	diamondback14'	袁琳
释光测年系统	TL/OSL DA-20	年小美
甲烷通量分析系统	LI-7700	黄颖
营养盐在线分析仪	Quattro	刘东艳
元素分析仪	FlashSmart NC soil	刘东艳
激光粒度仪	Lightmas plus	刘东艳
气相色谱仪	TRACE1300	刘东艳
开路式CO ₂ /H ₂ O浊度相关测量系统	LI-7500DS	黄颖
潮滩多光谱与地形无人机测量系统	精灵4多光谱版+经纬M300 RTK	李为华
荧光分光光度计	F-4700	张芬芬
多参数水质分析仪	EXO2	黄颖
冷冻干燥机	ALPHA 1-4/LD plus	刘东艳
声学多普勒流速剖面仪	HR Profiler	顾靖华
声学多普勒流速剖面仪	HR Profiler	顾靖华

野外调查 Field Observations

2019 年度长江口共享航次积极应对疫情、顺利完成三个航段调查任务

10月28日上午，执行长江口共享航次秋季航段任务的“润江1”号顺利返航，标志着2019年度长江口共享航次按计划圆满完成任务。本年度调查任务分为春季、夏季和秋季三个航段展开，共历时45天，圆满完成了多学科综合调查与研究任务。

本年度长江口科学考察实验研究主要围绕长江口及邻近海域的物质运输及其生态与环境效应这一主题，开展了水动力、物质运输、沉积特征、生态与环境等综合科学考察。汇集了来自全国14家高校、科研院所的34个共享航次搭载项目。

尽管受到疫情的影响，长江口航次冬季航段未能如期实施，但科考队积极应对，在得到管理部门的允许、支持下，及时调整航次航段和执行时间，增补秋季航段，在确保安全的前提下积极推进航次工作进度。

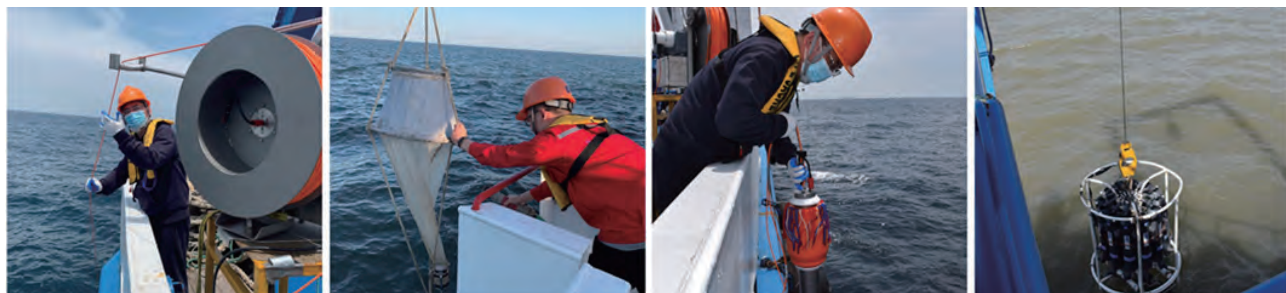
航次根据疫情防控的最新要求，编制了《航次疫情防控管理办法》，明确疫情防控措施、建立疫情处置应急预案，准备了充足的防疫防护用品。航段期间实施封闭式管理。所有科考队员经过严格的健康跟踪监测后，于航次出发日期前抵达出发码头集结。各航段首席科学家按照实施方案要求严格组织开展航前动员、疫情防控知识培训、海上作业安全教育和消防演习、救生应急演练等，以确保航次顺利执行。



春季航段调查人员合影



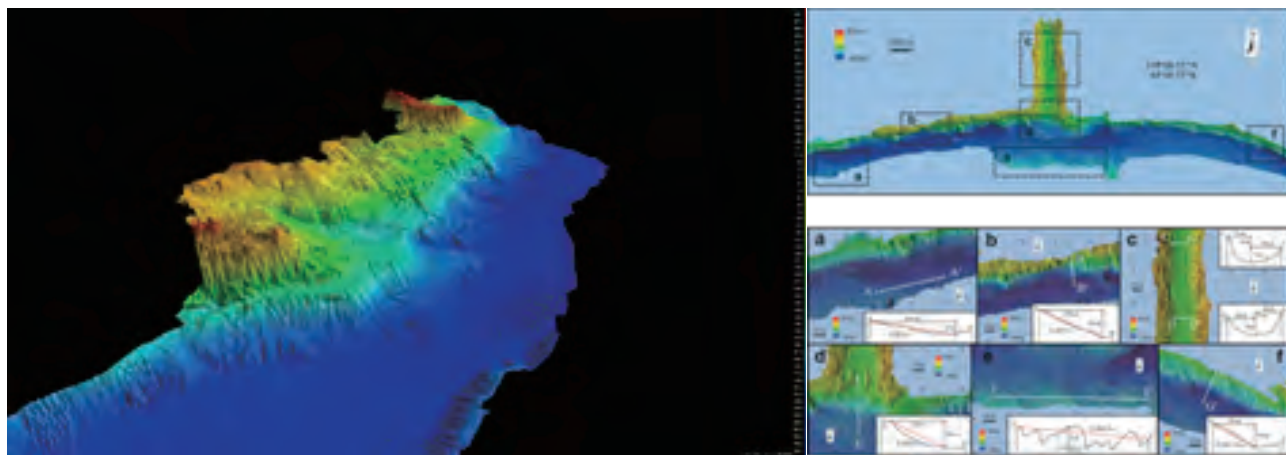
行前动员会



采样现场

程和琴教授团队开展长江中下游高陡边坡多模态水陆一体化岸坡稳定性智能测量与识别

2020年，华东师范大学河口海岸学国家重点实验室在中国地质调查局“重大水利工程对长江中下游地质环境影响研究”、中国国家自然科学基金委与荷兰科学研究组织及英国研究理事会共同资助项目“长江河口最大浑浊带的动力沉积过程对大型工程的自适应机理研究”等项目资助下，程和琴教授团队使用河口海岸智能移动观测系统，实现长江三峡库区和中下游干流河控与潮控河槽包括河口青草沙水库等高陡边坡水陆一体化地形、流速、浅层沉积结构同步智能观测数据880公里、并收集表层沉积物样品180个。而且，基于以上智能测量数据，开展了岸坡失稳风险和床面风险地貌的自动识别，并发现千年运河入干流河口岸坡失稳风险较大。



左：三峡库区滑坡水陆一体化地形

右：千年运河入干流河口水陆一体化地形

这些测量弥补了以往江、河、湖、海岸坡稳定性监测中陆域与水域、动力与沉积地貌数据获取与处理不同步、不配套、分析流程脱节的缺陷，形成了一个有机体系。实现江、河、湖、海临水岸坡失稳与崩岸、滑坡风险监测的技术装备水平和风险识别能力，为岸坡稳定监测与预警提供数据及技术支持。

9月，课题组博士研究生滕立志、唐明携河口海岸智能移动观测系统，赴广东珠海参与中央电视台《大国重器》纪录片拍摄。



《大国重器》拍摄现场照片（右二为本实验室河口海岸智能移动观测系统）

人才培养 Student Programs

2020年实验室在读研究生345人，其中博士研究生167人，硕士研究生178人。

学位授予 Degrees Offered

硕士学位：自然地理学；物理海洋学；海洋化学；海洋生物学；海洋地质；生态学；环境科学；港口、海岸及近海工程

博士学位：自然地理学；河口海岸学；物理海洋学；海洋化学；海洋生物学；海洋地质；生态学；环境科学

入学新生与毕业学生 The Freshmen and Graduates

2020年实验室共招收研究生89人，其中博士生35人，硕士生54人；招收的博士生中直博生4人、硕博连读16人。2020年共毕业52人，其中博士生17人，硕士生35人，彭谷雨、梅亚萍、张智伟、陈雅慧被评为2020年上海市优秀毕业生。



博士毕业生 List of Ph.D. Graduates

自然地理学 Physical Geography

姓名/Name	导师/Supervisor	毕业论文题目/Thesis	就业单位/Employment
赵小双	陈中原	尼罗河流域全新世气候演变与三角洲早期农业活动的响应	华东师范大学
姜 锋	陈中原	长江口下切古河谷全新世充填过程及其控制因素	华东师范大学

河口海岸学 Estuarine and Coastal Science

姓名/Name	导师/Supervisor	毕业论文题目/Thesis	就业单位/Employment
蒋 超	陈沈良	黄河口动力地貌过程及其对河流输入变化的响应	盐城师范学院
任剑波	何 青	台风驱动的长江口波浪动力场及其泥沙输运影响研究	杭州绍逸环境技术有限公司
朱礼鑫	李道季	溶解有机物在长江口和南大西洋湾中部河口及其邻近海域的不保守行为及絮凝、光降解影响研究	华东师范大学
Dearlyn Fernandes	吴 莹	氨基酸示踪中印热带河流沉积物和悬浮颗粒	回国
宋淑贞	李道季	近岸海域碳循环体系中碳水化合物浓度的调控因素及有机碱对CO ₂ 体系的影响	华东师范大学
陈 语	何 青	分汊河口横向环流及其格局转化研究	中交上海航道局有限公司
张 淼	吴 莹	利用光谱学及分子结构特性示踪南海-热带西太平洋水系有机质的输运与转化	深圳市福田区教育局
吕行行	朱建荣	长江口盐水入侵的预报精度提升及其对人类活动的响应	中交疏浚技术装备国家工程研究中心有限公司
强丽媛	程金平	新型污染物的水生生态毒理研究	石河子大学
钟强强	杜金洲	核素的大气沉降过程及其对上层海洋POC输出通量研究的启示	自然资源部第三海洋研究所
彭谷雨	李道季	沉积环境中的微塑料——河口区、海岸带及深海的比较研究	北京大学
王一鹤	吴 辉	长江口邻近海域浮游植物藻华锋面控制机理研究	华东师范大学
FOZIA	侯立军	印度河河口盐度梯度下沉积物脱氮过程与功能微生物菌群动态研究	回国

生态学 Ecology

姓名/Name	导师/Supervisor	毕业论文题目/Thesis	就业单位/Employment
赵丽侠	刘权兴	盐沼湿地空间自组织格局形成机理及其生态系统功能	上海栖星生态环境咨询有限公司

环境科学 Environmental Science

姓名/Name	导师/Supervisor	毕业论文题目/Thesis	就业单位/Employment
苏 磊	施华宏	微塑料在内陆至河口多环境介质中的污染特征及其迁移规律	华东师范大学

硕士毕业生 List of M. Sc. Graduates

自然地理学 Physical Geography

姓名/Name	导师/Supervisor	姓名/Name	导师/Supervisor
陈 锦	张卫国	黄 晶	王张华
梅亚萍	贾建军	牛淑杰	李茂田
同 萌	李茂田	杨照祥	贾建军
赵欣怡	田 波		

物理海洋学 Physical Oceanography

姓名/Name	导师/Supervisor	姓名/Name	导师/Supervisor
施沈阳	葛建忠	吴秋原	杨世伦
张智伟	吴 辉		

海洋化学 Marine Chemistry

姓名/Name	导师/Supervisor	姓名/Name	导师/Supervisor
邓彬彬	杜金洲	马文超	朱卓毅
王亚丽	张芬芬		

海洋地质 Marine Geology

姓名/Name	导师/Supervisor	姓名/Name	导师/Supervisor
陈 杰	陈 杰	成沁梓	张卫国

姜泽宇	程和琴	蒋亚梅	王张华
-----	-----	-----	-----

生态学 Ecology

姓名/Name	导师/Supervisor	姓名/Name	导师/Supervisor
陈雅慧	袁琳	胡梦瑶	葛振鸣
梁秋瑶	闫中正	孟蕾	李秀珍
潘家琳	袁琳		

环境科学 Environmental Science

姓名/Name	导师/Supervisor	姓名/Name	导师/Supervisor
梁桥	沈芳	唐玥	童春富
刘毛亚	童春富	宋张裕	李道季
王嘉颖	毛秀光		

港口、海岸及近海工程 Port, Coastal and Offshore Engineering

姓名/Name	导师/Supervisor	姓名/Name	导师/Supervisor
陈肖慧	张国安	何钰滢	戴志军
陆佳玉	丁平兴	石天	张二凤
徐圣	李占海	张靖婷	葛建忠

公派留学 Overseas Study Supported by China Scholarship Council

2020年，实验室共有13位同学获公派留学资格，赴美国、英国、德国、挪威、澳大利亚、荷兰等国家接受联合培养，其中3位同学为我室2018年申请获批的国家留学基金委“创新型人才国际合作培养项目”资助。

姓名 Name	国内导师 Supervisor	申报国别/地区 Country/Region	留学单位 Overseas institute	备注 Remarks
解丽娜	葛振鸣	挪威	挪威水资源研究所	创新型人才项目
李亚雷	葛振鸣	挪威	挪威水资源研究所	创新型人才项目
周相乾	葛建忠	挪威	挪威水资源研究所	创新型人才项目
张婷	周云轩	荷兰	荷兰皇家海洋研究所	
张齐琼	闫中正	澳大利亚	新南威尔士大学（悉尼校区）	
陈莹璐	张卫国	瑞典	乌普萨拉大学	
赵羚斌	高磊	美国	威斯康星大学密尔沃基校区	

盛 辉	汪亚平	英国	南安普顿大学
常 洋	汪亚平	德国	莱布尼茨波罗的海研究所
郭俊丽	陈沈良	英国	卡迪夫大学
王 黎	高 抒	美国	伊利诺伊大学香槟校区
刘桢娇	高 抒	美国	波士顿大学
张怡雪	吴 莹	德国	亥姆霍兹慕尼黑研究中心德国环境卫生研究中心

海外研修 Overseas Visiting

2020年，实验室有1位同学接受校级资助赴爱沙尼亚进行交流访学。

姓名 Name	国内导师 Supervisor	访学单位 Visiting institute	起止时间 Date
杨 斌	李秀珍	爱沙尼亚塔尔图大学	2020.02-2020.08

研究生科研成果 Research Outputs Contributed by Graduate Students

2020年研究生发表第一作者论文107篇，占实验室第一作者论文总数的66%，其中SCI/SCIE论文73篇（I区文章14篇，II区文章37篇），占实验室第一作者SCI/SCIE论文的59%。实验室学生中有3人次参加国际学术会议并做口头报告。

公众服务 Outreaches

为积极响应科技部、中宣部、卫健委和中国科协关于举办“科技战疫 创新强国”2020年全国科技活动周的号召，8月28日，河口海岸学国家重点实验室结合自身发展特色，立足科技强国，举办科技活动周云上科普讲座。讲座围绕“海岸生态系统与经济社会发展的关系”主题，从“海岸带经济承载力对于不同的海岸单元有明显的差异”、“海岸带经济承载力受到海湾生态承载力的制约”、“生态系统具有资源禀赋，可用以促进海湾经济的发展”和“全球变暖和人为干预下的海岸生态系统变化是一个重要科学问题，需要构建新理论新方法”四个论点展开探讨，吸引了来自全国各地的专家学者、科研新星及感兴趣的公众160余人参加。

为促进优秀大学生之间的思想交流，扩大河口海岸学国家重点实验室在国内相关院校中的影响力，提高实验室研究生生源质量，由我校研究生院主办、河口海岸学国家重点实验室承办的“2020年河口海岸学优秀大学生夏令营”于7月14日至16日在线上举行。此次夏令营设置院/室介绍、学术报告、实验室参观、师生在线交流、野外调查直播等环节，吸引了来自全国40余所知名院校的138名优秀大学生前来参加。

9-12月，为上海中学国际部学生开设科普课程《陆海相互作用（Land Ocean Interaction）》，12位教授、副教授参与授课，向国际中学生推广、普及陆海相互作用相关知识。

为了贯彻落实中央、上海市乡村振兴战略工作部署，积极参加上海市开展“结对百镇千村，助推乡村振兴”

行动，以教工党支部为引领，结对帮扶上海市崇明区长兴镇创建村，开展“生态科普 助建上海美丽乡村”活动。主要工作包括入村走访，开展科普讲座，提供专业知识和科普指导；利用微信平台推送“接地气”的村民生态科普知识，让老百姓理解村容村貌改造建设的重要意义，促进村民自觉自愿维护生态环境整洁与建设。

立足崇明西沙国家湿地公园，以崇明西沙湿地公园科普画廊建设为契机，开展河口海岸系列展板建设。累计制作展板总数超过200块。建成之后，将成为河口海岸科普教育基地的外部宣教设施。目前崇明西沙国家湿地公园年接待游客超过80万人次。

海洋科学（含港口、海岸及近海工程）学位评定分委员会

主任：高抒

副主任：何青、杜金洲

委员：高磊、贾建军、李道季、刘东艳、汪亚平、吴辉

研究队伍 Research Staff

2020年，重点实验室引进研究人员4人，现有固定人员113人（其中研究人员103人，技术人员7人，管理人员3人）。

固定人员 Faculty and Staff

教授

Professors

姓名 Title	研究专长 Research Interest	Email
Dr. BELLERBY R.	海洋生物地球化学循环 Marine Biogeochemical Cycles	Richard.Bellerby@niva.no richard@sklec.ecnu.edu.cn
陈 静 Dr. CHEN Jing	第四纪地质学 Quaternary Geology	jchen@geo.ecnu.edu.cn
陈启晴 Dr. CHEN Qiqing	微塑料的复合污染与生态效应研究；颗粒污染物对水生生物的生物富集和致毒机理研究 Compound Pollution and Ecological Effect of Microplastics; Biological Enrichment and Toxic Mechanism of Particulate Pollutants on Aquatic Organisms	chenqiqing@sklec.ecnu.edu.cn
陈庆强 Dr. CHEN Qingqiang	海洋沉积学；环境与生物地球化学 Marine Sedimentology; Environmental Geochemistry & Biogeochemistry	qqchen@sklec.ecnu.edu.cn
陈沈良 Dr. CHEN Shenliang	海岸动力地貌；三角洲侵蚀与脆弱性 Coastal Morphodynamics; Delta Erosion and Vulnerability	slchen@sklec.ecnu.edu.cn
陈中原 Dr. CHEN Zhongyuan	河流-三角洲沉积地貌过程；水文地貌过程；环境考古 River-Delta Sedimentological and Geomorphological Processes; Geoarchaeology	z.chen@sklec.ecnu.edu.cn
程和琴 Dr. CHENG Heqin	河口海岸动力沉积学；工程地貌与环境；海岸带管理 Estuarine and Coastal Dynamic Sedimentation; Engineered Morphodynamics and Environment; Integrated Coastal Management	hqch@sklec.ecnu.edu.cn
戴志军 Dr. DAI Zhijun	河口海岸动力地貌 Estuarine and Coastal Morphodynamics	zjdai@sklec.ecnu.edu.cn
丁平兴 Dr. DING Pingxing	潮流动力学及数值模型；波-流与泥沙输运 Coastal Dynamics and Numerical Modeling; Sediment Transport by Waves and Currents;	pxding@sklec.ecnu.edu.cn

姓名 Title	研究专长 Research Interest	Email
董宏坡 Dr. DONG Hongpo	海洋微生物分子生态; 海洋微生物适应环境的分子基础; 海洋微生物参与元素循环的过程和机理 Molecular Ecology of Marine Microorganisms; Molecular Foundation of Marine Microorganisms for Environmental Adaptation; Processes and Mechanisms of Marine Microorganisms Involved in Biogeochemical Cycles	hpdong@sklec.ecnu.edu.cn
杜金洲 Dr. DU Jinzhou	同位素海洋学; 环境放射化学 Oceanography of Isotopes; Environmental Radiochemistry	jzdu@sklec.ecnu.edu.cn
冯志轩 Dr. FENG Zhixuan	海洋生态系统动力学; 极地海洋学; 河口海岸带环境与动力过程 Marine Ecosystem Dynamics; Polar Oceanography; Estuarine-coastal Environments and Dynamics	zxfeng@sklec.ecnu.edu.cn
高磊 Dr. GAO Lei	河口海岸地区营养盐的生物地球化学过程 Nutrient Biogeochemistry in Estuarine and Coastal Areas	lgao@sklec.ecnu.edu.cn
高抒 Dr. GAO Shu	海洋沉积动力学 Marine Sediment Dynamics	sgao@sklec.ecnu.edu.cn shugao@nju.edu.cn
葛振鸣 Dr. GE Zhenming	气候变化与生态系统碳过程; 生态模型; 湿地生态学 Climate Change & Ecosystem Carbon-process; Ecological Model; Wetland Ecology	zmge@sklec.ecnu.edu.cn
韩平 Dr. HAN Ping	氮素生物地球化学循环的微生物过程 Microbial Processes of the Biogeochemical Nitrogen Cycle	phan@geo.ecnu.edu.cn
何青 Dr. HE Qing	河口海岸水动力学; 河口海岸泥沙运动学 Estuarine and Coastal Hydrodynamics; Estuarine and Coastal Sediment Transport	qinghe@sklec.ecnu.edu.cn
侯立军 Dr. HOU Lijun	环境地理学; 环境地球化学 Environmental Geography; Environmental Geochemistry	ljhou@sklec.ecnu.edu.cn
贾建军 Dr. JIA Jianjun	河口海岸沉积动力过程、记录与地貌效应; 海洋空间资源管理的支撑技术 Estuarine and Coastal Sediment Dynamics and Morphology; Techniques Supporting Marine Spatial Resources Management;	jjia@sklec.ecnu.edu.cn
姜晓东 Dr. JIANG Xiaodong	浮游动物适应与进化 Adaptation and Evolution of Zooplankton	xdjiang@bio.ecnu.edu.cn
姜雪峰 Dr. JIANG Xuefeng	硫循环化学 Sulfur Circulation Chemistry	xfjiang@chem.ecnu.edu.cn
李超 Dr. LI Chao	发育生物学 Developmental Biology	cli1@biochem.umass.edu
李道季 Dr. LI Daoji	生物海洋学; 河口和近岸海域生态系统 Biological Oceanography; Estuarine and Coastal Ecosystem	daojili@sklec.ecnu.edu.cn

姓名 Title	研究专长 Research Interest	Email
李秀珍 Dr. LI Xiuzhen	景观生态学; 湿地生态学; 遥感与地理信息系统应用 Landscape Ecology; Wetland Ecology; Application of Remote Sensing and GIS	xzli@sklec.ecnu.edu.cn
刘东艳 Dr. LIU Dongyan	海洋藻类生态学 Marine Algae Ecology	dylu@sklec.ecnu.edu.cn
刘权兴 Dr. LIU Quanxing	系统生态学 Systems Ecology	qxliu@sklec.ecnu.edu.cn
刘世昊 Dr. LIU Shihao	海洋地球物理; 海洋沉积; 高分辨率层序地层学 Marine Geophysics; Marine Sedimentology; High-resolution Sequence Stratigraphy	shliu@sklec.ecnu.edu.cn
彭 忠 Dr. PENG Zhong	波浪动力学; 河口海岸工程应用研究; 基于生态系统的海岸防护 Wave Dynamics; Applied Coastal Research and Engineering; Ecosystem-based Coastal Defence	zpeng@sklec.ecnu.edu.cn
沈 芳 Dr. SHEN Fang	河口近岸水色遥感; 遥感技术与GIS综合应用 Coast / Ocean Colour Remote Sensing; Integrated Applications of GIS and Remote Sensing Technology	fshen@sklec.ecnu.edu.cn
史贵涛 Dr. SHI Guitao	极地雪冰现代过程; 冰芯气候记录; 极地气候环境变化 The Geochemical Processes of Chemicals in Snow and Ice; Ice Core Records; Climate Changes in Polar Regions	gtshi@geo.ecnu.edu.cn
施华宏 Dr. SHI Huahong	生态毒理学; 生物监测; 环境与健康 Ecotoxicology; Biomonitoring; Environment and Health	hhshi@des.ecnu.edu.cn
孙千里 Dr. SUN Qianli	全新世环境与人类活动适应; 全新世海岸带环境演变与早期人类活动; 湖泊沉积学与全球变化 Holocene Environment Changes and Human Adaptation; Coastal Environment Evolution and Early Human Activity; Lake Sedimentology and Global change	qlsun@sklec.ecnu.edu.cn
唐剑武 Dr. TANG Jianwu	湿地生态学; 碳循环、全球变化生态学 Wetland Ecology; Carbon Cycling, Global Change Ecology	jwutang@sklec.ecnu.edu.cn
王锦龙 Dr. WANG Jinlong	同位素海洋学 Isotope Oceanography	jlwang@sklec.ecnu.edu.cn
王 群 Dr. WANG Qun	水生生物学 Aquatic Biology	qwang@bio.ecnu.edu.cn
汪亚平 Dr. WANG Yaping	海洋沉积动力过程与数值模拟; 河口海岸物质循环与输运 Ocean Sediments Dynamic Process and Numerical Simulation; Substances Transports and Circulation in Estuarine and Coastal Areas	ypwang@sklec.ecnu.edu.cn
王张华 Dr. WANG Zhanghua	河口-三角洲沉积地貌环境演变 Sedimentary and Morphological Evolution of Estuary and Delta	zhwang@geo.ecnu.edu.cn

姓名 Title	研究专长 Research Interest	Email
吴 辉 Dr. WU Hui	河口海岸动力过程及其三维数值模拟; 盐水入侵 Estuarine Dynamics and 3D Numerical Simulation; Saltwater Intrusion	hwu@sklec.ecnu.edu.cn
吴 莹 Dr. WU Ying	海洋有机地球化学; 海洋生物地球化学 Marine Organic Geochemistry; Marine Biogeochemistry	wuying@sklec.ecnu.edu.cn
Dr. WÜNNEMANN B.	气候与环境变化的湖泊地层记录 Lake Sedimentary Records for the Environmental and Climate Change	wuene@zedat.fu-berlin.de
夏建阳 Dr. XIA Jianyang	全球变化生态学 Global Change Ecology	jyxia@des.ecnu.edu.cn
杨嘉龙 Dr. YANG Jialong	海洋生物学 Marine Biology	jlyang@bio.ecnu.edu.cn
杨世伦 Dr. YANG Shilun	海岸湿地沉积动力过程; 河口对流域变化的响应 Sediment Dynamic Processes in Coastal Wetlands; Estuarine Response to Impacts from River Basin	slyang@sklec.ecnu.edu.cn
杨 毅 Dr. YANG Yi	新型有机污染物研究 Emerging Organic Pollutants	yyang@geo.ecnu.edu.cn
赵云龙 Dr. ZHAO Yunlong	水生生物学 Aquatic Biology	ylzhao@bio.ecnu.edu.cn
郑艳玲 Dr. ZHENG Yanling	河口近岸氮生物地球化学循环及其生态环境效应 Biogeochemical Cycle of Nitrogen in Estuarine and Coastal Ecosystems	ylzheng@geo.ecnu.edu.cn
张 经 (院士) Dr. ZHANG Jing Academician of CAS	生物地球化学与化学海洋学 Biogeochemistry and Chemical Oceanography	jzhang@sklec.ecnu.edu.cn
张卫国 Dr. ZHANG Weiguo	环境磁学; 环境演变; 环境污染 Environmental Magnetism; Environmental Change; Environmental Pollution	wgzhang@sklec.ecnu.edu.cn
赵 宁 Dr. ZHAO Ning	大陆边缘 (沉积物、珊瑚礁) 高分辨率气候与环境记录; 海洋沉积年代学; 海洋同位素地球化学; 古海洋环流与碳循环 High-resolution Records of Climate and Environment from Continental Margins (Marine Sediments, Coral Reefs); Chronology of Marine Sediments; Marine Isotope Geochemistry; Paleo Ocean Circulation and Carbon Cycle	nzhao@sklec.ecnu.edu.cn
周旭辉 Dr. ZHOU Xuhui	生态系统生态学 Ecosystem Ecology	xhzhou@des.ecnu.edu.cn
周云轩 Dr. ZHOU Yunxuan	海岸带资源与环境遥感; 土地利用与覆盖变化; 地理信息系统应用 Coastal Zone Remote Sensing; LUCC; Application of GIS	zhouyx@sklec.ecnu.edu.cn
朱建荣 Dr. ZHU Jianrong	河口海岸海洋动力学; 河口海岸海洋数值模式 Estuarine, Coastal and Ocean Dynamics; Estuarine, Coastal and Ocean Model;	jrzhu@sklec.ecnu.edu.cn

副教授

Associate Professor

姓名 Title	研究专长 Research Interest	Email
曹 芳 Dr. CAO Fang	海洋水色遥感 Ocean Color Remote Sensing	fcao@sklec.ecnu.edu.cn
陈雪初 Dr. CHEN Xuechu	湿地生态学 Wetland Ecology	xcchen@des.ecnu.edu.cn
邓 兵 Dr. DENG Bing	沉积地球化学; 沉积学; 古环境 Sedimentary Geochemistry; Sedimentology; Paleoenvironment	dengbing@sklec.ecnu.edu.cn
葛建忠 Dr. GE Jianzhong	水动力及泥沙运动数值模拟; 可视化系统及高性能计算 Numerical Modeling of Hydrodynamics and Sediment Transport; Visualization System and High-Performance Computing	jzge@sklec.ecnu.edu.cn
郭磊城 Dr. GUO Leicheng	河口海岸动力地貌及模拟 Morphodynamic Modelling in Estuarine and Coastal Areas	lguo@sklec.ecnu.edu.cn
黄 颖 Dr. HUANG Yin	滨海湿地生态遥感; 滨海湿地碳循环 Remote Sensing in Coastal Wetland Ecology; Carbon Cycle in Coastal Wetlands	yhuang@sklec.ecnu.edu.cn
何利军 Dr. HE Lijun	谱系生物地理学; 种群遗传学 Phylogeography; Population Genetics	ljhe@sklec.ecnu.edu.cn
蒋雪中 Dr. JIANG Xuezhong	流域--海岸带管理; 地表过程与变化; GIS&RS应用 Watershed and Coastal Zone Management; Land Surface Processes and Change; Application of GIS & RS	xzjiang@sklec.ecnu.edu.cn
李占海 Dr. LI Zhanhai	河口海岸沉积动力学 Coastal and Estuarine Sediment Dynamics	zhli@sklec.ecnu.edu.cn
梁 霞 Dr. LIANG Xia	河口碳氮生物地球化学循环; 污染土壤及水体生态修复 技术; 受损滩涂湿地植被恢复理论与技术 Biogeochemical Cycle of Carbon and Nitrogen in Estuaries, Reservoirs and Lakes; Ecological Remediation of Contaminated Soils and Waters; Ecological Restoration of Vegetation in Coastal Wetlands	xliang@sklec.ecnu.edu.cn
刘 演 Dr. LIU Yan	全新世气候与环境演变; 环境考古 Holocene Climatic and Environmental Changes; Geo- archaeology	liuyan@sklec.ecnu.edu.cn
梅雪菲 Dr. MEI Xuefei	流域-河口水文地貌过程; 河口海岸动力、沉积、地貌 River-Estuary Hydrological and Geomorphological Process; Estuarine and Coastal Dynamics, Sedimentation, Landform	xfmei@geo.ecnu.edu.cn
年小美 Dr. NIAN Xiaomei	第四纪地质年代学 Quaternary Geochronology	xmnian@sklec.ecnu.edu.cn



姓名 Title	研究专长 Research Interest	Email
史本伟 Dr. SHI Benwei	短周期潮滩沉积动力过程与机制; 生物作用影响下潮滩生物地貌学 Short Period Tidal Flat Sedimentary Dynamic Process and Mechanism; Tidal Beach Biogeomorphology under the Influence of Biological Processes	bwshi@sklec.ecnu.edu.cn
谭 凯 Dr. TAN Kai	河口海岸测绘遥感理论方法及应用; 潮滩地形与生态遥感监测; 激光雷达遥感点云数据处理方法和应用 Methods and Applications of Estuarine and Coastal Surveying and Mapping and Remote sensing Technologies; Remote Sensing Monitoring of Tidal Flat Topography and Ecology; LiDAR Remote Sensing Point Cloud Data Processing Methods and Applications	ktan@sklec.ecnu.edu.cn
田 波 Dr. TIAN Bo	海岸带遥感; 地理信息系统开发与应用 Coastal Zone Assessment and Remote Sensing; GIS Development and Application	btian@sklec.ecnu.edu.cn
童春富 Dr. TONG Chunfu	湿地生态学与系统生态学 Wetland Ecology and Systems Ecology	cftong@sklec.ecnu.edu.cn
王宪业 Dr. WANG Xianye	泥沙运动; 河流动力学 Sediment Transport; River Dynamics	xywang@sklec.ecnu.edu.cn
王玉珏 Dr. WANG Yujue	近海营养环境和生态; 营养盐和有机质同位素示踪 Coastal Ecological Environment; Nutrient and Organic Matter Tracing Using Stable Isotope	yjwang@sklec.ecnu.cn
许 媛 Dr. XU Yuan	河口湿地底栖原生动物生态学; 原生动物分类学及分子系统学 Wetland Protozoan Ecology; Protozoan Taxonomy and Phylogeny	yxu@sklec.ecnu.edu.cn
闫中正 Dr. YAN Zhongzheng	植物生理生态; 海洋水色遥感 Plant Ecophysiology; Ocean Color Remote Sensing	zzyan@sklec.ecnu.edu.cn
袁 琳 Dr. YUAN Lin	湿地生态; 资源环境遥感 Wetland Ecology; Remote Sensing Monitoring of Nature Resource	lyuan@sklec.ecnu.edu.cn
张 凡 Dr. ZHANG Fan	陆架河口动力过程对风暴的响应; 河口地区物理过程及生态过程的数值模拟 Response of Coastal Ocean to Tropical Cyclones; Numerical Modeling of Hydrodynamical and Biogeochemical Processes in The Estuary	Fzhang@sklec.ecnu.edu.cn
张芬芬 Dr. ZHANG Fengfeng	新技术(核磁共振、Raman光谱等)应用于海洋学的研究 Application of New Techniques (NMR and Raman spectroscopy) in Marine Science	ffzhang@sklec.ecnu.edu.cn
张文霞 Dr. ZHANG Wenxia	近岸动力过程及其生态效应; 数值模拟 Coastal Dynamics and Its Ecological Responses; Numerical Modeling	Wenxia.zhang@sklec.ecnu.edu.cn
朱卓毅 Dr. ZHU Zhuoyi	有机地球化学; 生物地球化学 Organic Geochemistry; Biogeochemistry	zyzhu@sklec.ecnu.edu.cn

管理人员

Administrative Staff

俞世恩 实验室党委书记 Dr. YU Shi'en, Communist Party secretary	江 红 实验室副主任 Dr. JING Hong, Deputy Director	张晓笛 主任助理 Ms. ZHANG Xiaodi, Director Assistant
吴 辉 实验室副主任 (兼) Dr. WU Hui, Deputy Director (part time)	张卫国 实验室副主任 (兼) Dr. ZHANG Weiguo, Deputy Director(part time)	高 磊 主任助理 (兼) Dr. GAO Lei, Director Assistant (part time)

技术人员

Technical Staff

姓名 Title	技术领域 Position	姓名 Title	技术领域 Position
瞿建国 副教授 Mr. QU Jianguo, Associate Professor	无机分析 Inorganic Elements Analysis	李为华 高级工程师 Dr. LI Weihua, Senior Engineer	野外仪器设备管理 Field Surveying Instrument
张文祥 高级工程师 Mr. ZHANG Wenxiang, Senior Engineer	野外仪器设备管理 Field Surveying Instrument	崔 莹 工程师 Dr. CUI Ying, Engineer	有机及无机分析 Organic and Inorganic Elements Analysis
顾靖华 工程师 Mr. GU Jinghua, Engineer	野外仪器设备管理 Field Surveying Instrument	张国森 工程师 Mr. ZHANG Guosen, Engineer	有机及无机分析 Organic and Inorganic Elements Analysis
张 婧 工程师 Ms. ZHANG Jing, Engineer	有机分析 Organic Elements Analysis		

博士后

Postdoctoral Fellows

姓名 Name	研究专长 Research Interest	Email
常 燕 Dr. CHANG Yan	化学海洋学和同位素地球化学 Marine Chemistry and Isotopic Geochemistry	ychang@sklec.ecnu.edu.cn
高灯州 Dr. GAO Dengzhou	河口氮循环和环境效应 Estuarine Nitrogen Cycle and Environmental Effect	dzgao@sklec.ecnu.edu.cn
胡 浩 Dr. HU Hao	河口及河流地貌动力过程 Estuarine and Fluvial Morphodynamics	hhu@sklec.ecnu.edu.cn
Dr. JABEEN K.	海洋微塑料污染 Marine Microplastic Pollution	khalidajabeen@sklec.ecnu.edu.cn
贾永颢 Dr. JIA Yonghao	海洋有机地球化学 Marine Organic Geochemistry	yhjia@sklec.ecnu.edu.cn
江 山 Dr. JIANG Shan	海洋生物地球化学 Marine Biogeochemistry	sjiang@sklec.ecnu.edu.cn

姓名 Name	研究专长 Research Interest	Email
刘建安 Dr. LIU Jian'an	放射性同位素海洋学 Radioisotopic Oceanography	jaliu@sklec.ecnu.edu.cn
梅衍俊 Dr. MEI Yanjun	海洋地质学 Marine Geology	yjmei@sklec.ecnu.edu.cn
牛玉慧 Dr. NIU Yuhui	土壤碳氮循环 Soil Carbon and Nitrogen Transformations	yhniu@sklec.ecnu.edu.cn
Dr. SENGUPTA D.	地理数据科学与海洋空间规划 Geodata Science and Marine Spatial Planning	dhritiraj@sklec.ecnu.edu.cn
尚 媛 Dr. SHANG Yuan	自然地理学 Physical Geography	yshang@sklec.ecnu.edu.cn
宋淑贞 Dr. SONG Shuzhen	无机碳化学 Inorganic Carbon Chemistry	szsong@sklec.ecnu.edu.cn
苏 磊 Dr. SU Lei	微塑料生态毒理学 Ecotoxicology of Microplastic	lsu@sklec.ecnu.edu.cn
王晓娜 Dr. WANG Xiaona	海洋有机地球化学 Marine Organic Geochemistry	xnwang@sklec.ecnu.edu.cn
王一鹤 Dr. WANG Yihe	河口生态动力学 Estuarine Ecological Dynamics	yhwang@sklec.ecnu.edu.cn
魏 稳 Dr. WEI Wen	河口动力沉积与动力地貌 Dynamic Sedimentation and Geomorphology of Estuary	wwei@sklec.ecnu.edu.cn
吴莹莹 Dr. WU Yingying	海洋微体古生物学 Marine Micropaleontology	yywu@sklec.ecnu.edu.cn
谢卫明 Dr. XIE Weiming	海岸动力地貌过程 Coastal Morphodynamics	wmxie@sklec.ecnu.edu.cn
邢 飞 Dr. XING Fei	海岸地貌动力学 Estuarine and Coastal Morphodynamics	fxing@sklec.ecnu.edu.cn
徐 凡 Dr. XU Fan	自然地理学 Physical Geography	fxu@sklec.ecnu.edu.cn
徐佳奕 Dr. XU Jiayi	海洋生物 Marine Biology	jyxu@sklec.ecnu.edu.cn
晏达达 Dr. YAN Dada	介形虫、沉积动力、气候环境重建 Ostracod, Sediment Dynamics and Process, Climate and Environmental Reconstruction	ddyan@sklec.ecnu.edu.cn
杨 阳 Dr. YANG Yang	海洋沉积动力学 Marine Sediment Dynamics	yyang@sklec.ecnu.edu.cn
赵小双 Dr. ZHAO Xiaoshuang	三角洲地貌演化与人类活动 Delta Evolution and Human Activity	xszhao@sklec.ecnu.edu.cn
周 鹏 Dr. ZHOU Peng	自然地理学 Physical Geography	pzhou@sklec.ecnu.edu.cn

客座人员 Adjuncts

Dr. BOJORCK S., Professor svante.bjorckgeol.lu.se	Dr. BOYLE E. A, Professor eaboyle@mit.edu	Dr. ITTEKOT V., Professor ittekot@uni-bremen.de
Dr. MOORE W. S, Professor moore@geol.sc.edu	Dr. MATSUMOTO E., Professor e2.matsumoto@nifty.com	Dr. KOCH B., Professor Boris.Koch@awi.de
Dr. SHEN Jian, Professor shen@viDr.edu	Dr. SU B. (Z), Professor b_su@itc.nl	Dr. HERTKORN N., Professor hertkorn@gsf.de
Dr. MITSCH W., Professor mitsch.1@osu.edu	Dr. VERHOEF W., Professor verhoef@nlr.nl	Dr. FINLAYSON B., Professor brianlf@unimelb.edu.au
Dr. CHEN Changsheng, Professor c1chen@umassd.edu	Dr. VRIEND H. J. de, Professor H.J.deVriend@sDr.utwente.nl	Dr. WEBBER M., Professor mjwebber@unimelb.edu.au
Dr. PEUCKER-EHRENBRINK B., Professor bpeucker@whoi.edu	Dr. STIVE M.J.F., Professor stive51@xs4all.nl	Dr. MANDER U., Professor ulo.mander@ut.ee
Dr. OLDFIELD F., Professor oldfield.f@gmail.com	Dr. YSEBAERT T., Professor Tom.Ysebaert@nioz.nl	Dr. ZHI Huang, Senior Research Scientist Zhi.Huang@ga.gov.au
Dr. PLATER A. J., Professor Gg07@liverpool.ac.uk	Dr. HERMAN P. M.J., Professor Peter.Herman@nioz.nl	Dr. TOWNEND I., Professor I.Townend@soton.ac.uk
Dr. DEARING J. A., Professor J.Dearing@soton.ac.uk	Dr. ROELVINK D., Professor d.roelvink@unesco-ihe.org	Dr. JONGE V. N de, Professor v.n.de.jonge@planet.nl
Dr. SAITO Y., Professor yoshiki.saito@aist.go.jp	Dr. KATTNER G., Professor Gerhard.Kattner@awi.de	Dr. ROTCHELL J. M, Associate Prof. J.Rotchell@hull.ac.uk
Dr. ZHANG Keqi, Professor keqizhang8@gmail.com	Dr. MATSUMOTO E., Professor e2.matsumoto@nifty.com	Dr. KOCH B., Professor Boris.Koch@awi.de
Dr. TOL C. van der, Associate Prof. c.vandertol@utwente.nl	Dr. MÜLLE M., Associate Prof. mmueller@swinburne.edu.my	Dr. WANG Xiaohua, Associate Prof. X.Wang@adfa.edu.au
潘顺琪 教授 Dr. PAN Shunqi, Professor PanS2@cardiff.ac.uk	Dr. LEONARDI N., Lecture N.Leonardi@liverpool.ac.uk	Dr. SOMPONGCHAIYAKUL P. spenjai@hotmail.com
Neven Cukrov, Senior Research associate ncukrov@irb.hr	Sheikh Aftab Uddin, Professor aftabims@cu.ac.bd	张茜 博士 Dr. ZHANG Qian zhangqian@hhu.edu.cn
孟 翊 副教授 Dr. MENG Yi, Associate Prof. ymeng@sklec.ecnu.edu.cn	张国安 副教授 Dr. ZHANG Guoan, Associate Prof. gazhang@sklec.ecnu.edu.cn	李茂田 副教授 Dr. LI Maotian, Associate Prof. mtli@sklec.ecnu.edu.cn
张二风 副教授 Dr. ZHANG Erfeng, Associate Prof. efzhang@sklec.ecnu.edu.cn	叶 祁 讲师 Dr. YE Qi, Lecture qye@sklec.ecnu.edu.cn	王艳娜 讲师 Dr. WANG Yanna, Lecture nywang@sklec.ecnu.edu.cn
毕倩倩 工程师 Dr. BI Qianqian, Engineer qqbi@sklec.ecnu.edu.cn	许 一 讲师 Dr. XU Yi, Lecture xuyi@sklec.ecnu.edu.cn	袁 庆 工程师 Dr. YUAN Qing, Engineer qyuan@sklec.ecnu.edu.cn



胡 进 工程师 Dr. HU Jin, Engineer jinhu@sklec.ecnu.edu.cn	张 丹 工程师 Dr. ZHANG Dan, Engineer dzhang@sklec.ecnu.edu.cn	李 月 工程师 Dr. LI Yue, Engineer yli@sklec.ecnu.edu.cn
Dr. SANDERS C. J. Professor Christian.Sanders@scu.edu.au	张安余 博士 Dr. ZHANG Anyu anyu.zhang@sio.org.cn	苏 函 工程师 Dr. SU Han, Engineer hsu@sklec.ecnu.edu.cn
冯 桓 教授 Dr. FENG Huan, Professor fengh@montclair.edu	倪寿清 教授 Dr. NI Shoutao, Professor sqni@sdu.edu.cn	Dr. WARD J.E., Professor evan.ward@uconn.edu
王 清 副研究员 Dr. WANG Qing, Associate Prof. qingwang@yic.ac.cn	张安国 副研究员 Dr. ZHANG Anguo, Associate Prof. zhanganguo2003@163.com	于 硕 助理研究员 Dr. YU Shuo, Assistant Prof. yushou2005@163.com
高 宇 助理研究员 Dr. GAO Yu, Research Assistant ygao@fudan.edu.cn	周晓静 讲师 Dr. ZHOU Xiaojing, Lecture zhouxiaojing@dlou.edu.cn	杨文卿 博士 Dr. YANG Wenqin givx@ustc.edu.cn
潘燕群 博士 Dr. PAN Yanqun yanqun_pan@uqar.ca	杨华蕾 副研究员 Dr. YANG Hualei, Associate Prof. hlyang@sklec.ecnu.edu.cn	禹定峰 副研究员 Dr. YU Dingfeng, Associate Prof. dfyu@qlu.edu.cn
李 鹏 讲师 Dr. LI Peng, Lecture pengli@ouc.edu.cn	陈大可 博士 Dr. CHEN Dake pengli@ouc.edu.cn	武国相 副教授 Dr. WU Xiangguo, Associate Prof. guoxiang@ouc.edu.cn
张 帆 博士 Dr. ZHANG Fan zhangf@sustech.edu.cn	苏 敏 副研究员 Dr. SU Min, Associate Prof. sumin@hhu.edu.cn	王宝利 教授 Dr. WANG Baoli, Professor baoli.wang@tju.edu.cn
刘 森 助理研究员 Dr. LIU Sen, Assistant Prof. sen_liu@sdu.edu.cn	苏应龙 研究员 Dr. SU Yinglong, Professor ylsu@des.ecnu.edu.cn	金 杰 工程师 Dr. JIN Jie, Engineer jjin@sklec.ecnu.edu.cn

固定人员在国际期刊和国际组织任职情况

Serving in International Academic Organizations and Journals

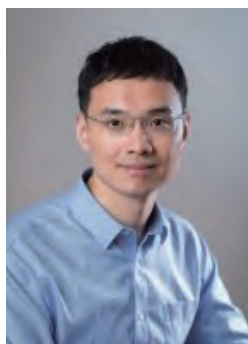
Name	International Organizations/Journals	Position	During
BELLERBY R.	SCAR Action Group on Ocean Acidification	Leader	2010-
	SCAR Integrated Climate and Ecosystem Dynamics (ICED)	SSC Member	2009-
	AMAP Working Group on Ocean Acidification	Leader	2010-
	IMBeR - Future Earth Coasts Continental Margins working group	Co-Leader	2017-
陈 静 CHEN Jing	Future Earth Coasts	Executive Committee Member	2019-
陈启晴 CHEN Qiqing	Environmental Science Europe	Subject Editor	2019-
陈中原 CHEN Zhongyuan	Environmental Management of Enclosed Coastal Seas	SPC Member	2004-
	Geomorphology	Editors-in-Chief	2017-
	Earth Surface Processes and Landforms	Advisory Editorial Board Member	2008-
程和琴 CHENG Heqin	Journal of Geology, Geophysics and Geosystems	Editorial Board Member	2009-
戴志军 DAI Zhijun	Scientific Reports	Editorial Board Member	2016-
	Frontiers of Earth Science	Associate Editor	2017-
	Geomorphology	Editorial Board Member	2018-
	Water	Editorial board member	2020-
高 抒 GAO Shu	Future Earth Coasts Academy	Member	2019-
	Mega-Delta Work Group, Future Earth Coasts	Chair	2019-
	Anthropocene Coasts	Founding Chief Editor	2017-
	Marine Geology	Editors-in-Chief	2017-
	Continental Shelf Research	Associate Editor	2011-
	Acta Oceanologica Sinica	Associate Editor	2016-
	China Ocean Engineering	Editorial Board Member	2013-
	Ocean Science Journal	Editorial Board Member	2015-
	Journal of Oceanology and Limnology	Editorial Board Member	2002-
何 青 HE Qin	INTERCOH	Member	2003-
侯立军 HOU Lijun	Estuaries and Coasts	Associate Editor	2017-
	Scientific Reports	Editorial Board Member	2017-

Name	International Organizations/Journals	Position	During
江山 JIANG Shan	Interdisciplinary Marine Early Career Network (IMECaN)	Committee Member	2020-2022
	Royal Society of Chemistry	Fellow of the Royal Society of Chemistry	2020-
	International Union for Pure and Applied Chemistry (IUPAC)	Executive Director	2016-
	International Union for Pure and Applied Chemistry (IUPAC)	Young Observer	2017-
姜雪峰 JIANG Xuefeng	International Younger Chemists Network (IYCN)	Member	2017-
	Organometallics	Editorial Advisory Board Member	2020-
	European Journal of Organic Chemistry	International Advisory Board Member	2019-
	Journal of Sulfur Chemistry	Editorial Board Member	2019-
	Heteroatom Chemistry	Editorial Board Member	2018-
	Phosphorus Sulfur Silicon and the Related Elements	Editorial Board Member	2018-
	Scientific Advisory Committee on Marine Plastic Litter and Microplastics of UNEP	Member	2019-
	Intergovernmental Oceanographic Commission of United Nations Educational, Scientific and Cultural Organization (UNESCO/IOC)	Expert	2017-
李道季 LI Daoji	UNESCO IOC/WESTPAC Research Project: Distribution, Source, Fate and Impacts of Marine Microplastics in the Asia Pacific Region	Principal Investigator	2017-2020
	UNEP- Northwest Pacific Action Plan (NOWPAP)	Expert	2018-
	UN Environment Programme, G6	Expert	2018-
	The North Pacific Marine Science Organization	Member	2018-
	UNESCO/IOC Regional Training and Research Center on Plastic Marine Debris and Microplastics (RTRC-PMDMP)	Director	2019-
	Advisory Committee on a Nordic Report on How to Strengthen the Global Knowledge Basis on Marine Litter and Microplastics	Member	2020-
	Scientific Advisory Board of European Quality Controlled Harmonization Assuring Reproducible Monitoring and assessment of plastic pollution	Member	2020-
	Anthropocene Coasts	Associate Editor	2018-
	Future Earth Coasts	Executive Committee Member	2019-
	李秀珍 LI Xiuzhen	Ocean and Coastal Management	Associate Editor
Wetlands Ecology and Management		Editorial Board Member	2012-
Chinese Geographical Science		Editorial Board Member	2009-

Name	International Organizations/Journals	Position	During
刘东艳 LIU Dongyan	Frontier in Marine Science: Marine Ecosystem Ecology	Associate Editor	2016-2020
史本伟 SHI Benwei	Scientific Reports	Senior Editorial Board	2020-
	Journal of Water Resources and Ocean Science	Editorial Board	2019
施华宏 SHI Huahong	Marine Pollution Bulletin	Associate Editor	2020-
	International Eco-Island Science Alliance	Founder	2019-
	UNEP Intertional Nitrogen Management System	Working Group Member	2018-
	Coastal Carbon Research Coordination Network	Steering Committee	2018-
唐剑武 TANG Jianwu	The Coastal Carbon Research Coordination Network Steering Committee	Member	2017-2021
	Ecosystem Health and Sustainability	Subject Editor	2017-
	Ecological Processes	Associate Editor	2017-
	Ecological Processes	Associate Editor	2017-
汪亚平 WANG Yaping	Coastal Education & Research Foudation, Inc. (CERF)	Society Member	
	Anthropocene Coasts	Associate Editor	2017-
	Acta Oceanologica Sinica	Editorial Board Member	2016-
吴 辉 WU Hui	Geoscience Letters	Editorial Board Member	2018-
吴 莹 WU Ying	IGBP/IMBER-Scientific Committee	Member	2019-2021
	Scientific Committee on Oceanic Research (SCOR), WG 161	Member	
夏建阳 XIA Jianyang	National Nature Foundation	Reviewer	2019-
	F1000 Prime Faculty member	Faculty Member	2019-
	Ecological Processes	Associate Editor	2018-
	Remote Sensing	Review Board Member	2019-
徐 凡 XU Fan	Journal of Plant Ecology	Associate Editor	2020-
	Frontiers in marine science	Review Editor	2020-
杨嘉龙 YANG Jialong	Fish & Shellfish Immunology Reports	Editorial Board Member	2020-
杨世伦 YANG Shilun	Scientific Reports	Editorial Board Member	2016-
杨 毅 YANG Yi	Applied Geochemistry	Associated Editor	2020-
	Journal of Hazardous Materials	Editorial Board Member	2019-
	Science of the Total Environment	Editorial Board Member	2019-

Name	International Organizations/Journals	Position	During
张 经 ZHANG Jing	IOC/WESTPAC-CorReCAP	Project Leader	2008-
	IOC/WESTPAC MPRM-III project (Atmospheric Input to the Ocean)	Project Leader	1993-
	IOC-UNESCO Global Ocean Oxygen Network	Chair	
	IGBP/IMBER -Capacity Building Working Group	Chair	2009-
	Joint IMBER/LOICZ Continental Margin Working Group	Member	2007-
	IOC Consulting Group on Capacity-Building	Member	2004-
	GOOS HOTO (Health of the Oceans Module of The Global Ocean Observing System) Panel	Member	1996-
	Water, Air and Soil Pollution	Editorial Board Member	1998-
张卫国 ZHANG Weiguo	Water, Air and Soil Pollution: Focus	Editorial Board Member	2001-
	Future Earth Coasts Academy	Member	2019-2029
	Current Pollution Reports	Editorial Board Member	2014-
	Estuarine Coastal and Shelf Science	Associate Editor	2017-
周旭辉 ZHOU Xuhui	Frontiers in Earth Science	Review Editor in Geomagnetism and Paleomagnetism	2015-
	Scientific Reports	Editorial Board Member	2020-2024
周云轩 ZHOU Yunxuan	Journal of Plant Ecology	Editorial Board Member	2014-
	Frontiers of Earth Science	Associate Editor	2008-

新聘人员 New Appointees



赵宁 研究员

主要经历:

美国麻省理工学院 博士 (2011-2017)
美国伍兹霍尔海洋研究所 博士后 (2017-2017)
德国马克思普朗克化学研究所 博士后 (2017-2020)
华东师范大学 研究员, 紫江优秀青年学者 (2020-)

研究专长:

大陆边缘 (沉积物、珊瑚礁) 高分辨率气候与环境记录;
海洋沉积年代学;
海洋同位素地球化学;
古海洋环流与碳循环

Dr. ZHAO Ning, Professor

Education and Major Experience:

Ph.D., MIT-WHOI Joint Program in Oceanography (2011-2017)
Post-doctoral Fellow, Woods Hole Oceanographic Institution (2017-2017)
Post-doctoral Scientist, Max Planck Institute for Chemistry (2017-2020)
Zijiang Excellent Young Scholar of ECNU, (2020-)

Research Interests:

High-resolution Records of Climate and Environment from Continental Margins (Marine Sediments, Coral Reefs),
Chronology of Marine Sediments,
Marine Isotope Geochemistry,
Paleo Ocean Circulation and Carbon Cycle



黄颖 副研究员

主要经历:

荷兰特文特大学 博士 (2010-2016)
华东师范大学 博士后 (2016-2019)
华东师范大学 副研究员 (2020-)

研究专长:

滨海湿地生态遥感;
滨海湿地碳循环

Dr. HUANG Ying, Associate Professor

Education and Major Experience:

Ph.D., University of Twente (2010-2016)
Post-doctoral Fellow, East China Normal University (2016-2019)
Associate Professor, East China Normal University (2020-)

Research Interests:

Remote Sensing of Coastal Wetland Ecology,
Carbon Cycle in Coastal Wetlands



谭凯 副研究员

主要经历:

同济大学 博士 (2011-2017)
华东师范大学 博士后 (2017-2020)
华东师范大学 副研究员 (2020-)

研究专长:

河口海岸测绘遥感理论方法及应用
潮滩地形与生态遥感监测
激光雷达遥感点云数据处理方法和应用

Dr. TAN Kai, Associate Professor

Education and Major Experience:

Ph.D., Tongji University (2011-2017)
Post-doctoral Fellow, East China Normal University (2017-2020)
Associate Professor, East China Normal University (2020-)

Research Interests:

Methods and Applications of Estuarine and Coastal Surveying and Mapping and Remote Sensing Technologies,
Remote Sensing Monitoring of Tidal Flat Topography and Ecology,
LiDAR Remote Sensing Point Cloud Data Processing Methods and Applications



张文霞 副研究员

主要经历:

美国德州农工大学 博士 (2010-2015)
加拿大达尔豪斯大学 博士后 (2015-2016)
华东师范大学 博士后 (2016-2020)
华东师范大学 副研究员 (2020-)

研究专长:

近岸动力过程及其生态效应
数值模拟

Dr. ZHANG Wenxia, Associate Professor

Education and Major Experience:

Ph.D., Texas A&M University (2010-2015)
Post-doctoral Fellow, Dalhousie University (2015-2016)
Post-doctoral Fellow, East China Normal University (2016-2020)
Associate Professor, East China Normal University (2020-)

Research Interests:

Coastal Dynamics and Its Ecological Responses, Numerical Modeling